



The  
Ionic Conductivity  
of  
p(2-Hydroxyethyl Methacrylate)  
Hydrogels

A thesis submitted for the degree of  
Doctor of Philosophy  
in the Department of  
Physical and Inorganic Chemistry.

The University of Adelaide,  
December 1995.

Darren A. Miller B.Sc.(Hons).

## *Table of Contents*

<b>Summary</b>		<b>vi</b>
<b>Statement</b>		<b>viii</b>
<b>Acknowledgements</b>		<b>ix</b>
<b>Abbreviations</b>		<b>x</b>
<b>Chapter One</b>	<i>Introduction</i>	<b>1</b>
<b>Chapter Two</b>	<i>Experimental Techniques</i>	<b>20</b>
2.1	Sample Source	20
2.2	Polymer Preparation	20
2.3	Sample Preparation	22
2.4	A.C. Impedance Measurements	23
2.5	A.C. Impedance Spectroscopy	25
2.6	Differential Scanning Calorimetry	29
2.6.1	Measurement of Freezing Water	30
2.7	Thermal Mechanical Analysis	30
2.8	Positron Annihilation Lifetime Spectroscopy	32
2.8.1	Theory	32
2.8.2	Experimental	34
<b>Chapter Three</b>	<i>The AC Conductivity of pHEMA</i>	<b>38</b>
3.1	Introduction	38
3.2	The AC Impedance Spectrum	39
3.3	The Conductivity of pHEMA	42
3.4	The Conductivity of EGDMA/HEMA Copolymers	46
3.4.1	Introduction	46

3.4.2 Results and Discussion	47
3.5 The Conductivity of OED/HEMA Copolymers.	53
3.5.1 Introduction	53
3.5.2 Results and Discussion	55
3.6 The Variation of AC Conductivity with Water Content	62
3.6.1 Water in pHEMA Hydrogels	62
3.6.2 Results and Discussion: pHEMA	66
3.6.3 EGDMA/HEMA Copolymers	72
3.6.4 OED/HEMA Copolymers	75
3.7 The Variation of AC Conductivity with Temperature	78
3.7.1 pHEMA	78
3.7.2 EGDMA/HEMA Copolymers	85
3.7.3 OED/HEMA Copolymers	89
3.8 Summary	92
<b>Chapter Four</b> <i>The AC Conductivity of ion doped pHEMA</i>	<b>94</b>
4.1 Introduction	94
4.2 AC Impedance Spectrum	99
4.3 The AC Conductivity of KBr doped pHEMA	99
4.4 The AC Conductivity of KBr doped EGDMA/HEMA Copolymers	104
4.5 The AC Conductivity of KBr doped OED/HEMA Copolymers	109
4.6 The Variation of Conductivity with Water Content.	114
4.6.1 KBr doped pHEMA	114
4.6.2 KBr doped EGDMA/HEMA Copolymers	120
4.6.3 KBr doped OED/HEMA Copolymers	129





5.4.2	Free volume characteristics of undoped pHEMA based gel electrolytes	173
5.4.3	Free volume characteristics of doped pHEMA based gel electrolytes	178
5.4.3a	KBr doped gel electrolytes	178
5.4.3b	The variation of dopant in pHEMA gel electrolytes	182
5.4.4	Summary	183
5.5	Summary	183
Chapter Six	<i>Conclusions</i>	185
References		194



## ERRATA

**- page 23, Table 2.1**

should read  $\text{Pb}(\text{NO}_3)_2$

**- page 51, line 11**

should read "The following equation can be used to evaluate capacitance."

**-page 64, line 8**

should read "...until water contents of 25wt%. As more water is absorbed  $T_2$  increases dramatically..."

**-page 83, lines 19-20**

should read "... (Fig. 3.25) would indicate that regions of the conductive phase had become non-conductive."

**page 84, last sentence**

should read "... of partially hydrated samples to determine if the glass transition results in a change in conductivity behaviour."

## *Summary*

Poly (2-hydroxyethyl methacrylate) (pHEMA) and a series of copolymers with various oligo (ethylene glycol) dimethacrylates, with the number of ethylene glycol units varying between one and nine, were prepared. These polymer samples were hydrated in a number of electrolyte solutions, primarily potassium bromide, of varying concentration. The resulting equilibrium water content (EWC) was found to be anion dependent. The conductivity of these hydrogel samples was evaluated using AC impedance spectroscopy. The interactions between polymer, water and electrolyte were investigated using several experimental techniques to assist in understanding of the conductivity data.

The AC impedance response of these samples was studied over the frequency range 10Hz-1MHz with an applied voltage of 1V. The resulting AC impedance spectra were used to model the behaviour of the polymeric systems in terms of resistors and capacitors and thus the the conductivity was resolved. The variation in conductivity was investigated with respect to variations in crosslinker concentration, crosslinker nature, water content, temperature, dopant concentration and dopant nature. The variation of these parameters resulted in corresponding changes in the conductivity. Changes in the gel structure were reflected in the locus of the AC impedance plot and yielded information on structural changes.

The interactions between polymer, water and electrolyte were investigated using several experimental techniques.

The amount of freezing and non-freezing water in the hydrogels was determined using differential scanning calorimetry. The variation in this ratio was measured for samples of varying crosslinker, concentration and nature, and

several dopants. Both factors were found to have a significant effects but the greatest change was found for specific electrolytes. Crosslinking led to a decrease in the relative amount of freezing water.

The free volume characteristics of the gels studied were investigated using thermal mechanical analysis and positron annihilation lifetime spectroscopy. It was found that the equilibrium water content of the copolymers studied varied in the same manner as  $I_3$ , the relative orthopositronium (oPs) annihilation intensity, an indication of the number of free volume sites within a polymer. TMA measurements revealed an increase in the free volume as the amount of water in pHEMA was increased.

### *Statement*

This work contains no material which has been accepted for the award of any other degree or diploma in any university or other tertiary institution and, to the best of my knowledge and belief, contains no material previously published or written by another person, except where due reference has been made in the text. I give consent for this copy of my thesis being made available for photocopying and loan when deposited in the University Library.

17<sup>th</sup> December 1995.

## *Acknowledgements*

I would like to thank both my supervisors, Dr Peter Allen and Dr David Williams, for their insights and guidance throughout the course of this work.

Mark Hodge ran the PALS experiments presented in this thesis and his experience in the field proved invaluable to the interpretation of the results presented in this thesis. Kym Ide was of great assistance in the use of the TMA. The technical staff of both the Departments of Physical and Inorganic Chemistry and Chemical Engineering provided excellent service and humour.

Darrell Bennett, Tony Clayton and Chee-Hoong Lai, graduates of the polymer group, all deserve mention for their advice and willingness to discuss my project, especially in its early stages.

I would also like to thank all my friends, my greatest assets, for their humour and support throughout the course of my studies.

My greatest thanks go to my family, especially my parents Brian and Carole, for their unfailing and unquestioning support of everything I do; words cannot adequately describe my gratitude to them.

## *Abbreviations*

AC	alternating current
DC	direct current
DiEGDMA	di (ethylene glycol) dimethacrylate
DMA	dimethyl acetamide
DMF	dimethyl formamide
DMSO	dimethyl sulfoxide
DSC	differential scanning calorimetry
EGDMA	ethylene glycol dimethacrylate
EWC	equilibrium water content
OED	oligo (ethylene glycol) dimethacrylate
oPs	orthopositronium
PAA	poly (acrylic acid)
PALS	positron annihilation lifetime spectroscopy
PAN	poly(acrylonitrile)
PC	propylene carbonate
PEO	poly (ethylene oxide)
PET	poly (ethylene terephthalate)
PHEMA	poly (2-hydroxyethyl methacrylate)
PPO	poly (propylene oxide)
pPs	parapositronium
Ps	positronium
PVam	poly (vinyl amine)
PVdF	poly (vinylidene difluoride)
P400	poly (400 (ethylene glycol) dimethacrylate)
RC	resistance/capacitance
T <sub>g</sub>	glass transition temperature

<b>TBO</b>	t-butyl per-2 ethyl hexanoate
<b>TEGDMA</b>	tetra (ethylene glycol) dimethacrylate
<b>TMA</b>	thermal mechanical analysis
<b>TMCS</b>	trimethyl chlorosilane
<b>triflate</b>	lithium trifluoromethanesulphonate ( $\text{LiCF}_3\text{SO}_3$ )





# CHAPTER ONE

## *Introduction*

The electrical conductivity of polymeric materials has been seen, until recently, as an undesirable phenomenon; only the insulating capabilities of polymers were considered important and of value in electrical applications. The first report of a conducting polymer in the literature appeared in 1910 when Burt<sup>(1)</sup> synthesized  $(S-N)_n$ , poly(sulfur nitride) and it was not until 1953 Goehrig and Voight<sup>(2)</sup> measured its conductivity. However, it was not until the mid 1970's that relatively high electronic and ionic conductivities were achieved for a number of polymers. Several reviews<sup>(3-7)</sup> list the projected applications and advantages of the use of conducting polymers. Some of the numerous proposed applications for conducting polymers (Table 1.1) are aircraft lightning protection, artificial muscles and nerves, batteries, capacitors, electrochromic windows, and various types of sensors (e.g. humidity and chemical). The field of conducting polymers has attracted much interest as these materials offer the potential to combine conductivity with other attractive properties of polymers (Table 1.1) such as biocompatibility, transparency, formability flexibility and low density.

Considerable research has been devoted to the development of a solid polymer electrolyte battery which would overcome existing limitations of liquid electrolytes such as leakproof containment and corrosion problems. The thin-film forming ability of solid polymer electrolytes would enable improved energy density and there would also be the added benefit of having no need to incorporate an inert electrode spacer in the design as the solid electrolyte could also provide this function. The flexibility of polymer electrolytes would not only result in good electrode/electrolyte contact but also enable cells to be designed in numerous configurations such as those

Representative proposed applications of conducting polymers	Anticipated attributes of conducting polymers
Aircraft lightning strike protection Antistatic carpet, fibres, films, paints Antitheft targets Antiradiation coating Architectural applications Artificial nerves and muscles Batteries Capacitors Catalysts, polymerization Coating for metal plating on plastic Conducting adhesives, fabrics, inks, sealants, wires Controlled-released medicine delivery systems Corrosion-preventing paints Displays Electrochromic displays, windows Electrodes (fuel cells, transparent, electrocardiograph) Electromagnetic shielding Electromagnetic shutters Electromechanical actuators for biomedical devices Electronic membranes Electronically-controlled catalysts and enzymes Electron-beam resists Electrostatic control Fuses (reversible) Gas separation membranes Heating elements (de-icer panels) Infrared reflectors Lithographic resists Loudspeakers (electrostatic, transparent) Memory devices (electrical, optical) Microwave shielding Nonlinear optics Packaging materials pH modulators Polymer/solid electrolytes Radar dishes Redox capacitors Resistive heaters Semiconducting devices (i.e. transistors) Sensors (i.e. humidity, chemical, temperature) "Smart" materials (i.e. actuators, sensors) Supercapacitors Thermal clothing Transparent conductors Waveguides Welding of plastic composites	High, metal-like conductivity Semiconductivity Large polarizabilities Bistability ( $\geq 2$ "stable" states) Low density Flexibility Film and/or fibre formation Processibility Transparency Solubility/dispersibility Low environmental contamination Biocompatibility Compatibility with other polymers for composites High strength Modulation/tuning of properties via organic chemistry Thermoelectric power Redox active Optical changes (linear and nonlinear) Fast optical response High threshold for optical damage

**Table 1.1**

Suggested applications and anticipated attributes of conducting polymers.

(Reproduced from [4].)

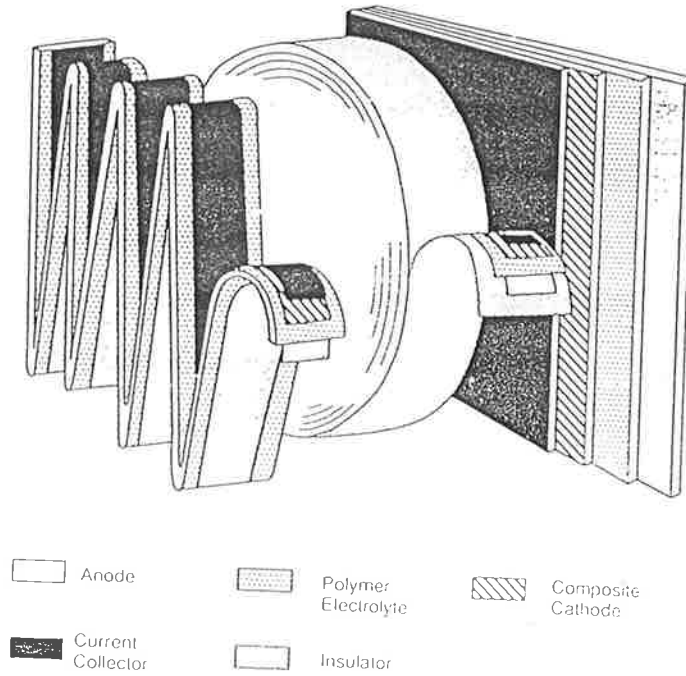


Figure 1.1

Various proposed configurations for extended area solid polymer electrolyte batteries. (Reproduced from (8).)

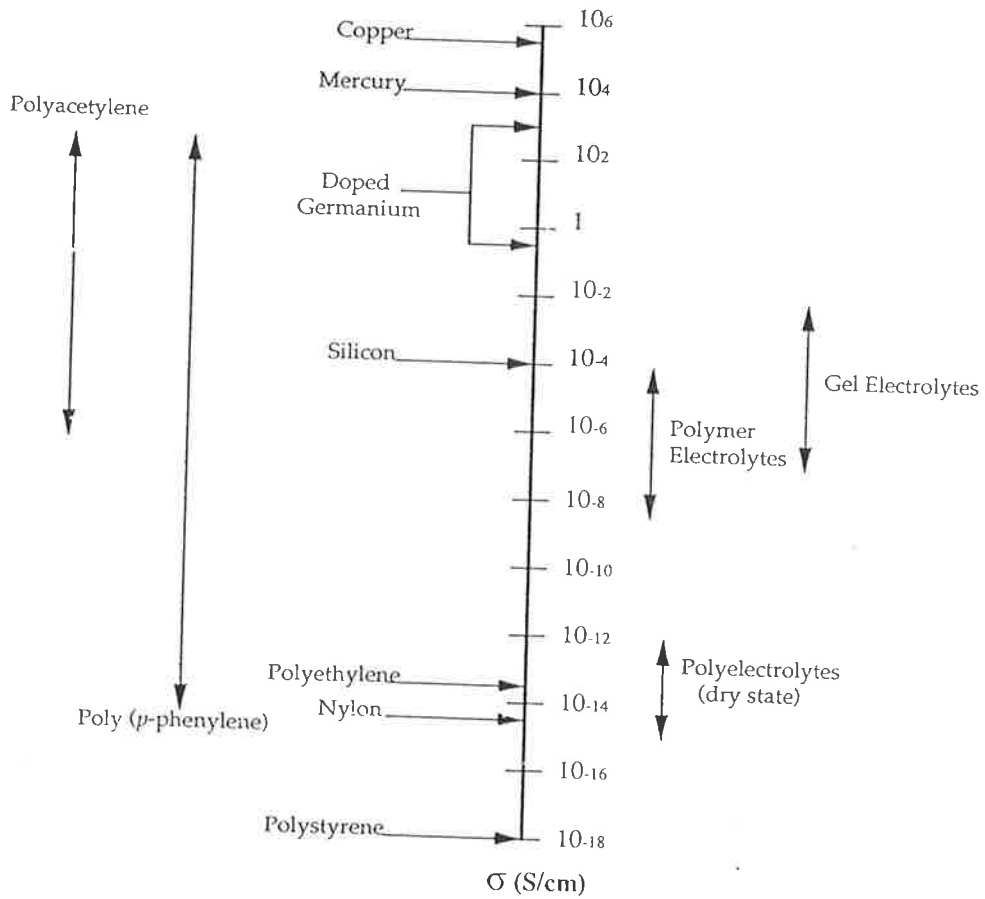


Figure 1.2

The conductivity of several materials.

proposed by Tofield et al.<sup>(8)</sup>(Fig 1.1) The manufacture of solid polymer electrolyte batteries is anticipated by Gray<sup>(3)</sup> to be easier than that of present cells due to the elimination of the liquid component. The new procedure could utilise or adapt existing thin film manufacturing technology thus minimising the costs of changing the battery construction process.

High electronic conductivity was first shown for doped poly(acetylene) systems by MacDiarmid and coworkers<sup>(9)</sup>; this stimulated research into numerous conjugated polymeric systems such as poly(*p*-phenylene)<sup>(10)</sup> and polypyrrole<sup>(11)</sup>. The formation of a highly conductive polymer results from either the removal or the addition of electrons by accepting or donating moieties <sup>(12)</sup>. This procedure has been termed doping<sup>(13)</sup> in analogy with the doping of inorganic semiconductors. Despite achieving high conductivities, present forms of electronically conductive polymers suffer from chemical instability and have limited processability<sup>(14)</sup>.

High ionic conductivities can be achieved in polymer systems by the incorporation of additives in the form of salts and or solvents into the matrix. Poly (ethylene oxide) [PEO]/ sodium iodide complexes were first formed and characterized by Wright and coworkers<sup>(15)</sup>. However, the potential for these systems in electrical applications was first reported by Armand<sup>(16)</sup>. This initial discovery has led to the investigation of ionic conductivity in such a wide range of polymer systems that further classification is required.

Ionically conducting polymeric media have been classified by Gray<sup>(17)</sup> as either polymer electrolytes, polyelectrolytes or gel electrolytes.

Polymer electrolytes are a group of polymers with the ability to solvate a number of inorganic salts by coordination. This ion-solvating ability was first reported for polyethers such as poly(ethylene oxide) [PEO]<sup>(15,16)</sup> and poly(propylene oxide)<sup>(16)</sup> [PPO] but other polymers have been shown to exhibit electrolyte solvating capabilities; these include poly(ethylene imine)<sup>(18)</sup>, poly(ethylene succinate)<sup>(19)</sup>, poly(ethylene adipate)<sup>(20)</sup>, poly( $\beta$ -

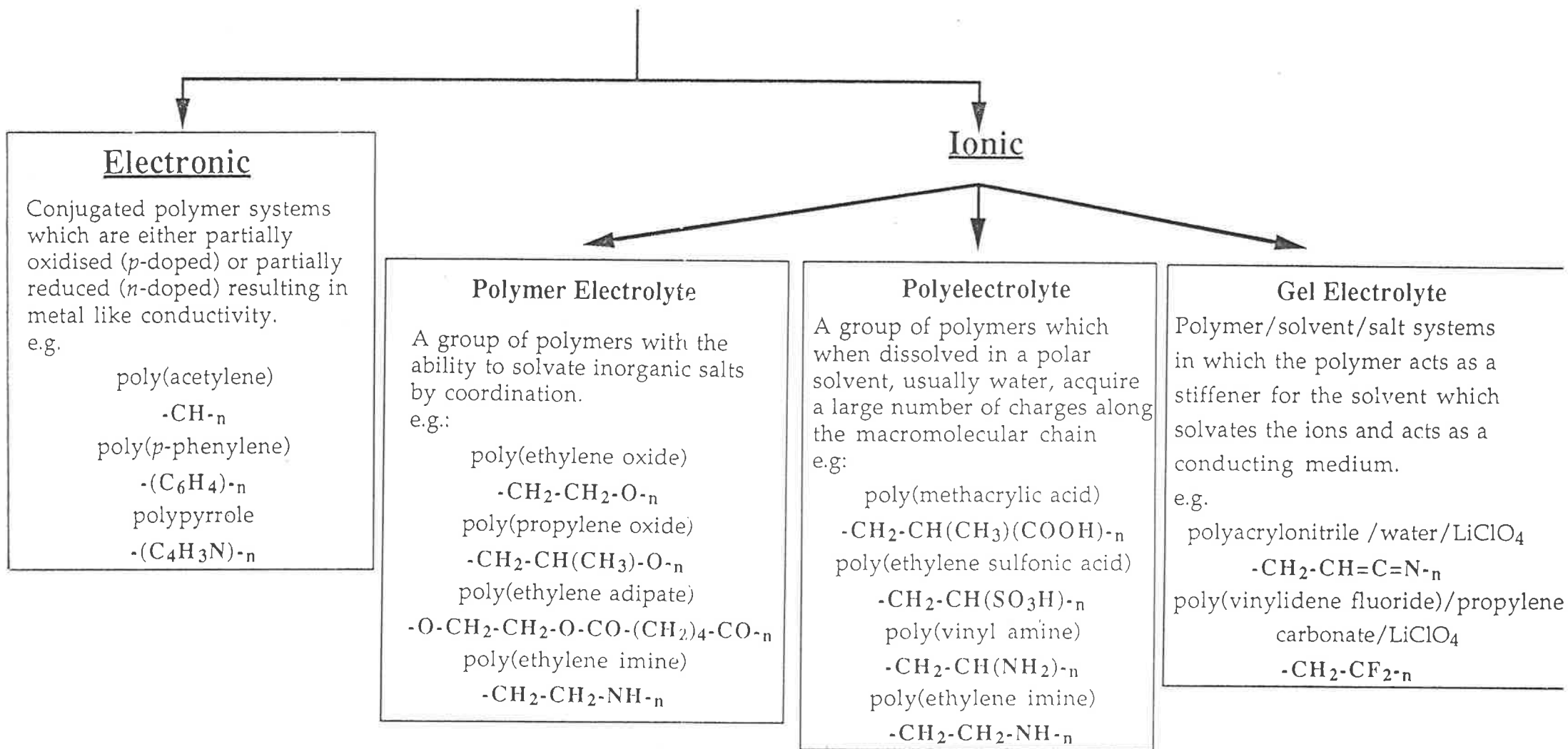
propiolactone)<sup>(21)</sup>, poly(methylene sulphide)<sup>(22)</sup> and polyphosphazenes<sup>(23)</sup>. The most commonly used salts are lithium perchlorate [LiClO<sub>4</sub>], sodium thiocyanate [NaSCN] and lithium trifluoromethanesulphonate [triflate, CF<sub>3</sub>SO<sub>3</sub><sup>-</sup>]. The conductivity of such systems is generally studied well above their glass transition temperature [T<sub>g</sub>] as it is dependent on the cooperative motion of ions and the polymer network. The conductive behaviour of such systems is usually interpreted in terms of the Vogel-Tamman-Fulcher equation:

$$\sigma = A_0 T^{1/2} \exp[-E_a/R(T-T_0)] \quad \text{Eqn. 1.1}$$

where A<sub>0</sub> is a weakly temperature dependent pre-factor, T<sub>0</sub> corresponds to T<sub>g</sub>, and E<sub>a</sub> is an activation energy. Ionic conductivity in these systems is discussed in terms of a model in which ion transport is facilitated by the large amplitude motion of the polymer backbone as cation-heteroatom interactions are formed and broken at different sites on the backbone.

Polyelectrolytes are a class of macromolecular compounds which when dissolved in a suitable polar solvent, usually water, spontaneously acquire, or can be made to acquire, a large number of elementary charges distributed along the macromolecular chain. They are formed by the interaction of cationic and anionic moieties, one of which is polymeric and the other a counter ion. The interaction between these moieties is controlled by the density of the charged groups on the polymer chain and the nature of the counter ion. The conductivity of these polymers in the dry state is typically in the range 10<sup>-12</sup> to 10<sup>-15</sup> Scm<sup>-1</sup>(17). The addition of water solvates the ions which tend to form stable immobile clusters in the dry state. Ionic conductivity is a function of water content as water has a twofold effect on the system; it increases the local dielectric constant of the polymer, aiding ion dissociation, and also plasticises the polymer, enhancing ionic mobility.

# Conducting Polymers



These systems are reviewed by Seanor<sup>(24)</sup> and Mandel<sup>(25)</sup>. Polyelectrolytes can be polyacids such as poly(acrylic acid)(PAA) or polybases such as poly(vinylamine) (PVAm). On interacting with water these polymers form polyanions and polycations respectively. Macromolecules which bear both acidic and basic functionalities are termed polyampholytes and are positively charged at low pH and negatively charged at high pH. They are neutral at isoelectric pH where charge balance is achieved.

A gel electrolyte is a polymer/ solvent/ salt system in which the polymer is secondary in the conducting matrix and acts merely as a stiffener or support for the low molecular weight high dielectric solvent which solvates the ions and acts as the conducting medium. In the absence of solvent there is some residual conductivity which probably arises from ion hopping between localised sites, although the salt would be expected to be dispersed, primarily as ion pairs, throughout the polymer matrix. Gel electrolytes are attracting interest as they benefit from the fact that the conducting phase also plasticises the polymer matrix; the ionic conductivity of polymer electrolytes has been enhanced by the addition of plasticisers but at the expense of mechanical rigidity.<sup>(26)</sup>

Several examples of research into such systems exist in the literature. Voice et al.<sup>(26)</sup> have investigated the conductivity of a range of gel electrolytes prepared from a number of commercially available polymers, e.g. poly(ethylene terephthalate) [PET], Poly(vinylidene fluoride) [PVDF], and solvents, e.g. N,N-dimethylacetamide [DMA], N,N-dimethylformamide [DMF], dimethylsulfoxide [DMSO], using lithium triflate as the ionic species incorporated for conduction. They report ionic conductivities in the region of  $10^{-3} \text{ Scm}^{-1}$  for their samples down to temperatures of  $-20^{\circ}\text{C}$ . Zygadlo-Monikowska et al.<sup>(27)</sup> have prepared gel electrolytes based on mixtures of 2,3-methoxypropyl methacrylate, propylene carbonate [PC] and  $\text{LiClO}_4$ . They report conductivities ranging from  $10^{-3} \text{ Scm}^{-1}$  at ambient temperature down

to  $10^{-5} \text{ Scm}^{-1}$  at  $-50^\circ\text{C}$ . Tsuchida and coworkers<sup>(28-31)</sup> have studied systems based on poly(acrylonitrile) [PAN] and PVDF. They report conductivities of around  $10^{-5} \text{ Scm}^{-1}$  at ambient temperature for PVDF/ PC/  $\text{LiClO}_4$  gel electrolytes of typical composition 50/ 30/ 20 (molar ratio) and  $2 \times 10^{-4} \text{ Scm}^{-1}$  at  $25^\circ\text{C}$  for PAN/ethylene carbonate [EC]/ $\text{LiClO}_4$  in the molar ratio 50.7/36.6/12.7. Crosslinked gel electrolytes have been formed by Kabata et al.<sup>(32)</sup>. They report that a material consisting of 13wt% monomer (ethoxypolyoxyethylene acrylate/ trimethylolpropane triacrylate), 67wt% (PC/ 1,2-dimethoxyethane) and 20wt%  $\text{LiBF}_4$  had an ambient conductivity of  $2.7 \times 10^{-3} \text{ Scm}^{-1}$ . Reich and Michaeli<sup>(33)</sup> report PAN/water/perchlorate salt gel electrolytes with ambient ionic conductivities in the range  $10^{-7}$  to  $10^{-2} \text{ Scm}^{-1}$ . Croce et al.<sup>(34)</sup> have studied gel electrolytes prepared from mixtures of PAN, EC, PC and  $\text{LiClO}_4$  or  $\text{LiAsF}_6$ . They report conductivities as high as  $10^{-2} \text{ Scm}^{-1}$  for a  $\text{LiAsF}_6$  containing sample.

It should be noted that the conductivity temperature dependence of gel electrolytes is not uniform for all systems. Reich and Michaeli<sup>(33)</sup> found that conductivity of PAN/water/perchlorate salt gel electrolytes showed an Arrhenius type temperature dependence both above and below  $T_g$  although the activation energy changed at this temperature. Non Arrhenius behaviour has been observed in Viton/ PC/  $\text{LiClO}_4$  solutions<sup>(35)</sup>.

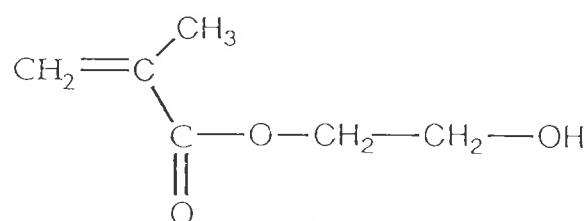
Polymer electrolytes tend to exhibit favourable mechanical properties but their conductivity is limited by the increase in crystallinity and ion-pair formation with an increase in ion content. Polyelectrolytes require aqueous dilution at the expense of mechanical properties to achieve favourable ionic conductivities. Gel electrolytes are attracting growing interest as they offer both mechanical integrity and enhanced conductivity. The polymer network supports the conducting phase, i.e. it acts as a stiffener, and the conducting phase both dissociates the charge carriers and plasticises the polymer network, decreasing the glass transition temperature.



We have chosen to study the conductivity of the poly (2-hydroxyethyl methacrylate) [pHEMA]/ salt/ water system. Such a system falls into the gel electrolyte category. The term gel can be used to describe a number of soft coherent substances including lamellar mesophases, clays, amorphous vanadium pentoxide, phospholipids and also three dimensional polymer networks. Polymeric gels are capable of absorbing large amounts of liquid (water in the system studied in this work) whilst still retaining essential properties of solids such as shear and compression moduli. Aharoni and Edwards<sup>(36)</sup> define a polymer gel as a system consisting of a polymer network swollen with solvent, where polymer network refers to the three dimensional polymeric structure excluding occluded solvent.

There are a number of reasons for opting to investigate pHEMA hydrogels. PHEMA is a relatively simple gel and its mechanical properties and water absorbing capabilities are easily controlled by crosslinking with ethyleneglycol dimethacrylate (EGDMA). PHEMA hydrogels have been the focus of considerable research as a result of their biocompatibility and thus there exists extensive data on its properties. The potential application of pHEMA to the field of gel electrolytes is reflected in the investigation of a humidity sensor<sup>(37)</sup> in which pHEMA was an active component.

2-Hydroxyethyl methacrylate was first synthesised and polymerised by du Pont in 1936<sup>(38,39)</sup> but gained widespread attention in the 1960's when Wichterle and Lim<sup>(40,41)</sup> reported on preparation techniques and its possible biological uses. HEMA monomer has the structure;



HEMA

The presence of polar moieties enables pHEMA to absorb large amounts of

water and leads to its classification as a hydrogel. It is able in some cases to absorb up to 40-45% of its total weight as a hydrogel.<sup>(42)</sup>

Synthetic hydrogels are suitable for potential medical applications such as soft contact lenses<sup>(43)</sup>, reverse osmosis membranes<sup>(44,45)</sup>, kidney dialysis membranes<sup>(46,47)</sup>, and drug delivery systems<sup>(48-50)</sup>. Hydrogels are of great use in the field of biomaterials where the absorbed water acts as a plasticiser, a transport medium for dissolved species, and a bridge between the disparate surface energies of synthetic polymers and body fluids<sup>(51)</sup>. PHEMA hydrogels are particularly useful for biomedical applications due to their mechanical integrity and chemical stability. They have been shown to be resistant to acid hydrolysis and reactions with amines<sup>(52)</sup> and incur alkaline hydrolysis only at high temperature and pH<sup>(53)</sup>.

The role of water in pHEMA has been studied by a number of techniques including nuclear magnetic resonance (NMR)<sup>(54-59)</sup> and differential scanning calorimetry (DSC)<sup>(57-63)</sup>. These studies provide evidence that water exists in more than one state within the hydrogel and that these states will affect the properties of the hydrogel. Several systems of nomenclature have been used to describe the states of water present within water absorbing polymers. Terms such as primary, secondary, bound, interfacial, bulk, free, freezing and non-freezing have been used to describe the various phases of water present<sup>(61)</sup>. Corkhill et al.<sup>(61)</sup> suggest that water is more likely to be present in a continuum of states between the two extremes rather than in a series of discrete phases. At one extreme is water which is strongly associated to the polymer through hydrogen bonding, sometimes called bound or non-freezing water, while at the other extreme is water unaffected by the polymer matrix, with a much greater degree of mobility, sometimes referred to as free or freezing water. The types and amounts of water measured are technique dependent and are also subject to hysteresis effects.

The water binding process in hydrogels has been described previously<sup>(61)</sup> using the concept of hydration shells. Hydrophilic groups on the polymer engage in hydrogen bonding with non-freezing water creating an inner hydration shell and this shell is surrounded by successive layers of freezing water molecules. McBrierty et al<sup>(58)</sup> have proposed that , in the case of pHEMA, less than 20 wt % of water is strongly bound to the polymer, corresponding to two water molecules per repeat unit. They define the next 15 wt% as interfacial, and additional water above a water content of 35 wt % as freely diffusable. In the gel electrolyte systems we have studied, the water absorbed by the pHEMA is the conducting medium and thus its structure within the hydrogel is directly relevant to an understanding of the conductive properties of the samples in this work.

The conductive properties of gel electrolytes can be measured by both DC and AC methods as discussed by Bruce<sup>(65)</sup>. We have chosen to use AC impedance spectroscopy for a number of reasons. Simple experimental cells with inert blocking electrodes (Fig. 2.1, 2.2) can be used to collect data: these blocking electrodes are stable over a wide temperature range enabling the temperature dependence of gel electrolyte conductivity to be readily determined. The analysis of complex impedance data gained from AC experiments enables us to model the electrical response of the gel electrolyte on an equivalent electrical circuit consisting of components such as resistors and capacitors. Although these circuits are an approximation of the real response they should enable us to quantify the resistive and capacitive components and relate them to fundamental electrical properties of the gel electrolyte. Sequential variation of experimental parameters (e.g. the amount of crosslinking, the nature of the crosslinking agent employed, water content, temperature and the concentration and the nature of the dopant) should enable the relative contribution of each to conductivity in pHEMA based gel electrolytes to be assessed.

The use of AC impedance spectroscopy may yield further insights into the structure of water in pHEMA hydrogels. Previous work by Watanabe and coworkers<sup>(66)</sup> on segmented polyether/ poly(urethane ureas) is representative of how AC impedance spectroscopy may give insight into morphological detail. Watanabe found that the AC impedance spectra in this system could be described as the superposition of two semi-circular loci. This phenomenon was attributed to the presence of two types of conductive pathway within the polymer network. Ionic conductivity takes place through the amorphous regions of the network and the presence of crystalline regions was used to rationalise the observed AC impedance locus.

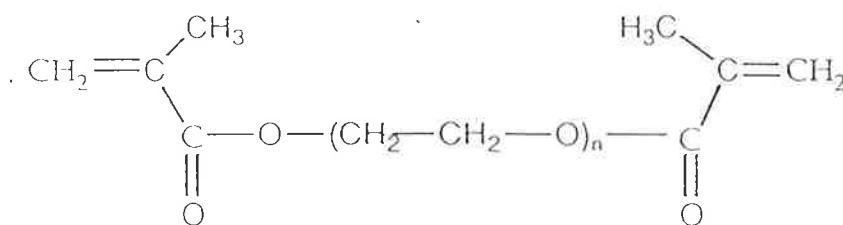
Initially the conductivity of pHEMA at full hydration (i.e. with an equilibrium water content of 40%) was measured. Subsequently, experiments were carried out to investigate the change in conductivity with respect to several environmental parameters.

pHEMA forms a three dimensional network which renders it insoluble despite its ability to absorb significant amounts of water; this results from a small amount of crosslinking which is in turn a consequence of the presence of small amounts of impurities in HEMA monomer. This impurity, a byproduct of the HEMA monomer production process, usually consists of ethylene glycol dimethacrylate (EGDMA). The EGDMA homopolymer is an extremely brittle glassy polymer with a very high glass transition temperature ( $T_g$ )<sup>(67)</sup>. The introduction of EGDMA decreases the amount of water which can be absorbed by the hydrogel as it is hydrophobic with respect to HEMA and also forms links between polymer chains which limit the swelling of the resultant network.

It has been reported<sup>(68,69)</sup> that the water uptake of pHEMA is relatively insensitive to low degrees of crosslinking with EGDMA, which has been taken to imply that secondary forces were responsible for the cohesion of the hydrogel. These secondary forces have been ascribed to hydrophobic

interactions between either  $\alpha$ -methyl groups or chain backbones<sup>(70)</sup>, hydrogen bonding<sup>(71)</sup> and polar interactions<sup>(72)</sup>. Higher degrees of crosslinking have been shown to lead to reduced water uptake<sup>(61)</sup>. We have prepared gels containing various EGDMA crosslinker concentrations and measured the resultant conductivities.

EGDMA is only the first in a series of oligo (ethylene glycol) dimethacrylates [OED] which have the general structure:



EGDMA

Where  $n$ , the number of ethylene glycol repeat units, regulates the length and flexibility of the crosslink which is formed as a result of the presence of the methacrylate functional groups at either end of the molecule. EGDMA crosslinker contains a single ethylene glycol unit between the methacrylate end groups. The conductivity of samples of varying EGDMA concentration has been investigated.

We have also prepared and measured the conductivity of several copolymers using OED's with  $n > 1$  as crosslinking agents: di-(ethylene glycol) dimethacrylate [DiEGDMA] ( $n=2$ ), tetra-(ethylene glycol) dimethacrylate [TEGDMA] ( $n=4$ ) and poly 400 (ethylene glycol) dimethacrylate [P400] ( $n \approx 9$ ). The name of P400 is based on the average molecular weight of the oligo ethylene glycol chain between methacrylate groups which corresponds to an average value of  $n$  being approximately nine.

Variation of the type of OED used as a crosslinking agent enables a number of parameters to be varied. As the length of the oligo ethylene glycol chain increases, the  $T_g$  of the respective OED homopolymer decreases, with P400 having a  $T_g$  of 268K<sup>(67)</sup>. It has also been noted<sup>(67)</sup> that the increase in

the polarity of the OED's as  $n$  increases, due to the increasing number of ether groups, results in an increase in water sorption with P400 absorbing much more water than EGDMA. The selection of OED as the crosslinking agent thus presents the possibility of being able to vary the hydrophilicity of the copolymer network, and therefore its water absorption properties, and also some of its bulk mechanical properties, such as  $T_g$ .

The relationship between water content and conductivity was investigated for all the copolymer gels produced by recording the AC response of samples subjected to a dehydration regimen.

The effect of temperature on the conductivity of fully hydrated gel electrolytes was also investigated by collecting AC impedance data for gel samples subjected to a standard temperature cycle. The temperature dependence of conductivity in these gel electrolytes will yield a measure of the activation energy of the conductivity and thus reflect the importance of the supporting polymer matrix in the gel electrolyte. PHEMA hydrogels, when cooled to sub-ambient temperatures, are noted for the anomalous freezing behaviour of the water absorbed within the polymer matrix<sup>(57-63)</sup>. The resultant morphological change in the gel should be reflected in its AC impedance response.

Copolymers based on pHEMA were also hydrated in a series of electrolyte solutions of varying concentration to produce ion doped gel electrolytes. The conductivity of polymer electrolytes can be described by the following equation<sup>(73)</sup>:

$$\sigma = \sum_i n_i(z_i e) u_i \quad \text{Eqn. 1.2}$$

where  $n_i$  is the number of charge carriers of type  $i$ ,  $z_i e$  is the net electronic charge on that ion or aggregate and  $u_i$  is its mobility in unit field. From Equation 1.2 it follows that increasing the concentration of the dopant will

result in an increase in conductivity. However, Equation 1.2 does not directly take into account the effect that the nature of the dopant will have on the supporting polymer in the gel electrolyte which in turn influences the structure of the conductive phase, the solvent.

The effect of the addition of electrolytes to pHEMA based hydrogel systems has been studied by swelling<sup>(74,75)</sup>, diffusion<sup>(78,81)</sup>, NMR<sup>(79,80)</sup>, DSC<sup>(78,79)</sup> and dynamic mechanical measurements<sup>(76,77)</sup>. Dusek et al.<sup>(74)</sup> and Refojo<sup>(75)</sup> have studied the influence of salts on the equilibrium swelling of pHEMA hydrogels. The introduction of ions may either improve the conditions for the mixing of the polymer and aqueous phase (salting in) or impair them (salting out). Refojo reported vastly differing water contents depending on the nature of the salt used, ranging from 58% for NaI to 33% for NaCl. These water contents refer to samples hydrated in 0.5M electrolyte solutions. Dusek et al. report that the anion plays a decisive role in determining the equilibrium swelling of pHEMA samples soaked in electrolyte solutions. They found iodides and perchlorates to be typical salting in anions, and fluorides and most chlorides to be typical salting out anions.

Nakamura<sup>(76)</sup> investigated the effect of the addition of NaCl, Na<sub>2</sub>SO<sub>4</sub> and NaI on the monomeric friction coefficient,  $\zeta$ . It was found that the addition of sodium chloride and sulphate resulted in an increase in  $\zeta$ , in direct contrast to the decrease resulting from the addition of sodium iodide. The plasticisation caused by the sodium iodide was attributed to specific ion polymer interactions. Allen et al.<sup>(77)</sup> studied the length contraction of aged pHEMA samples doped with KBr. They found that the magnitude of the contraction when quenched samples were heated through the glass transition decreased with KBr content which is consistent with role of an antiplasticising filler. The interaction of the electrolyte with the polymer is therefore dependent on the nature of the ions.

DSC has been used by Tighe et al.<sup>(78)</sup> and Quinn et al.<sup>(79)</sup> to investigate

the influence of dopants on the structure of water in pHEMA hydrogels. Quinn looked at the influence of saline solutions on pHEMA samples by recording cooling exotherms and melting endotherms. The introduction of NaCl was found to cause a small but significant increase in nonfreezable water which is consistent with the notion that  $\text{Na}^+$  is a structure forming ion. The presence of NaCl also led to a depression of the vitrification temperature. Tighe has recorded melting endotherms of pHEMA samples immersed in a range of potassium salt solutions. It was found that the presence of electrolyte not only altered the equilibrium water content but also the ratio of freezing to non freezing water. The EWC of the samples yielded the following trend:

$$\text{KI} > \text{KCl} > \text{K}_2\text{SO}_4$$

It should be noted that the sample in KI solution had a greater EWC than pHEMA hydrated in water while immersion in KCl and  $\text{K}_2\text{SO}_4$  solutions yielded samples with lower EWC's than pHEMA hydrated in water. The change in ratio of freezing to non-freezing water was even more drastic:

$$\text{KI} \gg \text{KCl} > \text{K}_2\text{SO}_4$$

Similarly, the freezing/non-freezing water ratio for a sample hydrated in water was less than for KI solution and greater than for KCl and  $\text{K}_2\text{SO}_4$  solutions.

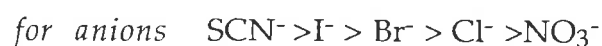
Quinn et al<sup>(79)</sup> have also used  $^1\text{H}$  NMR  $T_2$  measurements to investigate the effect of NaCl on the water present in pHEMA hydrogels. The change in  $T_2$  with respect to temperature reveals the onset of molecular motion and hysteresis associated with temperature cycling, whereas the  $T_2$  component intensity data enable the estimation of the relative amounts of distinguishably different types of water in the hydrogel. It was observed that the mobility achieved in the sample hydrated in water is appreciably greater than for the sample hydrated in saline solution for temperatures below ca. 250K. Another observation was that at 220K the ratio of tightly bound water is greater for the water hydrated sample than for the NaCl laden sample.



Quinn et al. also made  $^{23}\text{Na}$  NMR measurements on ion-doped pHEMA gels. The linewidth of the  $^{23}\text{Na}$  NMR signal is sensitive to environmental changes and is a measure of the interaction, whether through ionic or covalent bonding or a change in the degree of hydration, of the  $\text{Na}^+$  ion with its immediate surrounds. It was found that the linewidths for even the most hydrated samples were appreciably larger than for concentrated aqueous electrolytes of comparable concentration: this was interpreted as evidence that the immediate environment of the  $\text{Na}^+$  ions was affected by the polymer network, even in a heavily hydrated state.

Jhon and coworkers<sup>(80)</sup> have performed  $^{127}\text{I}$  and  $^{39}\text{K}$  NMR studies of water soluble polymers in KI solutions. The broad  $^{127}\text{I}$  linewidths obtained for isotactic pHEMA in KI solution were attributed to specific polymer/ion binding. Jhon suggested that the attractive force between the polarizable iodide anion and the electric dipoles of the polymer could be responsible for the polymer/iodide interaction.  $^{39}\text{K}$  NMR linewidths were relatively invariant with increased polymer concentration, providing evidence that potassium does not directly associate with the isotactic pHEMA in solution. This was further reinforced by the lack of variation in  $^{127}\text{I}$  NMR linewidths measured for polymers in various alkali iodide solutions: NaI, KI, RbI and CsI.

The diffusion of ions through hydrated pHEMA has been studied by Tighe et al.<sup>(78,81)</sup> who found that the nature of the anion exerted greater influence on the rate of permeation of the electrolyte than the cation. For membranes of a given structure anion permeation rates followed the Hoffmeister series:



It is obvious from all these results that the introduction of ions into pHEMA hydrogels further complicates an already complex system as ion/ion, ion/water and ion/polymer interactions will occur and compete with one

another. The addition of ions will alter the conductivity of the gel electrolyte, while the degree of alteration will be dependent on both the concentration and nature of the dopant used.

Initial investigations in this work focussed on HEMA based copolymers immersed in KBr solution of varying concentration. KBr was chosen as the electrolyte as it has been shown<sup>(81)</sup> to have a minimal effect on the equilibrium water content of pHEMA. The effect of varying the nature of the dopant employed was investigated for pHEMA gel electrolytes doped with a selection of alkali halides and other ions of interest. These samples were also subjected to dehydration and variable temperature experiments.

Physical characterization of the gel electrolytes studied was carried out using a number of experimental techniques. The effect of diluent and dopant addition on the polymer network was monitored by thermal mechanical analysis. The dimensional changes of samples were measured over a range of temperatures, yielding expansion coefficients. Differential scanning calorimetry was employed to investigate the nature of the water phase in the gel electrolytes and the effect of crosslinker and dopant on the structuring of the water phase. Positron annihilation spectroscopy was used to investigate the distribution of free volume.

The experimental apparatus and techniques employed in this work will be discussed in the next chapter. The bulk of the research undertaken in this project has been to investigate the variation in conductivity of pHEMA gel electrolytes. Changes in conductivity resulting from variation in crosslinking, that is alteration of both the amount and the nature of the crosslinking agent employed, water content and temperature have been investigated. In Chapter 3 the conductivity of undoped pHEMA hydrogels is discussed. The introduction of electrolytes to pHEMA hydrogels increased their conductivity. Chapter 4 deals primarily with the variation of conductivity in KBr doped pHEMA gel electrolytes subjected to similar

variations as the undoped samples in Chapter 3. The effect of the variation in the nature of the dopant on the conductivity is also investigated in Chapter 4. The results gained from the physical characterization of the gel electrolytes will be discussed in Chapter 5. The conclusions from this work will be addressed in Chapter 6 with the aim of providing a more complete understanding of the conductivity of the gel electrolytes investigated.

## CHAPTER TWO

### *Experimental Techniques.*

#### 2.1 Sample Source

HEMA was obtained from Mitsubishi Chemicals and contained 50 ppm hydroquinone monomethyl ether as inhibitor. NMR measurements<sup>(1)</sup> indicated the presence of 0.3 mol% EGDMA in the HEMA monomer. EGDMA, DiEGDMA, TEGDMA and P400 were obtained from Polyscience. The peroxide initiator used was t-butyl per-2-ethyl hexanoate (TBO) and was supplied by Interlox (Australia).



TBO

All electrolyte salts for soaking solutions were of analytical grade and were obtained from BDH. All chemicals were used as received without further purification.

#### 2.2 Polymer Preparation

All monomers were dried over anhydrous magnesium sulphate and then stored over activated 3Å molecular sieves at -15°C until required. The initiator was used at 0.2% v/v concentration in the monomer. To prevent inhibition of the polymerisation by oxygen, high purity dry nitrogen was bubbled through the monomer for approximately 15 minutes prior to casting. Casting was performed between two glass sheets separated by aluminium dividers with a silastic tubing (Dow Corning) gasket in the manner described by

Cowperthwaite<sup>(2)</sup>. Two methods were employed to prevent the strong adhesion of pHEMA and its copolymers to the curing mould: the surface of the glass sheets were either covered with teflon sheeting or treated with trimethylchlorosilane (TMCS) prior to casting. The TMCS reacts with the silanol groups on the glass surface precluding any interaction with the hydroxyl group of the HEMA repeat unit. These procedures enabled easy removal of the casts from their moulds.

HEMA was cured at 60°C until gelation occurred and the temperature was then increased in 10°C increments per hour until ultimately being held at 110°C for 12 hours. Curing above these temperatures for any extended period of time led to degradation of the sample indicated by the presence of brown discolouration. The casts were cooled slowly to ambient temperature over a few hours to avoid fracturing. The resultant casts were insoluble in water due to the presence of a three dimensional network caused by the presence of EGDMA in the monomer. All polymer casts produced were transparent and ca. 2mm thick. Similar cure profiles were employed for copolymers of HEMA with the oligo-(ethylene glycol) dimethacrylates except at higher concentrations of EGDMA and DiEGDMA. For these samples a further post cure was required at 120°C for one hour in order to ensure that maximum possible cure was attained.

Full sample cure was assumed when no detectable polymerization exotherm was measured by differential scanning calorimetry (DSC). It should be noted from previous work<sup>(3-7)</sup> that polymerized EGDMA, DiEGDMA and TEGDMA can have residual unsaturation at full cure in the form of trapped monomer and unreacted pendant double bonds that cannot be measured by DSC; this is unlikely to be the case with the relatively low crosslinker concentrations used in the HEMA copolymers in this work.

### 2.3 Sample Preparation.

Polymer sheets were placed in deionised water overnight to soften and facilitate cutting of the appropriately sized discs for conductivity studies. Sample discs were in a vacuum oven at 50 °C until a constant minimum weight was reached. The dry discs were immersed in approximately 50ml of either deionised water or dopant solution of the appropriate concentration in the range 0.10 to 1.0 M. Samples were left to equilibrate for 4-6 weeks until a constant maximum weight was achieved. All weights were measured on a Mettler AE166 balance with a reproducibility of  $\pm 0.2\text{mg}$ . Excess surface moisture was removed with soft tissue prior to weighing.

Water absorbed into hydrogel samples can be defined in a number of ways. The method that will be used in this work expresses the weight of water absorbed by the sample as a function of its total wet weight. The Equilibrium Water Content (EWC) is defined by the following equation<sup>(8)</sup>:

$$\text{EWC} = \frac{W_w - W_d}{W_d} \times 100 \% \quad \text{Eqn. 2.1}$$

$W_w$  is the weight of the wet polymer and  $W_d$  is the weight of the dry polymer. During dehydration experiments, initial measurements were made at full EWC whereupon samples were removed from their soaking solutions and allowed to dry for about 5 minutes. These samples had excess surface moisture removed with soft tissue before being placed in resealable polyethylene bags, which were kept at 25°C, to ensure the re-equilibration of remaining water in the polymer over 24 hours. The conductivity of the samples was measured and the samples were again partially dehydrated and allowed to re-equilibrate. This procedure was repeated until an EWC of 5% was attained and then the samples were dried in a vacuum oven at 50°C. All conductivity measurements were made at 25°C during the dehydration process.

Samples for TMA measurements at discrete EWC were fully hydrated in the appropriate dopant solution and then dried to constant weight in a 50°C vacuum oven. To reach the desired EWC, the dry samples were placed in a series of humid atmospheres achieved through the presence of various saturated salt solutions (Table 2.1) in sealed containers held at constant temperature (25°C).

**Table 2.1**

List of salts used to obtain different relative humidities at 25°C.<sup>(9)</sup>

Salt	%R.H.
NaOH	6
MgCl <sub>2</sub>	33
NH <sub>4</sub> Cl	79
PbNO <sub>3</sub>	98

#### 2.4 A.C. Impedance Measurements.

All impedance measurements were made using a Hewlett Packard HP4284 LCR bridge utilising the full 10Hz - 1MHz frequency range. The bridge was interfaced with an IBM compatible personal computer to facilitate repetition of data collection and manipulation of data. The recorded data was fitted by hand as manipulation with the available software proved unsuccessful. For all measurements the voltage applied was kept under 1 volt to minimise heat generation and any subsequent change in the equilibrium water content. Two separate cells were used to house the sample depending on the nature of the experiment performed. Short leads (<30cm) were used for all measurements to avoid impedance effects.

For conductivity measurements at constant temperature (25°C) the cell (Fig.2.4.1) consisted of two circular stainless steel electrodes mounted on a brass stand. Their separation was controlled by a micrometer spindle so as to ensure

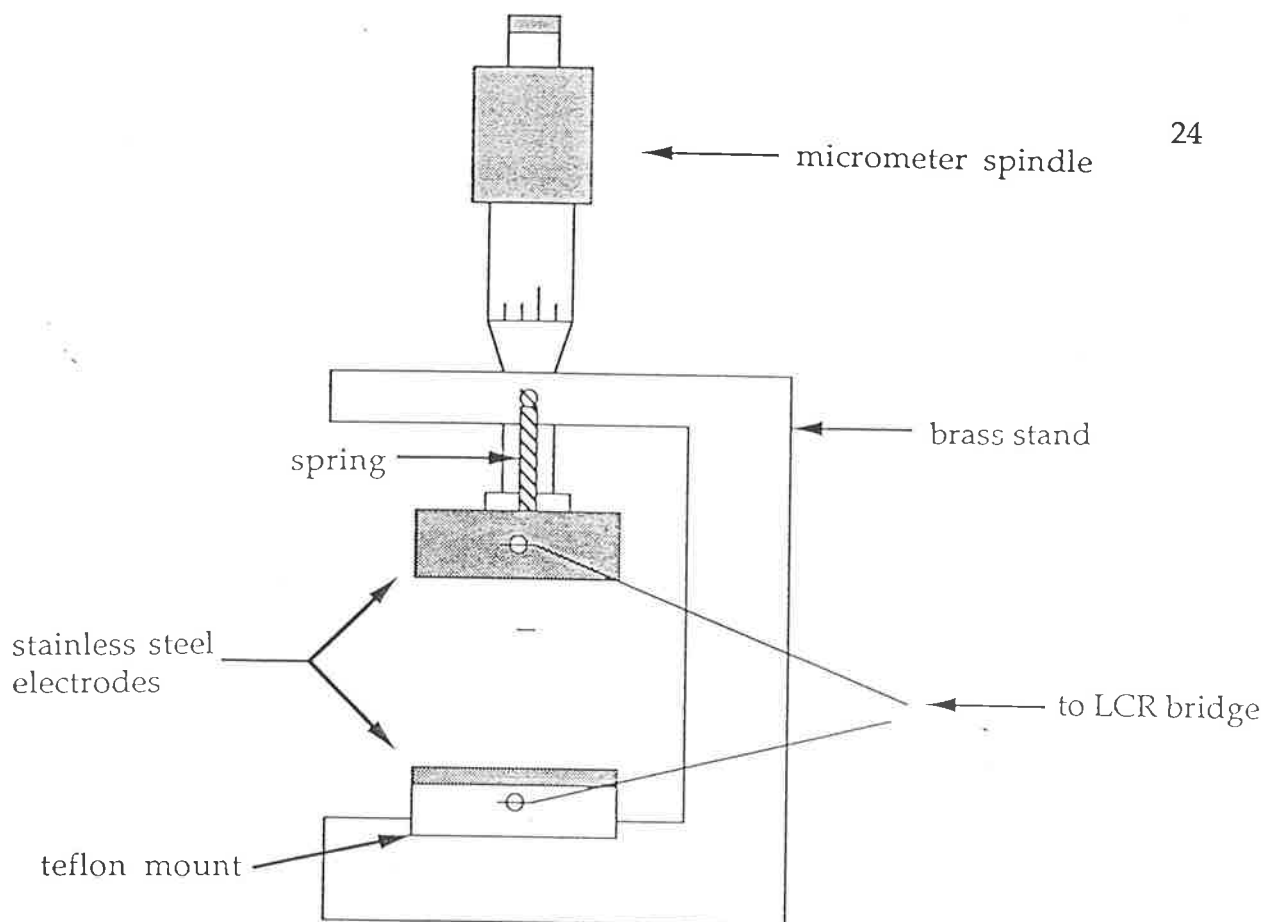


Figure 2.4.1

Experimental cell for conductivity measurements at constant temperature.

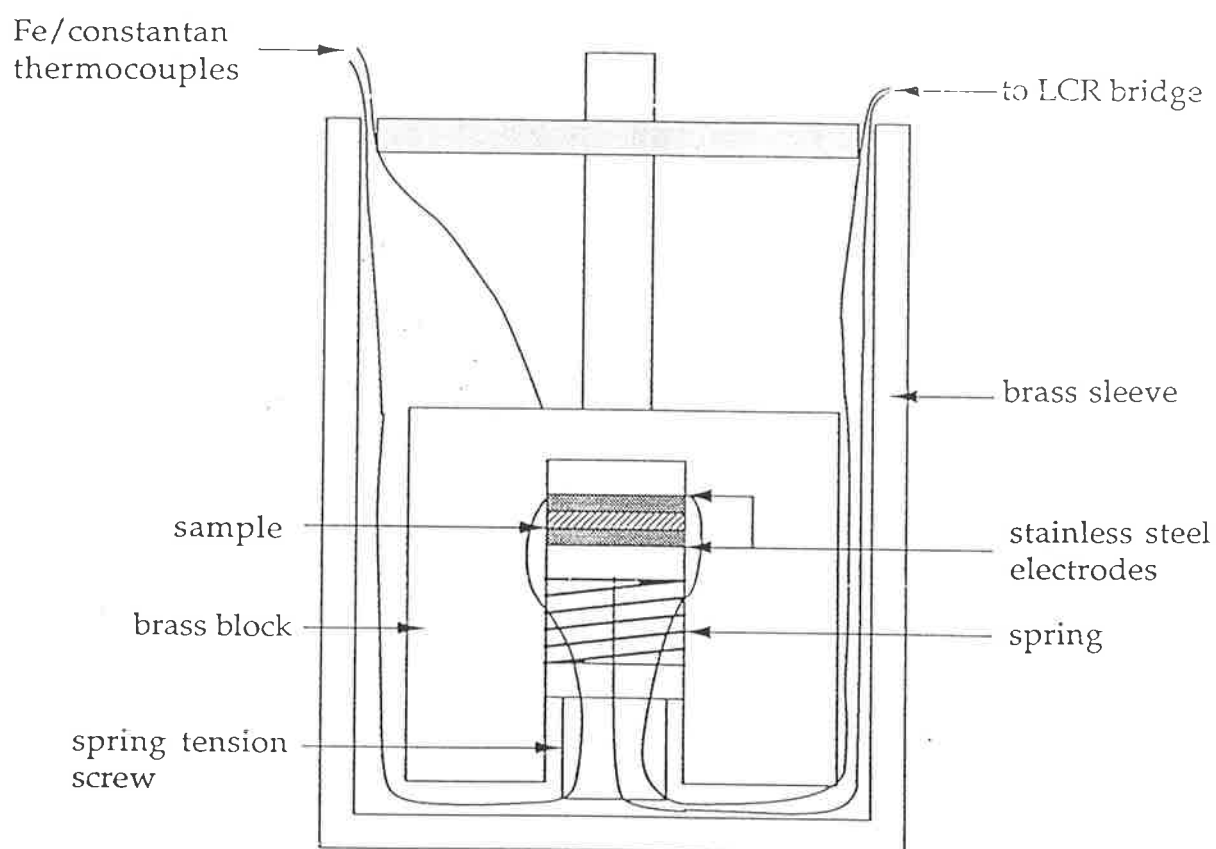


Figure 2.4.2

Experimental cell for conductivity measurements at variable temperature.



good electrical contact. Constant temperature was achieved by placing the cell in a brass sleeve which in turn was immersed in a constant temperature water bath ( $25.0 \pm 0.1$  °C).

For experiments which involved temperature cycling the cell (Fig.2.4.2) consisted of two circular stainless steel electrodes mounted in teflon and embedded within a large brass block. The lower electrode was spring loaded to ensure good electrical contact was maintained despite variation in sample thickness with change in temperature. Fe/constantan thermocouples were used to monitor the temperature at the electrodes and on the external surface of the brass block.

An average cooling rate of  $0.22$  °C/min was achieved by placing the cell in a brass sleeve which was in turn placed in a  $\text{MgCl}_2$ /ice bath in a freezer. This cooling rate was used to minimise the change in temperature during data collection at discrete temperatures. On achieving the required minimum temperature, the cell was removed from the sleeve and allowed to warm to ambient temperature. This resulted in an average heating rate of  $0.44$ °C/min.

## 2.5 AC Impedance Spectroscopy

A number of articles<sup>(10-12)</sup> have been published describing the application of AC impedance measurements to solid electrolytes, with Bruce<sup>(12)</sup> relating the technique to the specific needs of electrical measurements on polymer electrolytes. AC techniques have the advantage of avoiding polarisation of the sample being studied.

In an AC impedance experiment a sinusoidal voltage is applied to a cell and the resulting sinusoidal current measured. Such experiments differ from DC experiments in that it is necessary not only to observe the ratio of the applied voltage to the resultant current, i.e ohmic resistance, but also to measure the ratio of the maxima of the sinusoidal voltage and current and also the phase difference,  $\theta$ .(Fig.2.5.1) The AC impedance, analogous to resistance in

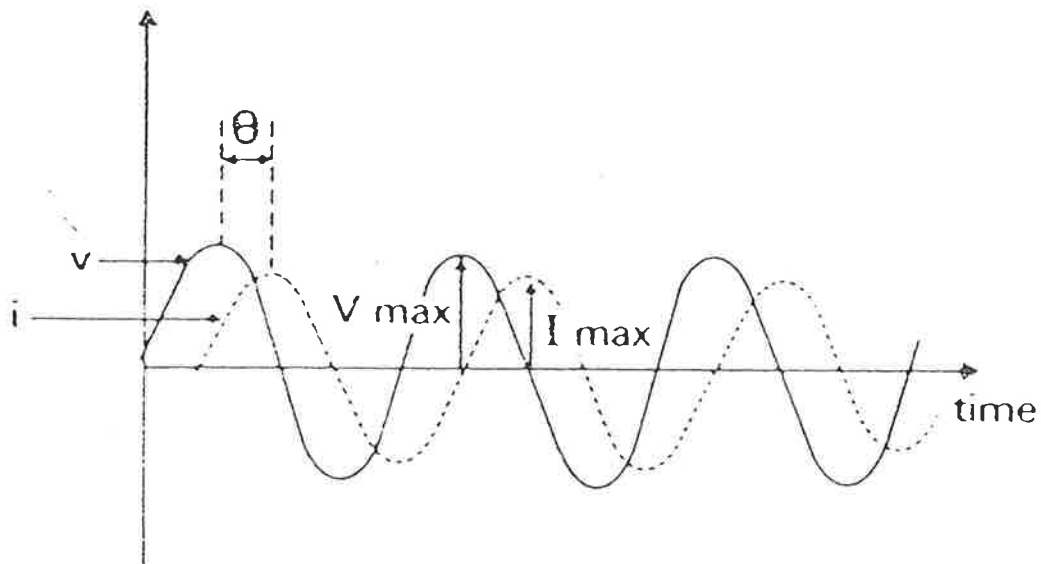


Figure 2.5.1

A representation of the sinusoidal voltage and current, at a given frequency, associated with a cell;  $v$ =voltage,  $i$ =current,  $\theta$ =phase difference between voltage and current. Generally the current is not in phase with the voltage. (Reproduced from (12).)

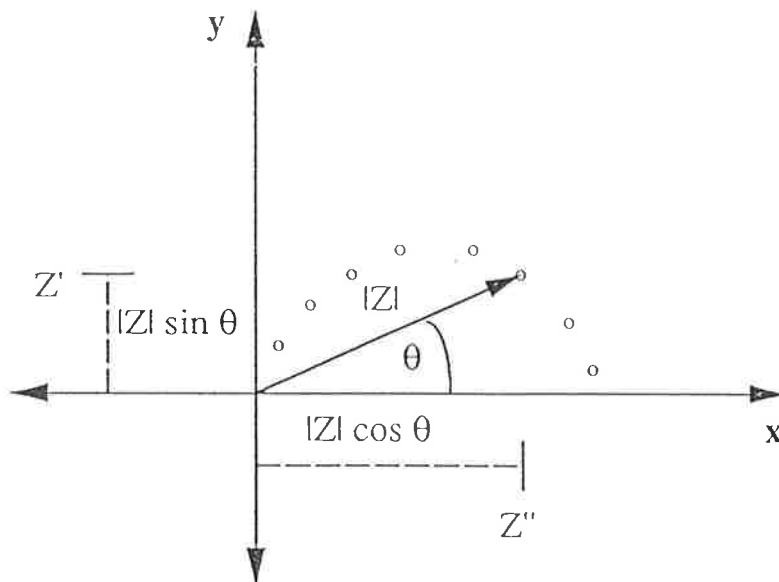


Figure 2.5.2

A representation of the impedance,  $Z$ , on an Argand diagram.  $Z'$  and  $Z''$  are the real and imaginary components of the complex impedance,  $Z = Z' - jZ''$ .

DC systems, is therefore a vector quantity with magnitude and phase. If we define the impedance as  $Z$ , then the impedance vector can be separated into  $x$  and  $y$  components where:

$$x = |Z| \cos\theta \quad \text{Eqn. 2.5.1}$$

$$y = |Z| \sin\theta \quad \text{Eqn. 2.5.2}$$

The term complex impedance is often used to describe impedance as its representation on a vector diagram is analogous to the representation of a complex number on an argand diagram (Fig. 2.5.2). Thus we can think in terms of complex numbers where:

$$Z^* = Z' - jZ'' \quad \text{Eqn. 2.5.3}$$

$$Z^* = \text{complex impedance}$$

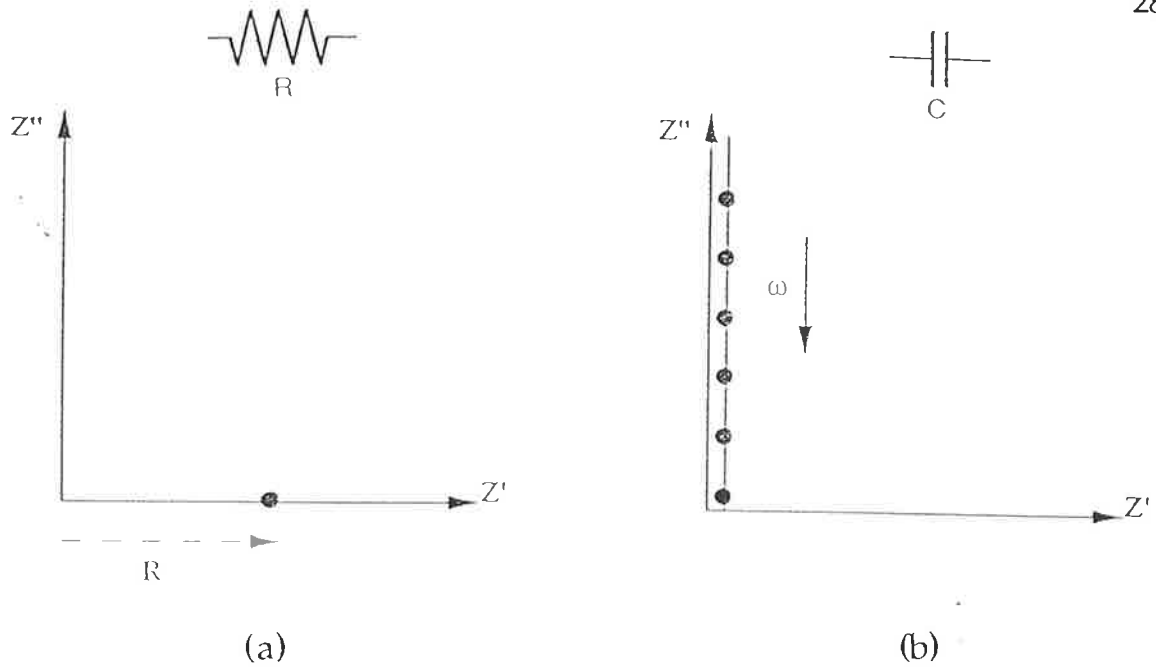
$$j = \sqrt{-1}$$

(Note:  $j$  is used rather than  $i$  to represent  $\sqrt{-1}$  so as to avoid confusion with the frequently used symbol for current.)<sup>(12)</sup>

The experiments employed in this thesis required the measurement of the complex impedance as a function of the frequency of the constant input voltage and the presentation of the results on a complex impedance plot. Various outcomes can be ascribed to representing differing equivalent circuits. The responses of simple components can be described as follows:

Resistor: the voltage applied to a resistor is in phase with the resultant current flowing through it, i.e.  $\theta=0$  and thus  $|Z|=R$ ,  $R$ =resistance. It is represented by a point  $R$  units along the real or  $x$ -axis of a complex impedance plot. (Fig.2.5.3(a))

Capacitor: the voltage applied to a capacitor lags behind the resultant current by  $90^\circ$ , i.e.  $\theta=-\pi/2$  and the magnitude of the impedance is frequency dependent.  $|Z|=1/\omega C$ ,  $C$ =capacitance. The impedance of a capacitor defines a vertical spike



(Note: the vertical spike in (b) should coincide with the imaginary axis but has been displaced for clarity)

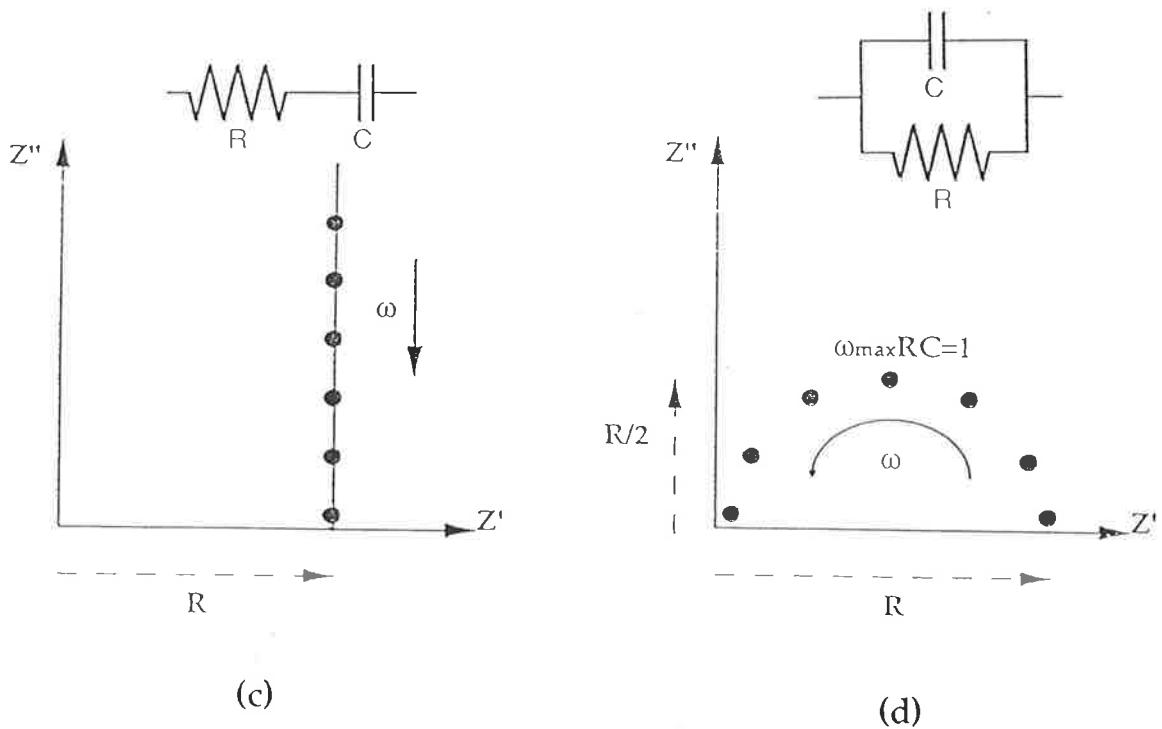


Figure 2.5.3

Complex impedance plots for (a) a resistor,  $R$ , (b) a capacitor,  $C$ , (c) a series combination of a resistor,  $R$ , and a capacitor,  $C$ , and (d) a parallel combination of a resistor,  $R$ , and a capacitor,  $C$ . Angular frequency,  $\omega = 2\pi f$  where  $f$  is the frequency of the applied voltage in hertz.

that coincides with the imaginary or y-axis of a complex impedance plot (Fig.2.5.3(b)). It is noteworthy that it is conventional for electrical engineers to regard the phase angle of a capacitor to be negative and thus the complex impedance becomes  $-i/\omega C$ , however electrochemical convention is to plot negative impedances above the real axis<sup>(12)</sup>.

In general, an equivalent circuit, a combination of such component impedance elements, is needed to map the more complex behaviour of an electrolyte. For example, it can be shown <sup>(12)</sup> that a series combination of a resistor and a capacitor will result in a vertical line that intersects the x axis of a complex impedance plot a distance from the origin equivalent to the magnitude of the resistance (Fig.2.5.3(c)). If these components are in parallel then the plot will be a semi-circle passing through the origin and the x axis a distance from the origin equivalent to the magnitude of the resistance.(Fig. 2.5.3(d)) At the maximum point in the y axis orientation of the plot,  $(R/2)$ ,  $\omega_{\max}RC=1$  where  $\omega = 2\pi f$ ,  $f$  being the frequency at which the measurement was made.

The AC impedance spectroscopic responses of real systems are often more complex than these examples but can be explained by the formation of equivalent circuits based on simple components<sup>(10-12)</sup>.

## 2.6 Differential Scanning Calorimetry.

In Differential Scanning Calorimetry (DSC) thermal transitions are measured by the continual monitoring of the differential heat flow from a sample with respect to a reference over a predetermined temperature range. The calorimeter balances the flow of thermal energy from the sample by the addition or subtraction, with respect to the reference, of an equivalent amount of electrical energy and thus a signal directly equivalent to the thermal transitions occurring in the polymer sample is provided by the calorimeter. All DSC measurements were made using a Perkin Elmer DSC II fitted with a dry

box with the output voltage monitored using the MacLab™ system. For above ambient temperature measurements high purity dry nitrogen was used as the purge gas and the instrument was calibrated with lead ( $\Delta H_f = 5.5$  cal/g,  $t_m = 600.65$  K) and indium ( $\Delta H_f = 6.8$  cal/g,  $t_m = 429.78$  K). For sub ambient temperature measurements water ( $t_m = 273.15$  K) and n-octane ( $t_m = 216.14$  K) were used as the temperature calibration standards. Liquid nitrogen was the coolant and helium the purge gas. All calibrations were determined at the same heating rate as that employed for samples (10 K/min).

### 2.6.1 Measurement of Freezing Water

Hydrated polymer samples were first dried with soft tissue to remove any surface water and then enclosed in volatile-sample pans (P.E. No. 219-0062) to minimise any water loss during measurement. Comparison of the area under melting endotherms for gel samples with that produced by a known weight of deionised water enabled the calculation of the amount of freezing water in the hydrogels.

## 2.7 Thermomechanical Analyser.

The Mettler TMA 4000 thermomechanical analysis system (TMA) (Figure 2.7.1) enabled the thickness of a polymer sample (ca. 5x5x2 mm) to be measured as a function of temperature. A static load of 0.1N was necessary to maintain probe contact.

Two types of measurements were carried out for dry and hydrated samples. Dry samples were heated rapidly to 430K, i.e.  $T > T_g$ , and then cooled slowly at 2K/min to remove any residual stresses within the polymer structure. The sample was then again heated at 2K/min to 430K and its dimensional changes monitored. Hydrated samples were cooled at 2K/min to 215K and subsequently heated at 2K/min to 295K whilst dimensional changes were recorded. Liquid nitrogen was used as the coolant for sub-ambient

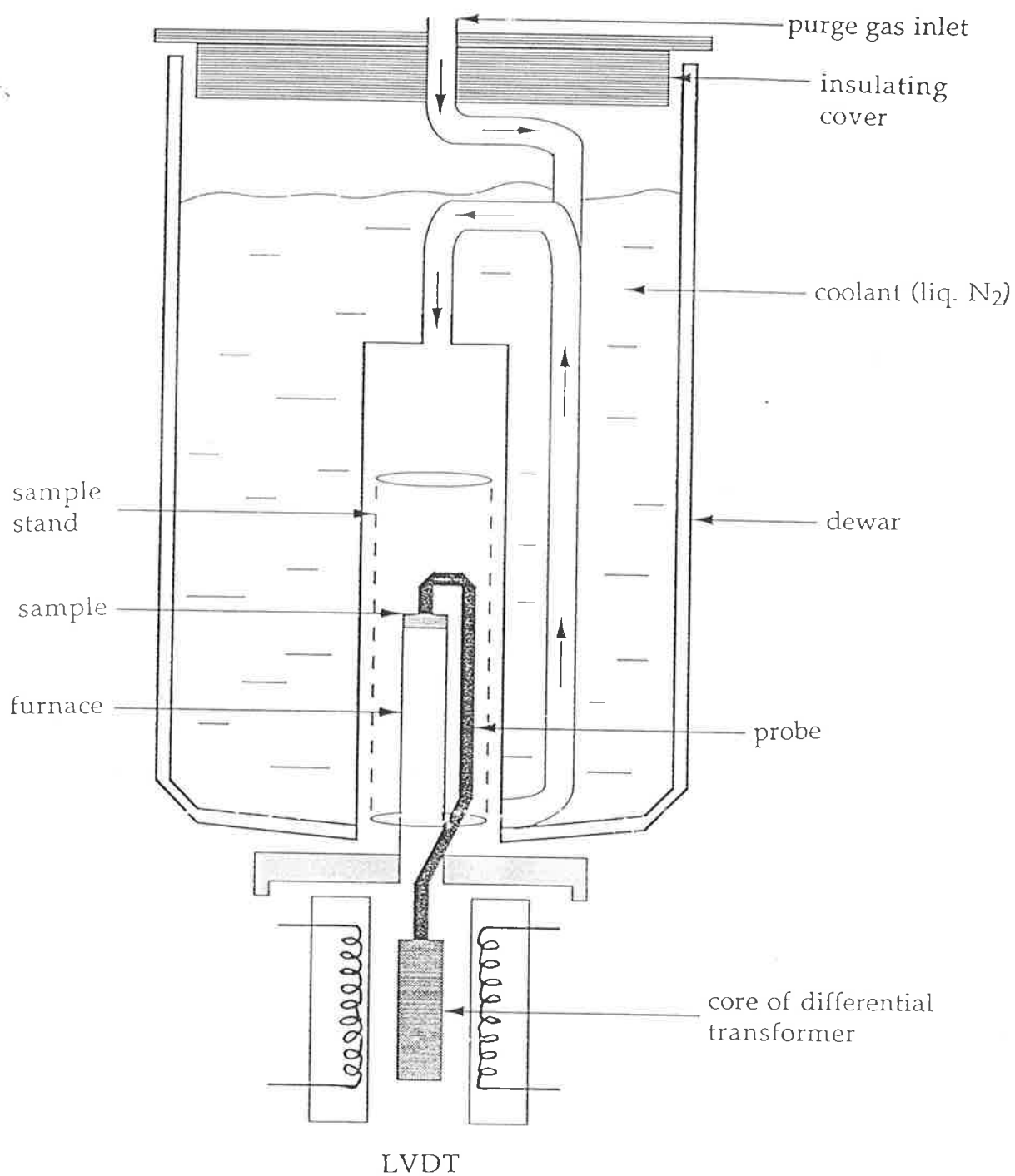


Figure 2.7.1

A schematic representation of a thermomechanical analyser set up for sub-ambient measurements.

measurements. Fully hydrated samples were covered with a thin glass microscope slide prior to the lowering of the probe to prevent the probe indenting the sample surface. To minimise water loss, hydrated samples were not heated above ambient temperature. All samples were weighed prior to and after TMA measurements to monitor weight loss.

## 2.8 Positron Annihilation Lifetime Spectroscopy.

Positron Annihilation Lifetime Spectrometry (PALS) is a technique which provides an indication of the free volume of a polymer and therefore provides an insight into the mobility of the 2-hydroxyethyl methacrylate polymer network. There are several sources<sup>(14-17)</sup> in the literature for information on this technique, both conceptual and technical.

### 2.8.1 Theory.

A positron is the antiparticle of an electron, having identical properties with the exception that the charge on the positron is positive. Positrons are emitted as a result of the natural decay of various radio-active isotopes and may exist in condensed matter in several forms. Immediate (time < 3ps) energy loss is associated with the injection of a positron into a solid via inelastic and elastic collisions with the polymer network and phonon interactions. During this process, positrons may either become bound to electrons to form an unstable atom like entity, known as positronium (Ps), or remain in free, singular positron form. After this energy loss has taken place, positrons localize to defects and or free volume within the solid and subsequently annihilate with neighbouring valence electrons.

Positronium exists in two states which are defined as a result of the spin states of the bound positron/electron entity. Para-Positronium (pPs), the singlet state, results from the positron and the electron exhibiting antiparallel spins, whereas ortho-Positronium (oPs) results from the positron and the electron



exhibiting parallel spins. pPs decays by a self annihilation mechanism with a short lifetime (0.125ns). oPs, with a much longer lifetime, decays by the pickoff process; the positron annihilates with an electron to which it is not bound. PALS data result in a spectra containing 3 decaying exponentials which can be ascribed to the three different annihilation mechanisms taking place in the sample. The short lifetime positrons (0.1 - 0.3ns) are attributed to pPs annihilations. Annihilations of free positrons lead to intermediate lifetimes (0.5 - 0.8 ns), and the third or long lifetime (1 - 5 ns) component of the spectrum is ascribed to pickoff annihilations of oPs. A flow chart depicting positron formation and annihilation is given in Figure 2.8.1.

The lifetime of positron species in molecular solids is dependent on the inverse of the electron density at the annihilation site. Consequently, a large site with a low mean electron density will result in a long lifetime, whereas a smaller annihilation site having a higher mean electron density will cause the positron to annihilate with a shorter lifetime. PALS measures the relative number ( $I$ ) and the lifetime ( $\tau$ ) of positron annihilations. Spectra are the sum of three separate exponential decays where:

$$Y_t = Ae^{-\alpha t} + Be^{-\beta t} + Ce^{-\gamma t} + \text{background.}$$

Where  $Y_t$  is the number of positrons annihilating at time  $t$ .  $\alpha, \beta, \gamma$  are the decay rates (slopes) for the three lifetime components  $\tau_1, \tau_2, \tau_3$ . ( $\tau_1=1/\alpha, \tau_2=1/\beta, \tau_3=1/\gamma$ ). The relative number of positrons ( $I_1, I_2, I_3$ ) giving rise to each lifetime component is determined by the area under the respective linear decay curve. The numerical notation is used to differentiate the data relevant to annihilations of a particular type. The subscripts 1,2 and 3 refer to pPs decay, free positron decay and oPs decay respectively. A typical PALS spectrum is shown in Figure 2.8.2.

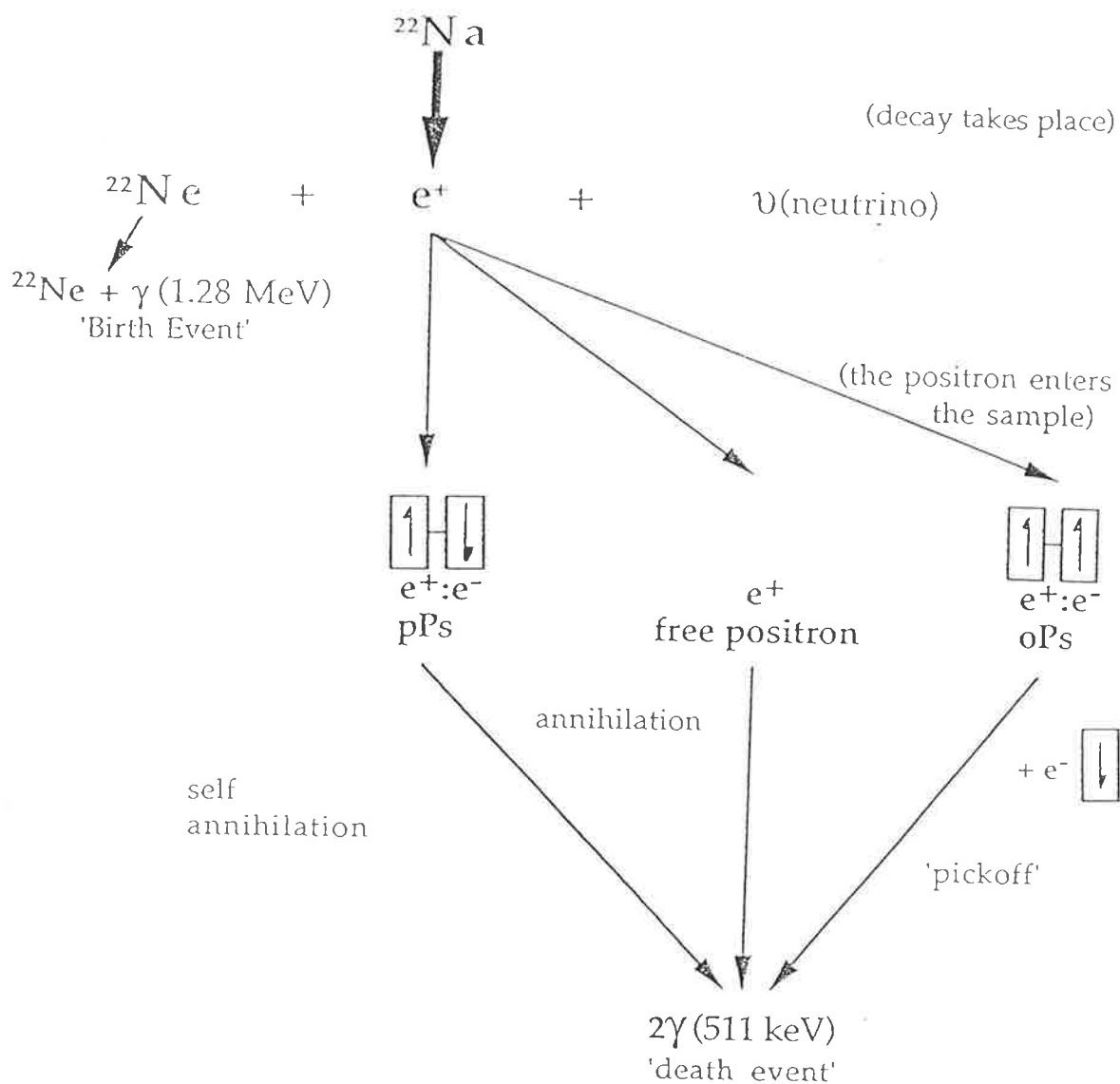


Figure 2.8.1

A flow chart of positron formation and annihilation in PALS

Given that positron decay is dependent on electron density and free volume within a polymer will be reflected by low electron density, it follows that PALS should be useful as a technique to investigate free volume. Brandt et al.<sup>(13)</sup> have shown that, in polymeric solids, oPs pickoff annihilations occur in free volume cavities. This study reports data recorded for  $\tau_3$  and  $I_3$ , the mean lifetime and relative intensity of oPs pickoff annihilations.

### 2.7.2 Experimental.

PALS data is collected by calculating the time between the emission of a positron from the radioactive source, characterized by the emission of a 1.28MeV  $\gamma$ -ray, and the annihilation of the positron in the solid sample, which is accompanied by the emission of twin 511 keV  $\gamma$ -rays. These two events are sometimes referred to as the birth and death events. A schematic representation of a positron annihilation lifetime spectrophotometer is given in Figure 2.8.3.

The PALS system used in this study was a thermally stabilized Batelle automated fast-fast coincidence system with a  $^{22}\text{Na}$  resolution of 250ps. Spectra were collected at 22°C utilising a  $^{22}\text{Na}$  source (35 $\mu\text{Ci}$ ) which had been heat sealed between two teflon coated kapton sheets, the teflon coating facing inwards. Data quoted are for 3 to 8 spectra of 30000 counts with collection time varying between ninety minutes and seven hours, depending on the experimental conditions. Spectra were analysed using the program PFPOSIT<sup>(18)</sup>.

Spectra were recorded for hydrogel samples and some solutions. For gel samples, the source was sandwiched between two identical samples of the gel after surface moisture of the samples had been removed by blotting with filter paper. The sandwich of source and hydrogel samples was placed in a partially evacuated polyethylene bag, in order to prevent moisture loss to the atmosphere, before being placed between the detectors.

For solutions, the source was placed in a 35mm slide frame which was then placed in a polyethylene bag. This bag was immersed in the solution under investigation in a specially prepared sample holder situated between the detectors. The sample holder was designed to force the bag to conform to rectangular geometry and thus maintain an even and constant thickness of solution between the source and detector.

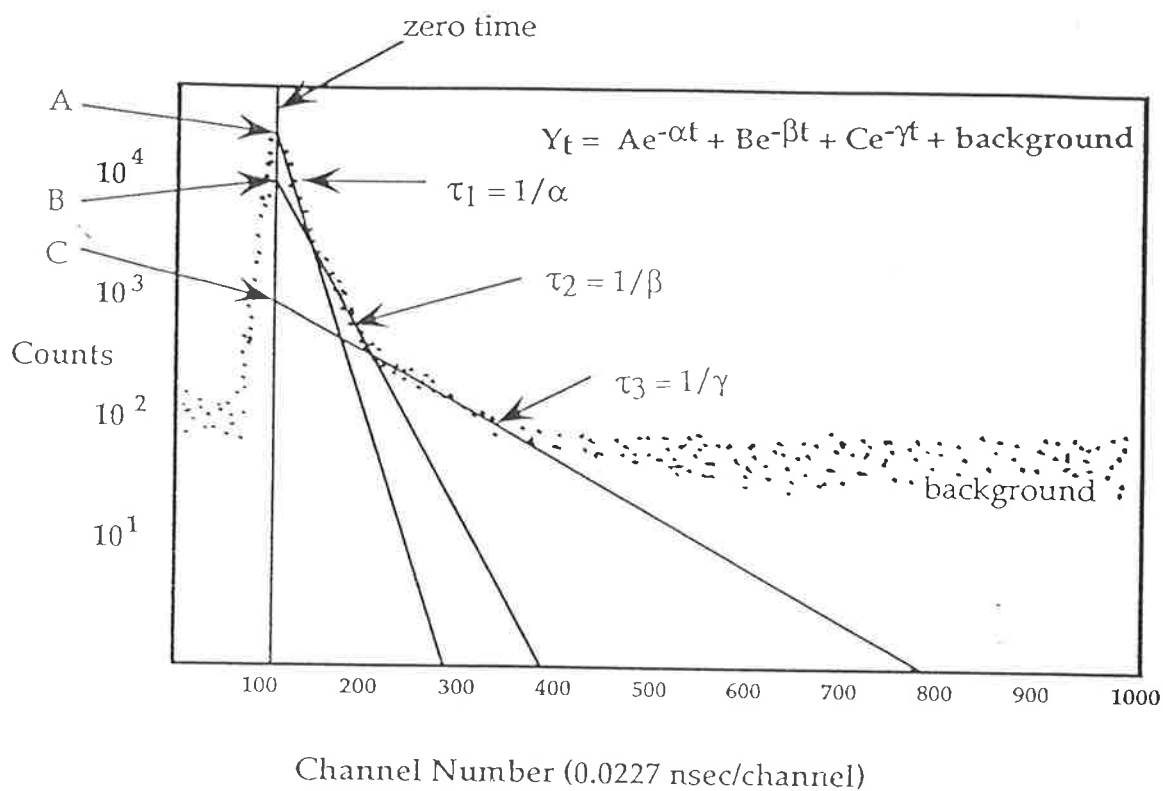


Figure 2.8.2  
A typical PALS spectrum.

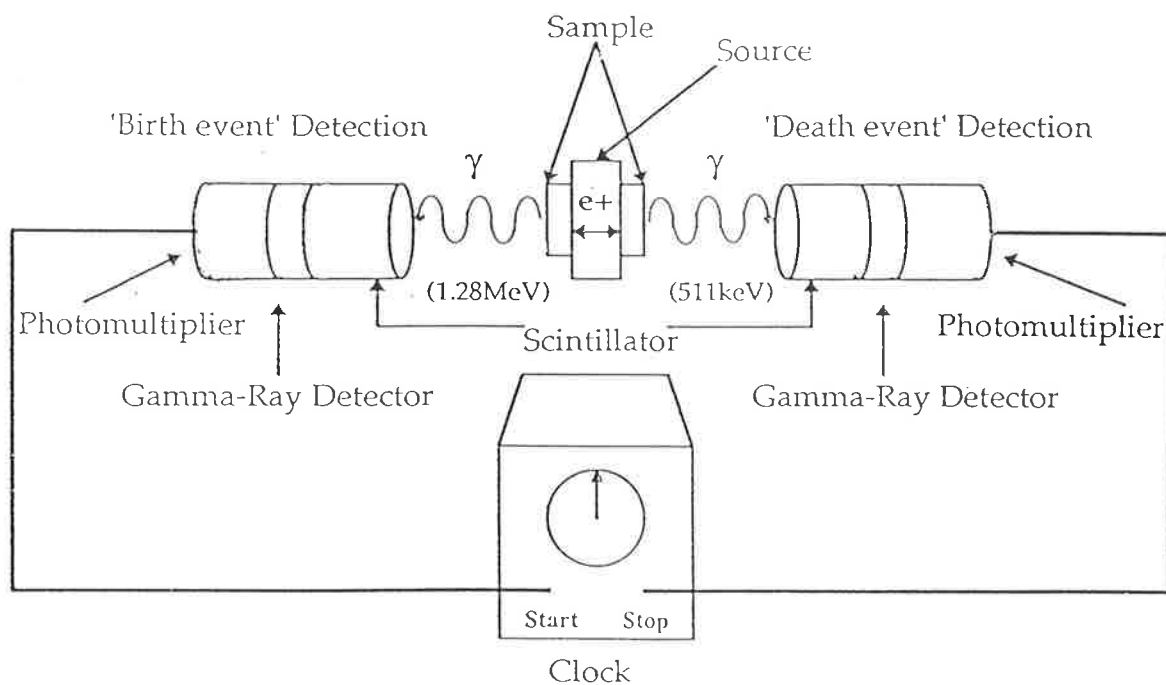


Figure 2.8.3  
A schematic representation of a PALS spectrophotometer.

## CHAPTER THREE

### *The AC Conductivity of pHEMA*

#### 3.1 Introduction

Initially in this work the conductivity of fully hydrated pHEMA was studied at 25°C by AC impedance spectroscopy. The properties of hydrogels can be changed by the variation of crosslinking, that is the amount and nature of the crosslinking agent employed, water content and temperature; changes in conductivity behaviour resulting from such variation have been investigated.

Previously, the specific resistance of membranes based on pHEMA had been studied by Vacik and Kopecek<sup>(1)</sup>. Dielectric analyses of this system have been carried out by M<sup>c</sup>Brierty et al.<sup>(2)</sup> and Pathmanathan and Johari<sup>(3)</sup>. The latter study yielded an Arrhenian DC conductivity relationship that was determined from the frequency-independent region of their conductivity spectra. The relationship can be described by the following equation:

$$\sigma_0 = \sigma_{0,0} \exp(-E_\sigma/RT) \quad (\text{Eqn. 3.1})$$

where  $\sigma_{0,0} = 0.6485 \text{ S.m}^{-1}$

$$E_\sigma = 27.8 \text{ kJ.mol}^{-1}$$

The DC conductivity of pHEMA (EWC= 38.6%, T= 25°C) calculated from this relationship is  $9.2 \times 10^{-4} \text{ S.cm}^{-1}$ .

Lee et al.<sup>(4)</sup> have measured AC conductivities at a frequency of one kilohertz for pHEMA samples over a range of water contents and found the conductivity of pHEMA, EWC=40%, to be ca.  $3.5 \times 10^{-5} \text{ S.cm}^{-1}$  at 25°C. In this work variable frequency measurements have been employed to elucidate

morphological information from the AC impedance response.

### 3.2 The AC Impedance Spectrum

The complex impedance of a fully hydrated pHEMA sample was measured at twenty-one frequencies over the range 10Hz to 1MHz. It should be noted that information gained from impedance spectra is dependent on the model chosen to rationalise the data collected and this can lead to ambiguity in some systems as discussed by Orazem et al.<sup>(7)</sup>. However, it can be seen from the complex impedance plot recorded for a fully hydrated pHEMA sample (Fig. 3.1) that the data gained is typical of the AC response expected for a real polymer electrolyte/blocking electrode experiment (Fig. 3.2) as described by Gray<sup>(5)</sup>. For such a system, an equivalent circuit of a capacitor in series with a parallel combination of a resistor and a capacitor is usually adopted as a model of the observed AC impedance behaviour. The series capacitor is indicative of the double layer that forms at the sample/electrode interfaces. The parallel combination of resistor and capacitor is representative of the motion of charge carriers through the hydrogel. Owen<sup>(6)</sup> attributes this capacitance to vibrating charge carriers that are trapped in potential wells and lead to an out of phase contribution to the resulting current flow.

It should be noted that the semicircular portion of the locus at high frequency is slightly flattened and thus non-ideal. Non-ideal behaviour of this nature has been attributed previously to the inhomogeneity of the conducting phase of the electrolyte<sup>(5)</sup>.

If we define  $\phi$ , where:

$$\phi = \frac{Z'^*}{Z''^*} \quad (\text{Eqn. 3.2})$$

given  $Z'^*$  is the real impedance at the non-zero intersection of the locus and  $Z''^*$  is the imaginary impedance at the highest point of the semi-circular

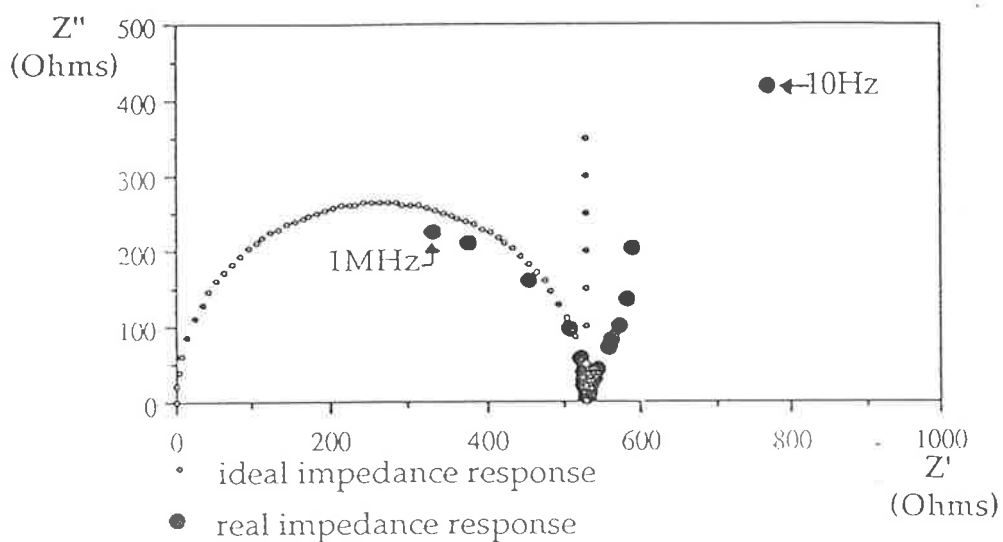


Figure 3.1

The anticipated ideal complex impedance plot and the experimentally recorded complex impedance plot for pHEMA (EWC=40.4%) measured with blocking electrodes and at 25°C.

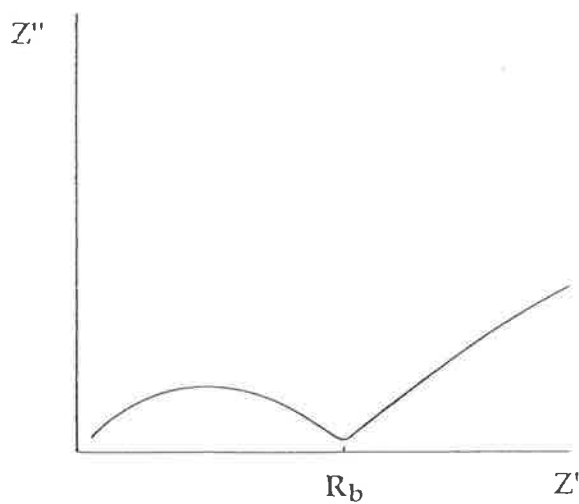


Figure 3.2

A typical complex impedance plot for a real, polymer electrolyte/ blocking electrode cell where  $R_b$  is the bulk resistance of the sample. Reproduced from [5].



portion of the complex impedance plot, then  $\phi$  should give an indication of the measure of non-ideality (i.e.  $\phi = 2$  for a regular semi-circle). A value of  $\phi = 2.07 \pm 0.02$  was obtained for the complex impedance plot for fully hydrated pHEMA (Fig.3.1). This slight deviation from ideality suggests that the water phase is almost homogeneous with respect to its conductive properties.

The low frequency spur is attributed to interfacial capacitance at the electrode/polymer interface and it is suggested<sup>(8)</sup> that its deviation from the vertical may be due to a number of physical properties such as surface roughness at the interface or incomplete blocking by the electrode.

The water in hydrated pHEMA provides the charge carriers and the mobile phase within the system. pHEMA lacks ionising functionalities in its repeat unit to contribute significantly to the conductivity of the polymer/water system. This is reflected by the pH of the water present in pHEMA at full hydration (i.e. pH=6)<sup>(9)</sup>.

The structure of water within hydrogels is not fully understood and has been the subject of many studies yielding several proposed models. The occluded water is believed to be present in a continuum of states ranging from tightly held to the network via hydrogen bonding to sufficiently removed from the polymer chains to behave as bulk water<sup>(10)</sup>. Hydrogels have also been described<sup>(3)</sup> as being composed of statistically distributed microchannels or fluctuating pores created by the mobility of the polymer segments within an interpenetrating network in the presence of a solvent where these pores are formed and removed as a result of the thermal motion of the polymer chains. It follows that the local continuity of the conducting phase will vary with respect to time and space and therefore there could be either insufficient water in parts of the network to readily support the motion of charge carriers, possibly near the more hydrophobic sections of the network, or the motion of charge carriers along a given path could depend upon the formation of a sufficiently large water filled pore which in turn would be subject to motion

of the polymer matrix. The large scale segmental motion of the polymer network, at temperatures above the glass transition, would result in the continual motion of the chains which would increase the probability of contact between water filled pores that could sustain charge carrier motion. The slight irregularity of the semi-circular section of the AC impedance plot can thus be attributed to the distribution of water throughout the polymer matrix resulting from the water/polymer interactions.

Allen et al.<sup>(11)</sup> reported six distinct freezing points in the DSC cooling thermogram of a saturated pHEMA sample previously subjected to five freeze-thaw temperature cycles (i.e. 293->173->293K), thus indicating the heterogeneous nature of absorbed water in pHEMA hydrogels.

### 3.3 The Conductivity of pHEMA.

The intercept of the semicircular portion of the locus with the real impedance axis of the complex impedance plot allowed the evaluation of the bulk resistance of the samples. The specific conductivity,  $\sigma$ , was calculated from the following equation:

$$\sigma = \frac{1}{R} \times \frac{l}{A} \quad (\text{Eqn. 3.3})$$

where R is the bulk resistance of the sample,  $l$  is the thickness of the sample and A is the cross sectional area of the sample in contact with the electrodes of the conductivity cell.

The conductivity of fully hydrated pHEMA (EWC=40.4%, T=298K) was found to be  $2.86 \times 10^{-5} \text{ S.cm}^{-1}$ . The frequency of the discrete impedance measurement at which the AC impedance plot intersected the real axis was ca. 2kHz. These results are in good agreement with those obtained by Lee<sup>(4)</sup>.

In the literature the conductivity of pure water has been reported by Kohlrausch and Heydweiller<sup>(12)</sup> to be  $4 \times 10^{-8} \text{ S.cm}^{-1}$ . The conductivity of

water in hydrated pHEMA can also be calculated from the equation<sup>(13)</sup>:

$$\sigma = \sum \frac{\lambda^{\circ}_i C_i}{1000} \quad (\text{Eqn. 3.4})$$

where  $\lambda^{\circ}$  ( $\Omega^{-1}\text{cm}^2\text{mol}^{-1}$ ) is the molar conductivity of an ionic species at infinite dilution and  $C$  ( $\text{mol dm}^{-3}$ ) is the concentration of the substituent charge carrier. In water the charge carriers would be protons and hydroxyl anions which have the following molar conductivities at infinite dilution:

$$\begin{aligned} \lambda^{\circ}(\text{H}^+) &= 349.8 \Omega^{-1}\text{cm}^2\text{mol}^{-1} \\ \lambda^{\circ}(\text{OH}^-) &= 198.3 \Omega^{-1}\text{cm}^2\text{mol}^{-1} \quad (13) \end{aligned}$$

Given that the  $\text{pH}=6^{(9)}$  for water in pHEMA, it follows that the conductivity of the polymer/water system would be expected to be no greater than  $3.52 \times 10^{-7} \text{S.cm}^{-1}$ .

However, the conductivity of the pHEMA hydrogel is some two to three orders of magnitude higher than either that of the theoretical or experimental values obtained for water. This can probably be explained in terms of the impurities associated with the water in the hydrogel. To investigate this, the conductivity of fresh deionised water and deionised water subjected to prolonged exposure to air, i.e. water used to hydrate samples, was measured with a Philips PW9527 conductivity meter (Table 3.1).

It is noted that the conductivity of the water used in hydrating the polymer samples is higher than that of the fresh deionised water. During the hydration procedure (3-4 weeks) it is possible that some ions may have diffused out of the glass itself, such as  $\text{Na}^+$ , into the water but is more likely to be due to the absorption of atmospheric carbon dioxide, leading to the presence of  $\text{HCO}_3^-$  and  $\text{CO}_3^{2-}$ , that would increase the conductivity of the solution. It should be noted that the conductivity of deionised water did not change significantly after seven days exposure to air. Heydweiller and

Kohlrausch<sup>(12)</sup> ensured purity of their samples by distillation in quartz apparatus whereas the theoretical calculation of the conductivity does not allow for impurities caused by atmospheric carbon dioxide.

**Table 3.1**

Comparison of conductivity data for various samples of water with the conductivity of fully hydrated pHEMA.

SAMPLE	CONDUCTIVITY (S $\text{cm}^{-1}$ )
H <sub>2</sub> O ( <i>experimental</i> ) <sup>a</sup>	$4.0 \times 10^{-8}$
H <sub>2</sub> O ( <i>theoretical</i> ) <sup>b</sup>	$3.5 \times 10^{-7}$
H <sub>2</sub> O ( <i>fresh deionised</i> )	$2.0 \times 10^{-5}$
H <sub>2</sub> O ( <i>hydration water</i> )	$6.6 \times 10^{-5}$
pHEMA (EWC=40%)	$2.86 \times 10^{-5}$

<sup>a</sup> Kohlrausch and Heydweiller (12)

<sup>b</sup> Using Eqn. 3.3

It is therefore reasonable to only compare the conductivity of the hydrated pHEMA sample (EWC=40.4%) with the conductivity of the deionised water that had been used in the hydration process. From this data it is clear that the conductivity of the hydrogel is less than that for the bulk water. This can be attributed to the role of the polymer matrix in the hydrogel system. It not only supports the conducting water phase but also forms an impediment to the motion of the charge carriers. The polymer also exhibits secondary interactions with the water phase via hydrogen bonding and dispersion forces that result in the water existing in a continuum of phases between tightly bound (via hydrogen bonding) and free bulk-like water<sup>(14)</sup>. These interactions lead to a decrease in the mobility of the occluded water molecules with respect to bulk water. Consequently, the viscosity of the conducting phase is increased resulting in a decrease in conductivity.

The relationship between viscosity  $\eta$  and charge carrier mobility  $\mu$  in electrolyte solution is given by:

$$\mu = \frac{e}{6\pi r\eta} \quad (\text{Eqn. 3.5})$$

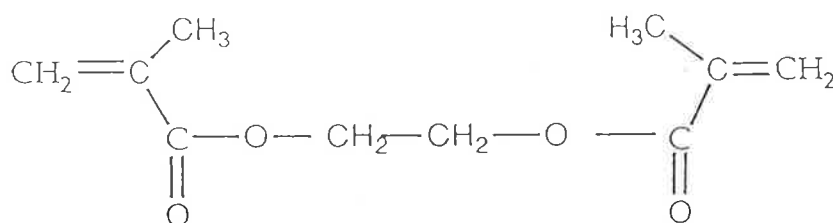
where  $e$  is the carrier charge and  $r$  is the radius of the carrier ion. The relation stating that carrier mobility is inversely proportional to viscosity is known as Walden's rule<sup>(15)</sup>. Shinohara et al.<sup>(15)</sup> found that this relationship does not hold for PAN/EC/LiClO<sub>4</sub> hybrids. It was discovered that on the addition of PAN to a solution of LiClO<sub>4</sub> in EC, viscosity increased but carrier mobility decreased only slightly, in apparent contradiction of Walden's rule. This result was rationalized by the distinction between microscopic and macroscopic viscosity. The addition of PAN increased the macroscopic viscosity of the hybrid but had little effect on the microscopic viscosity. The microscopic viscosity is concerned with the carrier migration and, in the case of this system, was dependent on the [EC]/[LiClO<sub>4</sub>], i.e. the ratio of the concentrations of the EC and LiClO<sub>4</sub>.

The change in microscopic viscosity between water and occluded water in a pHEMA gel sample is reflected by the <sup>1</sup>H NMR linewidths of occluded water and bulk water. Bulk water is able to tumble freely thus the resulting <sup>1</sup>H NMR signal has a linewidth of a few Hertz<sup>(16)</sup> at room temperature whereas absorbed water in pHEMA has been shown to have a linewidth of several hundred Hertz<sup>(11)</sup>. The broadening of the signal is due to the secondary interactions between the water and the polymer matrix which in turn lead to greater microscopic viscosity.

### 3.4 Conductivity of HEMA/EGDMA Copolymers

#### 3.4.1 Introduction

Despite their ability to absorb water, hydrogels remain insoluble because they form three dimensional networks on polymerisation. An impurity from the production of HEMA is ethylene glycol dimethacrylate (EGDMA) and on polymerisation the dimethacrylate functionalities react to form links between the HEMA chains rendering pHEMA insoluble in water. Hagias<sup>(17)</sup> has shown by NMR measurements that the optical grade HEMA used in this work contained 0.23% v/v EGDMA. The structure of EGDMA is shown below.



**Ethylene Glycol Dimethacrylate (EGDMA)**

Allen et al.<sup>(11,18-20)</sup> have studied the effect of EGDMA crosslinking on the properties of pHEMA hydrogels using several techniques. Proton enhanced magic angle spinning (PEMAS) <sup>13</sup>C NMR measurements<sup>(18)</sup> revealed that increasing EGDMA concentration led to an increase in  $T_{1\rho}(C)$ , the relaxation time in the rotating frame, indicative of the damping effect of the crosslinker on the molecular motions of the pHEMA network. Torsion pendulum experiments<sup>(19)</sup> revealed an increase in  $T_g$  with increasing EGDMA concentration. Sorption measurements<sup>(20)</sup> indicated decreasing ability to absorb water in copolymers with higher EGDMA concentrations. DSC measurements<sup>(11)</sup> revealed that an increasing EGDMA concentration results in a change in the absorbed water structure.

The water absorption capabilities and water structure of EGDMA/HEMA copolymers are of particular interest as the solvent phase of any gel electrolyte is primarily responsible for the conductivity. The

introduction of EGDMA into a HEMA copolymer has a twofold effect on the resulting polymer's ability to absorb water. EGDMA is more hydrophobic than HEMA and thus decreases the water sorption capabilities of the copolymer. EGDMA forms links between different polymer chains and consequently limits the ability of the network to expand upon swelling thus decreasing water uptake.

Copolymers of EGDMA with HEMA were made at four different EGDMA concentrations in the range 0.3mol% to 3.0mol%. Samples of these polymers were hydrated in deionised water and their conductivities evaluated using AC impedance spectroscopy.

### 3.4.2 Results and Discussion

The conductivities and equilibrium water contents for the five copolymers of EGDMA and HEMA are presented in Table 3.2. It is obvious

**Table 3.2**

The conductivities and EWC of several EGDMA/HEMA copolymers at full hydration and 25°C.

Copolymer	EWC (%)	$\sigma$ (S.cm <sup>-1</sup> )
pHEMA	40.4	$2.86 \times 10^{-5}$
0.3 mol% EGDMA co HEMA	37.5	$8.02 \times 10^{-6}$
0.6 mol% EGDMA co HEMA	36.3	$3.23 \times 10^{-6}$
1.5 mol% EGDMA co HEMA	32.9	$2.06 \times 10^{-6}$
3.0 mol% EGDMA co HEMA	27.7	$1.08 \times 10^{-6}$

that there is a rapid decrease in conductivity as the amount of EGDMA in the copolymer increases. As the concentration of EGDMA increases there is an accompanying decrease in equilibrium water content. However, the decrease

in conductivity as EGDMA concentration increases is much larger than the decrease in equilibrium water content. This is shown clearly in Figure 3.3. There is a sharp decrease in conductivity, ca.85%, as [EGDMA] increases to 0.6mol% which is in contrast to the smaller decrease in EWC ca.10%. The most significant decrease in conductivity occurred in samples of up to 0.6mol% EGDMA concentration. It would appear from these results that the presence of even small amounts of the dimethacrylate crosslinker perturb the conducting phase, that is the occluded water.

Previously, the water uptake of pHEMA has been observed to be relatively insensitive to low degrees of crosslinking<sup>(21,22)</sup>. This has been taken as an indication that there exists a secondary, non-covalent network along with the primary covalently bonded network. Proposed explanations describe this secondary structure as resulting from hydrophobic interactions between either  $\alpha$ -methyl groups or chain backbones<sup>(23)</sup> or hydrogen bonded hydroxyl groups probably stabilised by the exclusion of water from the regions containing the bonds<sup>(24)</sup>. The sharp decrease in conductivity for samples of relatively low crosslinker concentrations suggests that this secondary non-covalent bonding has little effect on the conductivity of hydrated p(EGDMA-co-HEMA) samples.

Similar AC impedance spectra were recorded for all samples, crosslinked with varying amounts of EGDMA, with respect to that of pHEMA (Fig 3.4). One interesting similarity of the impedance spectra of the crosslinked samples is lack of variation in the non-ideality of the semi-circular portion of the AC response, as indicated by  $\phi$  (Eqn 3.2), as the concentration of the crosslinker was increased from 0.30mol% up to 3.0mol% (Table 3.2a). On addition of 0.30mol% EGDMA,  $\phi$  only increased to  $2.10 \pm 0.02$ . No further variation in  $\phi$  was recorded until  $\phi = 2.12 \pm 0.02$  for 3.0mol% EGDMA. This would appear to suggest that, at the crosslinker



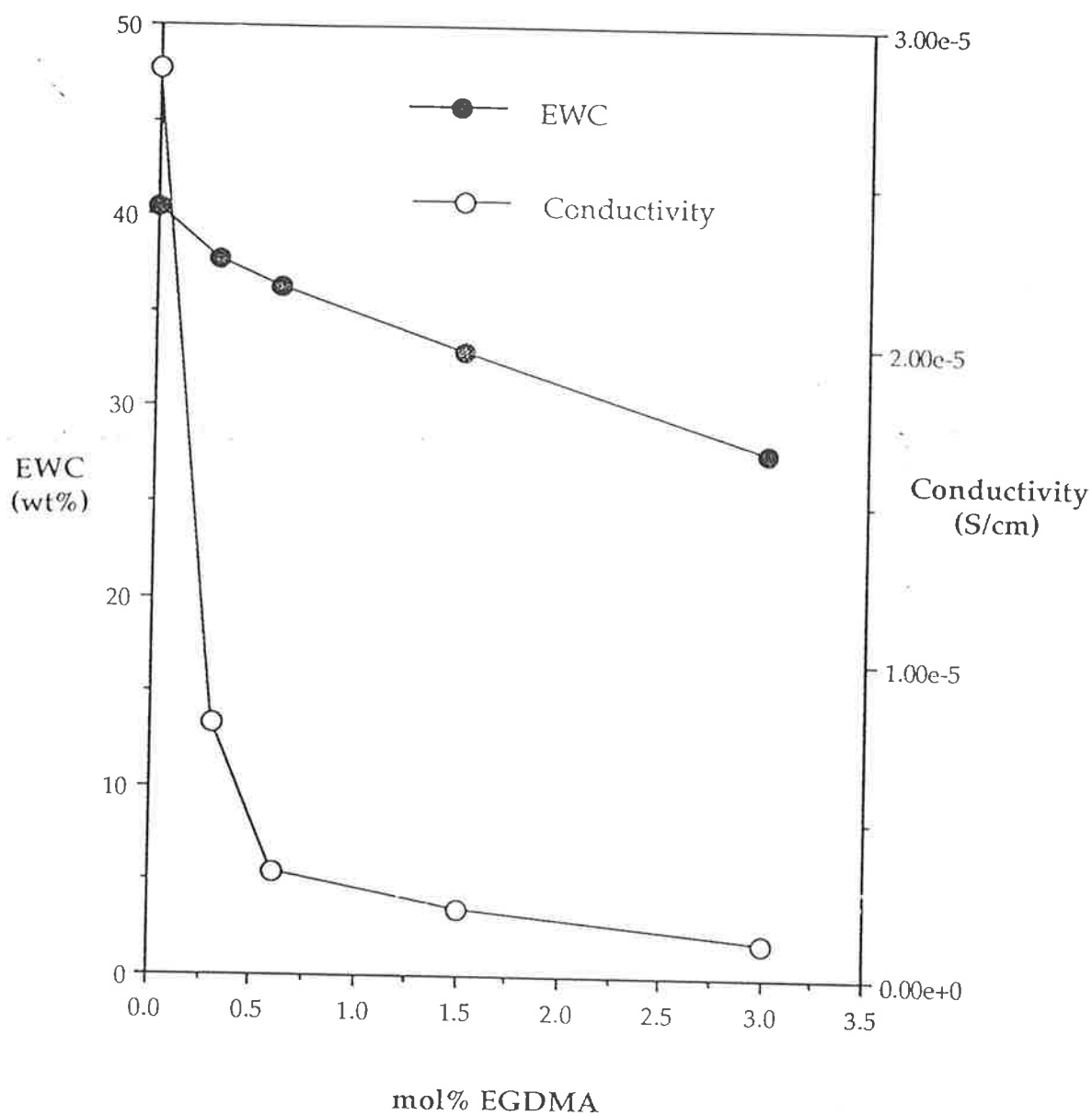


Figure 3.3

The variation of conductivity and equilibrium water content for several EGDMA/HEMA copolymers at 25°C.

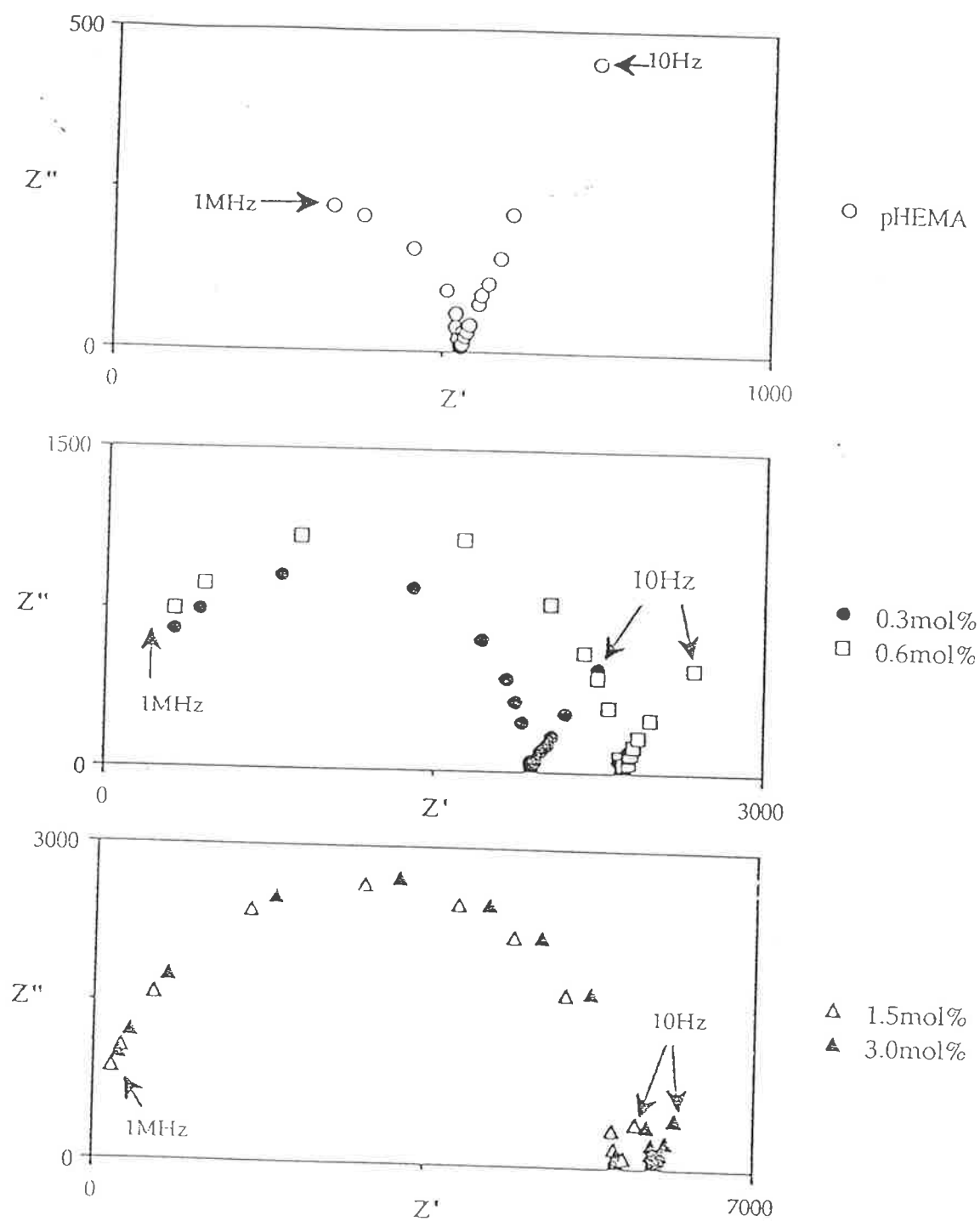


Figure 3.4

The AC impedance spectra of EGDMA/HEMA copolymers at full hydration and 25°C. EGDMA concentrations as listed above. ( $Z'$  and  $Z''$  in Ohms)

concentrations employed, the homogeneity of the conducting phase is not altered significantly by the introduction of the crosslinker.

**Table 3.2a**

The variation in capacitance,  $C$ , and  $\phi$  for EGDMA/HEMA copolymers of varying EGDMA concentration. All samples at full hydration and 25°C.

[EGDMA] (mol%)	$\phi$	$C$ (F)
0	2.07± 0.02	1.004 × 10 <sup>-10</sup>
0.30	2.10± 0.02	1.435 × 10 <sup>-10</sup>
0.60	2.10± 0.02	1.626 × 10 <sup>-10</sup>
1.5	2.10± 0.02	1.686 × 10 <sup>-10</sup>
3.0	2.12± 0.02	2.293 × 10 <sup>-10</sup>

It is also possible to evaluate the capacitance of the gels from their AC impedance responses. This capacitance has been attributed<sup>(6)</sup> to vibrating charge carriers that are trapped in potential wells and lead to an out-of-phase contribution towards the resulting current flow. The evaluation of the capacitance of the crosslinked samples should give an indication of the effect of the crosslinker on the network and thus the conductivity.

The capacitance of a parallel RC circuit can be evaluated from the maximum value, in the y-axis orientation, of the resultant semi-circular AC impedance spectrum. The following relationship can then evaluate the capacitance<sup>(5)</sup>:

$$\omega_{\max}RC = 1 \quad \text{Eqn 3.6}$$

where  $R$  is the bulk resistance of the sample,  $\omega_{\max} = 2\pi f$  and  $f$  is the frequency at the highest point of the semicircular portion of the recorded locus.

The capacitances for several EGDMA/HEMA copolymers are given in Table 3.2a. It should be noted that all the capacitances evaluated are of the

order of  $10^{-10}$  Farads and such low values are indicative of the lack of trapping of charge carriers in the polymer network; these copolymers are only very lightly crosslinked. However, there is a slight increase in capacitance as the concentration of the crosslinker increases which results from the polymer network becoming less mobile with greater crosslinking.

Allen et al.<sup>(11)</sup> investigated the effect of increased EGDMA concentration on the ratio of freezing to non-freezing water from DSC measurements. The variation of EWC, the amounts of freezing and non-freezing water and conductivity with EGDMA concentration are shown in Table 3.3.

**Table 3.3**

Comparison of EWC and conductivity of pHEMA and 3mol% EGDMA/HEMA copolymers with DSC evaluations of freezing water,  $(\text{H}_2\text{O})_f$ , and non-freezing water,  $(\text{H}_2\text{O})_{nf}$ , of similar copolymers by Allen et al.<sup>(11)</sup>

[EGDMA] (mol%)	EWC <sub>A</sub> (%)	$\sigma$ (S/cm)	EWC <sub>B</sub> (%)	$m(\text{H}_2\text{O})_f$ (g/g <sub>gel</sub> )	$m(\text{H}_2\text{O})_{nf}$ (g/g <sub>gel</sub> )
0	40.4	$2.86 \times 10^{-5}$	39.2	0.130	0.262
3.0	27.7	$1.08 \times 10^{-6}$	28.0	0.019	0.261

\* f=freezing, nf= non-freezing

\*\* EWC<sub>A</sub> refers to the samples prepared by the author, EWC<sub>B</sub> refers to the samples prepared by Allen et al.<sup>(11)</sup>

It should be noted that as the crosslinker concentration was increased to 3mol%, the mass of non-freezing water per gram of hydrogel sample decreased marginally. This contrasts with the amount of freezing water which decreased seven fold. However, the conductivity of similar hydrogels was observed to decrease twenty five fold. It could be suggested that the physical impediment to the motion of charge carriers created by the crosslinks themselves also contributes to the decrease in the conductivity. It follows that

the conducting phase is dependent not only on the structure of the occluded water but also the structure of the polymer network.

Allen et al.<sup>(11)</sup> studied mobile water present in several crosslinked HEMA copolymers from  $^1\text{H}$  NMR measurements. However, it should be noted that  $^1\text{H}$  NMR techniques only enable the observation of water molecules that exhibit some degree of tumbling. Free water has a linewidth of only a few Hz at room temperature<sup>(16)</sup>. Constrained or bound water is not seen as the linewidth will broaden into the baseline and thus reflect the increased viscosity of occluded water. Allen et al. found the linewidth of water in pHEMA (EWC=39.2%) to be ca. 300 Hz at 25°C whereas the linewidth for water in 3mol% EGDMA/HEMA copolymer is ca. 200 Hz at 25°C indicating greater mobility of water in the more crosslinked sample. This is in contrast with the conductivities of similar samples. However Allen et al. deduced from correlation with their DSC data that 82% of the water present in the 3mol% EGDMA crosslinked sample was constrained whereas only 13% in the pHEMA sample was constrained. It is necessary to not only consider the mobility of the occluded water but also the amount of constrained water present in each sample when considering the viscosity of the conducting phase.

In the samples we have studied the concept of microscopic viscosity is complex due to the dynamic nature of polymer water interactions. The mobility of the water phase is reflected in  $^1\text{H}$  NMR linewidths but the nature and relative proportions of the water present must also be taken into account.

### 3.5 The Conductivity of OED/HEMA Copolymers.

#### 3.5.1 Introduction

EGDMA is the first monomer in the OED series with one ethylene glycol repeat unit situated between two terminal methacrylate functionalities, which provide the crosslinking capability. By altering the number of repeat

ethylene glycol units,  $n$ , in the OED it is possible to produce hydrogels with varying properties.

Bennett<sup>(25)</sup> used several techniques to investigate the effect of varying the OED crosslinker on the properties of the OED/HEMA copolymers. Dynamic mechanical tests revealed an interesting trend in  $T_g$  as  $n$  was increased. For 3mol% OED/HEMA copolymers the following  $T_g$ 's were observed:

$n=1$	3mol%EGDMA/HEMA	$T_g = 137^\circ\text{C}$
$n=4$	3mol%TEGDMA/HEMA	$T_g = 127^\circ\text{C}$
$n=9$	3mol%P400/HEMA	$T_g = 111^\circ\text{C}$

If we compare this to the  $T_g$  of pHEMA ( $125^\circ\text{C}$ )<sup>(19)</sup> it is obvious that for small values of  $n$  the  $T_g$  of the copolymers increases but as  $n$  increases  $T_g$  decreases until eventually being lower than the  $T_g$  of pHEMA. Several models exist to predict the variation in the glass temperature resulting from copolymerisation and such models are generally based around free volume considerations<sup>(38-41)</sup> or statistical mechanical interpretation of composition effects<sup>(42,43)</sup>. Bennett ascribed this trend to the copolymer effect previously employed by Simon<sup>(26)</sup> to rationalise a similar phenomenon shown by TEGDMA/MMA copolymers. The copolymer effect suggests that a sufficiently flexible and mobile crosslinker, such as an OED with a long oligo-ethylene glycol chain, could influence local main chain motion. If this effect was significant it could outweigh the damping effect of crosslinking and lead to a decrease in  $T_g$ . Sorption measurements<sup>(20)</sup> revealed that EWC increased with  $n$  for crosslinked samples of the same OED concentration. By increasing  $n$  we not only increase the hydrophilicity of the crosslinker, and thus the water uptake of the resultant copolymer, but also increase the length and flexibility of the crosslink enhancing the ability of the copolymer to swell. DSC measurements<sup>(11)</sup> showed that freezing water increased and the fine structure of the melting endotherm changed as  $n$  increased for copolymers of like OED

concentration. The variation of  $n$  causes significant structural changes for the copolymers in both the dry and hydrated states.

Several OED/HEMA copolymers with crosslinker concentration 3mol% were prepared and their conductivities measured at full hydration at 25°C. The copolymers that were investigated in this study utilised the following crosslink agents: EGDMA ( $n=1$ ), DiEGDMA ( $n=2$ ), TEGDMA ( $n=4$ ) and P400 (average  $n=9$ ).

### 3.5.2 Results and Discussion

The variations in EWC and conductivity obtained as  $n$  was increased for several 3mol% OED/HEMA copolymers are presented in Table 3.4. The addition of any crosslinker was shown to both decrease EWC and conductivity of the resultant copolymer samples with respect to the pHEMA hydrogel sample. The EWC results are in good agreement with those obtained by Bennett<sup>(25)</sup> for similar samples.

**Table 3.4**

The conductivities and EWC of OED/HEMA copolymers at full hydration and 25°C.

Copolymer	EWC (%)	$\sigma$ (S/cm)
pHEMA	40.4	$2.86 \times 10^{-5}$
3 mol% EGDMA co HEMA	27.7	$1.08 \times 10^{-6}$
3 mol% DiEGDMA co HEMA	33.3	$1.55 \times 10^{-6}$
3 mol% TEGDMA co HEMA	33.8	$2.47 \times 10^{-6}$
3 mol% P400 co HEMA	34.7	$5.47 \times 10^{-6}$

Both the EWC and the conductivity of pHEMA hydrogels decrease appreciably on copolymerization with any of the OEDs used in this study. However, the variation of EWC is significantly different from the variation of

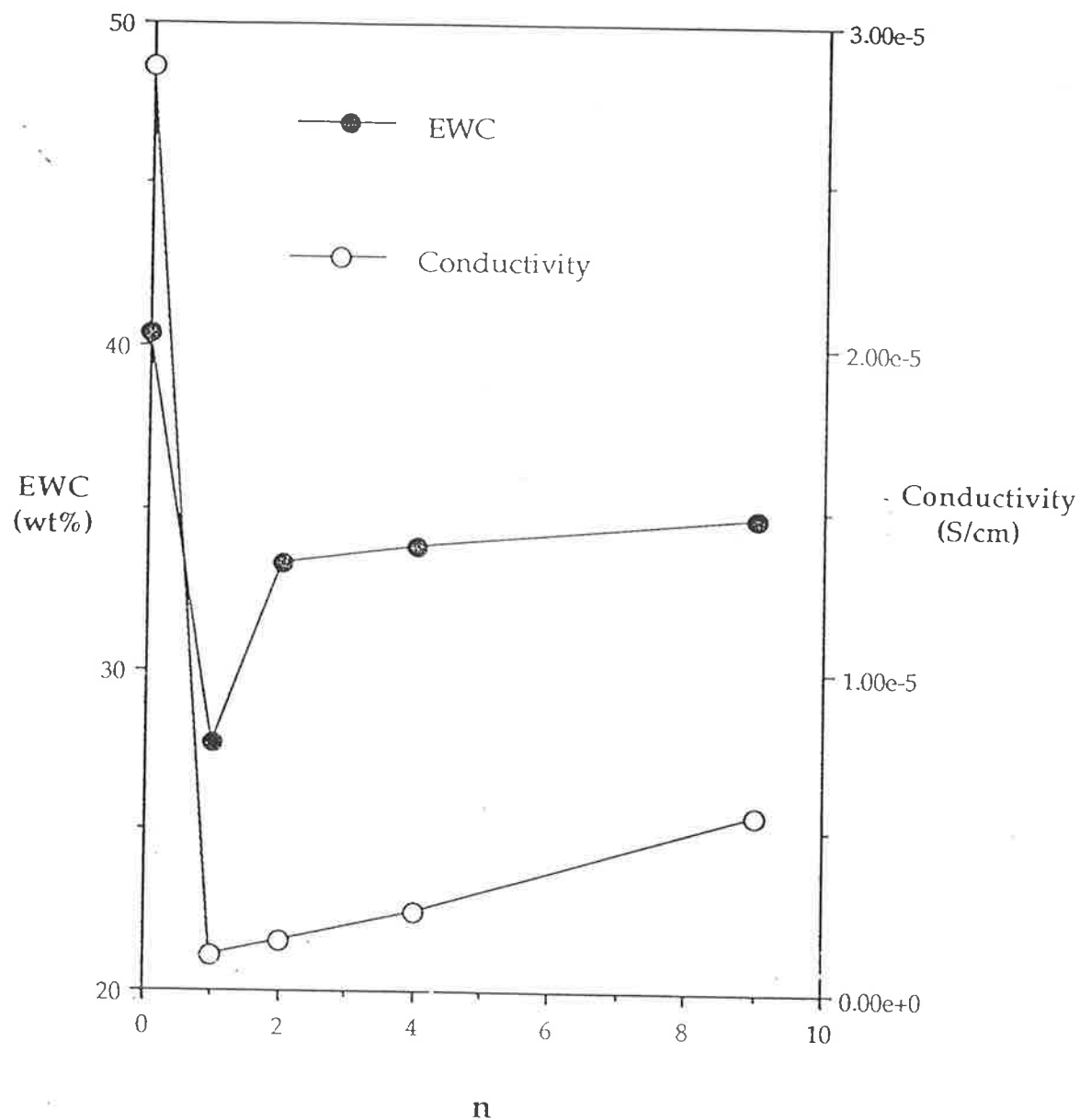


Figure 3.5

The variation in conductivity and equilibrium water content for several 3mol% OED/HEMA copolymers at full hydration and 25°C. (n is the number of ethylene glycol units in the OED)



conductivity when both are considered with respect to the increase in  $n$  from  $n=1$  to  $n=9$  (Fig. 3.5). The increase in conductivity with respect to  $n$  yields a linear relationship whereas the increase in EWC is sharp as  $n$  is increased from 1 to 2 yet the EWC appears to be approaching a limiting value as  $n$  is increased from 2 to 9.

The results of DSC measurements by Allen et al.<sup>(11)</sup> on the effect of altering the nature of the crosslinking agent on the ratio of freezing to non-freezing water are presented in Table 3.5 together with the variation in conductivity for similar samples prepared in this work.

**Table3.5**

Comparison of EWC and conductivity of various 3mol%OED/HEMA copolymers with DSC evaluations of freezing water,  $(\text{H}_2\text{O})_f$ , and non-freezing water,  $(\text{H}_2\text{O})_{nf}$ , of similar copolymers by Allen et al.<sup>(11)</sup>

Crosslink Agent	EWC <sub>A</sub> (%)	$\sigma$ (S/cm)	EWC <sub>B</sub> (%)	$m(\text{H}_2\text{O})_f$ (g/g <sub>gel</sub> )	$m(\text{H}_2\text{O})_{nf}$ (g/g <sub>gel</sub> )	$m_f/m_{nf}$
-	40.4	$2.86 \times 10^{-5}$	39.2	0.130	0.262	0.496
EGDMA	27.7	$1.08 \times 10^{-6}$	28.0	0.019	0.261	0.073
DiEGDMA	33.3	$1.55 \times 10^{-6}$	33.0	0.022	0.308	0.071
TEGDMA	33.8	$2.47 \times 10^{-6}$	33.7	0.031	0.306	0.101
P400	34.7	$5.47 \times 10^{-6}$	34.5	0.062	0.283	0.219

EWC<sub>A</sub> refers to samples prepared by the author.

EWC<sub>B</sub> refers to samples prepared by Allen et al.

There are a number of effects on the structure of water resulting from the increase in the number of ethylene glycol repeat units,  $n$ , in the crosslinking agent employed reflected in the results of Allen et al.. As  $n$  increased so did the amount of freezing water per gram of sample, with all crosslinked samples having much less freezable water than the pHEMA homopolymer. In contrast, the amount of non-freezing water increased

initially, as  $n$  was increased from 1 to 2, but was found to decrease slightly as  $n$  was increased from 2 to 4 before decreasing more rapidly as  $n$  was increased to 9.

Non-freezing water is ascribed to the water that is able to form strong secondary interactions with the hydrophilic portions of the polymer, such as the hydroxyethyl moieties or the ethylene glycol repeat units in the crosslinks. The amount of non-freezing water increased as  $n$  was increased to 2 due to the increase in hydrophilicity of the crosslinking agent but then was shown to decrease as  $n$  was increased from 4 to 9. This suggests that after the crosslink reaches a certain length, the flexible nature of the repeat ethylene glycol units could favour structural conformations of the copolymer that would in turn facilitate intramolecular hydrogen bonding and thus sterically hinder interaction between absorbed water and hydrophilic sites of the network.

The mass of freezing water per gram of hydrogel sample was found by Allen et al.<sup>(11)</sup> to increase as  $n$  was increased from 1 to 9 in a linear manner. This is most likely indicative of the more open nature of the polymer network formed resulting from the use of a longer crosslinking agent. The increase in EWC as  $n$  increases is also indicative of the formation of looser networks as the length of the crosslinks employed also increases.

The most interesting aspect of this data is that if the ratio of freezing water to non-freezing water is examined as a function of  $n$ , then a similar relationship is seen compared to the change in conductivity (Fig. 3.6). It would appear that the conductivity is influenced by the ratio of freezing water to non-freezing water which is in turn controlled by the polymer network and thus the nature of the crosslink.

AC impedance spectra were recorded for all the copolymer samples at full hydration and 25°C (Fig.3.7). All the OED/HEMA copolymers investigated yielded spectra typical of gel electrolytes, that is a combination of a high frequency semi-circle and a low frequency spur. However, it should be

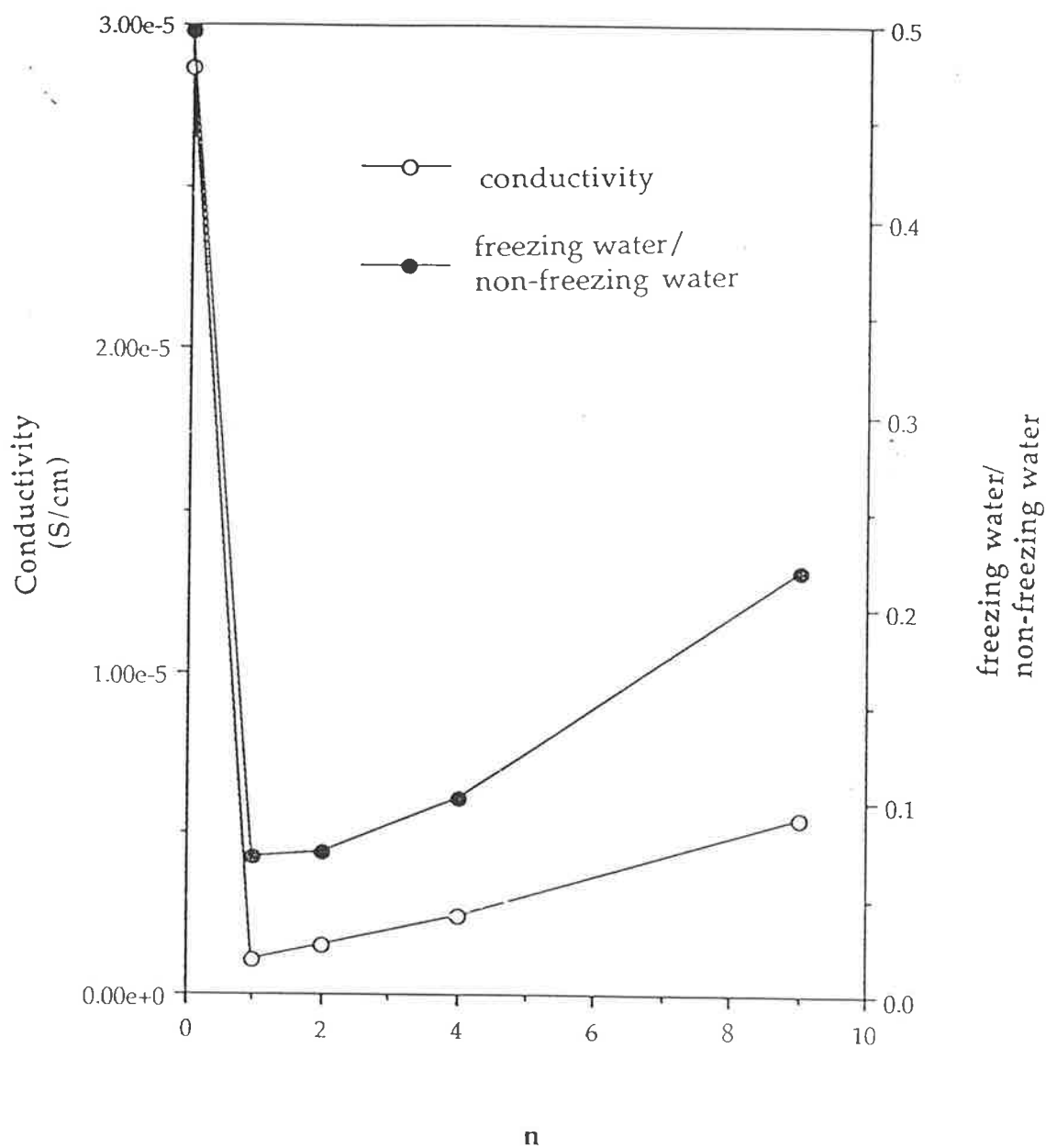


Figure 3.6

The variation of conductivity and the ratio of freezing water/non-freezing water<sup>‡</sup> for several 3mol% OED/HEMA copolymers at full hydration and 25°C ( $n$  is the number of ethylene glycol units in the OED).

[<sup>‡</sup> as measured by Allen et al.<sup>(11)</sup>]

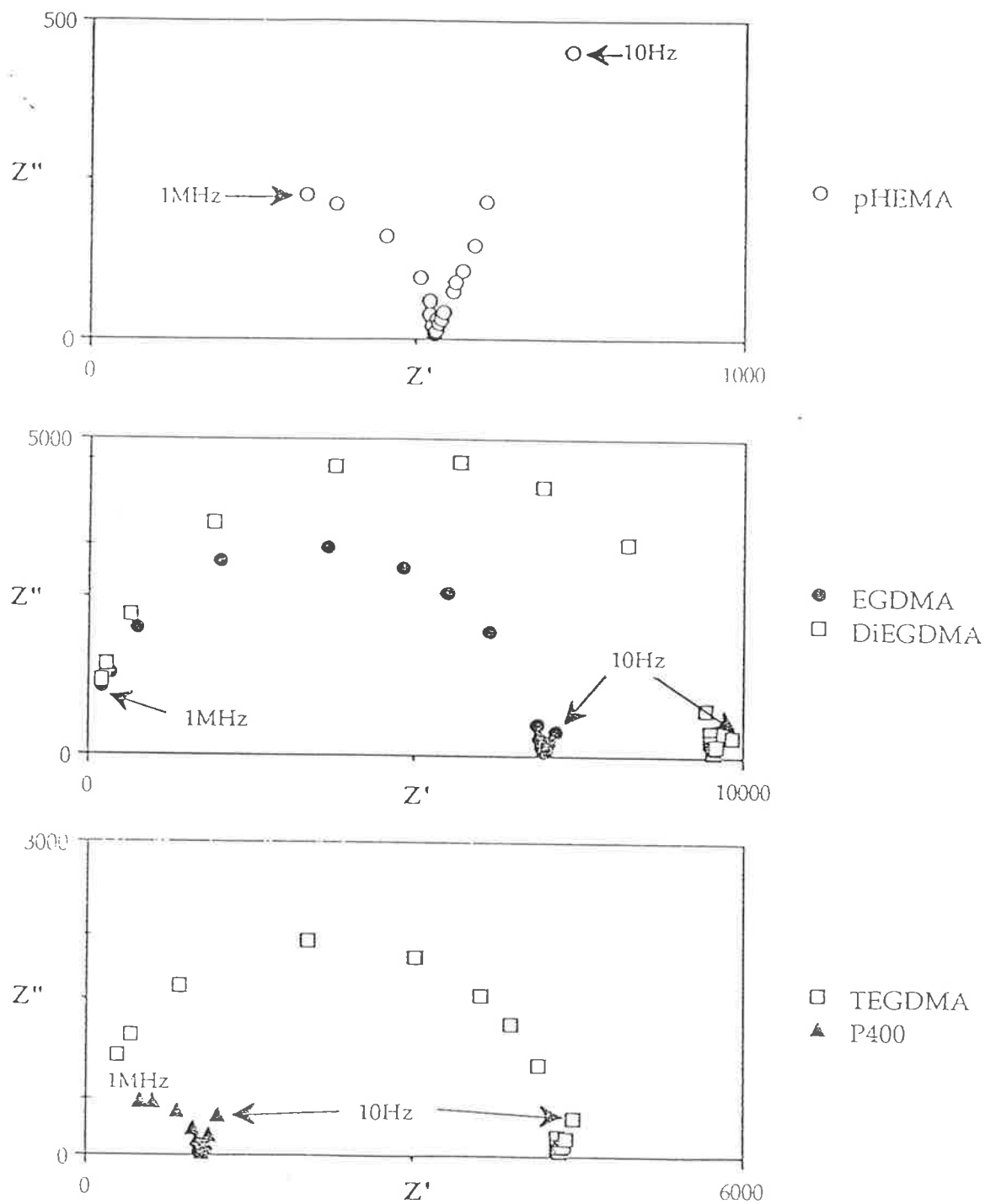


Figure 3.7

The AC impedance spectra of several 3mol% OED/HEMA copolymers at full hydration and 25°C. OED as listed above. ( $Z'$  and  $Z''$  in Ohms)

noted that the spectra vary with respect to the nature of the crosslinker present in the crosslinked sample. Given that the samples were of similar thickness, the bulk resistance decreased as  $n$  increased in the OED. The frequency at which the highest point in the semi-circular portion of the locus was recorded increased as  $n$  increased. The capacitance,  $C$ , and  $\phi$  were calculated for all the spectra and are presented in Table 3.6.

**Table 3.6**

Capacitance and  $\phi$  for 3mol%OED/HEMA copolymers at full hydration and 25°C.  $n$  represents the number of ethylene glycol units in the OED.

Copolymer	$n$	$C$ (F)	$\phi$
pHEMA	-	$1.004 \times 10^{-10}$	$2.07 \pm 0.02$
3mol%EGDMA/HEMA	1	$2.293 \times 10^{-10}$	$2.12 \pm 0.02$
3mol%DiEGDMA/HEMA	2	$1.661 \times 10^{-10}$	$2.10 \pm 0.02$
3mol%TEGDMA/HEMA	4	$1.506 \times 10^{-10}$	$2.09 \pm 0.02$
3mol%P400/HEMA	9	$1.493 \times 10^{-10}$	$2.10 \pm 0.02$

Again the introduction of the crosslinker has lead to a slight increase in  $\phi$  but there appears to be no dependence on the nature of the crosslinker other than that the presence of any crosslinker slightly perturbs the homogeneity of the conducting phase. The crosslinker concentration, 3mol%, is relatively low and as the samples studied are at full water content, the nature of the crosslink is unlikely to have any significant effect on  $\phi$ .

The introduction of EGDMA has already been shown to cause an increase in capacitance. As the nature of the crosslinker was altered, the capacitance was shown to increase with  $n$ , the number of repeat ethylene glycol units. As  $n$  increases the flexibility and length of the crosslinker also increases, which results in looser polymer networks able to absorb more water. The more open nature of the networks as  $n$  increases would decrease

the chance of entrapment of charge carriers leading to lower capacitance.

### 3.6 The Variation of Conductivity with Water Content .

#### 3.6.1 Water in pHEMA hydrogels.

Water in hydrogels performs many roles<sup>(27)</sup>. It can act as a plasticiser, a transport medium for dissolved species and, in biomedical applications, a bridge between the very different surface energies of synthetic polymers and body fluids. Andrade and Jhon<sup>(28)</sup> and Hoeve<sup>(29)</sup> have reviewed the interaction of water with polymers.

Given the unique role of water in hydrogels, it is first necessary to review the current understanding of the nature of water in pHEMA hydrogels and its effect on structure before discussing the change in conductivity with water content.

Considerable evidence exists<sup>(10)</sup> to suggest that water in hydrogels exists in more than one state and that these states of water in the hydrogel will also effect its properties. The desire to understand the distribution of occluded water in hydrogels has been the target of many studies. However, the outcomes have been varied and technique dependent. This has led to several classification systems which, whilst useful in explaining specific experimental results, are not readily interconvertible.

Studies utilising the DSC technique<sup>(4,10,11,30,31)</sup> have found it convenient to refer to the experimentally determined states, i.e. freezing water and non-freezing water. The difference arises as the freezing behaviour of water in hydrogels is irregular; when hydrated pHEMA samples are cooled to sub-zero temperatures not all of the available water freezes. This enables a quantitative analysis of the two states and further indication of changes in freezing behaviour are available from the fine structure of the melting endotherms<sup>(25)</sup>. Allen et al.<sup>(11)</sup> reported that approximately 33% of the water present in saturated pHEMA was capable of freezing. Comparison between

studies is hindered by the need for samples of similar thermal history as results are dependent on the temperature cycle employed. Allen et al. found that not only did the amount of freezing water vary with any alteration of the cooling and heating procedures but the nature of the recorded heating endotherm was also found to vary. The introduction of water has also been shown to cause a decrease in the glass transition temperature as a result of interfering with secondary interactions between polymer chains.

$^1\text{H}$  NMR studies have been used to probe the mobility of the water in hydrogels and thus monitor the interaction of absorbed water with the polymer matrix<sup>(11,14,32-34)</sup>. McBrierty et al.<sup>(14)</sup> proposed the existence of three types of water in hydrated pHEMA: bound water ( $\leq 20\text{wt}\%$ ), which corresponds to on average two hydrogen bonded water molecules per repeat unit, interfacial water, which is ascribed to dipole-dipole interactions with hydroxyl groups or hydrophobic interactions with polymer segments, and freely diffusable water in samples where the water content is greater than 35wt%. Values measured experimentally for  $T_1$ , the proton spin-lattice relaxation time, have been considered<sup>(33,34)</sup> as an average of the  $T_1$ 's of the three proposed classes of water present on the gels such that:

$$\frac{1}{T_1} = \frac{f_W}{T_{1W}} + \frac{f_I}{T_{1I}} + \frac{f_B}{T_{1B}} \quad (\text{Eqn. 3.7})$$

where  $f_W$ ,  $f_I$  and  $f_B$  are the fractions of the bulk water, interfacial water and bound water respectively and  $T_{1W}$ ,  $T_{1I}$ , and  $T_{1B}$  are the corresponding relaxation times of protons in these three classes of water.  $T_{1B}$  was taken as the relaxation time recorded for samples of water content less than 20wt% whereas  $T_{1W}$  was considered to be the same as for bulk water (4.5s at 34°C).  $T_{1I}$  was estimated using equation 3.9 and the experimental results. As the water content of the samples increased from 20-40wt%  $T_1$  increased and thus, by calculation, did  $T_{1I}$  which is indicative of increased mobility of the interfacial

water. One flaw in this work is the assumption that the bulk-like water in the polymer samples is the same as bulk water. It should be noted<sup>(11)</sup> that  $^1\text{H}$ NMR linewidths for occluded water are of the order of several hundred Hz as opposed to that of bulk water which yields linewidths of a few Hz, i.e. there exists no water domain in such gels that could be classified as a true water phase that is large enough to permit free tumbling. Measurements of  $T_2$ , the spin-spin relaxation time, by Sung et al.<sup>(33)</sup> reveal that  $T_2$  is relatively invariant until water contents of 25wt% are achieved when  $T_2$  increases dramatically revealing the presence of increased amounts of interfacial and bulk water.

$^{13}\text{C}$  NMR can be used as a probe to investigate the effect of water on the molecular motions of the polymer network. CPPEMAS (cross polarised proton enhanced magic angle spinning) experiments were carried out by Allen et al.<sup>(18)</sup> to evaluate  $T_{1\rho}(\text{C})$ , the  $^{13}\text{C}$  relaxation time in the rotating frame, for the various carbon centres of the repeat unit of the polymer network as the water content was varied.  $T_{1\rho}(\text{C})$  was found to increase progressively for all carbon environments with increasing water content revealing the plasticising action of the water. The  $T_{1\rho}(\text{C})$  data for carbons present in the hydroxyethyl moiety and the quaternary backbone carbon was scattered at low water contents and did not decrease appreciably until the glass transition fell below the probe temperature ( $25^\circ\text{C}$ ) at ca. 20% water content. The carbonyl carbon and the backbone methylene carbon showed a decrease in  $T_{1\rho}(\text{C})$  over the whole water content range investigated. The  $\alpha$ -methyl carbon was relatively unaffected by the addition of water at low water contents but  $T_{1\rho}(\text{C})$  decreased sharply when the glass transition fell below the probe temperature. This data is consistent with the notion of bound water being present up to water contents of 20wt% which equates to two water molecules per repeat unit involved in hydrogen bonding, presumably to the carbonyl and hydroxyl moieties.



Dynamic mechanical measurements are also helpful in revealing the effect of absorbed water on the molecular structure of pHEMA networks. Allen et al.<sup>(19)</sup> utilised torsion pendulum measurements to study storage and loss moduli ( $G'$ ,  $G''$ ) and  $\tan \delta$  for pHEMA samples of varying water content. A  $\tan \delta$ -temperature plot for dry pHEMA yielded three transitions:  $\alpha$ , taken to be the glass transition, at 125°C,  $\beta$ , ascribed to the motion of the complete side group, at 30°C and  $\gamma$ , indicative of rotation of the terminal hydroxyl group on the side group, which was barely perceptible at ca. -125°C. It was found that as the water content increased the  $\alpha$ -transition shifted to lower temperature, broadened and subsequently developed a shoulder on the low temperature side until at 13.5wt% water, two broad peaks could be distinguished at 43°C and 103°C. At higher water contents (> 22.8wt%) single sharp transitions were observed. The broadening and splitting of the  $\alpha$ -transition was ascribed to the heterodispersion of the absorbed water. The decrease in temperature of the  $\alpha$ -transition is indicative of the plasticising action of water. The  $\beta$ -transition is obscured by the broadening of the  $\alpha$ -transition as water content increases with the  $\gamma$ -transition becoming more distinct as water content increases.

Dielectric spectroscopic experiments have been carried out by Xu et al.<sup>(2)</sup> and Johari and Pathmanathan<sup>(3)</sup>. Both studies reflect the complex nature of the interaction of water with the pHEMA matrix. Again the increase of water content has been shown to decrease the temperature of the  $\alpha$ -transition at the expense of resolution of the  $\beta$ -transition<sup>(2)</sup>. The  $\gamma$ -transition has been shown to be profoundly affected by the behaviour of the water phase<sup>(2)</sup>.

All these techniques reflect the complex nature of the polymer/ water interaction in hydrated pHEMA gels. The most obvious effect is that the hydrophilicity of pHEMA leads to water sorption and thus the polymer swells to become a gel. As the water content increases the presence of the water molecules liberates polymer chains from inter-chain secondary bonding thus

enabling and enhancing several modes of molecular motion. The effect of the matrix on the water molecules is quite different. Initially absorbed water molecules experience a decrease in mobility, compared to the bulk, as they hydrogen bond to polar moieties of the matrix. As more water is absorbed (>20wt%) it fills voids and is shielded from the polymer network by already sorbed water until the network can swell no more. The cohesive force that limits the swelling of the gels has been ascribed to a secondary non-covalent network which has been proposed to be due to hydrophobic interactions<sup>(23)</sup> and hydrogen bonding<sup>(24)</sup>. The mobility of the absorbed water increases with water content but never reaches that of water in the bulk. It is the combination of the mobilities of the water and the polymer network that will be of interest in rationalising the conductive behaviour of samples of varied hydration.

The conductivity of several fully hydrated polymer samples was evaluated at 25°C and subsequent measurements were made after progressive dehydration. The dehydration regimen involved the exposure of the sample to the ambient environment for a brief period before being placed in a resealable polyethylene bag at 25°C and left for 24 hours before subsequent AC impedance analysis. The sample was stored in this manner to ensure re-equilibration of the remaining water.

### 3.6.2 Results and Discussion: pHEMA

Conductivity was found to decrease with the decrease in water content of pHEMA hydrogels (Figure 3.8). Although the decrease in conductivity is continuous as water is removed, it is convenient to discuss the behaviour in terms of three water content regions defined by McBrierty et al.<sup>(14)</sup>, namely 0 to 20wt%, 20 to 35wt% and 35wt% and above. It will be seen that these regions also correlate with distinct changes in the conductivity behaviour.

The first 20wt% of water that is absorbed by pHEMA (Region 1) has the

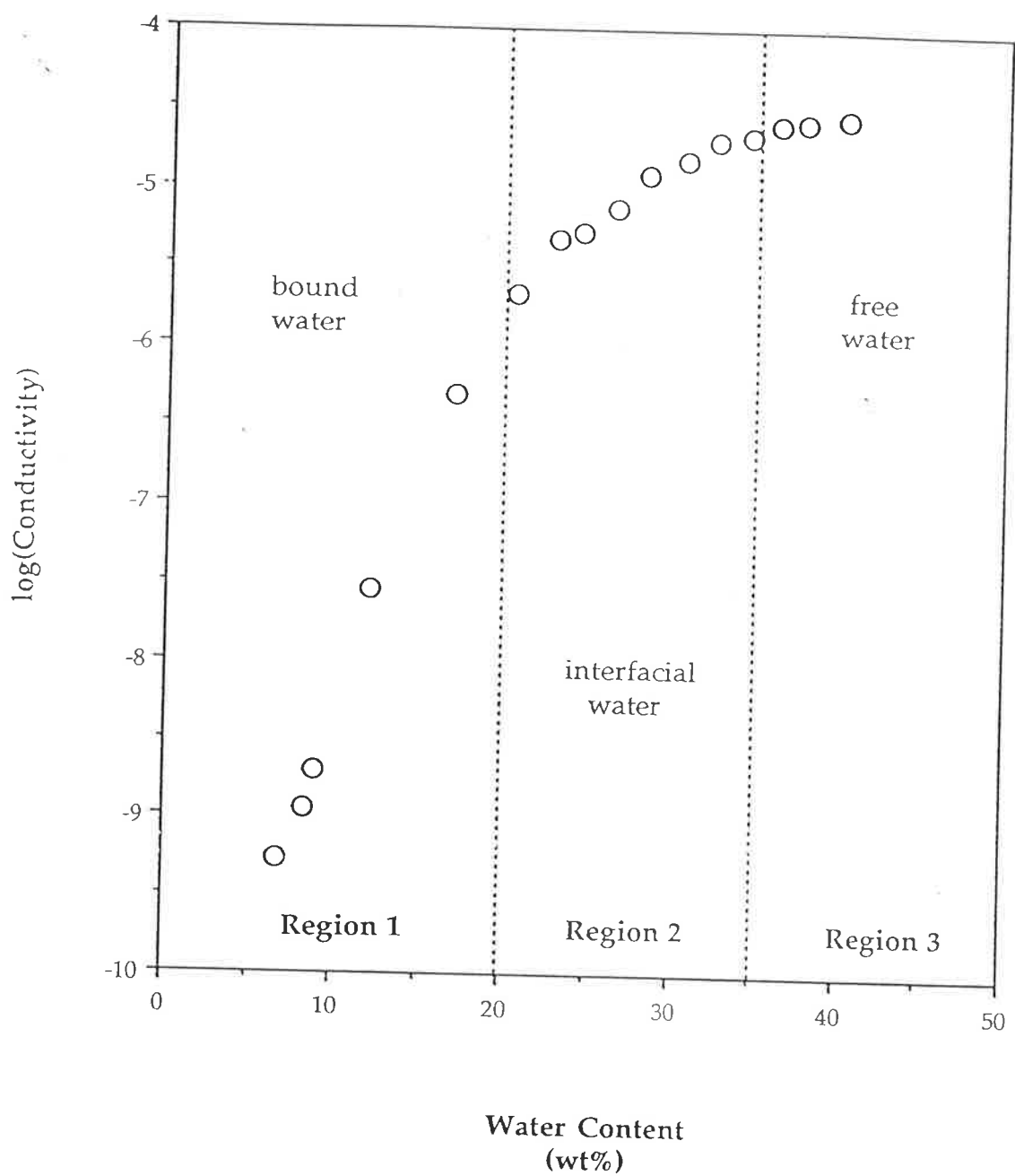


Figure 3.8  
The variation of  $\log(\text{conductivity})$  with water content for pHEMA at 25°C

greatest effect on the conductivity and is ascribed to the hydrogen bonding of two water molecules per repeat unit to polar moieties of the polymer. In Region 2, between 20wt% and 35wt% water the effect of increasing the water content is not as great as in Region 1. McBrierty describes water in this range as interfacial, that is it has no direct secondary bonding with the polymer but interacts with the hydrogen bound water and as such is influenced to some extent by the polymer network. The effect of water added above 35wt% (Region 3) is less than for Region 2, and this water is referred to as bulk-like, that is water which is sufficiently shielded from the polymer by other absorbed water that it behaves similarly to water in the bulk.

The increase in conductivity is greatest with increasing water content in Region 1 as water in this hydration range not only provides the conducting phase, initially, but it also liberates molecular motion of the polymer network. Dynamic mechanical analysis by Allen et al.<sup>(19)</sup> found the glass transition temperature of pHEMA increases from ca. 25°C to 125°C over the same hydration range. The  $\beta$ -transition was found to decrease by 10-15°C with the addition of just 10wt% water. The plasticising action of the absorbed water liberates modes of molecular motion of the polymer network which will assist in the continuity of the conductive water phase.

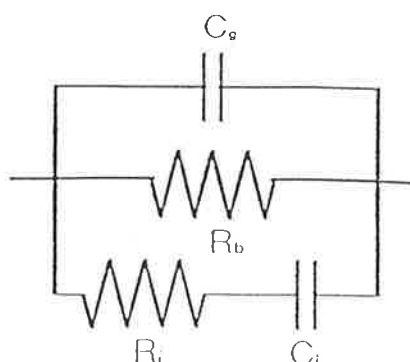
The effect of water on the motion of the polymer network is less in Region 2 and further decreases for Region 3. The plasticising action of the interfacial water is not as effective as the bound water and is reflected by the lower increase of T<sub>g</sub> recorded by Allen et al.<sup>(19)</sup> over this hydration range, i.e. 5°C at 31.7% to 20°C at 22.8%. The water absorbed in Region 3 has the least effect on the glass transition (5°C at 31.7%, 0°C at 39.2%)<sup>(19)</sup>.

Despite the decreased effect on the molecular motion of the polymer network it should be noted that the mobility of the bulk water is greater than that of the interfacial water which is in turn greater than that of the bound water which is reflected in the <sup>1</sup>H NMR T<sub>2</sub> data of Sung et al.<sup>(33)</sup>. The

mobility of water is an indication of the microscopic viscosity which decreases as we increase the water content from Region 1 to Region 3. It should also be noted that the addition of water will always increase the amount of the conductive phase. Both these factors lead to enhanced conductivity with increased water content.

The AC impedance spectra recorded for pHEMA at several stages of dehydration are shown in Figure 3.9. A number of changes in the nature of the AC impedance spectra take place as the hydration level decreases. As the hydration level decreases from 40.4% to 17.1% not only does the real intercept, the bulk resistance, increase but the semi-circular portion of the locus becomes more flattened and irregular. This is revealed by the variation in  $\phi$  from  $2.07 \pm 0.02$  at 40.4% water content to  $2.43 \pm 0.02$  at 17.1% and would suggest that the ideality of the conducting phase, the occluded water, is decreasing. As water is removed from the sample, the deswelling of the sample coupled with the decrease in the mobility of the polymer chains leads to an increase in the microscopic viscosity of the conducting phase and a decrease in the amount of conducting phase which results in a less ideal conductive phase.

A distinct change in AC impedance behaviour was observed at a water content of 12.1%. The broadened semi-circular locus transformed into a superposition of two separate semi-circles. This type of response has been observed previously by Watanabe et al.<sup>(35)</sup> in the study of the ionic conductivity of polymer complexes formed by segmented polyether poly(urethane ureas) and lithium perchlorate. They modelled their results on the following equivalent circuit:



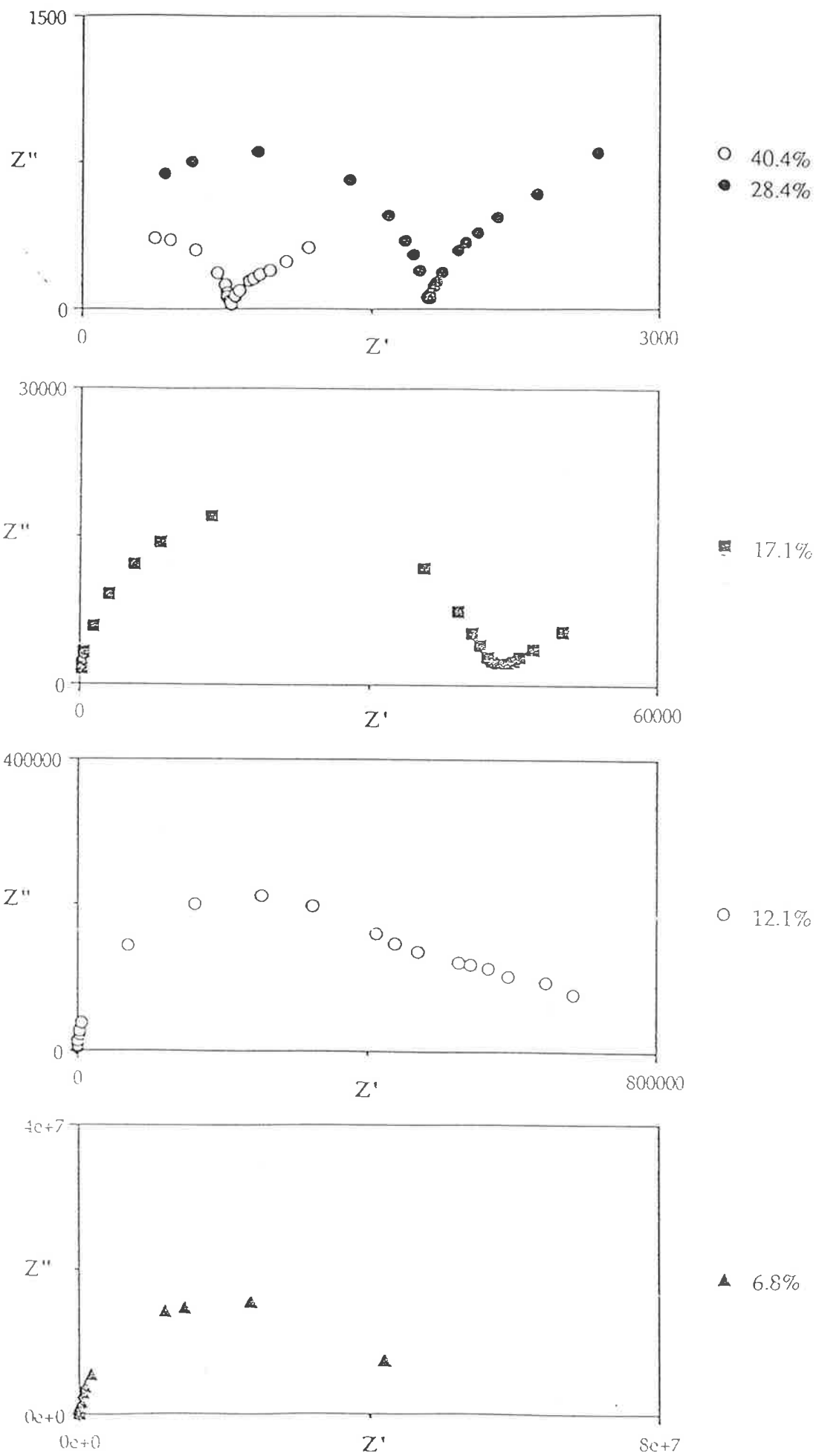


Figure 3.9

The AC impedance spectra of pHEMA at 25°C and several water contents as listed above.

( $Z'$  and  $Z''$  in Ohms)

$C_g$  is the geometrical capacitance and  $R_b$  is the bulk resistance of the continuous pathways for conduction provided by polyether regions with dissolved  $\text{LiClO}_4$ . The series combination of  $C_i$  and  $R_i$  refer to the pathways of polyether that are blocked by the presence of regions of semi-crystalline poly(urethane urea).  $C_i$  corresponds to the interfacial capacitance between the separate phases, the polyether soft segment in which the  $\text{LiClO}_4$  dissolved selectively and the poly(urethane urea) hard segment.

It would appear that similar morphological changes could occur in pHEMA as it is progressively dehydrated. It is suggested that at a water content of 12.1% there exists regions of the pHEMA network that are not sufficiently hydrated to support conductivity. This is indicative of the heterodispersion of water at these levels of hydration in pHEMA. As the water content was further decreased the locus again reverted to a singular semi-circle indicative of an increase of the discontinuous nature of the conducting phase. Similar behaviour was reported for the variation in the nature of the  $\alpha$ -transition in the dynamic mechanical analysis of hydrated pHEMA by Allen et al.<sup>(19)</sup>

The data suggests that the decrease in conductivity with water content is caused by three factors. Primarily, the amount of the conducting phase is decreased. The modes of molecular motion of the polymer are also inhibited, which will lead to decreases in both continuity of the conducting phase, and the microscopic viscosity of the water phase decreases. As the water content is decreased to 35% the resultant decrease in conductivity is due primarily to the decrease in microscopic viscosity of the conducting phase caused by the removal of the bulk-like water. As the water content is further decreased to 20% the conductivity decreases at a greater rate as not only is the microscopic viscosity decreasing but the removal of water has a more significant effect on the molecular motions of the polymer chains which in turn limits the continuity of the conducting phase. As the water content decreases from 20%

the microscopic viscosity decreases further but, more significantly, the continuity of the conducting phase is drastically affected by not only the decrease in molecular motion of the polymer ( $T_g = 25^\circ\text{C}$  at ca.  $\text{WC} = 20\%$ ) but also the lack of conducting phase itself as the water content approaches zero.

### 3.6.3 EGDMA/HEMA Copolymers.

The variation of conductivity with water content for a number of EGDMA/HEMA copolymers is presented in Figure 3.10, with a decrease in conductivity with water content being exhibited by all copolymers. One distinct difference between the behaviour of the copolymers investigated is that, over the entire range of water content, the conductivity is lower for copolymers of greater crosslinker concentration.

The three stage behaviour of the decrease in conductivity with hydration level of pHEMA is different from the trends exhibited by the EGDMA/HEMA copolymers. For crosslinker concentrations of 0.6 and 1.5 mol% there appears to be only two separate trends whereas for 3.0 mol% the variation of conductivity with water content is almost linear. Given that McBrierty et al.<sup>(14)</sup> proposed that bulk-like water is only present in pHEMA samples at water contents greater than 35% and the introduction of crosslinker results in polymer networks of lower equilibrium water contents, it is unlikely that any of the samples investigated will exhibit an increase in conductivity with water content due to the presence of bulk-like water.

Dynamic mechanical measurements by Allen et al.<sup>(19)</sup> at discrete water contents for a 3 mol% EGDMA/HEMA copolymer can be used to show that the  $T_g$  is  $25^\circ\text{C}$  at a water content of ca. 26%. The almost linear decrease in  $\log(\text{conductivity})$  3 mol% EGDMA/HEMA could be ascribed to the fact its glass transition temperature exceeds the experimentation temperature over nearly the entire water content range investigated. Although currently there is no data, given the conductivity behaviour for samples of 0.6 mol% and 1.5 mol%



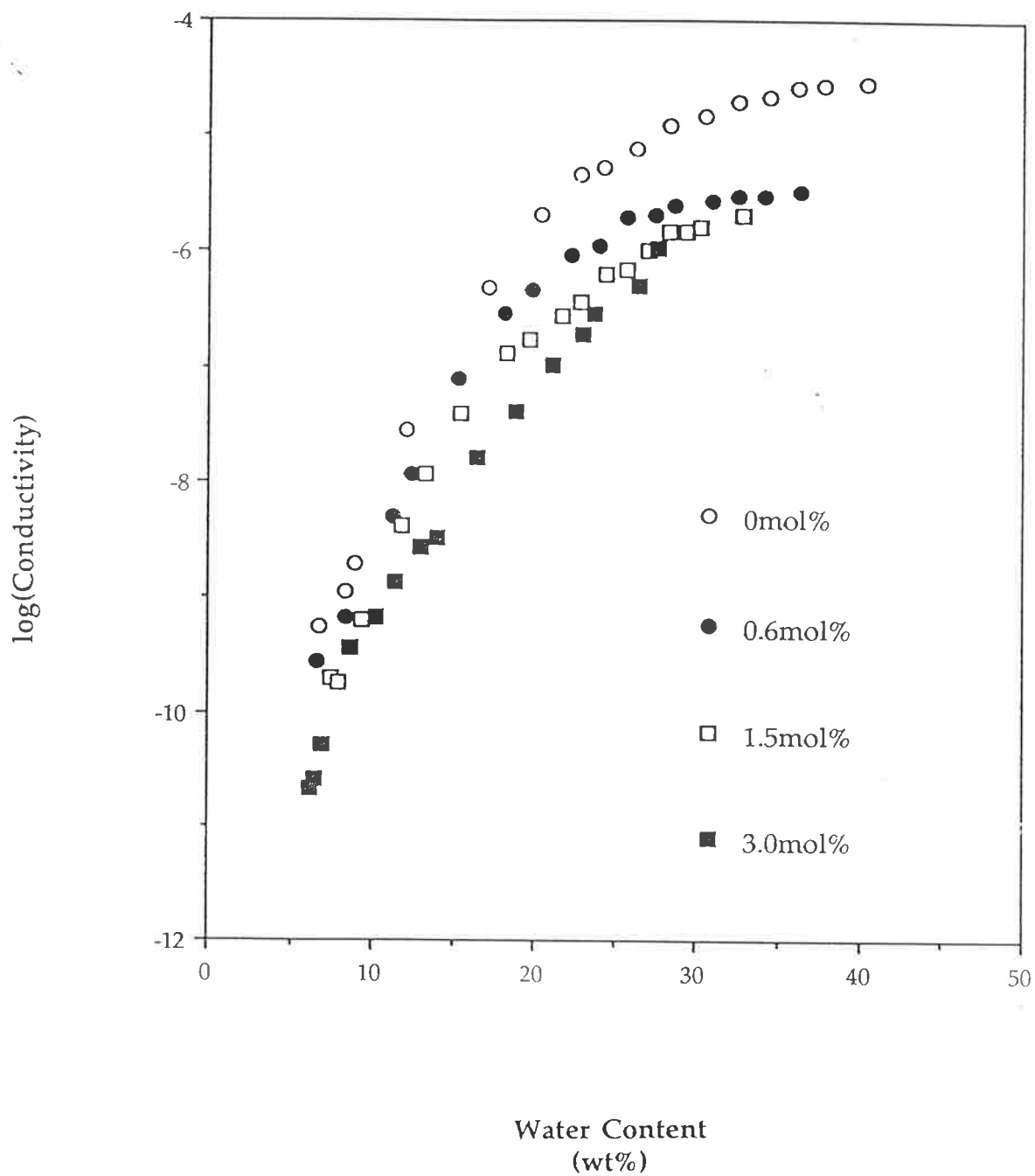


Figure 3.10

The Variation of Log(conductivity) with Water Content for several EGDMA/HEMA Copolymers at 25°C and EGDMA concentrations as listed above.

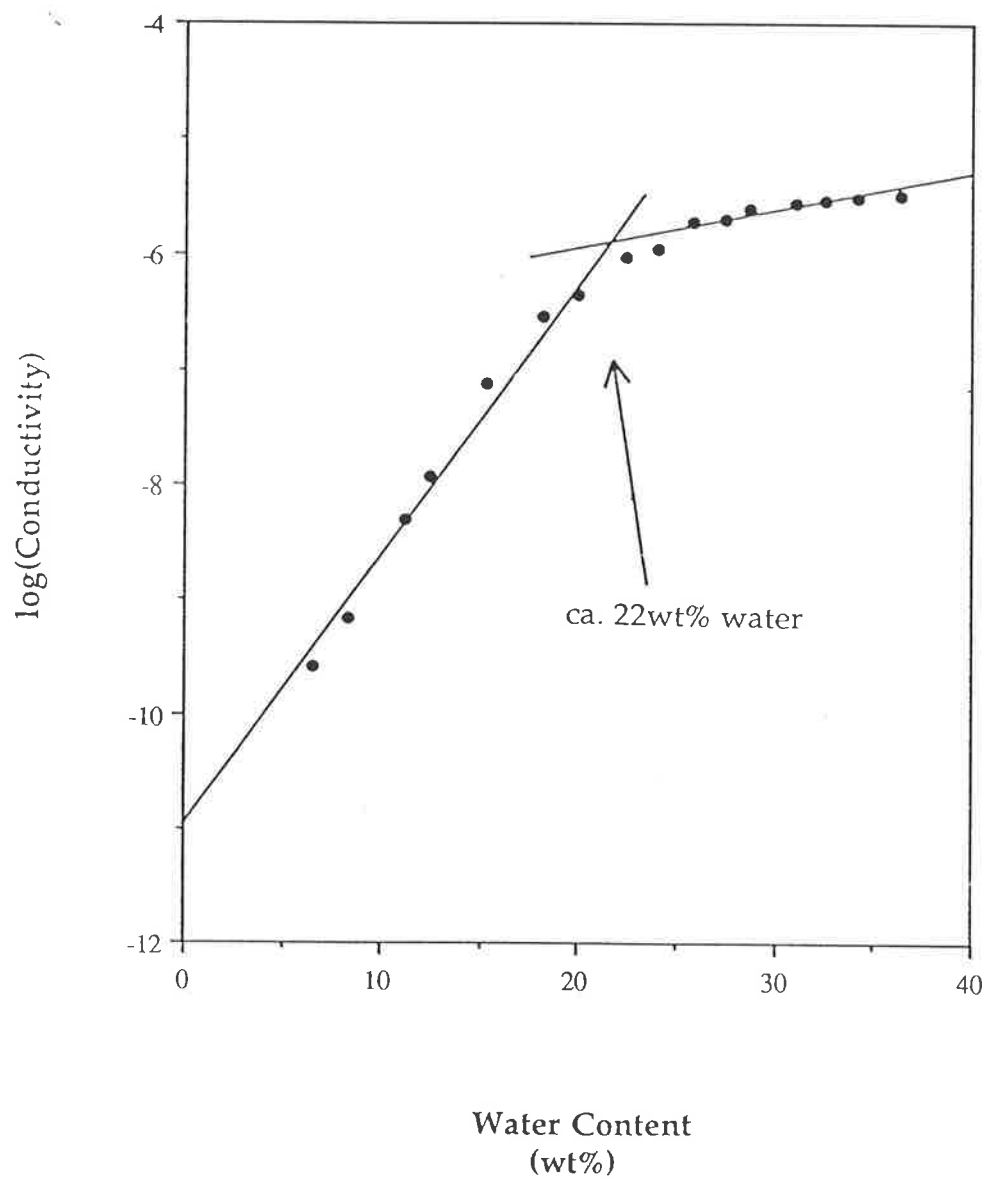


Figure 3.10a

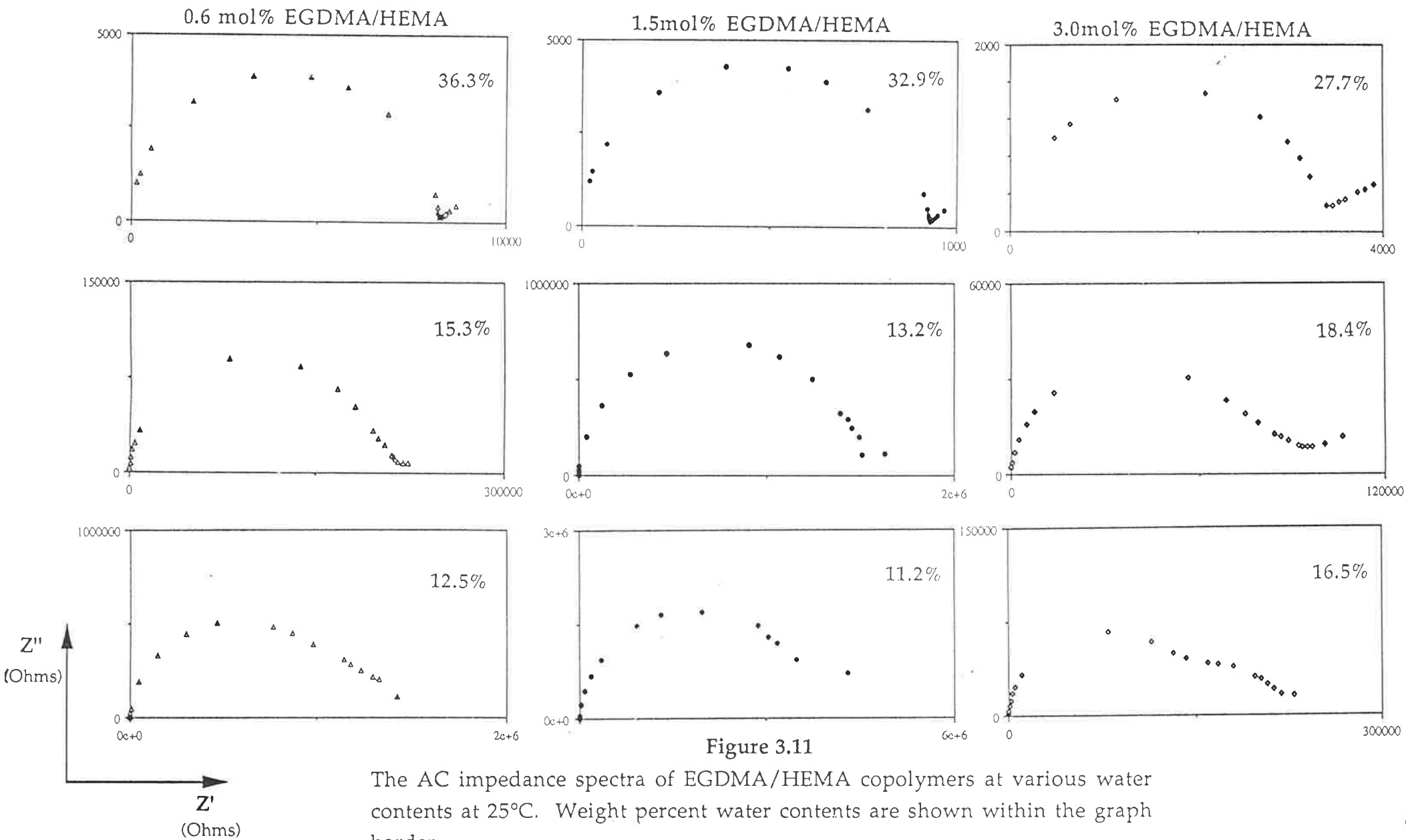
The estimation of the water content at which  $T_g=25^\circ\text{C}$  for 0.6mol% EGDMA/HEMA based on the variation of  $\log(\text{conductivity})$  with water content at  $25^\circ\text{C}$ .

EGDMA with decrease in hydration level, it could be suggested that  $T_g$  for these samples would be  $25^\circ\text{C}$  at water contents of approximately 22% and 26% respectively. As an example, Figure 3.10a shows how this estimation was carried out for the 0.6mol% EGDMA/HEMA copolymer.

The AC impedance spectra of the crosslinked samples underwent similar transformations with decrease in water content as exhibited by pHEMA. The semi-circular portion of the locus for all samples broadened with continued dehydration until the spectra resembled two superimposed semi-circles (Fig 3.11). It is of interest to note that the water content at which the change in the AC impedance response takes place is not significantly affected until the crosslinker concentration is 3mol% when it occurs at a higher water content. This appears to indicate that the continuity of the conductive water phase is more affected by the polymer network in the case of increased crosslinking.

### 3.6.3 OED/HEMA Copolymers.

The variation of conductivity with water content for a number of 3mol% OED/HEMA copolymers is presented in Figure 3.12. Again dehydration of these samples results in a dramatic decrease in the conductivity. The samples crosslinked with OEDs where  $n$  is 2 or more, i.e. DiEGDMA, TEGDMA and P400, exhibit behaviour similar to pHEMA but are distinct from the more rapid decrease in  $\log(\text{conductivity})$  shown by the EGDMA/HEMA copolymer. It appears that the behaviour of these copolymers is restricted to the two regions associated with bound and interfacial water; the third region of behaviour, attributed to bulk water, is unlikely given that none of these copolymers have EWCs greater than 35%. The copolymers, apart from the 3mol% EGDMA/HEMA, exhibit a change in the rate of decrease of the  $\log$  of conductivity with decrease in hydration level at approximately 22% water content. It is suggested that at 22wt% hydration



The AC impedance spectra of EGDMA/HEMA copolymers at various water contents at 25°C. Weight percent water contents are shown within the graph border.

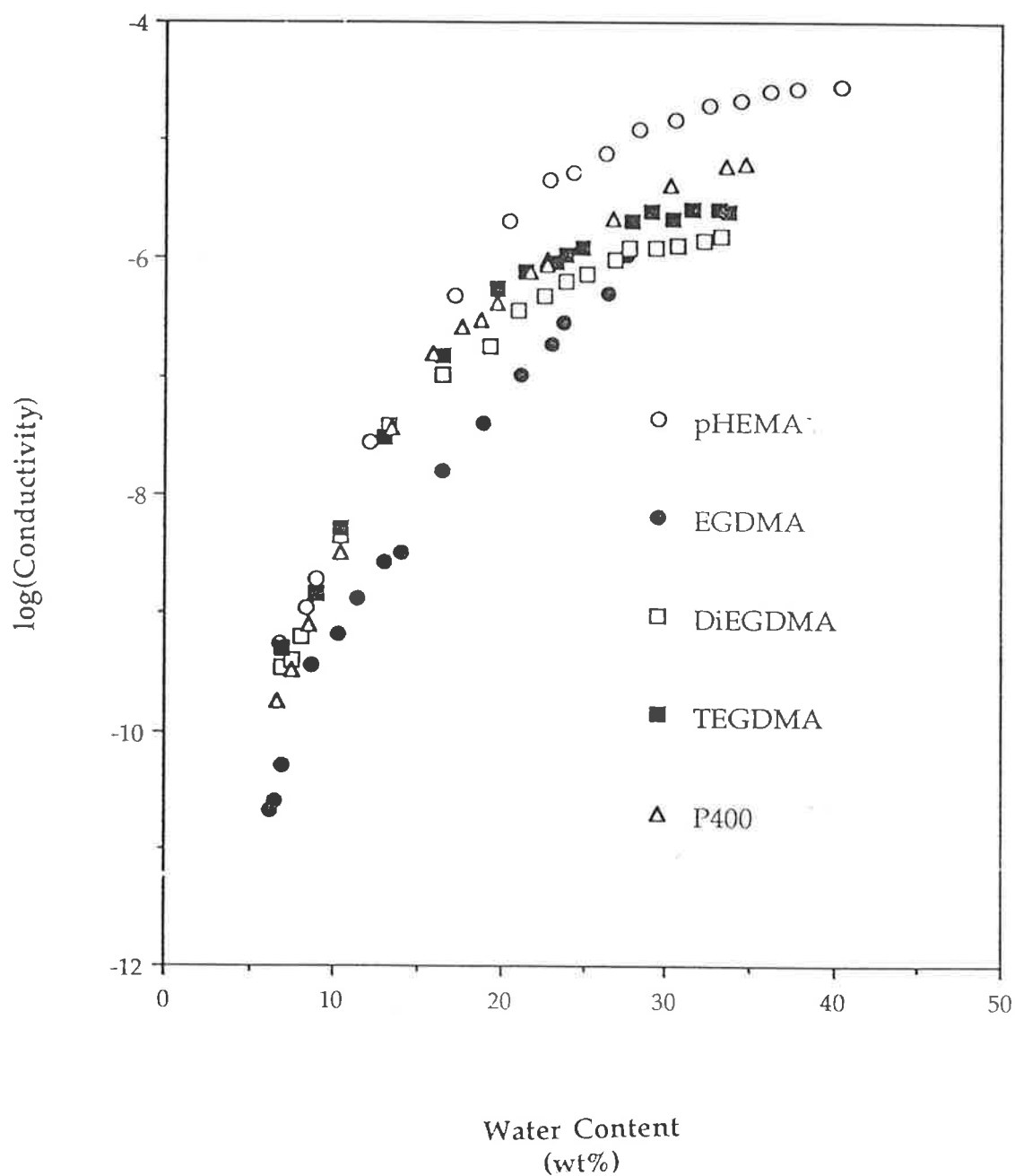


Figure 3.12

The Variation of Log(conductivity) with Water Content for several 3mol% OED/HEMA Copolymers at 25°C. OED as listed above.

the  $T_g$ s of the copolymers exceed the experimental temperature (25°C). Data from dynamic mechanical measurements by Bennett<sup>(25)</sup> reveal that 25°C is the  $T_g$  for both 3mol%TEGDMA and 3mol%P400 copolymers of around 24% water content. It should also be noted that as  $n$ , the number of ethylene glycol units in the OED, increases so does the conductivity at discrete water contents. However, the difference between the conductivity of different copolymers decreases as the hydration content under investigation decreases. It is suggested that this difference results from the effect the crosslink has on the structure, that is when  $n$  is larger, the crosslink is more flexible and able to promote interaction of regions of the water phase of suitable size to allow conductivity by the motions of the crosslink. It should be noted that the flexibility of the crosslink is also dependent on the level of plasticisation.

The AC impedance response of the OED copolymers at various hydration levels are shown in Figure 3.13. The transition in AC impedance behaviour from single semi-circle to the superposition of two semi-circles reflected a change in morphology with respect to the conductive phase for all copolymers subjected to dehydration. It should be noted that for DiEGDMA, TEGDMA and P400 crosslinked samples the change in AC response is first recognized at around the same level of hydration (ca. 10.4%). The 3mol% EGDMA/HEMA sample first exhibited such behaviour at 16.5% water content (Fig 3.10). It would appear that flexibility of the crosslink gained by the introduction of a second (and subsequently up to eight more) ethylene glycol units in the crosslink enhances the continuity of the conductive phase as the water content is decreased, that is the increased molecular motion of the crosslink enhances the continuity of the conducting phase.

### 3.7 The Variation of Conductivity with Temperature

#### 3.7.1 pHEMA.

The conductivity of a fully hydrated (EWC=40.4%) pHEMA sample was

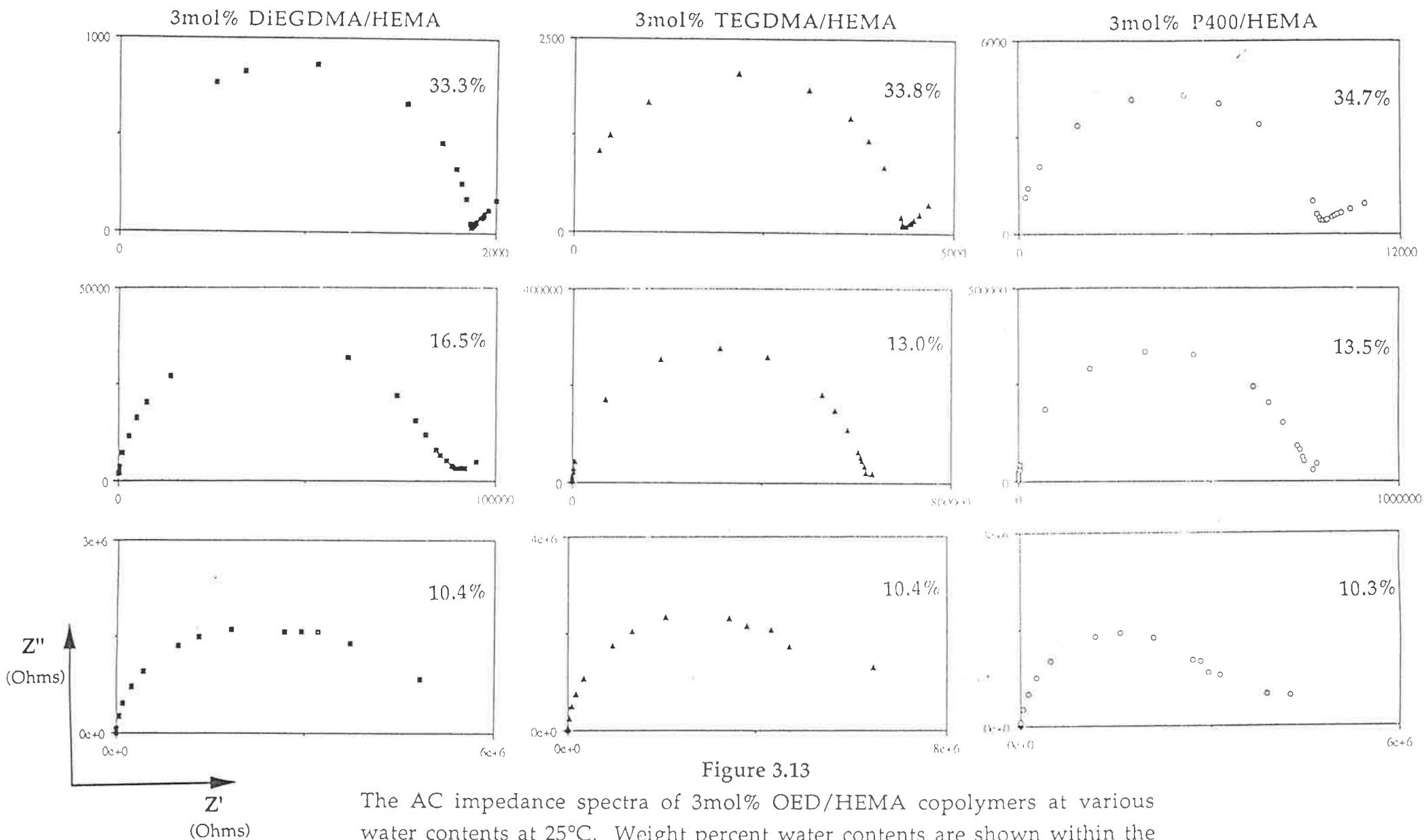


Figure 3.13  
 The AC impedance spectra of 3mol% OED/HEMA copolymers at various water contents at 25°C. Weight percent water contents are shown within the graph border.

recorded as it was cooled from room temperature to  $-10^{\circ}\text{C}$  and subsequently warmed to  $+10^{\circ}\text{C}$ . The cooling rate was  $0.22^{\circ}\text{C}/\text{min}$  and the heating rate was  $0.44^{\circ}\text{C}/\text{min}$ . The effect of temperature on the conductivity of pHEMA is shown in Figure 3.14. The change in  $\log(\text{conductivity})$  with  $1/T$  yields linear relationships indicating an Arrhenian dependence on temperature. Previous work by Reich and Michaeli<sup>(36)</sup> on ion doped, hydrated PAN systems yielded similar Arrhenian behaviour and activation energies were calculated using Equation 3.10 :

$$\sigma = A \exp(-E_a/RT) \quad \text{Eqn. 3.10}$$

The temperature dependent behaviour is best discussed by examining the change in conductivity over several temperature ranges. As the gel is cooled from room temperature, the  $\log(\text{conductivity})$  decreases linearly with an activation energy of  $15.0 \text{ kJ/mol}$  until at  $-5.8^{\circ}\text{C}$  when a sudden decrease in the  $\log(\text{conductivity})$  is observed. The  $\log(\text{conductivity})$  continues to decrease with temperature, but with a different activation energy of  $36.2 \text{ kJ/mol}$  until the minimum temperature is reached. On warming, the  $\log(\text{conductivity})$  increases linearly with no change in activation energy until the sample exhibits a large increase in  $\log(\text{conductivity})$  at  $2.5^{\circ}\text{C}$ . Again the  $\log(\text{conductivity})$  of the sample increases linearly with temperature, however it should be noted that the  $\log(\text{conductivity})$  values in this temperature range appear to be slightly greater than at similar temperatures on cooling. The increase in conductivity was greater the acceptable range of error anticipated for repeated measurements and thus this is deserving of further investigation.

The AC impedance response of the sample (Fig 3.15) also changed as the temperature was varied. As the sample was cooled the intercept of the semi-circular portion of the locus increased as did the sample's resistance and



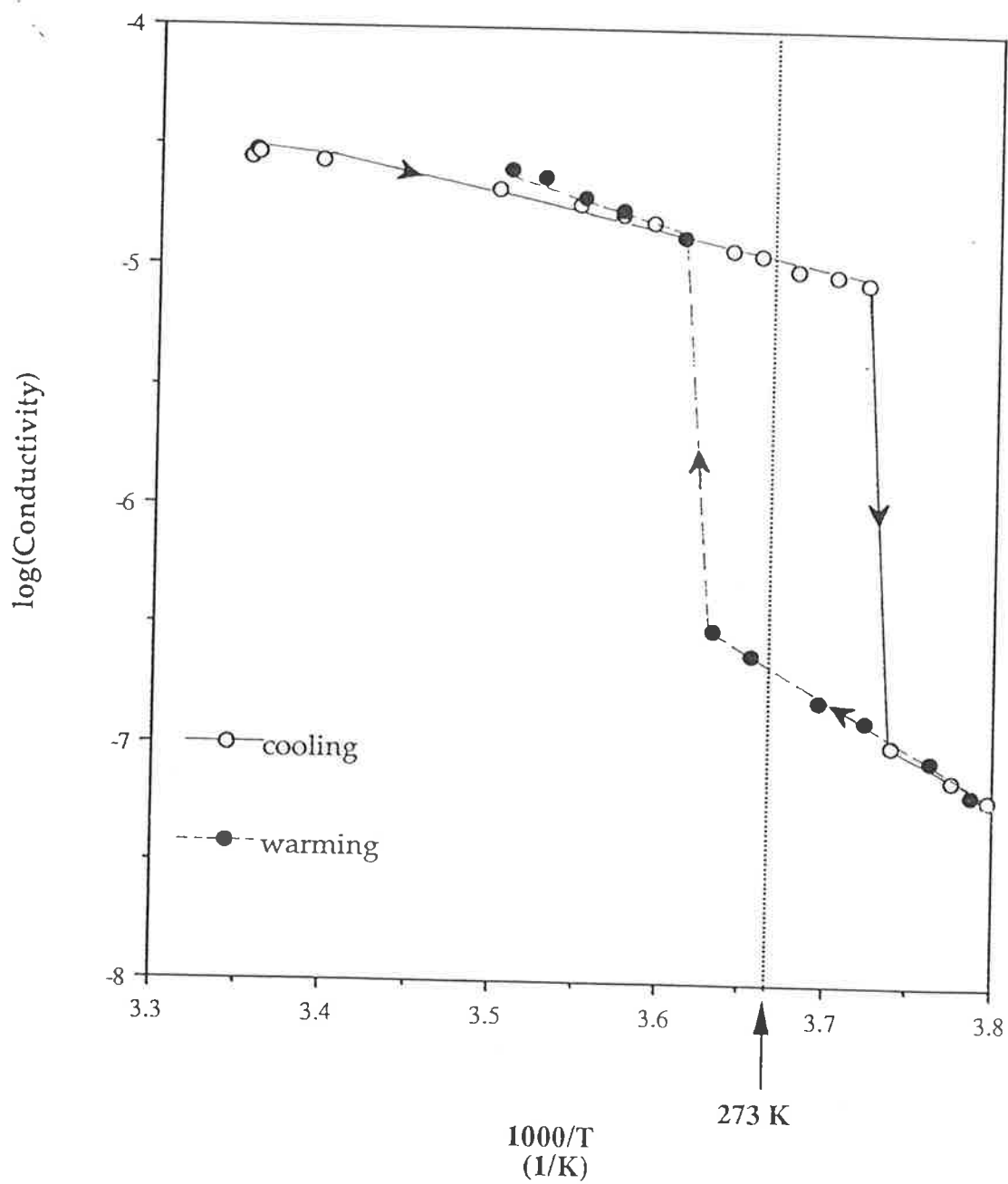


Figure 3.14  
The variation of log(conductivity) with  $1000/T$  for pHEMA at full hydration.  
(EWC=40.4%)

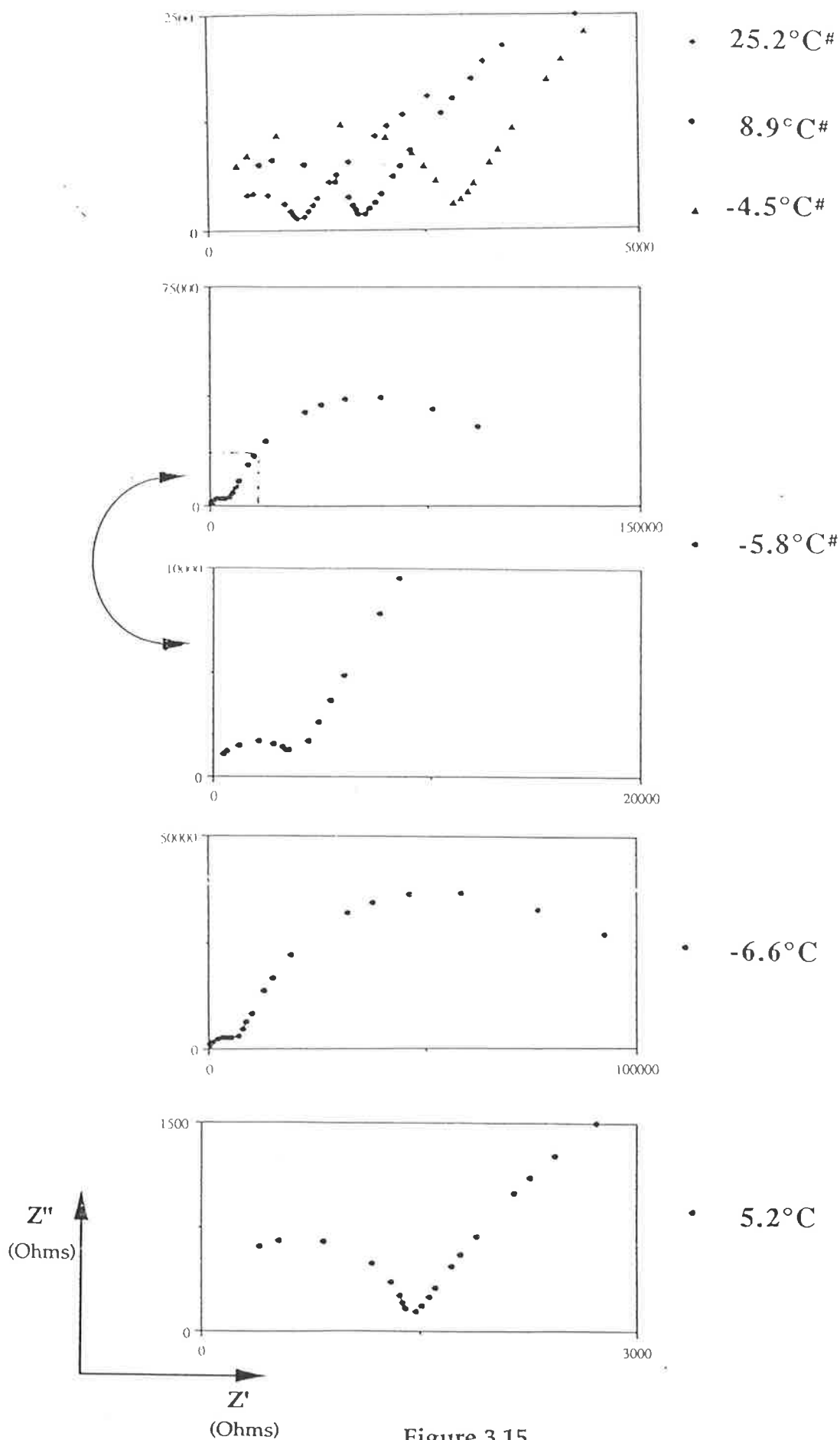


Figure 3.15

The AC impedance spectra of fully hydrated pHEMA (EWC=40.4%) at various temperatures as listed above.

(# indicates measurements made on cooling)

hence conductivity. However, at  $-5.8^{\circ}\text{C}$  the single semi-circular response transformed into the superposition of two semi-circles indicative of a morphological change with respect to the conductive phase, the absorbed water. Similar AC responses were observed for the sample as it was cooled to the minimum temperature ( $-10^{\circ}\text{C}$ ) and then warmed. At  $2.5^{\circ}\text{C}$  the nature of the AC impedance spectrum reverted to the anticipated semi-circular locus. This implies that the morphological change was temperature dependent and also reversible.

The change in morphology of the gel electrolyte may be a result of the freezing of some of the occluded water. It is documented that pHEMA hydrogels are subject to anomalous freezing of the occluded water when subjected to sub-zero temperatures. Allen et al.<sup>(11)</sup> reported that up to 33% of the available water can freeze in pHEMA samples. It should be noted that the amount of available water that freezes is dependent on the thermal history of the sample. Clearly, the variation of conductivity with temperature supports this hypothesis. The sharp decrease in conductivity does not occur until  $T = -5.8^{\circ}\text{C}$  which can be explained by the interactions of polymer and water leading to a depressed freezing point. The accompanying change in the nature of the AC impedance spectra (Fig.3.15) would indicate that regions of the conductive phase had become non-conductive to conductivity. Such regions could result from the formation of ice which has a much lower conductivity than of liquid water.

The change of activation energy can be ascribed to the appearance of crystalline ice regions impeding the path of charge carriers. Given that the density of ice is less than liquid water, the formation of ice will also lead to distortion of the polymer network on a microscopic scale which in turn could increase the local microscopic viscosity of the conducting phase thus contributing to the increase in activation energy. The return to the initial type of response at  $T = 2.5^{\circ}\text{C}$  can be explained by the thawing of the previously

frozen water. The deviation of this melt temperature from that expected for water (0°C) can be explained by the design of the experimental cell (Fig. 4.2.2); the sample was in the centre of the cell which was warmed from the outside, thus the recorded temperatures were slightly higher than those experienced at the same time by the sample during the warming cycle.

If the data of Allen et al.<sup>(11)</sup> is used and it is assumed that 33% of available water freezes during the cooling cycle it follows that the conductivity of the sample after freezing should be of the same order as that for a sample of ca.27% water. The decrease in conductivity after occluded water has frozen is comparable to the difference between the conductivities of pHEMA samples of 40.4% and 27%.

The observed change in activation energy occurs when the water freezes. This differs from the results obtained by Reich and Michaeli<sup>(36)</sup> for PAN/water/electrolyte systems where it was found that a change in activation energy corresponded to the onset of large scale molecular motion of the polymer network, i.e. at the glass transition temperature. The T<sub>g</sub> of fully hydrated pHEMA is reported as 0°C<sup>(19)</sup>. Clearly there is no transition revealed in the conductive behaviour at that temperature. It is suggested that at full hydration (EWC=40.4%) the polymer network plays very little role in the conductivity other than to support the conducting phase in this gel electrolyte. This is also reflected in the activation energy of conductivity for the sample (15.0kJ/mol) which is comparable to that of water (15.5kJ/mol\*)<sup>(37)</sup>.

The polymer network has been shown through dehydration experiments (Section 3.6) to exhibit influence on the conductivity of the gel electrolytes at lower water contents. Possible further work could include the investigation of the change in conductivity with temperature of partially hydrated samples to see if the glass transition results in a change in the conductivity behaviour.

---

\* activation energy calculated from data reported by Dobos (37)

### 3.7.2 EGDMA/HEMA Copolymers.

The conductivity of several EGDMA/HEMA copolymers at full hydration was measured for samples subjected to the same temperature cycle as used for pHEMA. The resultant variation of log(conductivity) with temperature is presented in Figures 3.16a-d.

All copolymers exhibited two regions of linear behaviour during the cooling/warming temperature cycle. The log(conductivity) decreased linearly for all samples until at some sub-zero temperature a sudden decrease in log(conductivity) was experienced. The temperature at which this decrease occurred increased with EGDMA concentration until for the 3mol% EGDMA/HEMA sample the decrease coincided with the initiation of warming. The decrease in log(conductivity) experienced by the samples decreased as the concentration of the crosslinker increased. However, the 1.5mol% EGDMA/HEMA did not follow this trend and showed an unexpectedly small decrease in log(conductivity). Associated with this sharp decrease in log(conductivity) was a change in the activation energy (Table 3.7).

**Table 3.7**

The activation energies of conductivity for EGDMA/HEMA copolymers at full hydration.

[EGDMA] (mol%)	$E_{a1}$ (kJ/mol)	$E_{a2}$ (kJ/mol)
0.0	15.0	36.2
0.3	16.3	24.2
0.6	16.9	24.5
1.5	16.9	22.6
3.0	22.5	-

$E_{a1}$  is the activation energy on cooling.

$E_{a2}$  is the activation energy at subzero temperatures on warming.

It should be noted that as the concentration of EGDMA increased the activation energy of the initial cooling conductivity behaviour,  $E_{a1}$ , increased

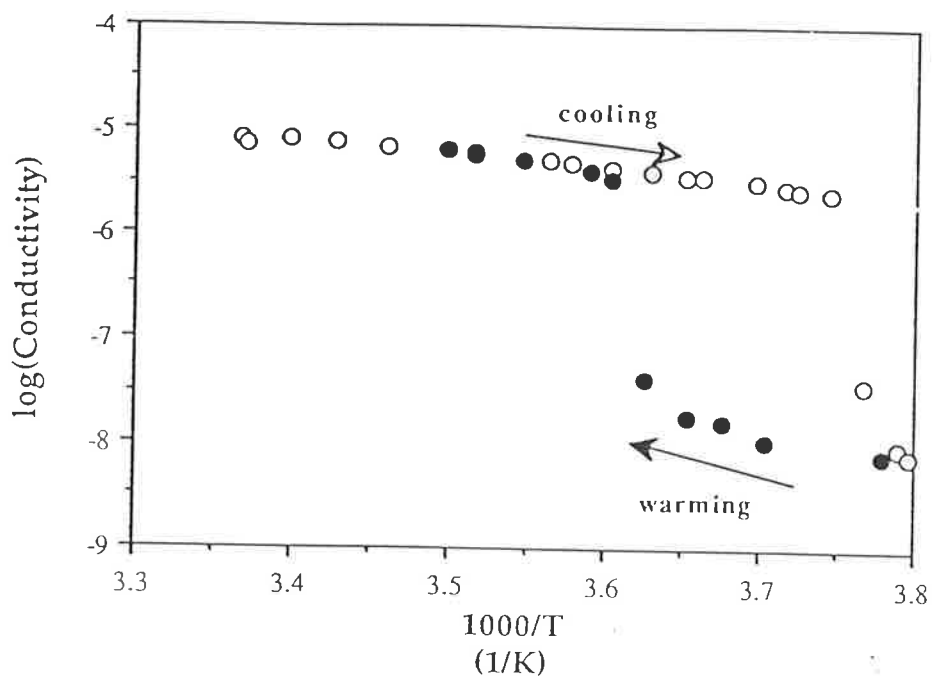


Figure 3.16a

The variation of  $\log(\text{conductivity})$  with  $1000/T$  for 0.3mol% EGDMA/HEMA at full hydration.

Hollow markers indicate that measurement taken during cooling cycle. Solid markers indicate measurement during warming cycle.

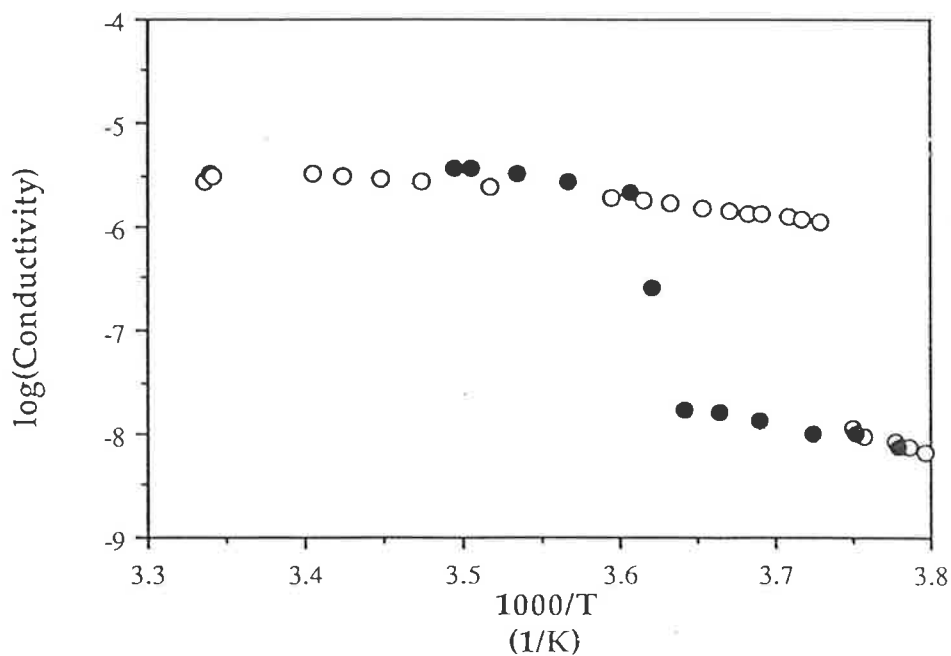


Figure 3.16b

The variation of  $\log(\text{conductivity})$  with  $1000/T$  for 0.6mol% EGDMA/HEMA at full hydration.

Hollow markers indicate that measurement taken during cooling cycle. Solid markers indicate measurement during warming cycle.

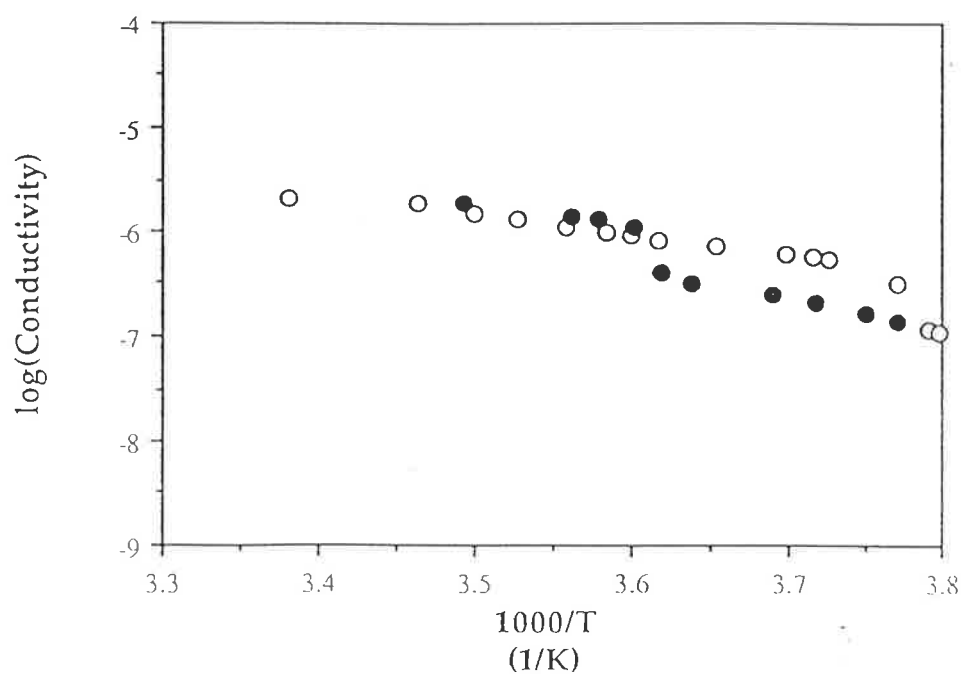


Figure 3.16c

The variation of  $\log(\text{conductivity})$  with  $1000/T$  for 1.5mol% EGDMA/HEMA at full hydration.

Hollow markers indicate that measurement taken during cooling cycle. Solid markers indicate measurement during warming cycle.

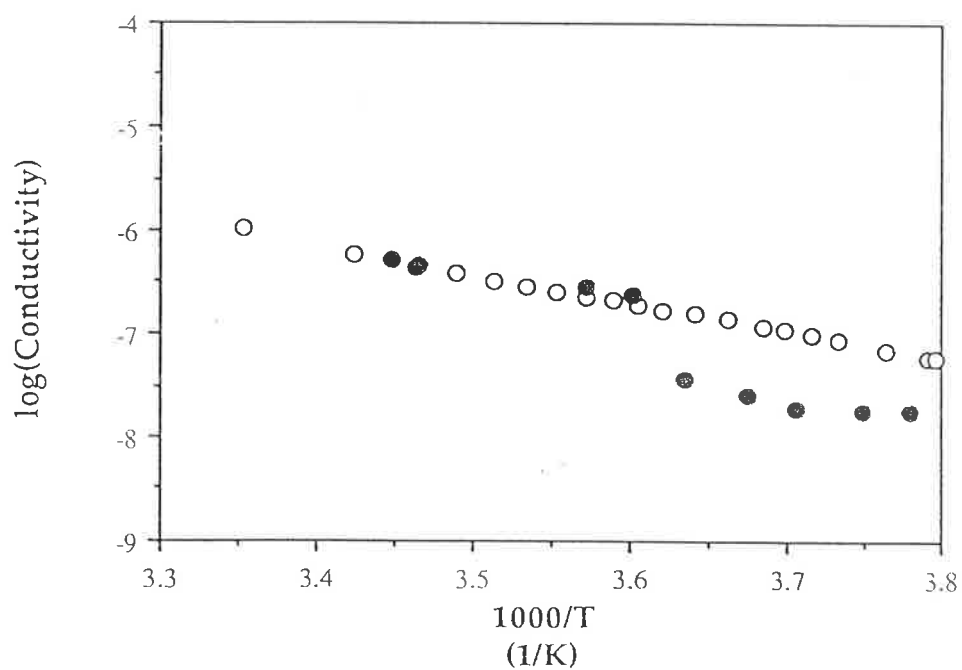


Figure 3.16d

The variation of  $\log(\text{conductivity})$  with  $1000/T$  for 3.0mol% EGDMA/HEMA at full hydration.

Hollow markers indicate that measurement taken during cooling cycle. Solid markers indicate measurement during warming cycle.

whereas the activation energy of the conductivity behaviour prior to the transition at ca.0°C on warming decreased.

$E_{a2}$  was not calculated for 3mol% EGDMA/HEMA because there was insufficient linear conductivity data on warming prior to the increase in  $\log(\text{conductivity})$  at ca.0°C.

All samples exhibited a sharp increase in  $\log(\text{conductivity})$  when they were warmed past 0°C and subsequently increased linearly in a manner similar to the initial cooling behaviour. However, it should be noted that there appears to be a slight increase in the  $\log(\text{conductivity})$  in this temperature range in comparison to the initial cooling behaviour.

These results reinforce the hypothesis that the transition in the conductivity data is due to the freezing of water within the copolymer samples. The sudden decrease in  $\log(\text{conductivity})$  at subzero temperatures is consistent with the freezing behaviour of water in polymers as the change in behaviour is reversible and reverts on warming at ca.0°C, the melting point of water. Allen et al.<sup>(11)</sup> have shown by DSC and <sup>1</sup>H NMR that the amount of freezable water in EGDMA/HEMA copolymers decreases as the concentration of EGDMA increases. The decrease in  $\log(\text{conductivity})$  at the transition on cooling also decreases as EGDMA increases, that is less of the conducting phase is frozen. Allen et al. claimed that ca. 7% of available water in 3mol% EGDMA/HEMA copolymers is able to be frozen. The decrease in conductivity on the removal of 2wt% water (EWC=27.7wt%) from the 3mol% EGDMA/HEMA sample, i.e. ca.7% of available water at full hydration, is comparable to the decrease in conductivity of a fully hydrated sample that has been subjected to a cooling temperature cycle. The activation energy ( $E_{a2}$ ) of the conductivity at temperatures below 0°C on warming decreases as EGDMA increases. This could be ascribed to less of the conducting phase freezing reducing any impediment to remaining conductive pathways in comparison to the pHEMA sample.



The increase in  $E_{a1}$  as EGDMA concentration increases is indicative of the effect of crosslinking of the polymer network on the structure of the occluded water. Increased crosslinking decreases the hydrophilicity of the network and its ability to swell. This in turn leads to decreases in the mobility, the amount and the continuity of the conductive phase and is reflected in the increase in activation energy.

Allen et al.<sup>(19)</sup> report the  $T_g$  of 3mol% EGDMA/HEMA to be 13.9°C at full hydration. No transition was observed at this temperature for such a sample, reinforcing the belief that at full hydration the polymer matrix plays a minimal role in the conductivity of the hydrogel.

### 3.7.3 OED/HEMA Copolymers.

The conductivity of several 3mol%OED/HEMA copolymers at full hydration was measured for samples subjected to the same temperature cycle as that for pHEMA. The resultant variation of  $\log(\text{conductivity})$  with temperature is presented in Figures 3.17a-d.

Again the copolymers exhibited two regions of linear behaviour during the cooling/warming temperature cycle. The sudden decrease in conductivity at subzero temperatures on cooling and the subsequent increase at ca.0°C on warming again is indicative of water freezing and thawing during the temperature cycle. The activation energies of the samples exhibited during the temperature cycle are given in Table 3.8. It should be noted that  $E_{a1}$  was found to increase as  $n$ , the number of ethylene glycol units in the crosslinker, increased. The magnitude of the decrease in  $\log(\text{conductivity})$  at the subzero transition was also found to increase as  $n$  increased.

The conductivity behaviour observed is attributable to partial freezing of the occluded water. Allen et al.<sup>(11)</sup> have shown through DSC and  $^1\text{H}$  NMR investigations that as  $n$  is increased for OED/HEMA copolymers of the same crosslinker concentration the amount of absorbed water increases as does the

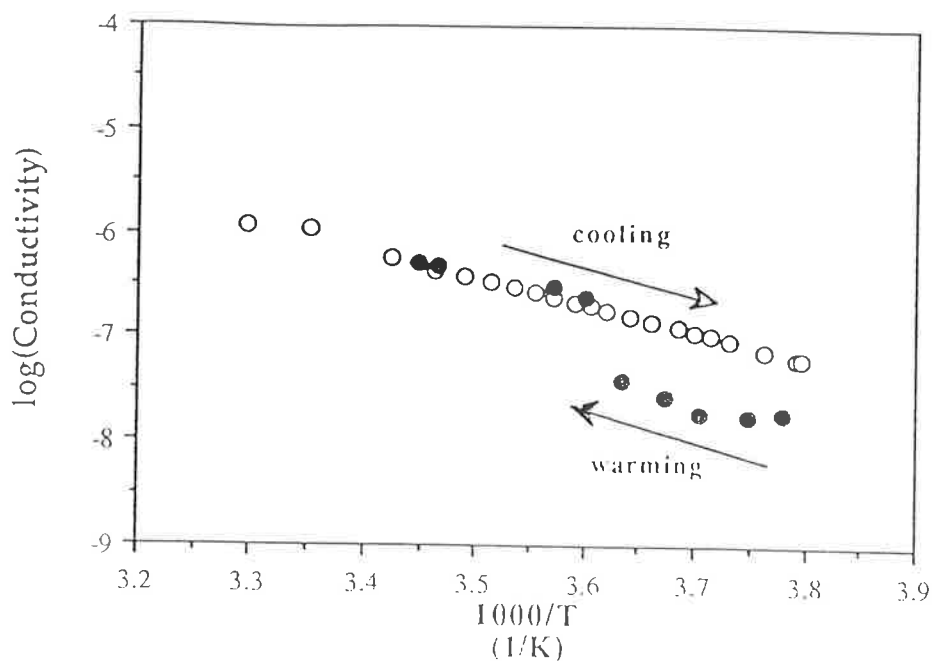


Figure 3.17a

The variation of  $\log(\text{conductivity})$  with  $1000/T$  for 3.0mol% EGDMA/HEMA at full hydration.

Hollow markers indicate that measurement taken during cooling cycle. Solid markers indicate measurement during warming cycle.

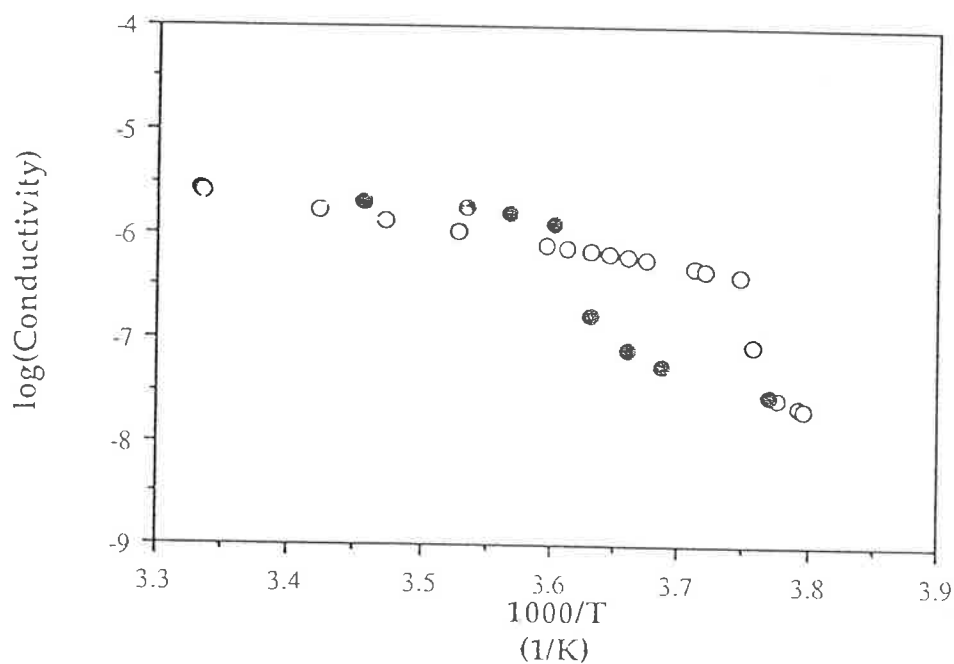


Figure 3.17b

The variation of  $\log(\text{conductivity})$  with  $1000/T$  for 3.0mol% DiEGDMA/HEMA at full hydration.

Hollow markers indicate that measurement taken during cooling cycle. Solid markers indicate measurement during warming cycle.

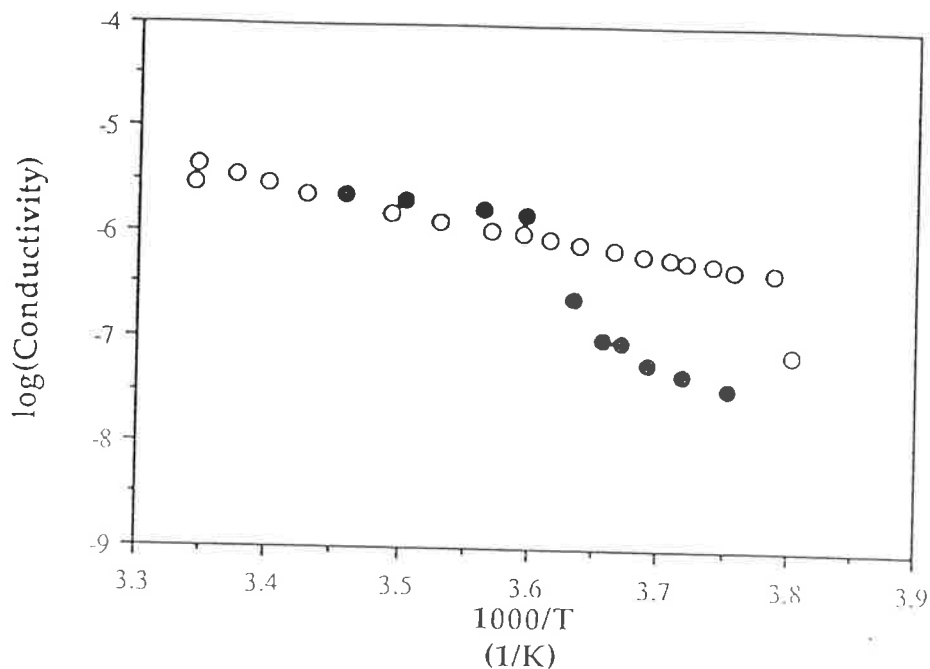


Figure 3.17c

The variation of log(conductivity) with  $1000/T$  for 3.0mol% TEGDMA/HEMA at full hydration.

Hollow markers indicate that measurement taken during cooling cycle. Solid markers indicate measurement during warming cycle.

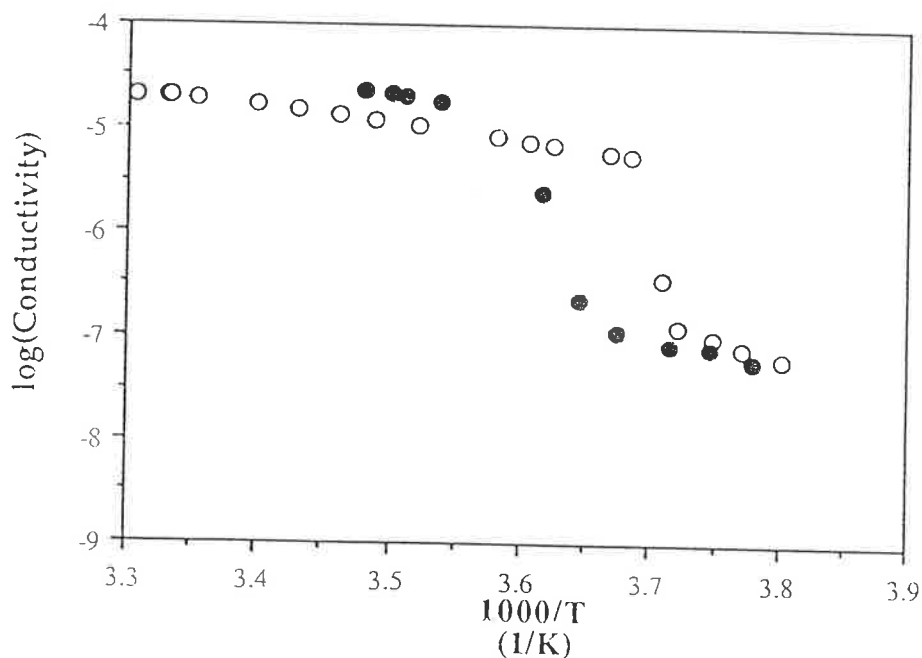


Figure 3.17d

The variation of log(conductivity) with  $1000/T$  for 3.0mol% P400/HEMA at full hydration.

Hollow markers indicate that measurement taken during cooling cycle. Solid markers indicate measurement during warming cycle.

relative proportion of this water that is capable of freezing. An increase in  $n$  results in an increase in hydrophilicity and extends the length of the crosslink thus enhancing the ability of the copolymer to swell. This explains the greater decrease in  $\log(\text{conductivity})$  and also the decrease in  $E_{a1}$  as  $n$  increases.

**Table 3.8**

The activation energies of conductivity for 3mol%OED/HEMA copolymers at full hydration.

OED	n	$E_{a1}$ (kJ/mol)	$E_{a2}$ (kJ/mol)
EGDMA	1	22.5	-
DiEGDMA	2	15.5	31.9
TEGDMA	4	15.4	35.2
P400	9	15.3	32.8

$E_{a1}$  is the activation energy on cooling.

$E_{a2}$  is the activation energy at subzero temperatures on warming.

No transitions in the conductivity data appeared at the glass transition of the P400 and theTEGDMA crosslinked samples, Allen et al.<sup>(19)</sup> report their  $T_g$ 's at full hydration to be 5.7°C and 4.0°C.

### 3.8 Summary.

The conductivity of fully hydrated pHEMA (EWC=40.4%) at 25°C is  $2.86 \times 10^{-5} \text{ Scm}^{-1}$ . As is the case for gel electrolytes, the conductivity is dependent on the nature and quantity of the conductive phase (the occluded water) with the polymer functioning as a support.

The introduction of several OED crosslinkers decreased the conductivity of the resultant gels by decreasing the water absorbing capabilities of the copolymers and also decreasing the mobility of the occluded water. Dehydration experiments suggested the three roles that water has in determining the nature of the conducting phase. The absorbed water

provides the conducting phase, it plasticises the polymer matrix, liberating segmental motion of the polymer matrix, which in turn increases the continuity of the conducting phase and swells the polymer which results in the increased mobility of the conducting phase as the water content increases.

The investigation of the conductivity with variable temperature revealed that conductivity was dependent on the phase transitions of the conductive phase. For all hydrogels studied, no temperature dependent transition corresponded to the glass transition indicating the minimal influence of the polymer matrix on the conductivity at full hydration. However, a change in the conductivity behaviour exhibited by pHEMA during dehydration when  $T_g$  was equivalent to the temperature of investigation ( $25^\circ\text{C}$ ) would infer that this is not necessarily the case for samples of lower water content and warrants further investigation.

AC impedance measurements reflected structural changes taking place in the hydrogel samples as various environmental parameters were altered.

## CHAPTER FOUR

### *The AC Conductivity of ion doped pHEMA*

#### 4.1 Introduction

The introduction of ions to hydrogels further complicates an already complex system. To understand ion motion, and thus conductivity, it is necessary to consider the numerous interactions that can take place between ions, absorbed water and the polymer matrix. These interactions have been summarised in a table by Zaikov et al.<sup>(1)</sup> (Table 4.1).

The structure of bulk water can be considered to consist of long range tetrahedrally co-ordinated hydrogen bonds<sup>(2)</sup>. The introduction of electrolytes interferes with this dynamic equilibrium structure and induces the formation of three different water phases<sup>(3,4)</sup>. The primary water phase, in the immediate vicinity of the ions, is strongly associated and ordered by the ions. The secondary phase exists beyond the primary phase water and is less ordered by the electrolyte than the primary phase. The tertiary phase is unaffected by the electrolyte and is bulk water.

The nature of the electrolyte determines the ratio of primary phase ordering to secondary phase disordering. Relatively small ions, i.e. Na<sup>+</sup>, Li<sup>+</sup>, and multivalent ions, i.e. Ca<sup>2+</sup>, are described as structure-making ions. They order and electrostrict near-neighbour water molecules and their higher charge density induces order in water molecules beyond the primary hydration shell resulting in a long range hydration shell. Large monovalent ions, i.e. K<sup>+</sup>, Cl<sup>-</sup>, Br<sup>-</sup>, I<sup>-</sup>, ClO<sub>4</sub><sup>-</sup>, have lower charge density and, consequently, are only capable of ordering near-neighbour water molecules. This in turn leads to a more extensive secondary phase. Such ions are referred to as net structure breakers.

Type of interaction	Characteristic of interaction	Physico-chemical phenomena involved
Polymer-polymer	Electric, polar, dispersion interactions.	Variety or ordered crystal and submolecular structures. Three main states: glassy, highly elastic and viscoplastic.
Electrolyte-electrolyte	Electric forces (ion-ion). Monopole-dipole interactions (between undissociated electrolyte molecules). Hydrophobic interactions (between large organic).	Coulomb interactions, presence of ionic atmosphere, mass action law, dissociation, complexing.
Water-Water	Dipole-dipole interactions.	Hydrogen bonds, formation of ordered structures (clusters), equilibrium between clustered water and monomeric (free) water.
Electrolyte-water	Monopole-dipole interactions.	Hydration, formation of crystalline hydrates.
Water-polymer	Polar and hydrophobic interactions.	Hydration of polymer groups and segments, plasticisation, antiplasticisation, conformational transformations, crystalline transformations, amorphization, degradation etc.
Electrolyte-polymer	Electric and polar forces, hydrophobic interactions (for large organic ions).	Conformational transformations of macromolecules, crystalline transformations, complexation, structurization (with polyvalent ions), plasticization.

Table 4.1

A summary of the possible interactions in polymer/water/electrolyte systems.  
[Reproduced from (1).]

Although most descriptions of the nature of water in pHEMA refer to bulk or free water, it should be noted that there does not exist any bulk water in its true form; this is reflected in the narrow  $^1\text{H}$  nmr linewidths of bulk water (a few Hz)<sup>(5)</sup> compared to the water phase in pHEMA hydrogels (several hundred Hz)<sup>(6)</sup>. The interaction of ions and water will also depend in part on water/polymer, ion/polymer and water/ion/polymer interactions. The interaction of electrolyte solutions with pHEMA gels has been the subject of several investigations.<sup>(7-12)</sup>

The most evident effect of electrolyte solutions on pHEMA is the resultant alteration of the hydrogels ability to swell when placed in electrolyte solutions of varying concentration<sup>(7,8)</sup>. Refojo<sup>(7)</sup> investigated the hydration of pHEMA samples soaked in different electrolyte solutions. The nature of the anion was found to play the dominant role in determining the hydration achieved. However, it is believed that the nature of the ion/polymer interactions control the level of hydrophobic interaction of the polymer matrix and subsequently the resultant hydration level. Samples soaked in chloride solutions were found to have greatly reduced water contents compared with samples soaked in water, whereas bromides reduced hydration minimally and iodides drastically increased water contents. Differences in the equilibrium water contents of ion doped compared to ion free gels generally levelled off with increasing solute concentration. This behaviour was found to be more pronounced for electrolytes that enhanced hydration.

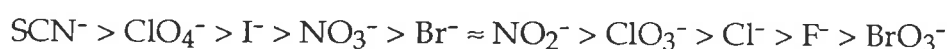
Refojo suggests that the increase in hydration of samples in iodide solutions can be ascribed to polymer/ion interactions. It is believed that iodide ions adsorb to portions of the polymer network resulting in a polyelectrolyte effect. The electrostatic repulsion between adsorbed iodide anions impairs hydrophobic interactions and causes the expansion of the polymer network and increased EWC. PHEMA samples hydrated in iodide



solutions were reported to be yellow. Refojo described this as evidence for a direct association between the polymer and the iodide (or more likely triiodide) anions. Refojo postulates that as the concentration of solute increases the swelling effect should decrease as ions may be shielded from one another with increasing hydration.

It would appear that as the charge density of the anion increases the likelihood of the polyelectrolyte effect taking place decreases. Bromide solutions yielded slight decreases in the EWC of pHEMA whereas chloride solutions led to greater reductions in the EWC. It would appear that the relatively greater water ordering ability of the chloride anion leads to the greatest enhancement of the hydrophobic bonding, thus limiting gel swelling to a greater extent than for the bromide anion.

Dusek et al.<sup>(8)</sup> obtained similar results with a wide range of anions. Gel swelling decreased in the following order:



No ordering of cations was achieved in the same study due to a lack of accurate data. However, in the case of pHEMA they believe that cations may also directly interact with the polymer matrix via association of polar groups (i.e OH) into their hydration sphere. This type of interaction would be most likely to occur between cations of high charge density and polar groups with high dipole moments. Conformational stability measurements on pHEMA by Kang and Jhon<sup>(9)</sup> correlated increases in swelling with the exposure of the hydrophobic portions of the pHEMA network at the surface due to interaction with anions whereas they found cations to have considerably less influence.

The interaction of ions with pHEMA hydrogels has also been studied using nmr. <sup>127</sup>I nmr measurements of 0.1M solutions of isotactic pHEMA in 0.1M KI solutions by Oh et al.<sup>(10)</sup> resulted in significant broadening of the <sup>127</sup>I signal, when compared to the signal of an aqueous solution of KI of the same concentration; this was attributed to specific binding of the iodide anion to the

polymer.  $^{39}\text{K}$  nmr measurements in the same study showed only a slight increase in the signal linewidth with increasing polymer concentration, and this was attributed to the lack of direct association of potassium cations to the polymer matrix. However  $^{23}\text{Na}$  nmr investigation of pHEMA hydrogels hydrated in 2wt% NaCl solution by Quinn et al.<sup>(10)</sup> found that even in a heavily hydrated state the  $^{23}\text{Na}$  linewidths were significantly broader than for saline solutions of comparable concentration. It would appear from this result that  $\text{Na}^+$  ions have limited association with the polymer at high hydration levels.

The nature of the water present in pHEMA hydrogels hydrated in electrolyte solutions has been shown by DSC<sup>(11-13)</sup> to be dependent on the nature of the electrolyte employed. Tighe et al.<sup>(12,13)</sup> have shown that both water uptake and the amounts of freezing and nonfreezing water present in a series of pHEMA samples hydrated in a range of potassium salts were dependent on the nature of the anion. Structure breaking anions increased both the water uptake and the amount of freezing water present yet decreased the amount of nonfreezing water present. Structure making anions yielded decreases in water uptake and freezing water and increases in nonfreezing water. DSC thermograms recorded for all the samples<sup>(12)</sup> hydrated in electrolyte solutions exhibited significant variation in the fine structure of the melting endotherms indicative of the influence of the electrolytes on the water structure.

The introduction of electrolytes to pHEMA hydrogels at full hydration will undoubtedly lead to an increase in conductivity as this will increase the number of available charge carriers (Eqn 1.2). However conductivity is also dependent on the mobility of these charge carriers which will depend on the various polymer/water/electrolyte interactions.

In this study the conductivity of pHEMA samples hydrated in KBr solutions of varying concentration has been investigated. KBr was chosen

due to its minimal effect on the water uptake of pHEMA<sup>(7,8)</sup>. Conductivity of KBr solution hydrated samples subjected to variations in crosslinker concentration, nature of crosslinking agent, water content and temperature was determined as for samples hydrated in water in Chapter 3. The conductivity of pHEMA samples hydrated in a range of different electrolytes has also been studied to investigate the effect of the nature of the electrolyte.

## 4.2 The AC Impedance Spectrum

The AC impedance plots, recorded at 25°C, of pHEMA samples hydrated in solutions of varying KBr concentration are shown in Figure 4.1. All samples exhibited similar behaviour in the frequency range studied. Non vertical spikes were recorded for all samples whose EWCs decreased as the concentration of the soaking solution increased. Although no high frequency semi-circle was recorded it was assumed that the bulk resistance of the sample was equivalent to the intercept value of the locus on the real impedance axis. This intercept was larger in value for samples hydrated in solutions of lower KBr concentration.

## 4.3 The AC conductivity of KBr doped pHEMA

pHEMA discs were soaked in a range of KBr solutions varying in concentration from 1.0M to 0.10M at a constant temperature of 25°C until they reached a constant maximum weight (3-4 weeks). All gels swollen in KBr solutions were colourless and clear at full hydration. Their conductivities were measured at 298K and the results are given in Table 4.2. After the conductivities of the samples were evaluated, the pHEMA discs were placed in a vacuum oven (50°C) until a constant dry weight was reached and then KBr uptake and EWC were calculated.

The hydration of pHEMA in KBr led to EWCs that were in agreement with the work by Refojo<sup>(7)</sup> and Dusek et al.<sup>(8)</sup>; that is the addition of KBr led

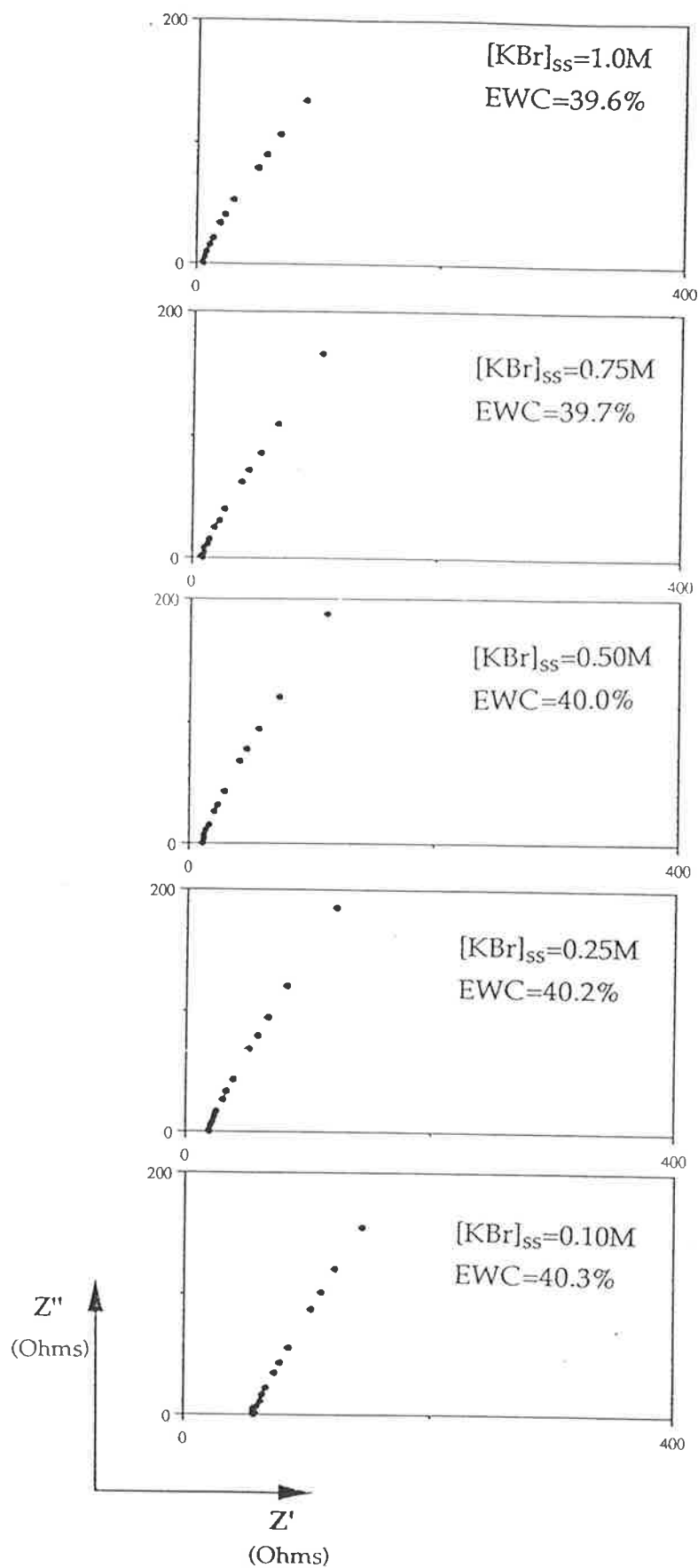


Figure 4.1

The AC impedance plots of PHEMA samples fully hydrated in KBr solutions of varying concentration. EWC and KBr solution concentration as listed above. Hydration and AC measurements carried out at 25°C.

to a decrease in the EWC, with the decrease being greater for samples hydrated in solutions of greater concentration. It should be noted that the concentration of KBr in the water phase of the gels is similar to that of the KBr in the soaking solution employed. (e.g. for pHEMA in 1M KBr:  $[KBr]_{gel} = ((4.17 \times 10^{-4} / 0.396) \times 1000) = 1.05M$ ).

Table 4.2

The variation in KBr uptake, EWC and conductivity of pHEMA samples hydrated in KBr solutions of varying concentration at 25°C.

$[KBr]_{ss}^{\dagger}$ (M)	$\sigma_{ss}^{\dagger}$ (S/cm)	$[KBr]_p^{++}$ (mol/g)	EWC (%)	$\sigma$ (S/cm)
1.0	0.152	$4.17 \times 10^{-4}$	39.6	$4.13 \times 10^{-3}$
0.75	0.114	$3.05 \times 10^{-4}$	39.7	$2.86 \times 10^{-3}$
0.50	0.076	$1.25 \times 10^{-4}$	40.0	$2.12 \times 10^{-3}$
0.25	0.038	$0.64 \times 10^{-4}$	40.2	$1.16 \times 10^{-3}$
0.10	0.015	-	40.3	$4.19 \times 10^{-4}$
0	-	0	40.4	$2.86 \times 10^{-5}$

$\dagger [KBr]_{ss}$  is the concentration of the electrolyte solution.

$^{++} [KBr]_p$  is the concentration of the KBr in the polymer sample in mol/g of dry polymer.

$\ddagger \sigma_{ss}$  is the conductivity of the soaking solution using Eqn. 3.4 .

$(\lambda_0(Br^-) = 78.1 \Omega^{-1} cm^2 mol^{-1}, \lambda_0(K^+) = 73.5 \Omega^{-1} cm^2 mol^{-1})(14)$

The introduction of KBr into the pHEMA hydrogels led to a major increase in conductivity in comparison to the undoped sample. Conductivity was found to increase with KBr concentration despite the accompanying decrease in EWC caused by the presence of the KBr in the gel. These trends are shown clearly in Figure 4.2. It would appear that for fully hydrated, KBr doped pHEMA samples the conductivity is determined by the number of charge carriers which must outweigh the effect of the decrease in water content resulting from the increase in KBr concentration.

However, if we compare the conductivities of the various KBr doped pHEMA samples with KBr solutions of similar concentration we can see that

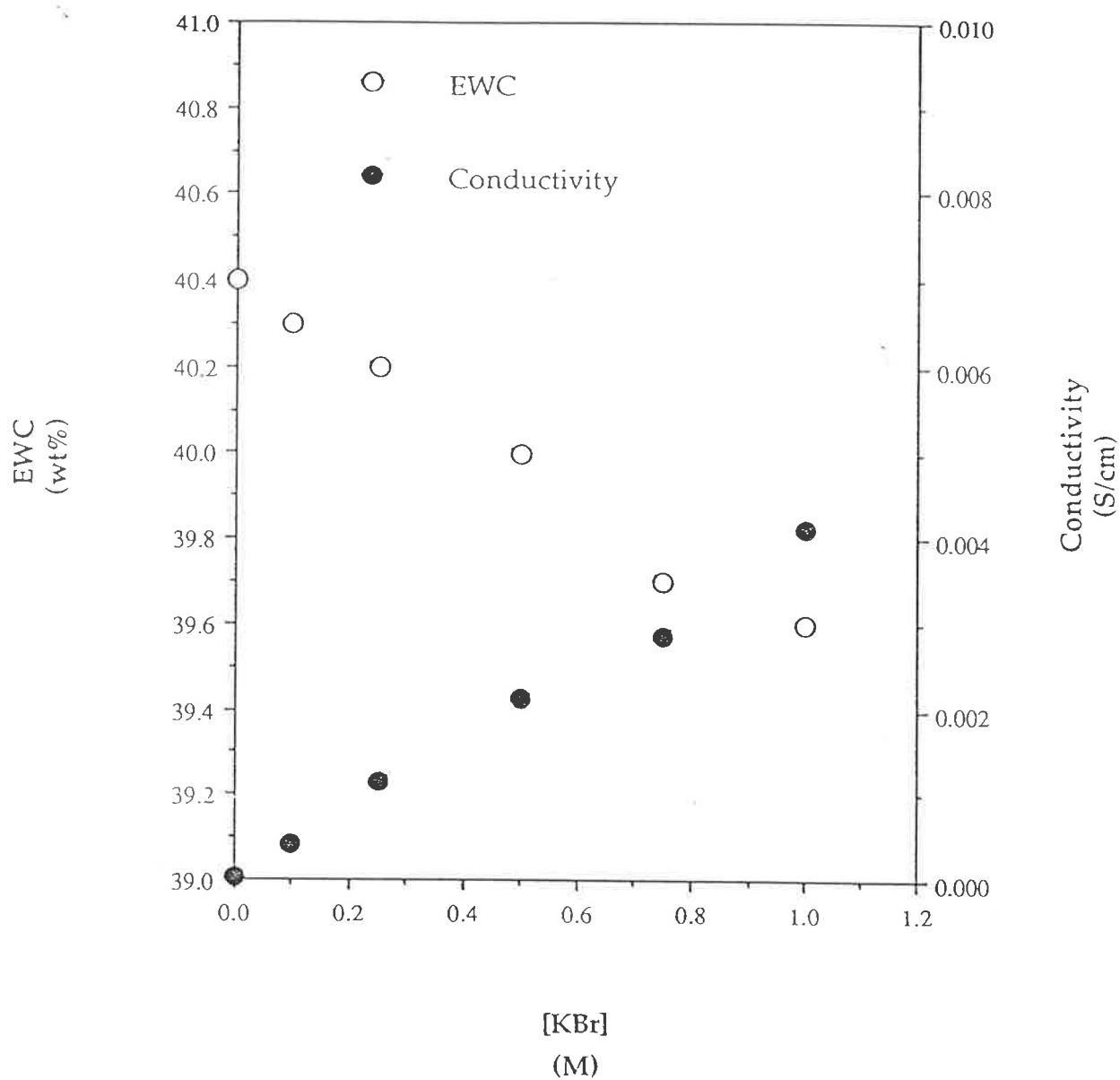


Figure 4.2

The variation of EWC and conductivity of pHEMA gels hydrated in KBr solutions of varying concentrations at 25°C.

the presence of the polymer network causes the conductivity to decrease to between 2.5 and 3.0% of the conductivity of the bulk solution. Primarily the polymer matrix provides a physical impediment to the motion of ions and their associated water molecules. The polymer also re-orders the water phase which will result in increased viscosity of the conducting phase and decreased charge carrier mobility.

In solutions, as the electrolyte concentration increases, the average separation of the ions decreases (Table 4.3). For a 1:1 electrolyte the average separation decreases from 44Å for a 0.01M solution to 9.4Å for a 1.0M solution. It is therefore only reasonable to consider ions with successive hydration layers at concentrations less than or equal to 0.10M.

**Table 4.3**

Average separation of ions in a solution of a 1:1 electrolyte.

Concentration(M):	0.001	0.01	0.10	1.0	10.0
Separation (Å):	94	44	20	9.4	4.4

Reproduced from (14).

At higher concentrations it is conceivable that more than one ion may have an ordering effect on a given water molecule. This will increase both the electrophoretic effect and the relaxation effect that contributes to a decrease in conductivity as the concentration of an electrolyte solution increases. The electrophoretic effect<sup>(14)</sup> refers to drag experienced by a moving ion as it moves in an electric field surrounded by an atmosphere of associated water molecules.

The application of an electric field will lead to the distortion of the local electric field around the ion in motion as it moves ahead of its hydration sphere resulting in an elliptical local field. The ion will subsequently experience a restoring force from the hydration sphere to return to the initial spherical distribution; this restoring force is referred to as the relaxation effect<sup>(14)</sup>. These effects may be responsible for the slight deviation from linear

behaviour at high KBr concentrations in the conductivity plot of fully hydrated pHEMA/KBr (Fig. 4.2).

#### 4.4 The Conductivity of KBr doped EGDMA/HEMA Copolymers

Several EGDMA/HEMA copolymers of varying EGDMA concentration, i.e. [EGDMA] = 0.3, 0.6, 1.5, 3.0 mol%, were prepared and samples of each copolymer were hydrated in a range of KBr solutions ([KBr] = 0.25, 0.50, 0.75, 1.00 M) at 25°C until a constant maximum weight was achieved. The AC impedance plot was recorded for each sample at 25°C and the conductivity was evaluated. Samples were dried in a vacuum oven (50°C) to enable calculation of KBr uptake and EWC. The results of these measurements are shown in Table 4.4.

The AC impedance plots of samples hydrated in KBr solutions of 0.25 M and 1.0 M for each copolymer are presented in Figure 4.3. At full hydration most of the KBr doped EGDMA/HEMA copolymers yield plots similar to those recorded for pHEMA, i.e. non vertical spikes which intercepted the real impedance axis. The intercept was assumed to be equivalent to the bulk resistance of the sample. For each copolymer the intercept value increased as the concentration of the KBr solution decreased. It should be noted that for 1.5 mol% EGDMA/HEMA samples hydrated in low concentration KBr solutions and for all 3 mol% EGDMA/HEMA samples, the AC impedance plot included, at high frequencies, a portion of a semi-circle that is assumed to pass through the origin. The touch-down frequency of these AC impedance plots decreased with increasing crosslinker concentration and decreasing KBr concentration. One advantage of using variable frequency AC impedance analysis is that it enables a more accurate calculation of the bulk resistance from the AC impedance plot than is possible with measurements at one frequency.



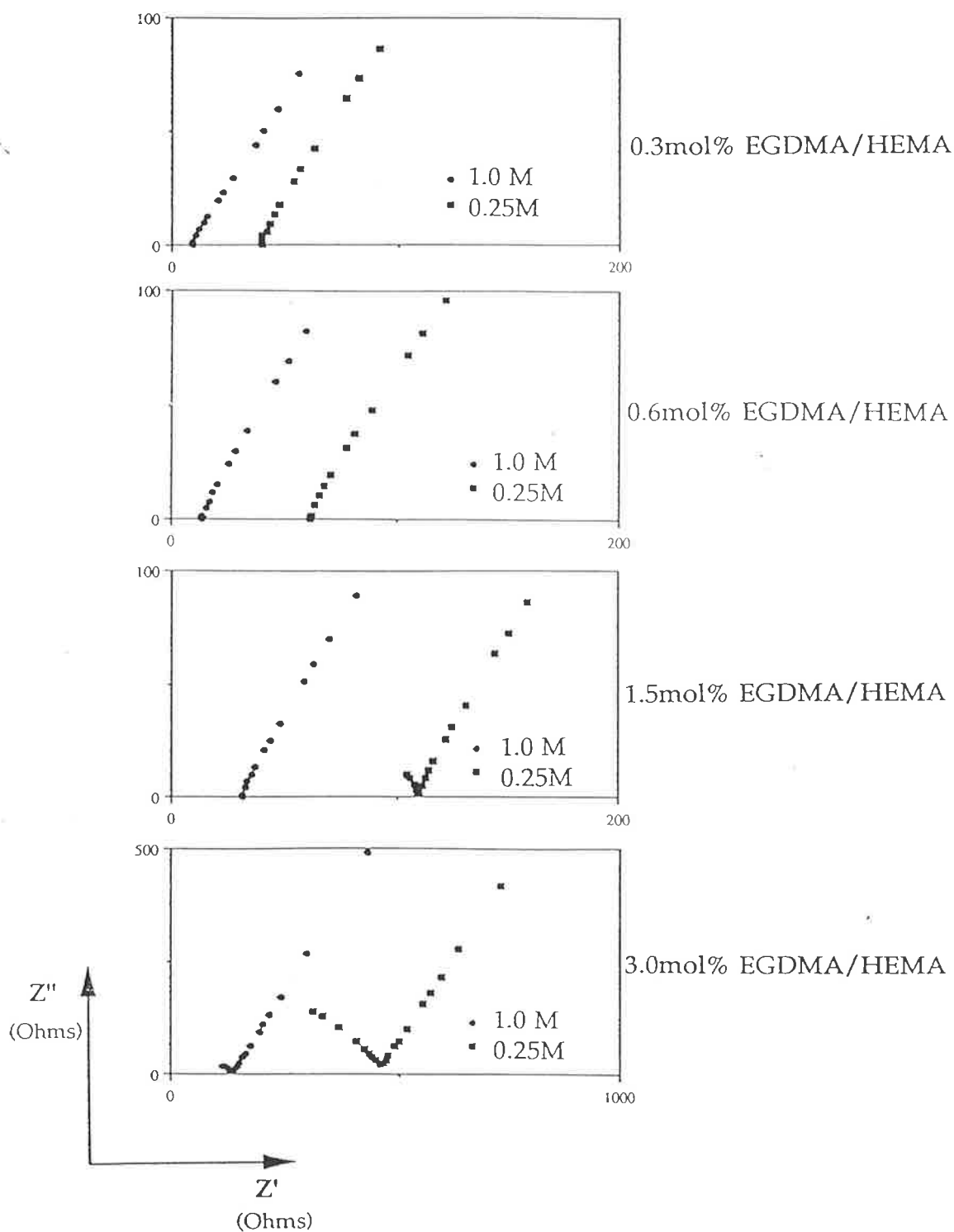


Figure 4.3

The AC impedance plots of several EGDMA/HEMA copolymers hydrated in 1.0M and 0.25M KBr solutions. Hydration and AC measurements carried out at 25°C. EGDMA concentrations as listed above.

Table 4.4

The variation in KBr uptake, EWC and conductivity of several EGDMA/HEMA copolymers hydrated in KBr solutions of varying concentration at 25°C.

Copolymer	[KBr] <sub>ss</sub> <sup>†</sup> (M)	[KBr] <sub>p</sub> <sup>††</sup> (mol/g)	EWC (%)	σ (S/cm)
pHEMA	1.00	4.17x10 <sup>-4</sup>	39.6	4.13x10 <sup>-3</sup>
	0.75	3.05x10 <sup>-4</sup>	39.7	2.86x10 <sup>-3</sup>
	0.50	1.25x10 <sup>-4</sup>	40.0	2.12x10 <sup>-3</sup>
	0.25	0.64x10 <sup>-4</sup>	40.2	1.16x10 <sup>-3</sup>
	0	0	40.4	2.86x10 <sup>-5</sup>
0.3 mol%EGDMA co HEMA	1.00	3.33x10 <sup>-4</sup>	36.8	2.18x10 <sup>-3</sup>
	0.75	2.47x10 <sup>-4</sup>	37.0	1.48x10 <sup>-3</sup>
	0.50	1.26x10 <sup>-4</sup>	37.2	1.04x10 <sup>-3</sup>
	0.25	0.35x10 <sup>-4</sup>	37.3	5.02x10 <sup>-4</sup>
	0	0	37.5	8.02x10 <sup>-6</sup>
0.6 mol%EGDMA co HEMA	1.00	3.43x10 <sup>-4</sup>	35.9	1.50x10 <sup>-3</sup>
	0.75	2.75x10 <sup>-4</sup>	36.0	1.09x10 <sup>-3</sup>
	0.50	1.39x10 <sup>-4</sup>	36.1	6.66x10 <sup>-4</sup>
	0.25	0.81x10 <sup>-4</sup>	36.3	3.51x10 <sup>-4</sup>
	0	0	36.3	3.23x10 <sup>-6</sup>
1.5 mol%EGDMA co HEMA	1.00	3.43x10 <sup>-4</sup>	32.3	6.61x10 <sup>-4</sup>
	0.75	2.49x10 <sup>-4</sup>	32.4	5.00x10 <sup>-4</sup>
	0.50	1.65x10 <sup>-4</sup>	32.5	3.57x10 <sup>-4</sup>
	0.25	0.90x10 <sup>-4</sup>	32.5	1.87x10 <sup>-4</sup>
	0	0	32.9	2.06x10 <sup>-6</sup>
3.0 mol%EGDMA co HEMA	1.00	1.39x10 <sup>-4</sup>	27.0	1.70x10 <sup>-4</sup>
	0.75	1.20x10 <sup>-4</sup>	27.2	1.28x10 <sup>-4</sup>
	0.50	1.09x10 <sup>-4</sup>	27.4	1.06x10 <sup>-4</sup>
	0.25	0.58x10 <sup>-4</sup>	27.4	4.87x10 <sup>-5</sup>
	0	0	27.7	1.08x10 <sup>-6</sup>

<sup>†</sup> [KBr]<sub>ss</sub> is the concentration of the electrolyte solution.

<sup>††</sup> [KBr]<sub>p</sub> is the concentration of the KBr in the polymer sample in mol/g of dry polymer.

The hydration of EGDMA/HEMA copolymers in KBr solutions again led to reduced EWCs with the reduction in EWC greater for samples hydrated in more concentrated KBr solutions. All crosslinked samples hydrated in 1M samples experienced ca.1wt% decrease in EWC in comparison to undoped samples. However, if we take into account the decrease in EWC caused by the increase in EGDMA concentration then it appears that the salting out effect caused by KBr is more significant in more tightly crosslinked samples.

For all EGDMA/HEMA copolymers the introduction of KBr led to significant increases in conductivity. The increase in conductivity experienced was greater for samples with lower EGDMA concentration. It must be noted that increasing crosslinker concentration results in copolymers of decreased EWC and will thus limit the KBr uptake by sorption. Consequently the conductivity of these samples will be less, when compared to less crosslinked samples hydrated in similar electrolyte solutions, on the basis of having decreased numbers of charge carriers. However if we compare the conductivity of samples based on their KBr concentrations with respect to the dry polymer (Figure 4.4) we can see the effect of increased crosslinking and decreased EWC on the conductivity.

It is clear that the increase in crosslinking leads to a significant decrease in conductivity for samples with the same KBr concentration with respect to the dry polymer. This decrease can be ascribed to a number of effects. Increases in EGDMA concentration lead to more hydrophobic and tighter networks with lower EWC. If the description for a hydrogel's structure given by Pathamanathan and Johari<sup>(15)</sup> is accepted, i.e. a hydrogel consists of statistically distributed microchannels or fluctuating pores created by the mobility of the polymer segments within an interpenetrating network in the presence of a solvent where the pores are formed and removed as a result of the thermal motion of the polymer, then an increase in EGDMA concentration will hinder the formation and removal of these pores.

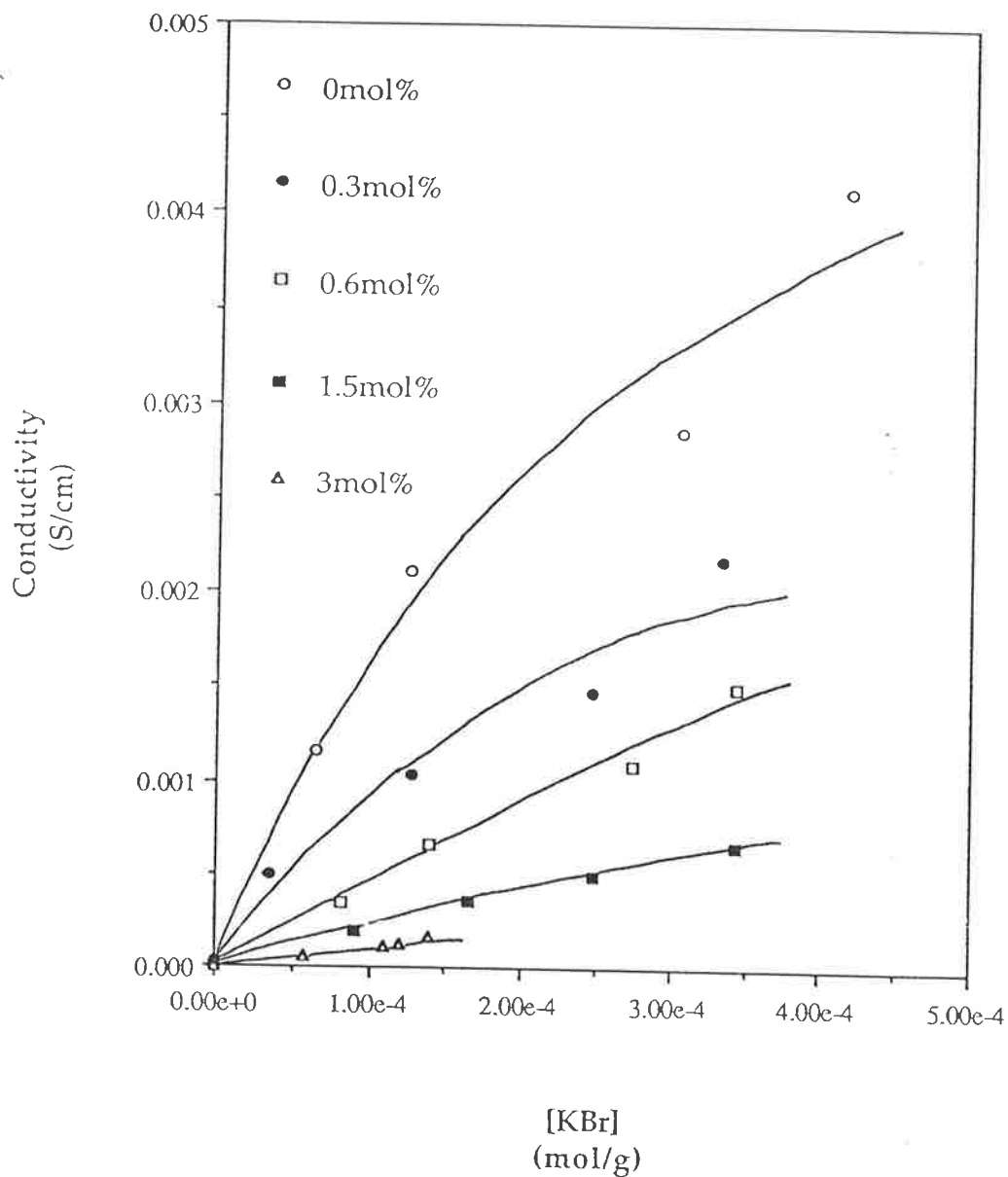


Figure 4.4

The variation of conductivity, at 25°C and full hydration, with respect to KBr concentration of several EGDMA/HEMA copolymer gels. EGDMA concentration as listed above. KBr concentration is given in moles KBr per gram dry polymer.

Additional crosslinker will result in a tighter network with decreased segmental mobility. Given that ion motion will take place between pores of sufficient size to support motion of the ions and their hydration clouds, an increase in EGDMA effectively decreases the continuity of the conducting phase with respect to space and time. The mobility of the water is lower, in relative terms, in a more crosslinked network as a result of polymer/water interactions. It should also be noted that a decrease in EWC at a constant KBr concentration leads to decreased distances between ions increasing the electrophoretic and relaxation effects experienced by the mobile ions.

#### 4.5 The Conductivity of KBr doped 3mol% OED/HEMA Copolymers

Several 3mol% OED/HEMA copolymers (OED= EGDMA, DiEGDMA, TEGDMA, P400) were prepared and samples of each copolymer were hydrated in a range of KBr solutions ( $[KBr]= 0.25, 0.50, 0.75, 1.00M$ ) at  $25^{\circ}C$  until a constant maximum weight was achieved. The AC impedance plot was recorded for each sample at  $25^{\circ}C$  and the sample conductivity evaluated. Samples were dried in a vacuum oven ( $50^{\circ}C$ ) to enable calculation of KBr uptake and EWC. The results of these measurements are shown in Table 4.5.

The AC impedance plots of samples hydrated in KBr solutions of 0.25M and 1.0M KBr for each copolymer are presented in Figure 4.5. A similar AC response to that of pHEMA samples hydrated in KBr solutions was recorded for most of the copolymers hydrated in solutions of identical concentration. Non vertical spikes which intercept the real impedance axis were recorded for most copolymer samples, yet as  $n$ , the number of repeat ethylene glycol units in the OED decreased and the KBr concentration of the soaking solution decreased the likelihood of the presence of a portion of a semi-circle in the AC impedance locus increased. Such behaviour was exhibited by EGDMA/HEMA samples hydrated in all KBr solutions and DiEGDMA/HEMA samples hydrated in solutions of lower KBr concentration.

Table 4.5

The variation in KBr uptake, EWC and conductivity of several 3mol%OED/HEMA copolymers hydrated in KBr solutions of varying concentration at 25°C.

Copolymer	[KBr] <sub>ss</sub> <sup>†</sup> (M)	[KBr] <sub>p</sub> <sup>††</sup> (mol/g)	EWC (%)	σ (S/cm)
pHEMA	1.00	4.17x10 <sup>-4</sup>	39.6	4.13x10 <sup>-3</sup>
	0.75	3.05x10 <sup>-4</sup>	39.7	2.86x10 <sup>-3</sup>
	0.50	1.25x10 <sup>-4</sup>	40.0	2.12x10 <sup>-3</sup>
	0.25	0.64x10 <sup>-4</sup>	40.2	1.16x10 <sup>-3</sup>
	0	0	40.4	2.86x10 <sup>-5</sup>
3.0 mol% EGDMA co HEMA	1.00	1.39x10 <sup>-4</sup>	27.0	1.70x10 <sup>-4</sup>
	0.75	1.20x10 <sup>-4</sup>	27.2	1.28x10 <sup>-4</sup>
	0.50	1.09x10 <sup>-4</sup>	27.4	1.06x10 <sup>-4</sup>
	0.25	0.58x10 <sup>-4</sup>	27.4	4.87x10 <sup>-5</sup>
	0	0	27.7	1.08x10 <sup>-6</sup>
3.0 mol% DiEGDMA co HEMA	1.00	3.46x10 <sup>-4</sup>	32.5	7.73x10 <sup>-4</sup>
	0.75	2.59x10 <sup>-4</sup>	32.8	5.41x10 <sup>-4</sup>
	0.50	1.64x10 <sup>-4</sup>	32.7	3.72x10 <sup>-4</sup>
	0.25	0.75x10 <sup>-4</sup>	33.1	1.96x10 <sup>-4</sup>
	0	0	33.3	1.55x10 <sup>-6</sup>
3.0 mol% TEGDMA co HEMA	1.00	3.82x10 <sup>-4</sup>	32.8	8.57x10 <sup>-4</sup>
	0.75	2.85x10 <sup>-4</sup>	32.9	7.23x10 <sup>-4</sup>
	0.50	1.91x10 <sup>-4</sup>	33.0	5.03x10 <sup>-4</sup>
	0.25	0.94x10 <sup>-4</sup>	33.4	2.96x10 <sup>-4</sup>
	0	0	33.8	2.47x10 <sup>-6</sup>
3.0 mol% P400 co HEMA	1.00	3.74x10 <sup>-4</sup>	34.0	8.70x10 <sup>-4</sup>
	0.75	2.74x10 <sup>-4</sup>	34.3	6.60x10 <sup>-4</sup>
	0.50	1.93x10 <sup>-4</sup>	34.3	5.45x10 <sup>-4</sup>
	0.25	0.85x10 <sup>-4</sup>	34.6	2.68x10 <sup>-4</sup>
	0	0	34.7	5.47x10 <sup>-6</sup>

<sup>†</sup> [KBr]<sub>ss</sub> is the concentration of the electrolyte solution.

<sup>††</sup> [KBr]<sub>p</sub> is the concentration of the KBr in the polymer sample in mol/g of dry polymer.

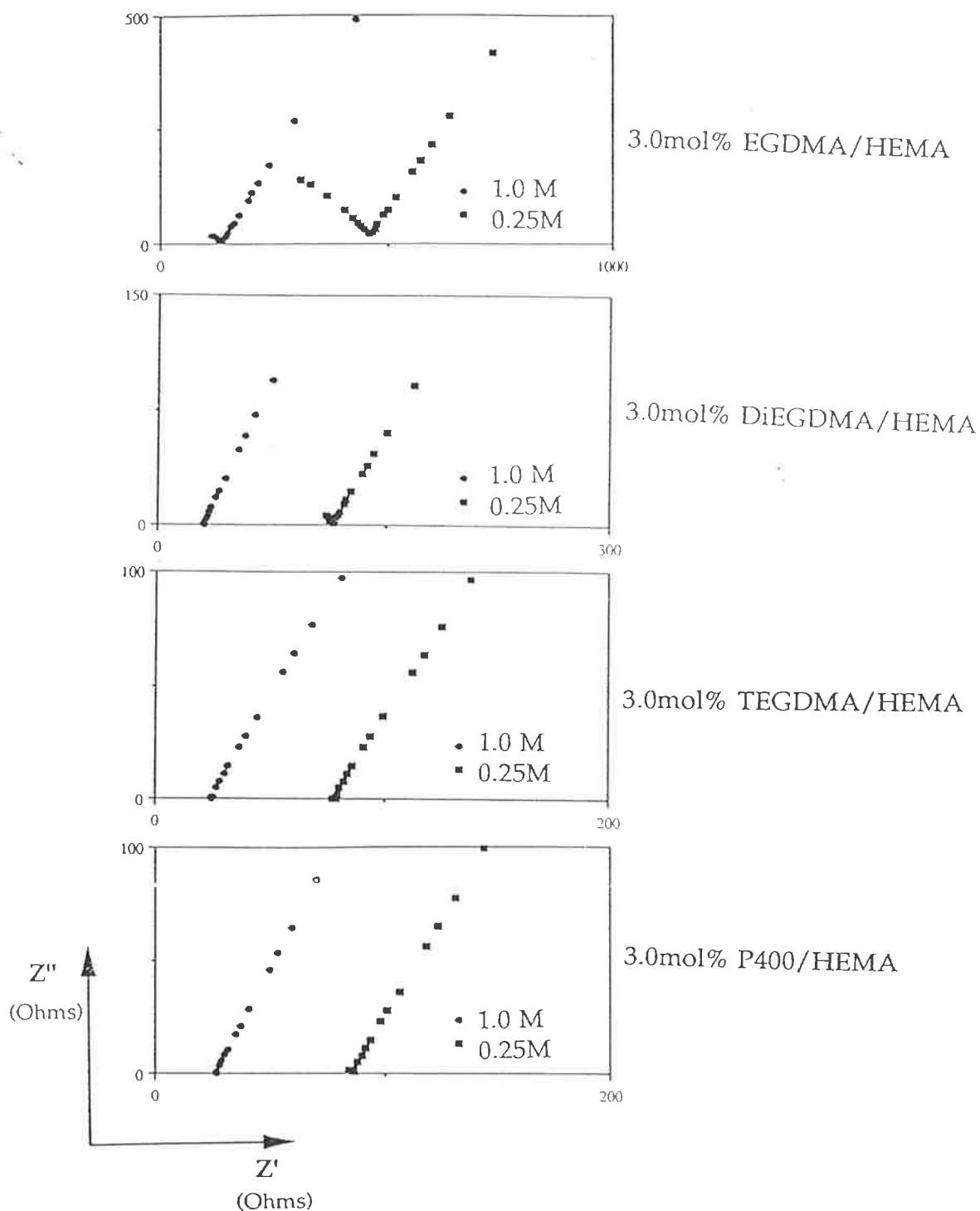


**Figure 4.5**

The AC impedance plots of several 3mol% OED/HEMA copolymers hydrated in 1.0M and 0.25M KBr solutions. Hydration and AC measurements carried out at 25°C. OED as listed above.

In OED/HEMA samples that had portions of a semi-circle in the high frequency region of the AC impedance plot, the touch down frequency decreased as the KBr concentration of the soaking solution decreased. It was assumed that this semi-circle would have passed through the origin. There was insufficient AC impedance data for  $\phi$  or the bulk capacitance of these samples to be calculated. The bulk resistance of the OED/HEMA samples was calculated from the intercept of the non vertical spike with the real impedance axis.

The hydration of OED/HEMA copolymers in KBr solutions has led to reduced EWCs. Again the decrease in EWC was greatest for samples hydrated in the most concentrated KBr solutions. The maximum decrease in EWC for all OED copolymers was ca.1wt%. This, however, represents a more significant decrease in EWC for OED/HEMA copolymers where  $n$  is smaller. As  $n$  decreases, for copolymers of like OED concentration, the crosslink becomes smaller and more hydrophobic resulting in tighter polymer networks with decreased EWC. The salting out effect caused by the presence of KBr appears to be greater for tighter networks.

The presence of KBr in all of the OED/HEMA systems has led to significant increases in conductivity. The increase in conductivity of 3mol% OED/HEMA copolymers was found to increase as the number of ethylene glycol repeat units in the OED increased. Given that the nature of the OED employed will affect the EWC and this in turn will limit the KBr uptake by diffusion, it is more appropriate to compare conductivity of the various copolymers with respect to the KBr concentration, i.e. moles KBr per gram of dry polymer (Figure 4.6).

As  $n$  is increased from 1 to 2 (i.e. EGDMA to DiEGDMA) there is a considerable increase in conductivity of samples of similar KBr concentration, however, as  $n$  is increased to 4 (TEGDMA) and then 9 (P400) it is evident that the increase in  $n$  has a reduced effect on the conductivity with there being



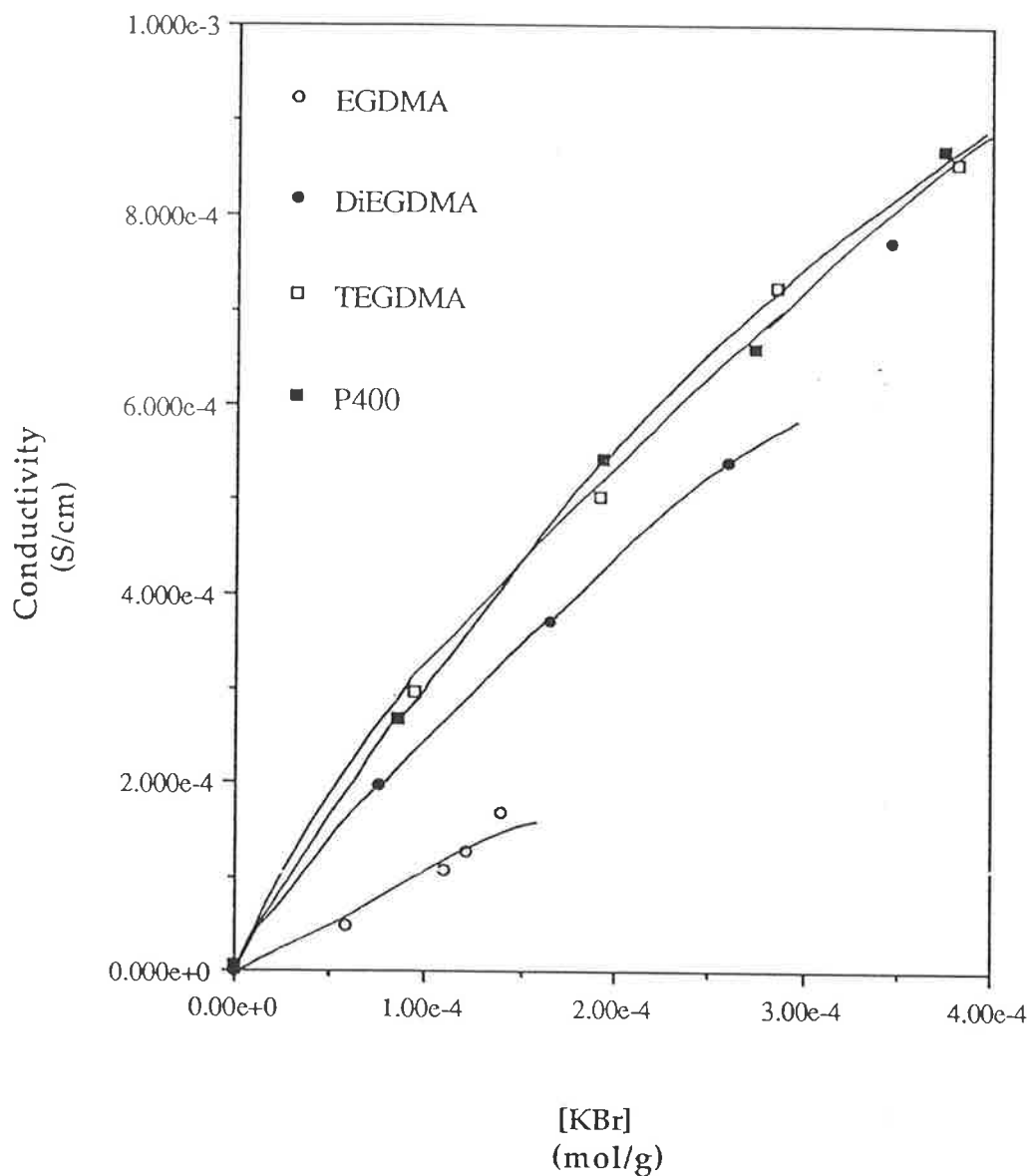


Figure 4.6

The variation of conductivity with KBr concentration for several fully hydrated 3mol% OED/HEMA copolymer gels at 25°C. OED as listed above. KBr concentration is given in moles per gram dry polymer.

little difference between the conductivities of 3mol% TEGDMA/HEMA and 3mol% P400/HEMA copolymers hydrated in like KBr solutions. This conductivity trend mirrors the effect that altering  $n$  has on the EWC; EWC for 3mol% OED/HEMA copolymers increases as  $n$  increases but the rate of increase in EWC decreases as  $n$  increases. This is as expected for a gel electrolyte, since the polymer provides the role of supporting the conducting phase, in this case the occluded water. In the case of the 3mol% OED/HEMA copolymers investigated here the conductivity increases as the EWC increases. Increasing  $n$  leads to both the greater hydrophilicity of the crosslinking agent and looser networks. These factors lead to increased EWC and thus KBr uptake. However, the flexibility of the crosslink as  $n$  increases that enhances intramolecular secondary bonding and limits EWC may also sterically impede the motion of the ions and limit conductivity. Consequently, the increase in the slope of the plot of conductivity versus KBr content decreased as  $n$  increased

All OED/HEMA copolymers exhibited an increase in conductivity as KBr content of the copolymer increased despite the corresponding decrease in EWC. The rate of increase in conductivity decreased as KBr increased and could be ascribed to the ion motion retarding electrophoretic and relaxation effects associated with increasing ion concentration.

## 4.6 The Variation of Conductivity with Water Content

The variation of conductivity with water content was investigated for a number of KBr doped copolymer samples. All conductivity measurements were made at 25°C and the dehydration regimen employed was the same as that used for pHEMA (Section 3.6.2).

### 4.6.1 KBr doped pHEMA

The variation of conductivity at 25°C for pHEMA hydrated in several

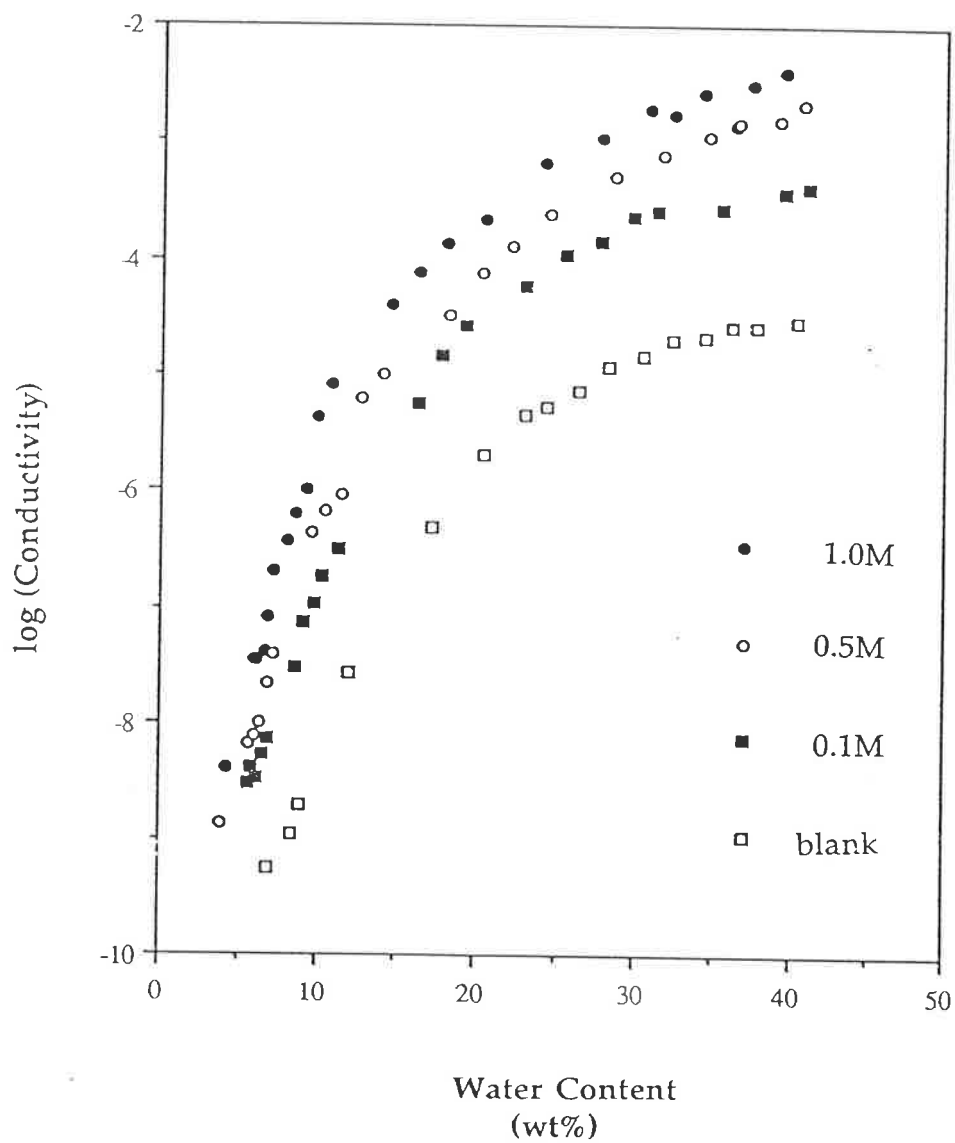


Figure 4.7

The variation of  $\log(\text{Conductivity})$  with water content at 25°C for pHEMA samples hydrated in a range of KBr solutions. KBr solution concentration as listed above.

KBr solutions (0.10, 0.50, 1.0M) with water content is shown in Figure 4.7. The conductivity of undoped pHEMA, when subjected to gradual dehydration, was found to decrease at differing rates dependent on the water content. The changes in the slope of the conductivity versus water content plot (Figure 3.8) were found to occur at water contents similar to those postulated by McBrierty et al.<sup>(16)</sup> to describe the nature of water in pHEMA. McBrierty describes absorbed water up to 20wt% water as bound to the polymer, 20 to 35wt% water is deemed interfacial and greater than 35wt% water is free. The dehydration behaviour of the ion doped pHEMA samples is similar in form to the behaviour exhibited by undoped pHEMA with a few differences.

As with the results obtained for undoped pHEMA (Section 3.6.2), there appears to be three distinct conductivity regions for each of the three KBr concentrations investigated. It appears that for all samples the first change of behaviour is at ca.35wt% suggesting that for all these samples water present above 35wt% is free water. Below 35wt% water content, the conductivity decreases at a slightly greater rate as so-called interfacial water is removed.

However, the transition to the third region of behaviour is at different water contents for samples of differing KBr concentrations, i.e. ca. 12wt% (1.0M KBr), ca. 14wt% (0.5M KBr), ca.17wt% (0.1M KBr) and 20wt% (0M KBr). For the sample hydrated in water, the major change at 20wt% was not only ascribed to the decrease in mobility of the conducting phase (bound water is less mobile than interfacial water) but also to the removal of plasticising water which would decrease the mobility of the polymer network disrupting the continuity of the conducting phase with respect to time. Torsion pendulum measurements by Allen et al.<sup>(17)</sup> found the T<sub>g</sub> of pHEMA to be ca.25°C at 20wt% water content. Given that the transition for conductivity behaviour occurs at lower water contents for higher KBr concentrations it appears that the ions are able to alter the structure of the water within the gel

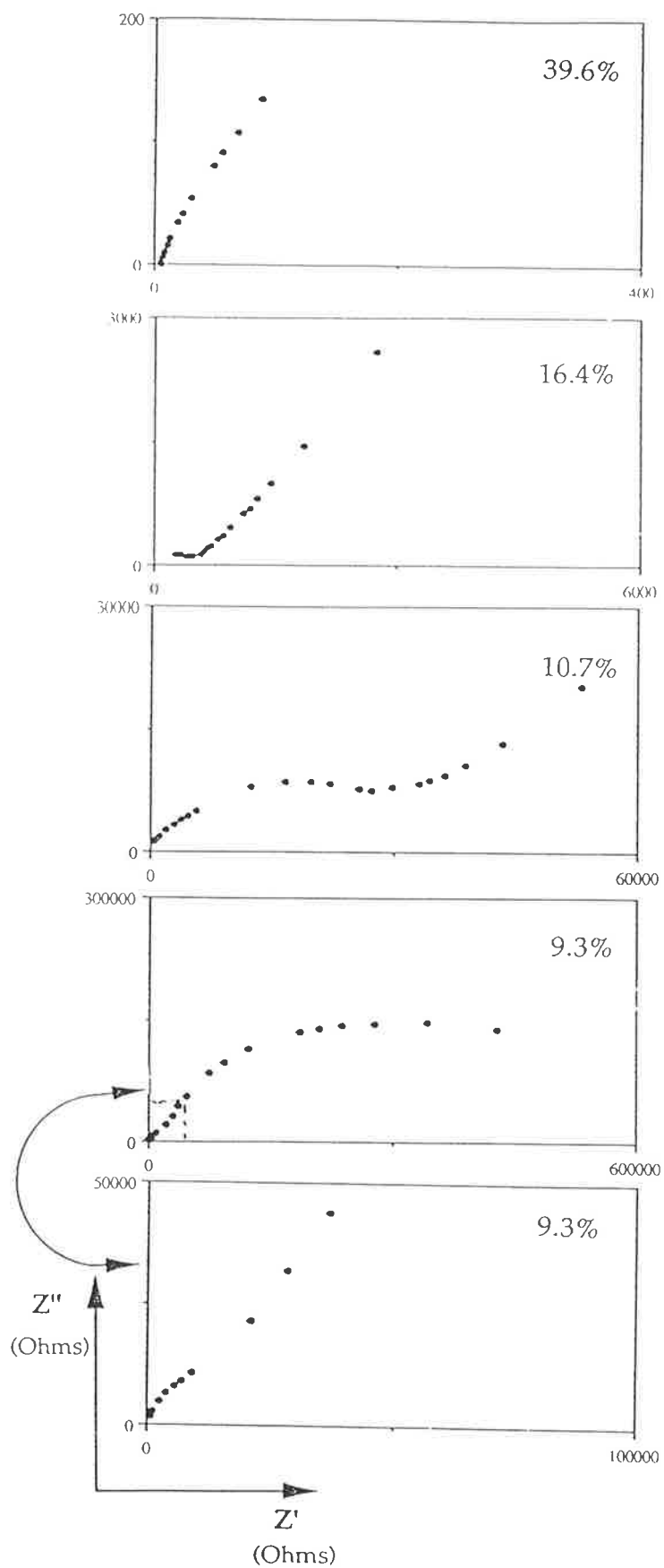


Figure 4.8

The AC impedance plots of pHEMA, hydrated in 1.0M KBr, at 25°C and several water contents as listed above.

at lower water contents in a manner that enhances conductivity.

Thermal mechanical analysis by Allen et al.<sup>(18)</sup> revealed that KBr has an antiplasticising effect on dry pHEMA resulting in increased glass transition temperatures. However, no data exists for the variation in  $T_g$  for KBr doped pHEMA samples of differing water contents, thus making it unclear whether the change in conductivity behaviour is associated to the cessation of large scale segmental motion of the polymer.

It should be noted that the rate of decrease in conductivity in each of the three regions of behaviour is greater for samples of higher KBr concentration. This can be ascribed initially to the increase in the electrophoretic and relaxation effects experienced by ions in more concentrated samples but it is conceivable at lower water contents that ion-pairing will take place forming clusters of ions, with decreased mobility compare to free ions, effectively reducing the number of charge carriers .

The AC impedance plots for pHEMA hydrated in 1.0M KBr at several water contents are shown in Figure 4.8. At full hydration (39.6wt% water), the AC impedance plot is a nonvertical spike that intercepts the real impedance axis at a point that is assumed to be the bulk resistance of the sample. As the water content was reduced (e.g. 16.4%) the high frequency behaviour changed such that the spike became joined to a portion of a semi-circle, which was assumed to pass through the origin. With further dehydration the touch down frequency decreased, and the semi-circular portion of the locus approached the origin. The semi-circular portion of the locus also broadened with decreased water content, indicative of a decrease in the continuity of the conducting phase<sup>(19)</sup>. At a water content of 9.3wt% the broadened semicircle locus transforms to the superposition of two semi-circles. In accordance with the results of Watanabe et al.<sup>(20)</sup> this has been taken to indicate that there is a two phase morphology with respect to conductivity. It is suggested that at 9.3wt% water there exists localised regions

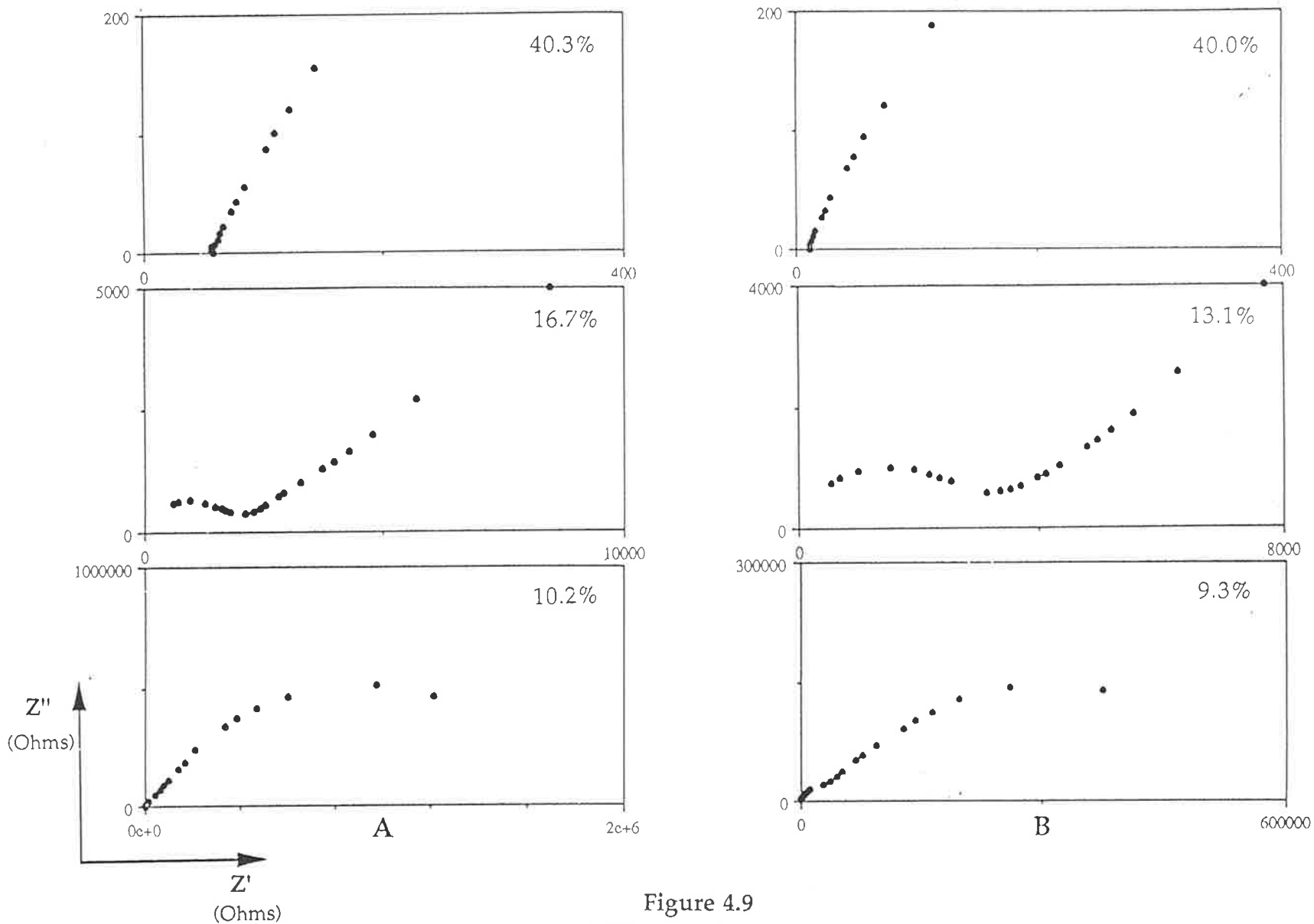


Figure 4.9  
 The AC impedance plots of PHEMA hydrated in A 0.1MKBr and B 0.5M KBr,  
 at 25°C and several water contents as listed above.

of the pHEMA gel network with insufficient water to support motion of KBr and thus conductivity. It is interesting that this behaviour occurs in the ion doped sample at a lower water content than in the undoped sample (12.1wt%). This suggests that the KBr ions may be able to order the water to provide a more continuous conductive phase at a lower water content.

Similar AC impedance behaviour was exhibited by the less concentrated KBr doped (0.5M, 0.25M) pHEMA gel samples when they were subjected to dehydration (Fig. 4.9). It is of interest to observe that the water content at which the impedance plot becomes the superposition of two semi-circles is at a lower water content than in the case of the undoped pHEMA (12.1wt%) and is also lower for the sample hydrated in 0.5M KBr (9.3wt%) than for the sample hydrated in 0.25M KBr (10.2wt%). This not only suggests that the KBr ions may be able to reorder water present at lower hydration levels, enhancing the continuity of the conducting phase, but also that this reordering is concentration dependent.

#### 4.6.2 KBr doped EGDMA/HEMA Copolymers

The variation of  $\log(\text{conductivity})$  at 25°C for several EGDMA/HEMA copolymers hydrated in different KBr solutions (0.25M, 1.0M) with water content is shown in Figures 4.10a-c. As in the case of the pHEMA samples the conductivity behaviour of the KBr doped EGDMA/HEMA samples on dehydration was similar in form to the behaviour shown by the undoped samples.

For the 0.6mol% EGDMA/HEMA copolymer, hydration in KBr solutions led to EWCs of 35.9wt% (1.0M) and 36.3 wt% (0.25M). It is not surprising that their conductive behaviour can be described in terms of two water content ranges; McBrierty et al.<sup>(16)</sup> believe free water is only present at water contents greater than 35wt%. These samples are only believed to contain interfacial and bound water. The introduction of KBr has again



shifted the change in behaviour to lower water contents for both the KBr doped samples with a slightly greater decrease shown by the sample hydrated in a 1.0M KBr solution. This change in behaviour occurs at ca. 22wt% for the undoped sample and ca.19wt% and 18wt% for samples hydrated in 0.25M and 1.0M KBr respectively.

Similar trends are exhibited by the data for the 1.5mol% EGDMA/HEMA copolymer samples (Fig. 4.10b). The additional increase in EGDMA concentration reduces the EWC further and also limits the KBr uptake (Table 4.4). The two stage conductive behaviour is once again exhibited as interfacial water is removed eventually leaving just bound water to provide the conducting phase. The transition in conductive behaviour occurs at lower water contents for the samples hydrated in 1.0M (ca. 20wt%) and 0.25M KBr (ca. 20wt%) than for the undoped sample (ca. 26wt%).

Fully hydrated undoped 3mol% EGDMA/HEMA when subjected to dehydration yields an almost linear decrease in  $\log(\text{conductivity})$  with respect to water content. This has already been ascribed to the fact that the  $T_g$  of this copolymer is 25°C at ca. 26wt%<sup>(17)</sup>. However, distinct two stage behaviour is exhibited by the samples hydrated in 1.0 and 0.25M KBr solutions with both samples exhibiting a transition at ca. 20wt% water.

Examples of the AC impedance plots obtained for these copolymers hydrated in 1.0M KBr and 0.25 M KBr are shown in Figures 4.11a and 4.11b respectively. The change in the AC impedance spectra is similar in style to that experienced by KBr doped pHEMA samples but a few trends emerge from the data gained. Compared to pHEMA samples hydrated in like KBr solutions, the water content at which the appearance of the superposition of two semi-circle response increases as the crosslinker concentration increases. This trend was also shown by samples without added KBr. This can be ascribed to the presence of the crosslinker leading to a less continuous conducting phase. The appearance of this style of AC impedance response,

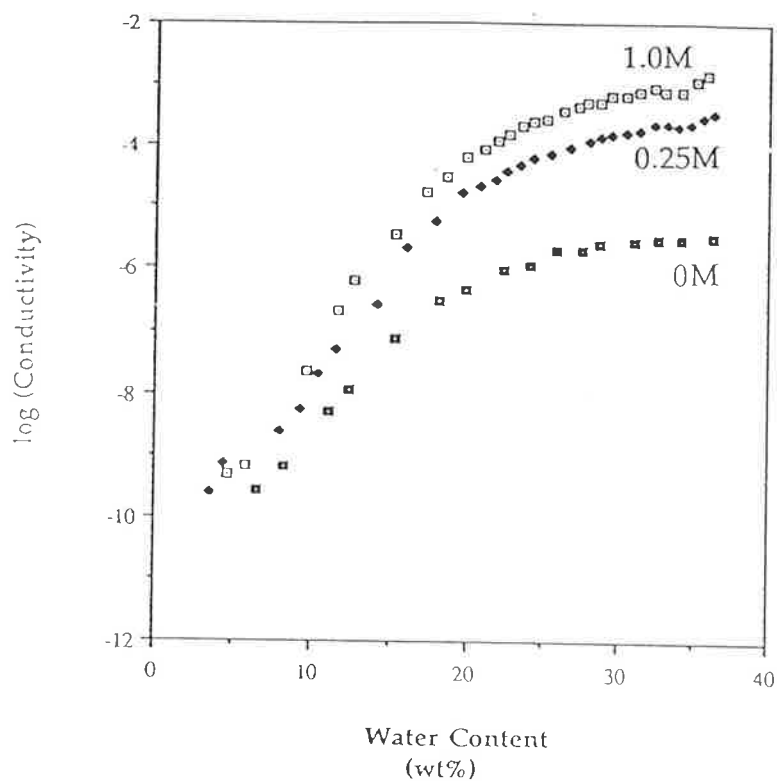


Figure 4.10a

The variation of  $\log(\text{Conductivity})$  with water content at 25°C for 0.6mol% EGDMA/HEMA samples hydrated in a range of KBr solutions. KBr solution concentration as listed above.

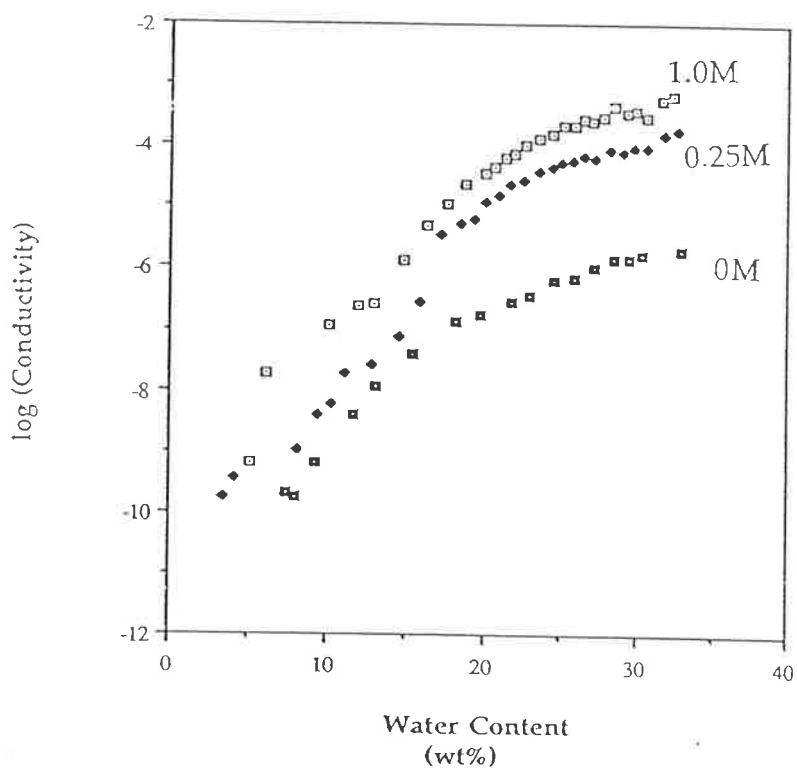


Figure 4.10b

The variation of  $\log(\text{Conductivity})$  with water content at 25°C for 1.5mol% EGDMA/HEMA samples hydrated in a range of KBr solutions. KBr solution concentration as listed above.

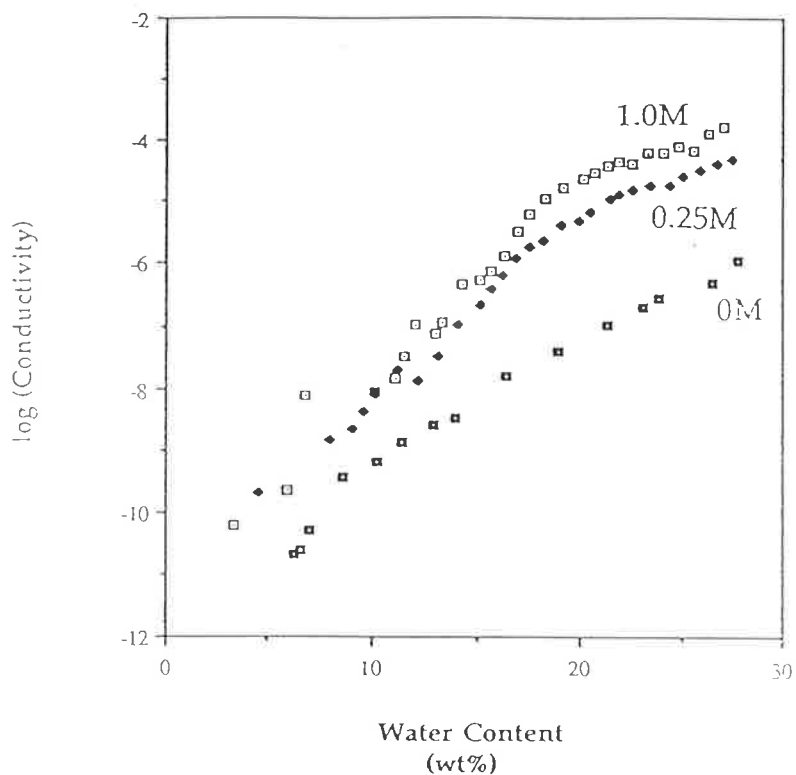


Figure 4.10c

The variation of  $\log(\text{Conductivity})$  with water content at 25°C for 3.0mol% EGDMA/HEMA samples hydrated in a range of KBr solutions. KBr solution concentration as listed above.

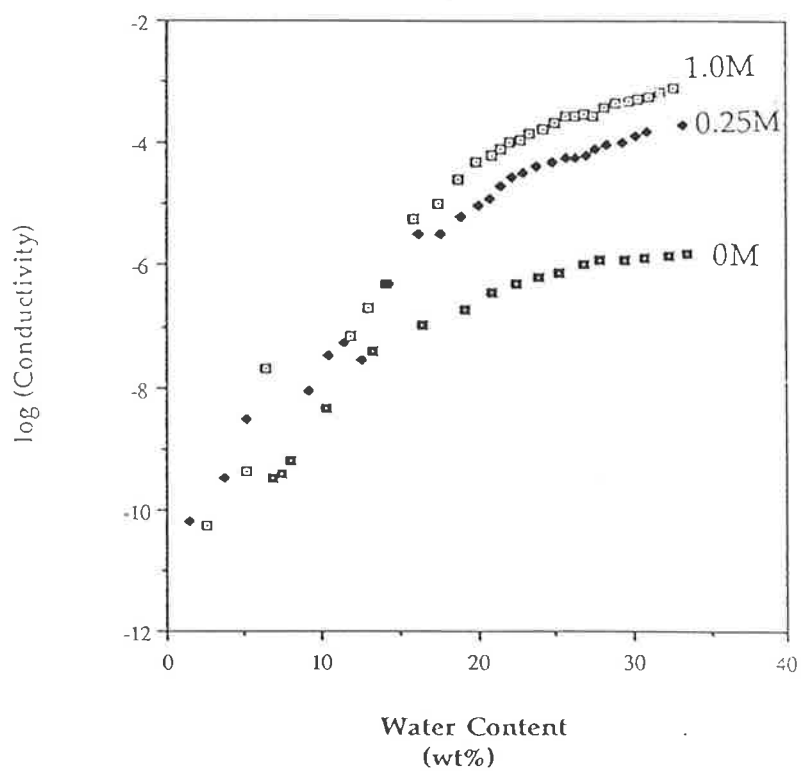


Figure 4.10d

The variation of  $\log(\text{Conductivity})$  with water content at 25°C for 3.0mol% DiEGDMA/HEMA samples hydrated in a range of KBr solutions. KBr solution concentration as listed above.

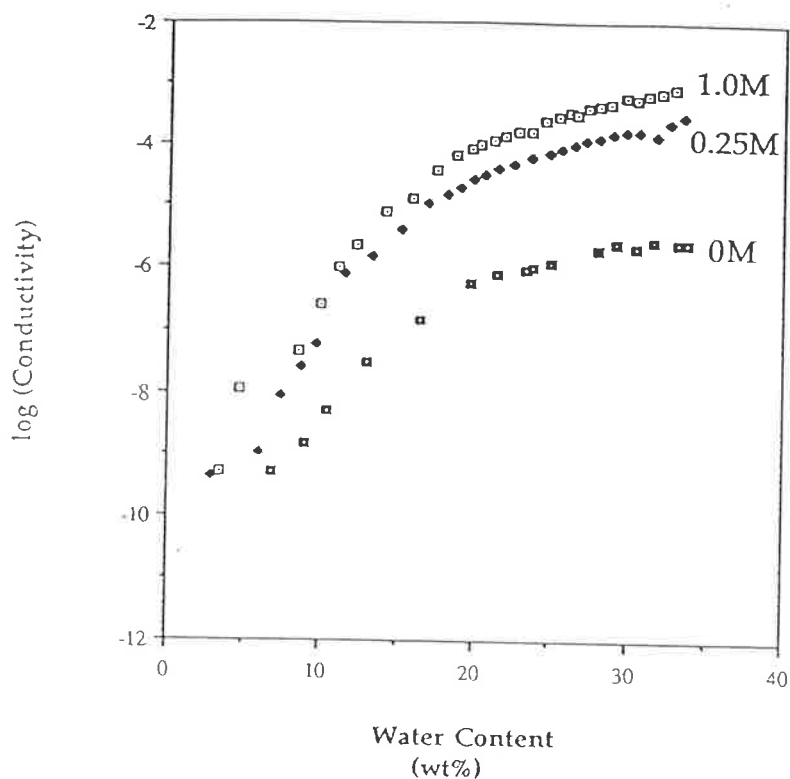


Figure 4.10e

The variation of  $\log(\text{Conductivity})$  with water content at  $25^\circ\text{C}$  for 3.0mol% TEGDMA/HEMA samples hydrated in a range of KBr solutions. KBr solution concentration as listed above.

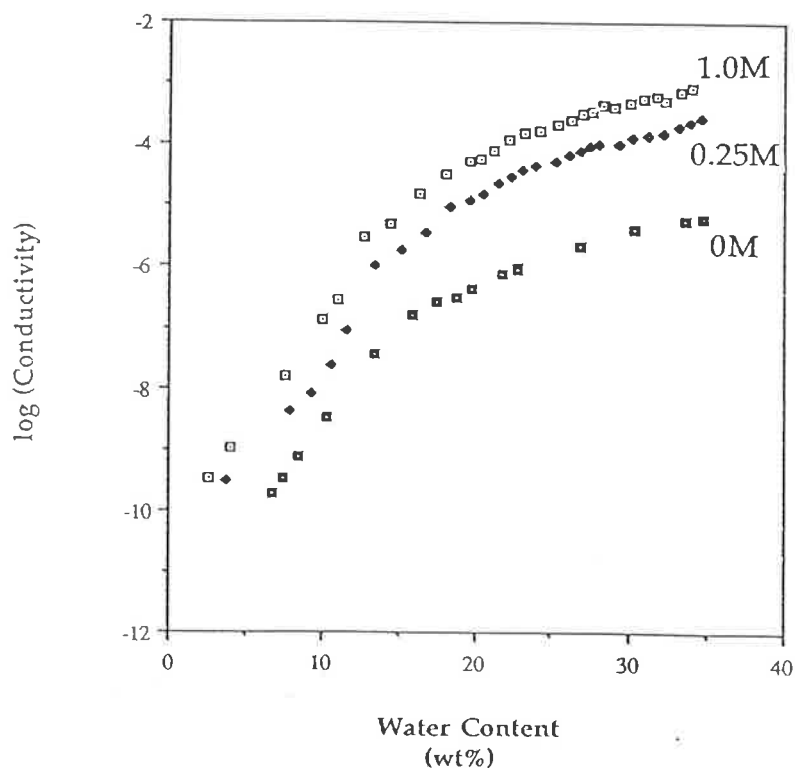


Figure 4.10f

The variation of  $\log(\text{Conductivity})$  with water content at  $25^\circ\text{C}$  for 3.0mol% P400/HEMA samples hydrated in a range of KBr solutions. KBr solution concentration as listed above.

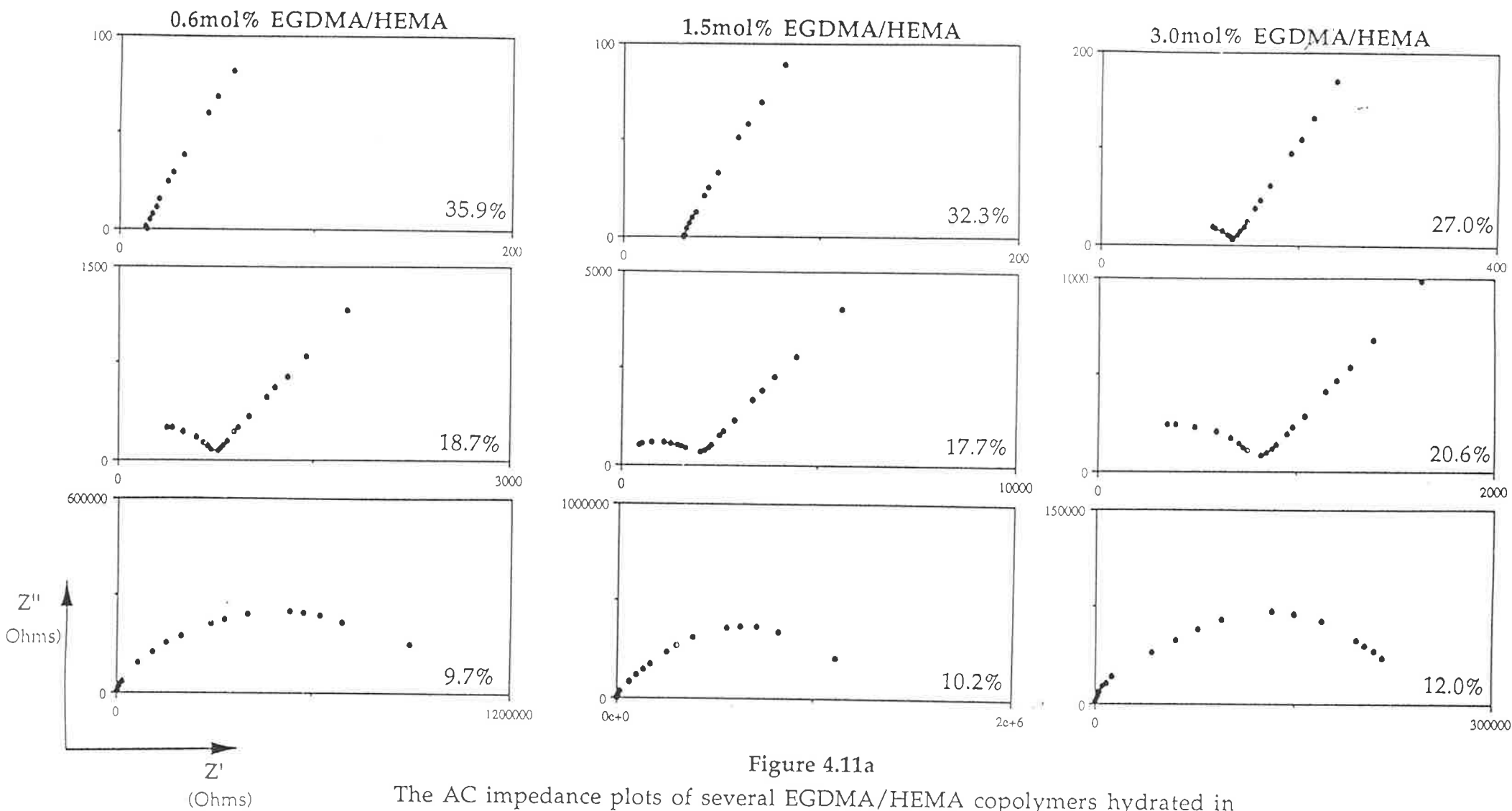


Figure 4.11a

The AC impedance plots of several EGDMA/HEMA copolymers hydrated in 1M KBr at various water contents and 25°C. EGDMA concentrations and water contents as listed above.

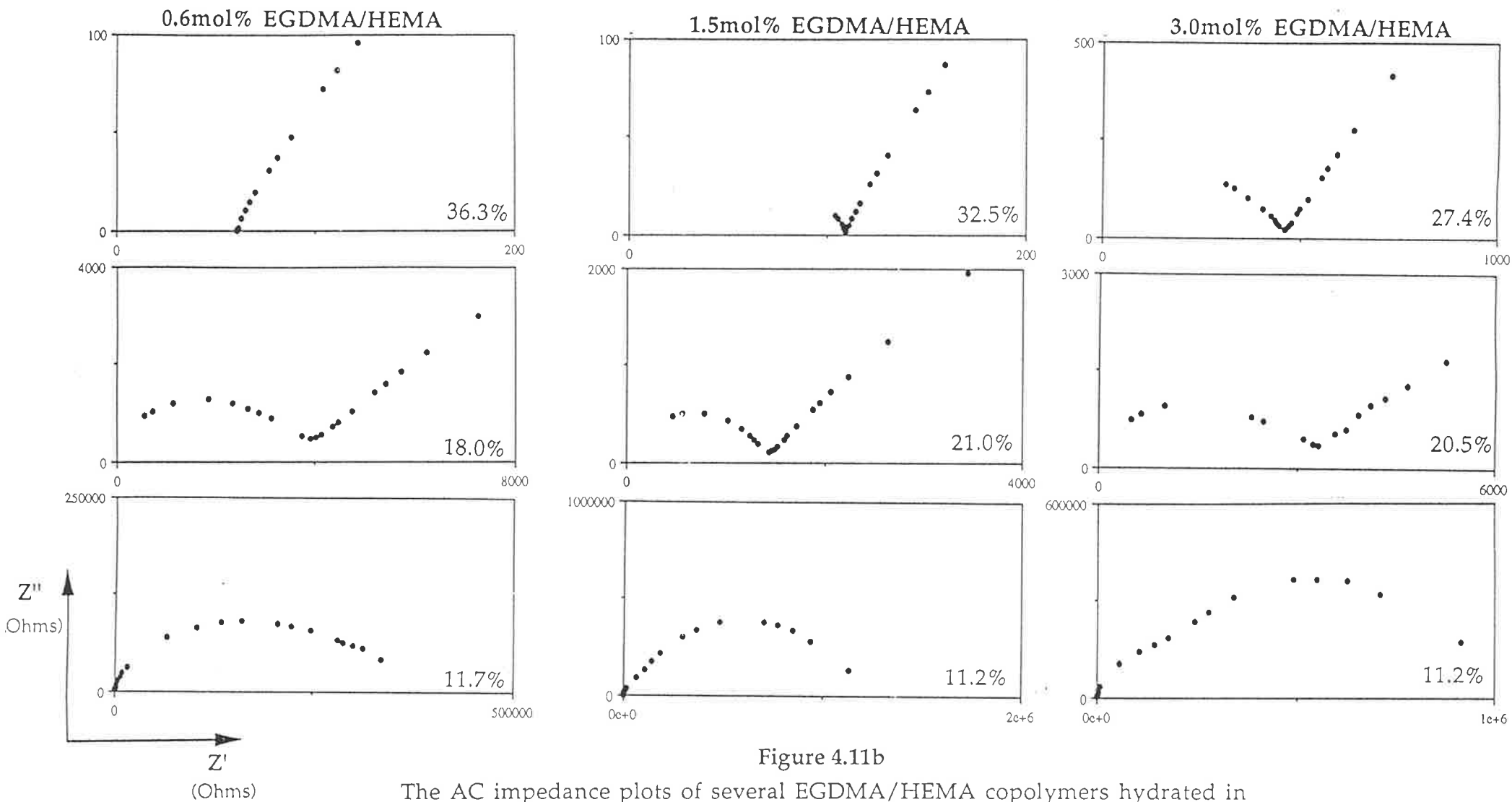


Figure 4.11b

The AC impedance plots of several EGDMA/HEMA copolymers hydrated in 0.25M KBr at various water contents and 25°C. EGDMA concentrations and water contents as listed above.

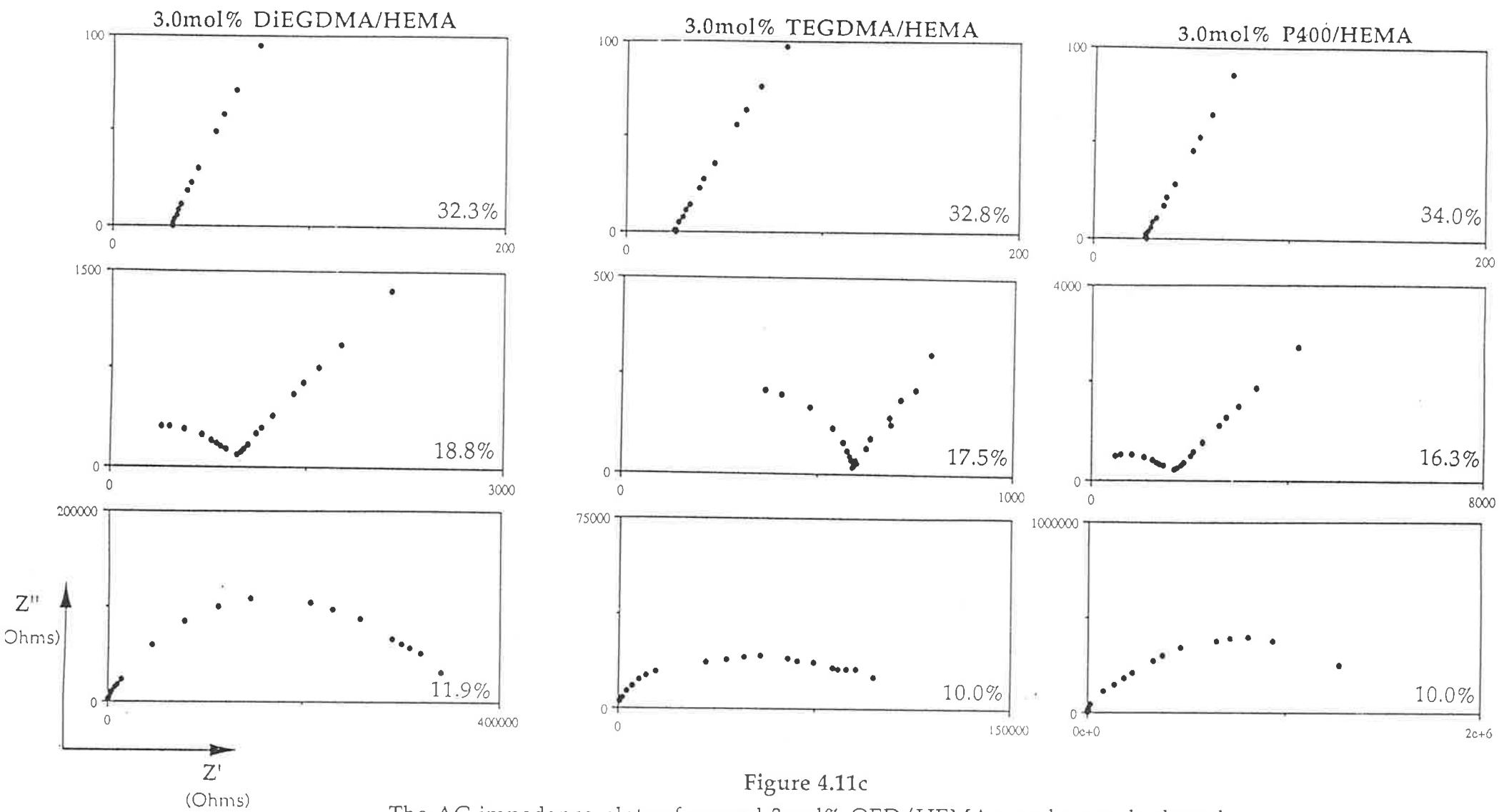


Figure 4.11c  
 The AC impedance plots of several 3mol% OED/HEMA copolymers hydrated in 1M KBr at various water contents and 25°C. OED and water contents as listed above.

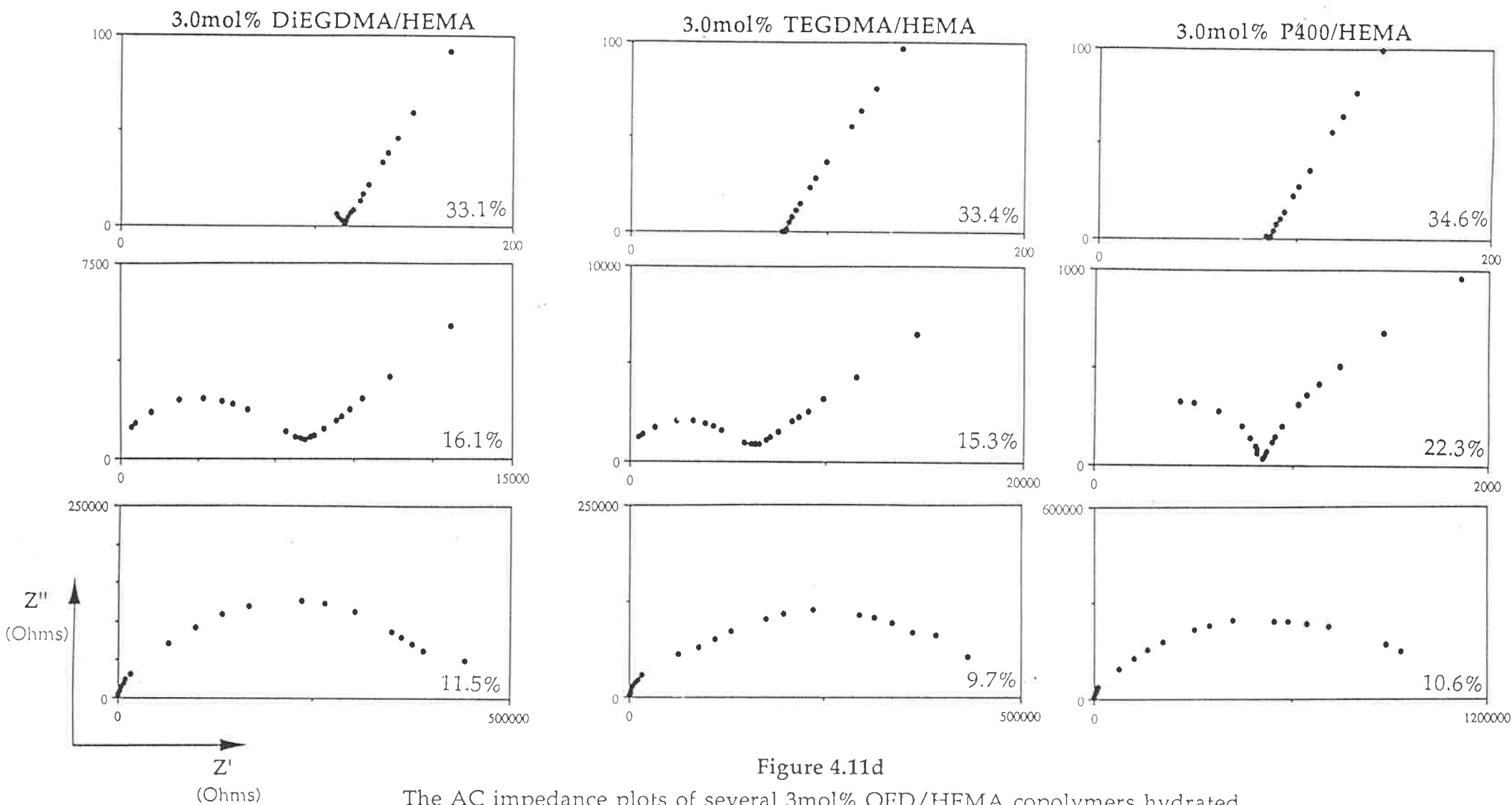


Figure 4.11d

The AC impedance plots of several 3mol% OED/HEMA copolymers hydrated in 0.25M KBr at various water contents and 25°C. OED and water contents as listed above.



indicative of two phase morphology with respect to conductivity, tended to occur at lower water contents for copolymer samples of higher KBr concentration. This suggests that the KBr ions are able to reorder water at lower hydration levels improving the continuity of the conducting phase thus facilitating ion motion and conductivity.

#### 4.6.3 KBr doped OED/HEMA Copolymers

The variation of  $\log(\text{conductivity})$  at 25°C for several 3mol% OED/HEMA copolymers hydrated in different KBr solutions (0.25M, 1.0M) with water content is shown in Figures 4.10c-f. As in the case of the pHEMA samples, the conductivity behaviour of the KBr doped EGDMA/HEMA samples on dehydration was similar in form to the behaviour shown by the undoped samples. The conductivity behaviour of KBr doped 3mol% EGDMA has already been discussed in Section 4.6.2.

3mol% OED/HEMA copolymers, where OED = DiEGDMA, TEGDMA, P400, all exhibit two regions of behaviour with the transition between the two regions occurring at approximately 22wt% water content. The two step behaviour was expected as these copolymers all have EWC<35wt% when hydrated in water and the addition of KBr further reduced the water content. The KBr doped samples of each of these copolymers exhibited similar two step behaviour, however the transition was at reduced hydration levels. The transition for DiEGDMA/HEMA samples was shown at ca.20wt% water, for TEGDMA/HEMA at ca.18wt% water and P400 at ca.17wt%.

Selected AC impedance spectra of 3mol% OED/HEMA copolymers subjected to dehydration are presented in Figures 4.11a-d. All the copolymers, at each of the concentrations, exhibited the same progression in the nature of the AC impedance plots as dehydration is carried out. At high water contents a non vertical spike is present. As water is removed gradually, the touch down frequency of the spike decreases as the high frequency behaviour results

in a semicircular portion of the locus. This semi-circle broadens as the water content decreases until the locus can be described as the superposition of two semi-circles. The emergence of the superposition of the semi circles is ascribed to a morphological change within the polymers that effects the conductivity, i.e. there exists localised regions of the gel network with insufficient water to support the motion of the charged particles.

A few differences exist in the changing of the nature of the AC impedance spectra of the copolymers. The emergence of the superposition of two semi-circles in the AC impedance plots occurred at higher water contents for 3mol% OED/HEMA polymers where  $n$ , the number of ethylene glycol units in the OED, was lower. Except for the DiEGDMA/HEMA copolymer, the addition of KBr resulted in this form of AC impedance plot occurring at lower water contents, implying that the KBr ions are able to reorder water at low hydration levels to enhance conductivity. The decrease in water content at which this change in the nature of the AC impedance plot took place did not change significantly for different KBr concentrations.

## 4.7 The Variation of Conductivity with Temperature

### 4.7.1 KBr doped pHEMA

The conductivity of fully hydrated pHEMA samples, hydrated in several solutions of varying KBr concentration, was evaluated as the samples were cooled from room temperature to  $-10^{\circ}\text{C}$  and then warmed to room temperature. The cooling rate was  $0.22^{\circ}\text{C}/\text{min}$  and the heating rate was  $0.44^{\circ}\text{C}/\text{min}$ . The conductivity of these samples is presented in Figure 4.12.

Except for the sample hydrated in 1M KBr, pHEMA/KBr gels exhibited similar behaviour to the undoped pHEMA hydrogel sample (Section 3.7.1).  $\text{Log}(\text{conductivity})$  decreased linearly as temperature decreased until a rapid decrease in conductivity occurred at sub-zero temperatures. The temperature

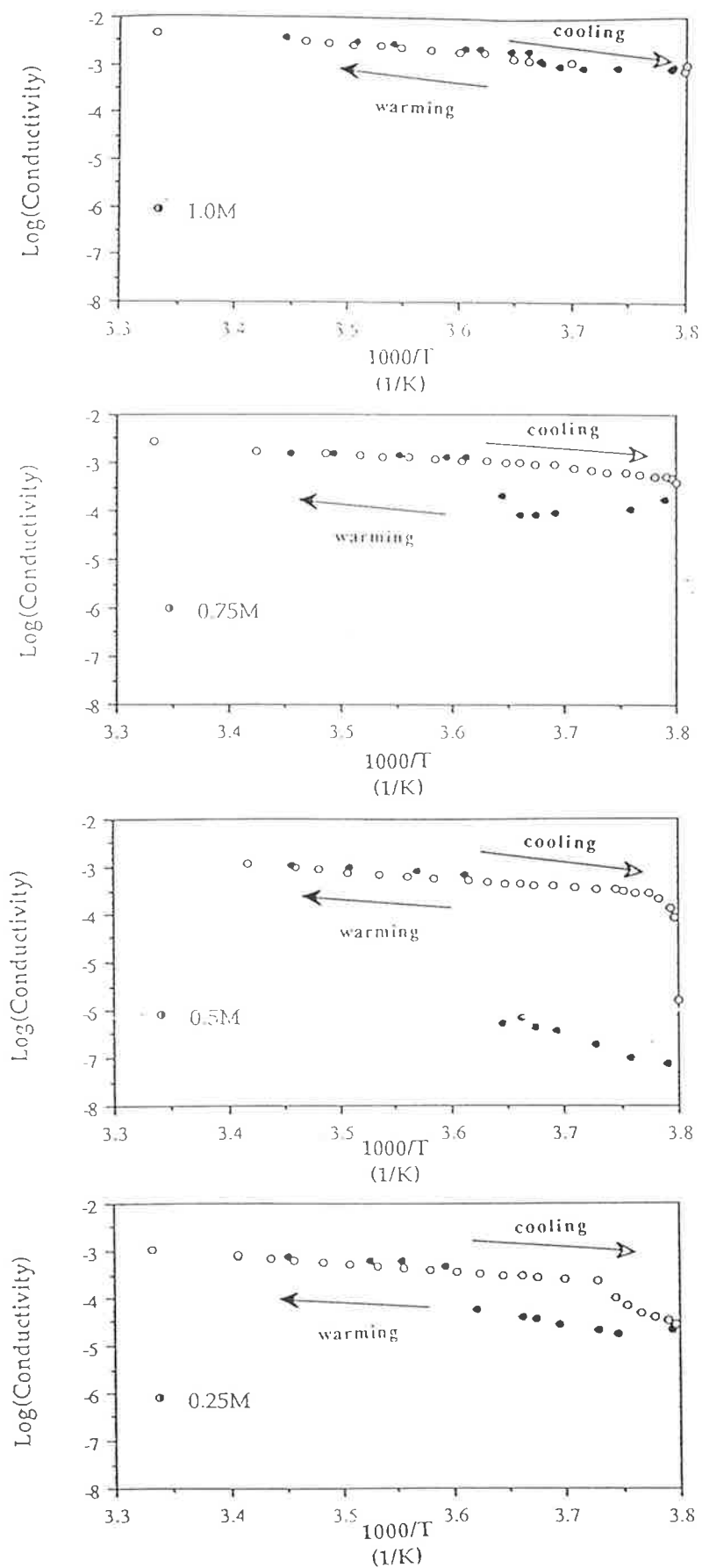


Figure 4.12

The variation of  $\log(\text{Conductivity})$  with  $1000/T$  for pHEMA samples, hydrated in a range of KBr solutions, at full hydration. KBr concentration of the hydration solution as listed above.

(hollow markers: cooling, solid markers: warming)

at which this decrease took place decreased with increased KBr content. On warming the samples, a second region of linear behaviour was exhibited as  $\log(\text{conductivity})$  increased with increasing temperature until at temperatures of ca.  $-2.0^{\circ}\text{C}$  when there was a sharp increase in conductivity.  $\log(\text{conductivity})$  increased linearly above this temperature in a manner similar to the initial decrease experienced by the samples when subjected to cooling. The sample hydrated in 1.0M KBr exhibited no transitions as  $\log(\text{conductivity})$  decreased linearly with temperature to  $-10^{\circ}\text{C}$  and then increased in a similar linear manner on warming.

As was the case for the undoped samples, the transition in conductive behaviour is believed to result from the freezing of some of the occluded water present in the gel electrolytes. The AC impedance spectra of pHEMA hydrated in 0.25M KBr at several temperatures are given in Figure 4.13. As the temperature decreases the frequency at which the non vertical spike intercepts the real impedance axis decreases and the bulk resistance of the sample increases. The sudden decrease in  $\log(\text{conductivity})$  is accompanied by a change in the nature of the AC impedance response. The AC impedance spectra is the superposition of two semi-circles: this has been previously attributed<sup>(20)</sup> to the presence of non conductive crystalline regions. In this case the crystalline regions are caused by the formation of ice which will disrupt the motion of charged entities through the occluded water phase. On warming from the minimum temperature, the AC impedance spectra maintained this general form yet the magnitude of the bulk resistance decreased as temperature increased. At ca.  $2.0^{\circ}\text{C}$  the nature of the AC impedance spectra reverted to the original type of response. As temperature was further increased the intercept frequency of the non vertical capacitance spike increased as the bulk resistance decreased. This transition in behaviour is ascribed to the thawing of the frozen water.

The AC impedance plots of the pHEMA sample hydrated in 1.0M KBr

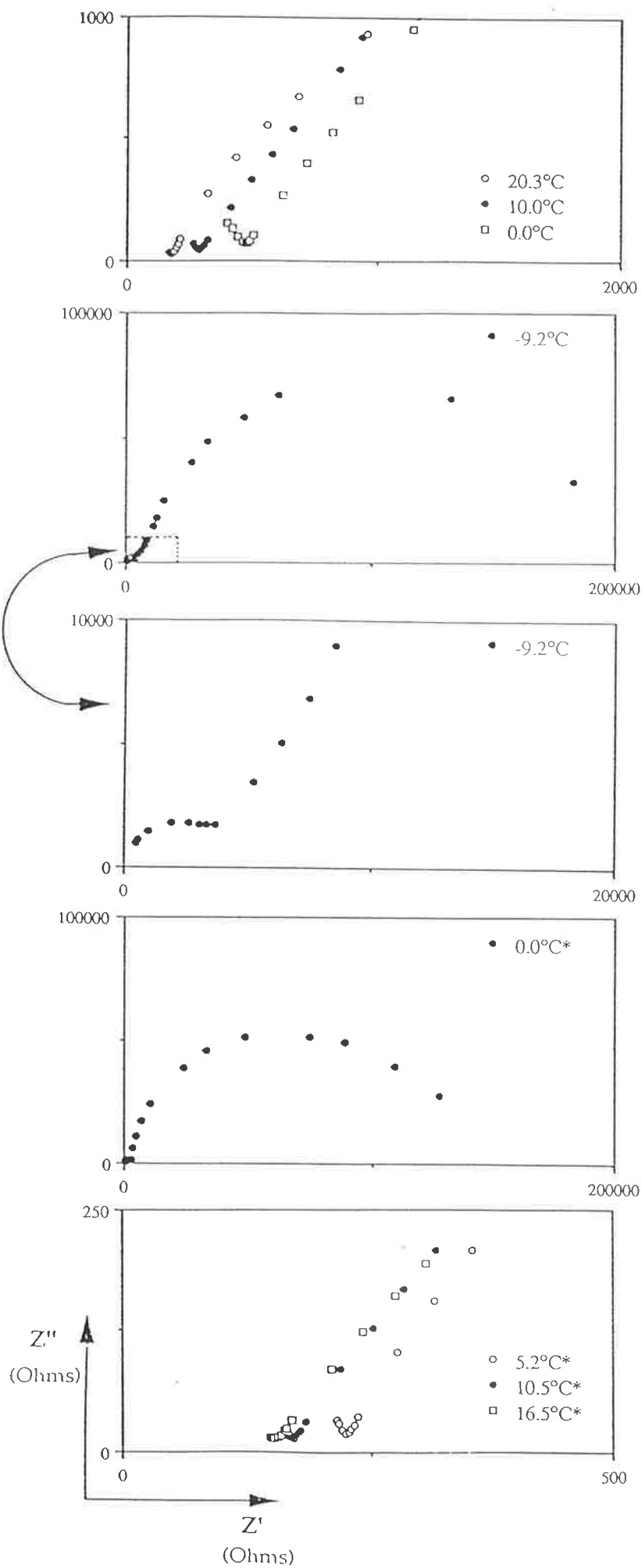


Figure 4.13

The AC impedance plots of a fully hydrated pHEMA sample solvated in 0.25M KBr at various temperatures as listed above.

(\* indicates measurement made when sample was being warmed)

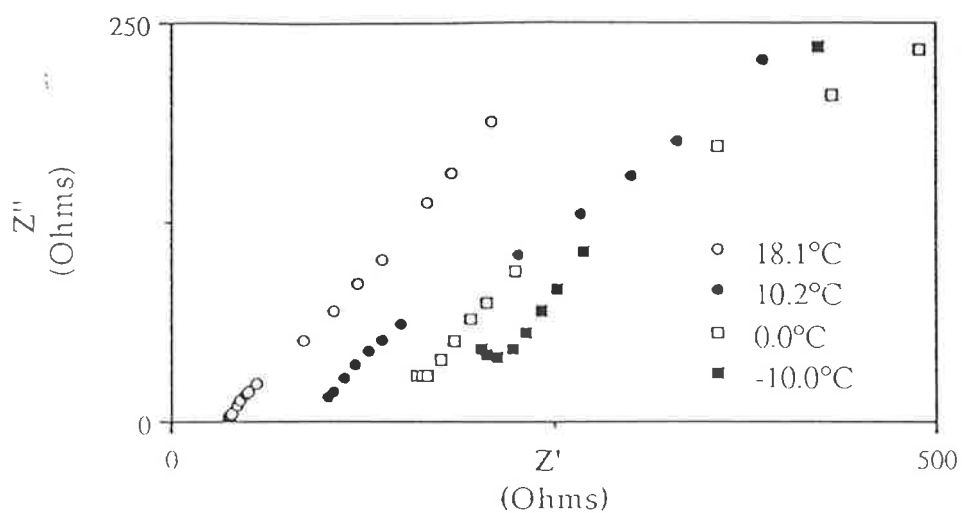


Figure 4.14a

The AC impedance plots of a fully hydrated pHEMA sample hydrated in 1.0M KBr at various temperatures as listed above. Data was collected as the sample was cooled.

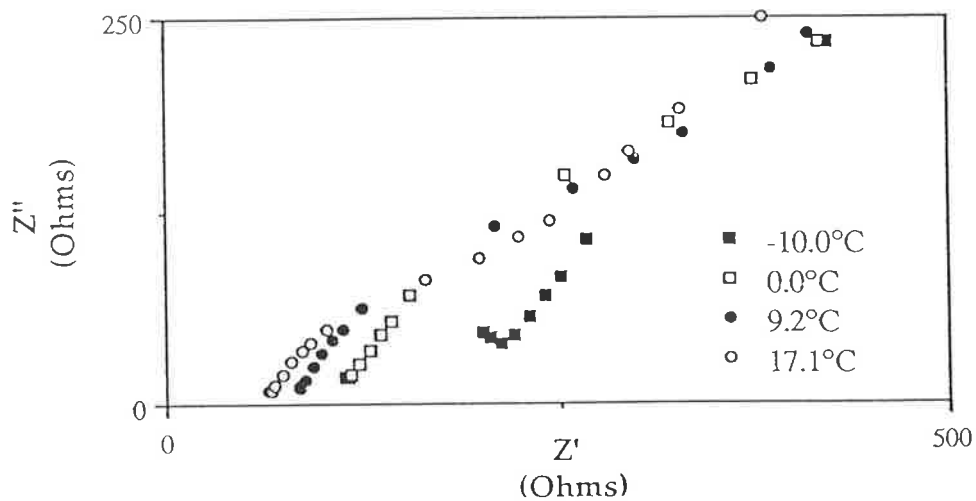


Figure 4.14b

The AC impedance plots of a fully hydrated pHEMA sample hydrated in 1.0M KBr at various temperatures as listed above. Data was collected as the sample was warmed.

at different temperatures are shown in Figure 4.14. As this sample was cooled to  $-10^{\circ}\text{C}$  there was no change in the nature of the AC impedance response. The frequency at which the non vertical capacitance spike intercepted the real impedance axis decreased and the bulk resistance increased as the temperature decreased. The opposite trends in touch down frequency and bulk resistance were observed as temperature was increased. It is interesting to note that the  $\log(\text{conductivity})$  of this sample at temperatures above  $0.0^{\circ}\text{C}$  is greater on warming than on cooling the sample. Samples exhibiting freezing behaviour often show a similar trend suggesting hysteresis arising from the thawing of the freezable water and thus it is deserving of future investigation.

The temperature at which the occluded water begins to freeze ( $T_{\dagger}$ ) is given in Table 4.6. The freezing point will be affected by the KBr concentration and in electrolyte solutions the freezing point depression of a solution can be estimated from the following equation:

$$\Delta T = i \cdot K_f \cdot m_2 \qquad \text{Eqn. 4.1}$$

where  $\Delta T$  is the freezing point depression,  $i$  is the van't Hoff factor (i.e. moles of particles in solution/ moles of solute),  $K_f$  is the molal freezing point depression constant ( $K_f=1.86^{\circ}\text{C/molal}$  for  $\text{H}_2\text{O}$ ) and  $m_2$  is the concentration of the solute (moles/kg solvent). The freezing point depressions that would be experienced by KBr solutions ( $\Delta T$ ) are given in Table 4.6.

The freezing point depression in the gel samples is greater for samples of higher KBr concentration, however when compared to the freezing point depression experienced by solutions of similar concentration ( $\Delta T$ ) it appears that the decrease in the freezing temperature is generally greater for gel samples. This can be ascribed to the water/polymer and ion/water/polymer interactions.

The activation energy,  $E_{a1}$ , was found not to vary significantly with variation in KBr content. This would appear to suggest that, in the concentration range studied, ion/ion and ion/polymer interaction had little

**Table 4.6**

The KBr concentration, EWC,  $E_{a1}$ ,  $E_{a2}$ , and  $T_{\ddagger}$  of pHEMA samples hydrated in KBr solutions of varying concentration.  $\Delta T$  is the freezing point depression calculated for the soaking solutions.

[KBr] <sub>ss</sub> (M)	[KBr] <sub>p</sub> (mol/g)	EWC (%)	$E_{a1}$ (kJ/mol)	$E_{a2}$ (kJ/mol)	$\Delta T$ (°C)	$T_{\ddagger}$ (°C)
1.0	$4.17 \times 10^{-4}$	39.6	14.1	-	3.72	<-10.0
0.75	$3.05 \times 10^{-4}$	39.7	12.8	-	2.79	-9.8
0.50	$1.25 \times 10^{-4}$	40.0	14.2	56.7	1.86	-8.2
0.25	$0.64 \times 10^{-4}$	40.2	14.3	34.3	0.93	-5.0
0	-	-	15.0	36.2	-	-5.8

$E_{a1}$  is the activation energy on cooling.

$E_{a2}$  is the activation energy at subzero temperatures on warming.

$T_{\ddagger}$  is the temperature at which freezing of the occluded water begins to take place

influence on the activation energy,  $E_{a1}$ . The activation energy of conductivity of 1.0M KCl over the temperature range 10°C-30°C is 5.8kJ/mol<sup>(21)\*</sup>. Gel electrolyte samples have higher activation energies resulting not only from polymer/water interaction, which result in a less mobile conducting phase, but also from the physical impediment that the polymer network presents to the motion of an ion and its associated hydration cloud.

$E_{a2}$ , the activation energy after freezing has taken place, was not calculated for all gel samples as they either did not exhibit freezing behaviour or insufficient linear data was recorded. The values of  $E_{a2}$  recorded for the KBr doped samples are of the same order of magnitude as that for the undoped sample, suggesting that the presence of ice is again the reason for the

\* Calculated from the data of Dobos (21).



decrease in conductivity and the change in the nature of the AC impedance plots.

#### 4.7.2 KBr doped EGDMA/HEMA Copolymers.

The conductivity of several fully hydrated EGDMA/HEMA copolymer samples, hydrated in solutions of varying KBr concentration, was evaluated as the samples were cooled from room temperature to  $-10^{\circ}\text{C}$  and then warmed to room temperature. The cooling and heating rates were the same as for the pHEMA samples. The variation in conductivity of these samples is presented in Figures 4.15a-d.

All samples exhibited a linear decrease in  $\log(\text{conductivity})$  as the temperature was decreased. The linear behaviour yielded the activation energy  $E_{a1}$  (Table 4.7) which was found to be, in general, higher for samples of increased KBr and EGDMA concentration. At some temperature below  $0^{\circ}\text{C}$ ,  $T_{\ddagger}$ , a sudden decrease in  $\log(\text{conductivity})$  was experienced by most samples and this is attributed to the partial freezing of the water phase. A second region of linear behaviour was exhibited for some samples on warming from  $-10^{\circ}\text{C}$  to  $0^{\circ}\text{C}$  which yielded another activation energy,  $E_{a2}$  (Table 4.7).

It should be noted that as EGDMA and KBr concentration increased,  $T_{\ddagger}$  decreased until, for samples of 1.5mol% EGDMA/HEMA and 3.0mol% EGDMA/HEMA which had been hydrated in 1.0M KBr, no freezing transition was observed; the presence of sufficient KBr and EGDMA had depressed the freezing point of the occluded water below  $-10^{\circ}\text{C}$  at the cooling rate employed. For less crosslinked samples, 0.3 and 0.6mol% EGDMA,  $T_{\ddagger}$ , increased with KBr concentration as expected.

An apparent anomaly in the recorded data was observed. The variation in  $\log(\text{conductivity})$  with temperature for 1.5mol% EGDMA/HEMA hydrated in 0.25M KBr is presented in Figure 4.15c. This sample exhibited a transition in behaviour on warming from  $-10^{\circ}\text{C}$ . This transition was

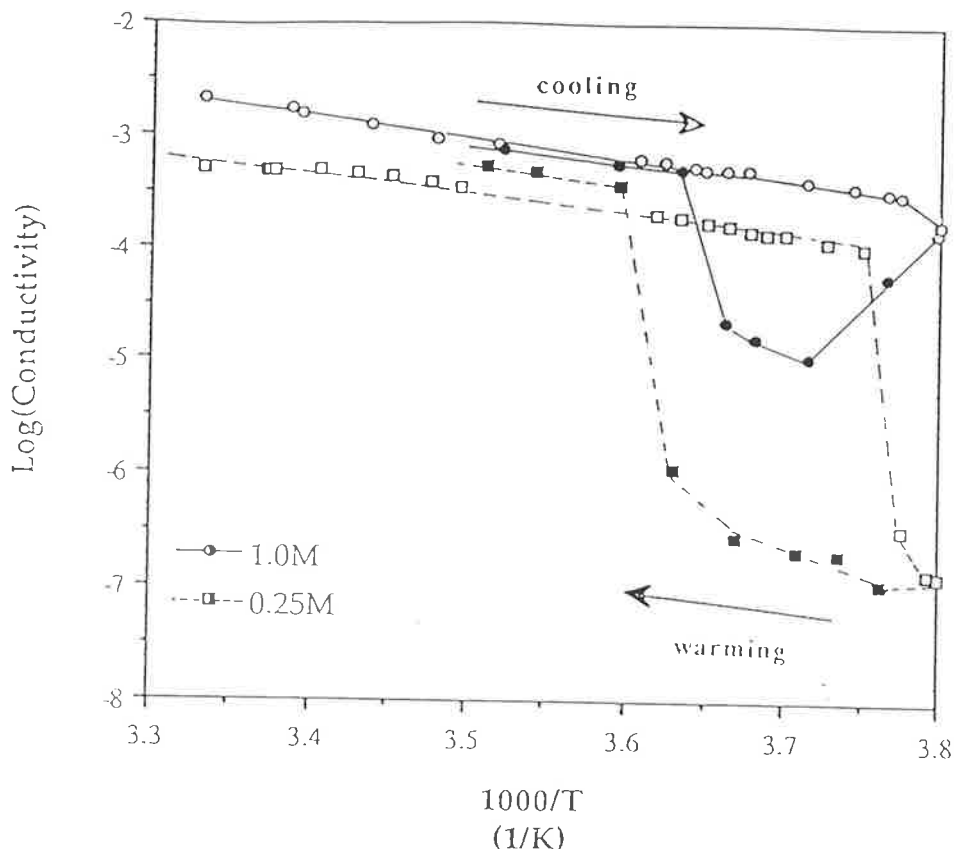


Figure 4.15a

The variation of  $\log(\text{Conductivity})$  with  $1000/T$  for 0.3mol% EGDMA/HEMA samples, hydrated in different KBr solutions, at full hydration. KBr concentration of the hydration solution as listed above.

(hollow markers: cooling, solid markers: warming)

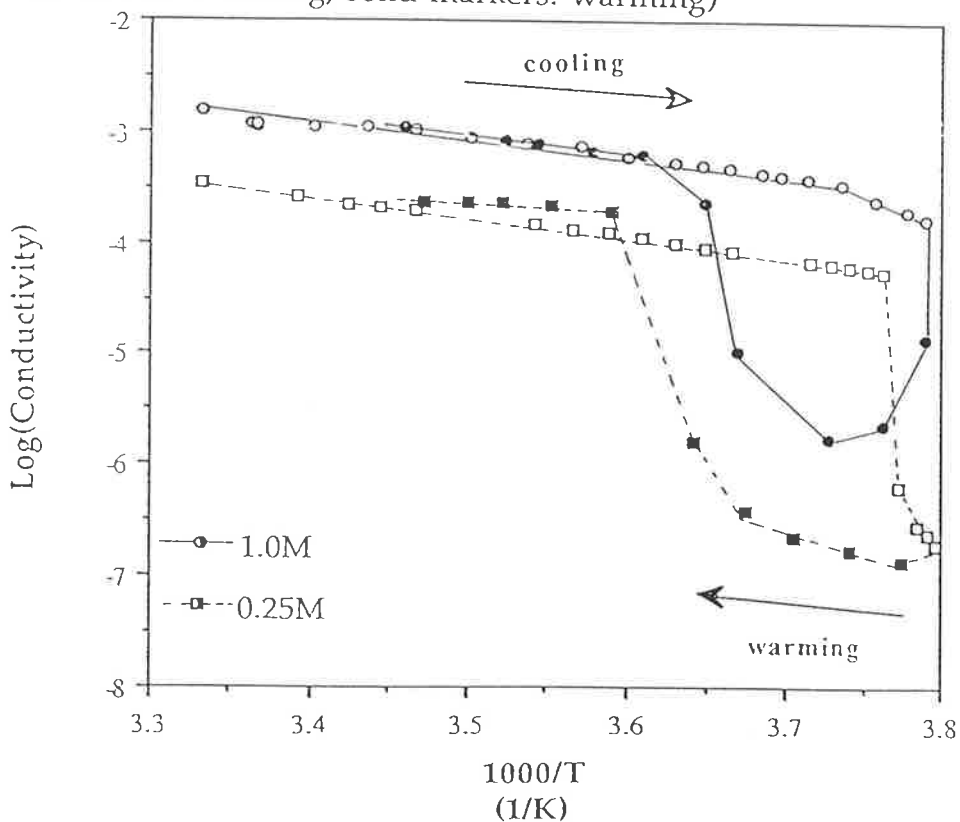


Figure 4.15b

The variation of  $\log(\text{Conductivity})$  with  $1000/T$  for 0.6mol% EGDMA/HEMA samples, hydrated in different KBr solutions, at full hydration. KBr concentration of the hydration solution as listed above.

(hollow markers: cooling, solid markers: warming)

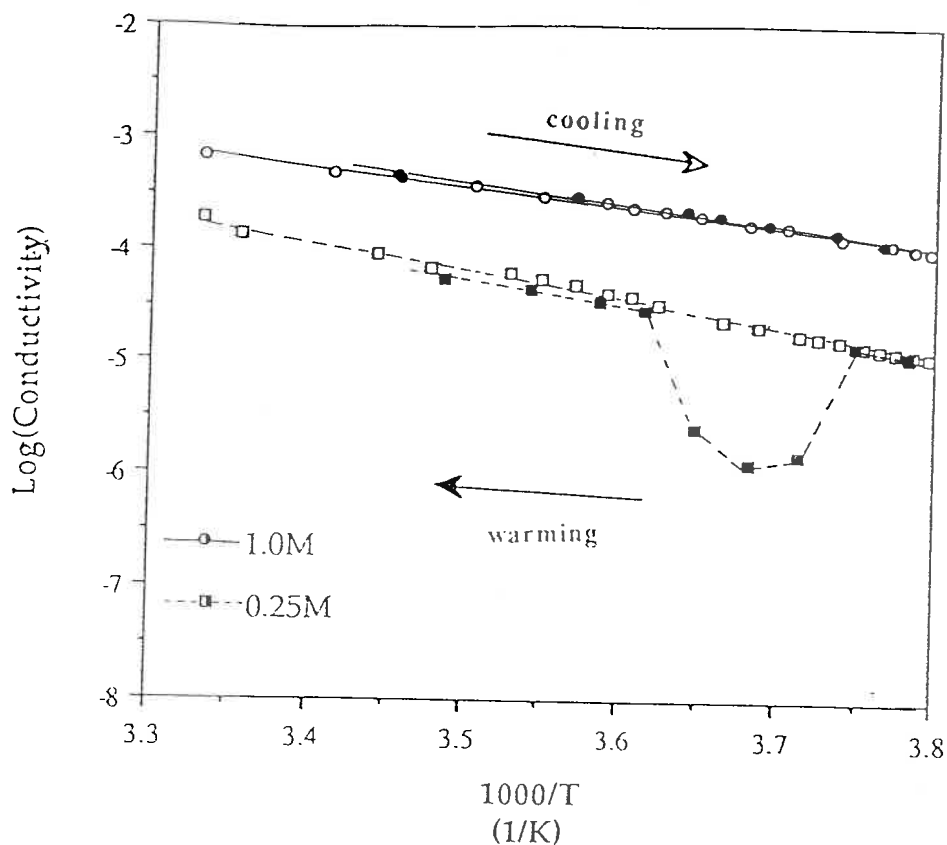


Figure 4.15c

The variation of  $\log(\text{Conductivity})$  with  $1000/T$  for 1.5mol% EGDMA/HEMA samples, hydrated in different KBr solutions, at full hydration. KBr concentration of the hydration solution as listed above.

(hollow markers: cooling, solid markers: warming)

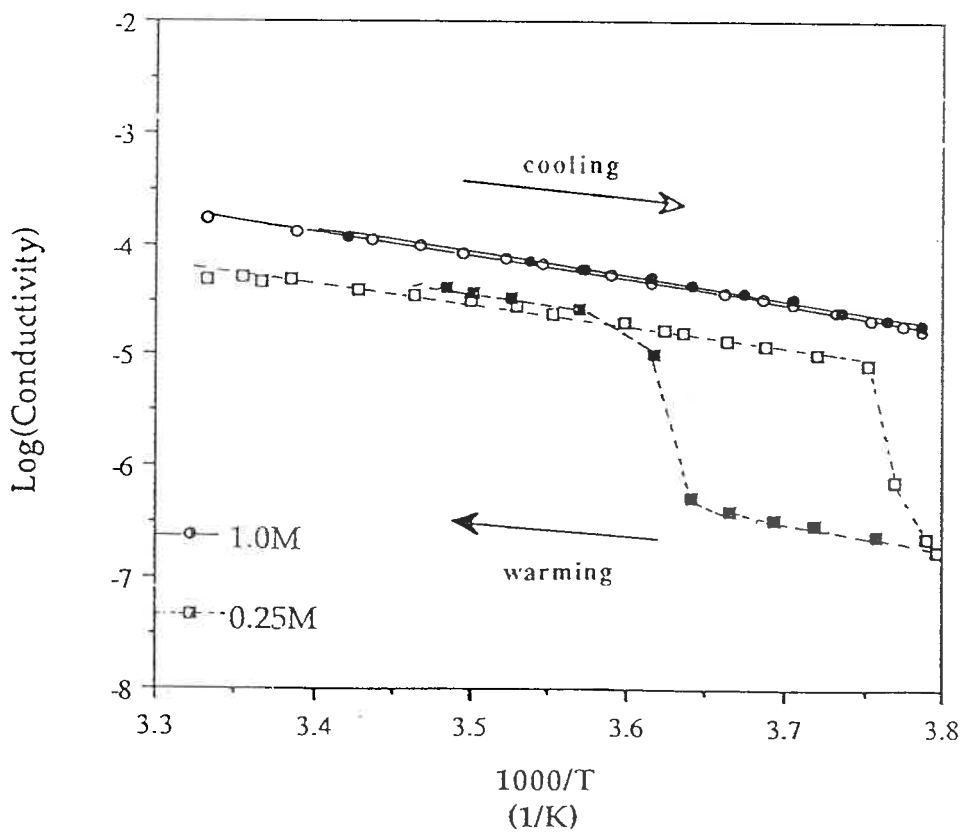


Figure 4.15d

The variation of  $\log(\text{Conductivity})$  with  $1000/T$  for 3.0mol% EGDMA/HEMA samples, hydrated in different KBr solutions, at full hydration. KBr concentration of the hydration solution as listed above.

(hollow markers: cooling, solid markers: warming)

attributed to partial freezing of the occluded water as  $\log(\text{conductivity})$  returned to its original linear behaviour at ca.2.0°C. A possible explanation for this response is that the freezable water present in this sample had undergone supercooling and warming of the sample allowed the water molecules to reorganise and subsequently freeze.

**Table 4.7**

The KBr concentration, EWC,  $E_{a1}$ ,  $E_{a2}$ , and  $T_{\ddagger}$  of several EGDMA/HEMA samples hydrated in KBr solutions of varying concentration.

Copolymer	[KBr] <sub>ss</sub> (M)	[KBr] <sub>p</sub> (mol/g)	EWC (%)	$E_{a1}$ (kJ/mol)	$E_{a2}$ (kJ/mol)	$T_{\ddagger}$ (°C)
0.3mol%	1.0	$3.33 \times 10^{-4}$	36.8	15.0	48.4	-8.2
EGDMA/HEMA	0.25	$0.35 \times 10^{-4}$	37.3	14.8	54.8	-6.5
	0	-	37.5	16.3	24.2	-6.1
0.6mol%	1.0	$3.43 \times 10^{-4}$	35.9	14.5	-	-8.4
EGDMA/HEMA	0.25	$0.81 \times 10^{-4}$	36.3	14.9	35.9	-7.4
	0	-	36.3	16.9	24.5	-6.0
1.5mol%	1.0	$3.43 \times 10^{-4}$	32.3	16.8	-	<-10.0
EGDMA/HEMA	0.25	$0.90 \times 10^{-4}$	32.5	19.9	-	-
	0	-	32.9	16.9	22.6	-7.0
3.0mol%	1.0	$1.39 \times 10^{-4}$	27.0	18.7	-	<-10.0
EGDMA/HEMA	0.25	$0.58 \times 10^{-4}$	27.4	16.8	23.0	-6.5
	0	-	27.7	22.5	-	-10.0

$E_{a1}$  is the activation energy on cooling.

$E_{a2}$  is the activation energy at subzero temperatures on warming.

$T_{\ddagger}$  is the temperature at which freezing of the occluded water begins to take place

The activation energy,  $E_{a2}$ , was calculated for samples that exhibited a transition in conductivity behaviour and also yielded sufficient linear data to enable reasonably accurate evaluation.  $E_{a2}$  decreased with increased EGDMA

concentration and was markedly higher for doped samples compared to similar undoped samples. This suggests that the major factor determining the amount of freezable water present in these KBr doped samples is the EGDMA concentration, as the  $E_{a2}$  was lower for more highly crosslinked samples. However, the large increase in  $E_{a2}$  for doped lightly crosslinked polymers compared to undoped samples indicates the importance of the freezable water to the motion of ions.

#### 4.8 Variation of Conductivity with Nature of Dopant

pHEMA samples were hydrated in 1.0M and 0.5M solutions of a range of alkali halides, lithium perchlorate and potassium carbonate. The alkali halides were chosen to monitor the effect of varying ion size whereas the polyatomic anionic electrolytes were chosen as a result of the influence anions have been shown to have on the EWC<sup>(7,8)</sup>. The resulting gels were all transparent and colourless except for the samples hydrated in iodide solutions which were transparent but yellow. This colouration has been ascribed<sup>(7)</sup> to the binding of iodide, or tri-iodide anions to the pHEMA network. The conductivity of these samples was measured at 25°C before the samples were dried to enable the calculation of EWC and the concentration of the dopant (mol/g dry polymer). The relevant data is presented in Table 4.8.

It should be noted that the nature of the dopant employed had a drastic effect on the EWC of the resulting gel electrolyte (Figure 4.16). Samples hydrated in iodide and  $\text{LiClO}_4$  solutions exhibited large increases in EWC when compared to a sample hydrated in water (EWC= 40.4wt%). Bromide solutions yielded samples of slightly reduced EWC whereas chloride solutions led to greater decreases in EWC. The greatest reduction in EWC was experienced by samples hydrated in  $\text{K}_2\text{CO}_3$  solutions. The nature of the anion in the electrolyte appears to have a greater effect on the EWC than the nature of the cation.

Table 4.8

EWC, dopant concentration and conductivity at 25°C of pHEMA samples hydrated in several dopant solutions of different concentrations.

Dopant	[Dopant] <sub>SS</sub> <sup>†</sup> (M)	[Dopant] <sub>P</sub> <sup>‡</sup> (M)	EWC (%)	σ (S/cm)
-	-	-	40.4	2.86 × 10 <sup>-5</sup>
LiCl	1.0	3.36 × 10 <sup>-4</sup>	33.3	1.06 × 10 <sup>-3</sup>
	0.5	1.84 × 10 <sup>-4</sup>	35.4	7.23 × 10 <sup>-4</sup>
LiBr	1.0	3.79 × 10 <sup>-4</sup>	38.3	2.66 × 10 <sup>-3</sup>
	0.5	2.01 × 10 <sup>-4</sup>	38.6	1.42 × 10 <sup>-3</sup>
LiI	1.0	6.18 × 10 <sup>-4</sup>	53.7	2.03 × 10 <sup>-2</sup>
	0.5	2.58 × 10 <sup>-4</sup>	52.1	7.87 × 10 <sup>-3</sup>
NaCl	1.0	2.88 × 10 <sup>-4</sup>	28.2	7.10 × 10 <sup>-4</sup>
	0.5	1.72 × 10 <sup>-4</sup>	33.7	5.82 × 10 <sup>-4</sup>
NaBr	1.0	3.56 × 10 <sup>-4</sup>	35.6	2.71 × 10 <sup>-3</sup>
	0.5	1.87 × 10 <sup>-4</sup>	37.2	1.36 × 10 <sup>-3</sup>
NaI	1.0	5.15 × 10 <sup>-4</sup>	51.5	1.34 × 10 <sup>-2</sup>
	0.5	2.23 × 10 <sup>-4</sup>	44.8	6.91 × 10 <sup>-3</sup>
KCl	1.0	3.01 × 10 <sup>-4</sup>	29.7	8.05 × 10 <sup>-4</sup>
	0.5	1.77 × 10 <sup>-4</sup>	34.1	6.20 × 10 <sup>-4</sup>
KBr	1.0	4.17 × 10 <sup>-4</sup>	39.6	4.13 × 10 <sup>-3</sup>
	0.5	1.25 × 10 <sup>-4</sup>	40.0	2.12 × 10 <sup>-3</sup>
KI	1.0	5.89 × 10 <sup>-4</sup>	50.5	1.84 × 10 <sup>-2</sup>
	0.5	2.30 × 10 <sup>-4</sup>	47.2	7.55 × 10 <sup>-3</sup>
K <sub>2</sub> CO <sub>3</sub>	1.0	2.47 × 10 <sup>-4</sup>	21.4	1.43 × 10 <sup>-4</sup>
	0.5	1.46 × 10 <sup>-4</sup>	28.6	3.42 × 10 <sup>-5</sup>
LiClO <sub>4</sub>	1.0	5.02 × 10 <sup>-4</sup>	50.9	8.63 × 10 <sup>-3</sup>
	0.5	2.37 × 10 <sup>-4</sup>	45.3	4.36 × 10 <sup>-3</sup>

<sup>†</sup>[Dopant]<sub>SS</sub> is the concentration of the dopant soaking solution.

<sup>‡</sup>[Dopant]<sub>P</sub> is the concentration of the dopant in the pHEMA samples in mol/g dry polymer.

Previous studies by Refojo<sup>(7)</sup> and Dusek et al.<sup>(8)</sup> have yielded similar trends. It appears that the ability of the anion to interact with the polymer network and impede any hydrophobic bonding will control the EWC. The

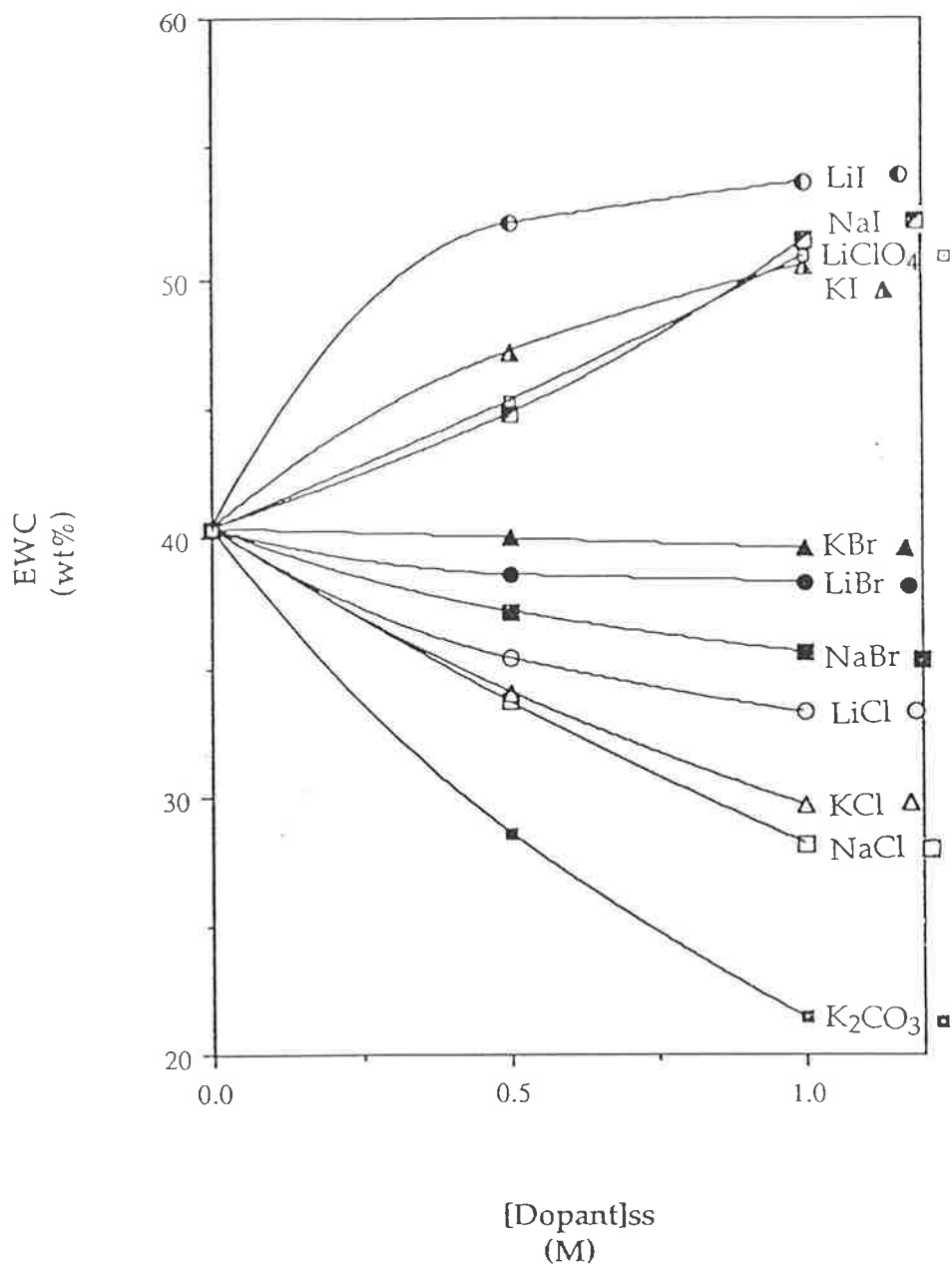


Figure 4.16

The EWC of pHEMA samples hydrated in 1.0M and 0.5M solutions of several electrolytes at 25°C.

iodide ion,  $I^-$ , is a large monovalent anion and will be repelled from the more electronegative hydrophilic moieties on the polymer network. Given the low charge density of the  $I^-$  anion, it will only be able to order near-neighbour water molecules, it is a structure breaker<sup>(12)</sup>, and thus its approach to the more hydrophobic portions of the network will be less hindered by the need to move with an extended hydration sphere. This would lead to an iodide anion/polymer interaction causing a polyelectrolyte effect<sup>(7)</sup> and a subsequent increase in EWC as suggested by Refojo. This is supported by the  $^{127}I$  nmr measurements of Oh et al.<sup>(9)</sup> which indicate that there is specific binding of iodide anions to isotactic pHEMA gels.

Bromide and chloride electrolytes led to salting out and thus reduced EWCs of the pHEMA network. Given that both anions are also considered to be structure breaking<sup>(12)</sup> it would appear that the polarisability of the anion, or the ability of its electron cloud to be distorted, is a determining factor, i.e. anions with an easily distorted electron cloud are more likely to associate with the polymer and impede hydrophobic bonding thus increasing EWC.

Polyatomic anions,  $ClO_4^-$  and  $CO_3^{2-}$ , were found to have opposite effects on the EWC. Samples hydrated in perchlorate solutions had an increased EWC whereas the EWC was greatly reduced for samples hydrated in carbonate solutions. This could be due to the difference in charge density of the anions as the carbonate anion would be more likely to structure its aqueous environment.

The nature of the cation appears to have a secondary role in determining the EWC of a pHEMA sample hydrated in an electrolyte solution. It appears from the samples hydrated in alkali halide solutions that lithium solutions result in higher EWC than sodium or potassium. Cations have the ability to interact with the hydrophilic groups of the polymer network and this is reflected in the  $^{23}Na$  nmr data of Quinn et al.<sup>(11)</sup> for pHEMA hydrated in a saline solution. In summary, the EWC is determined



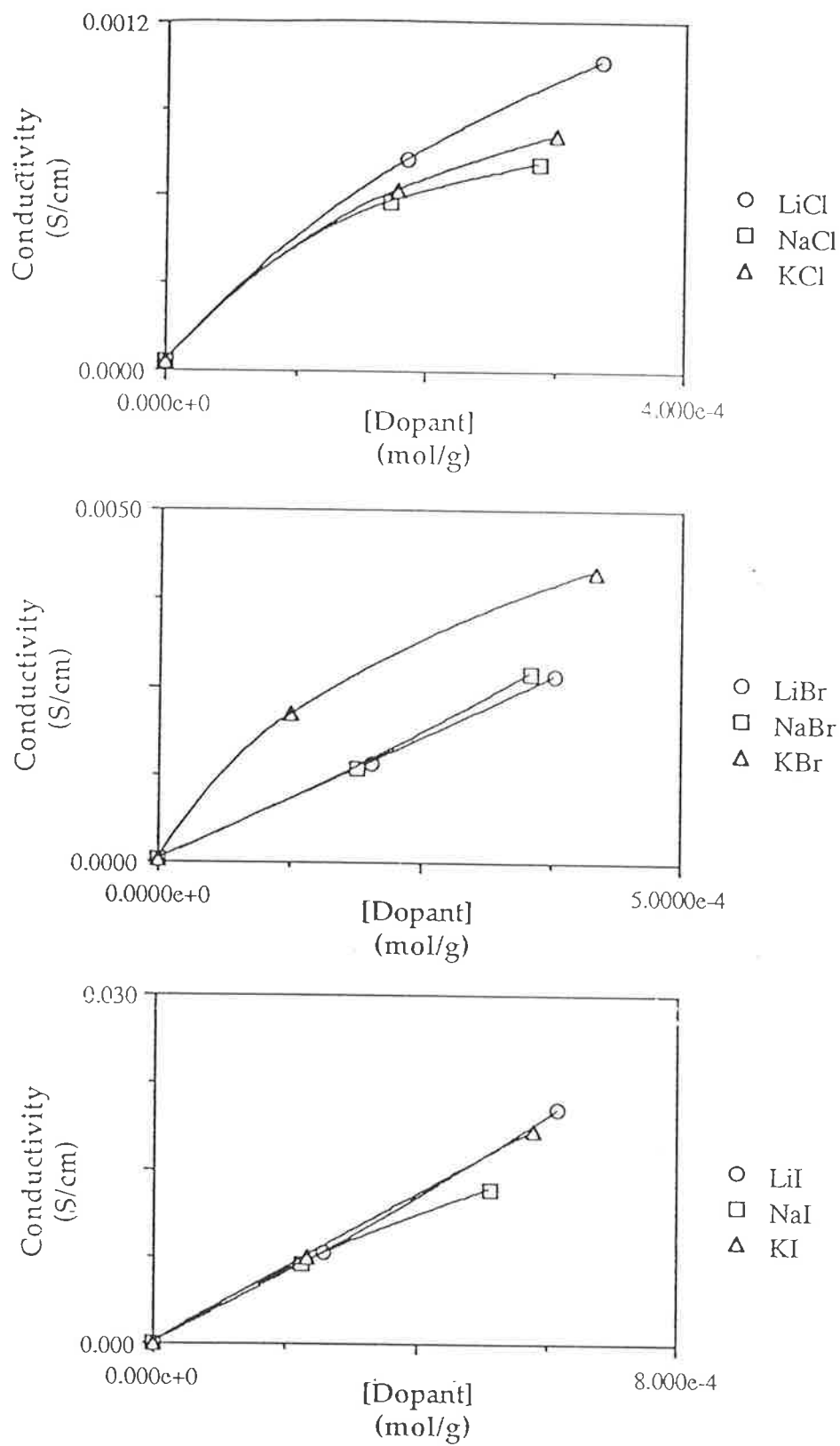


Figure 4.17a

The variation of conductivity with dopant concentration for pHEMA samples hydrated in alkali halide solutions; the effect of varying the cation.

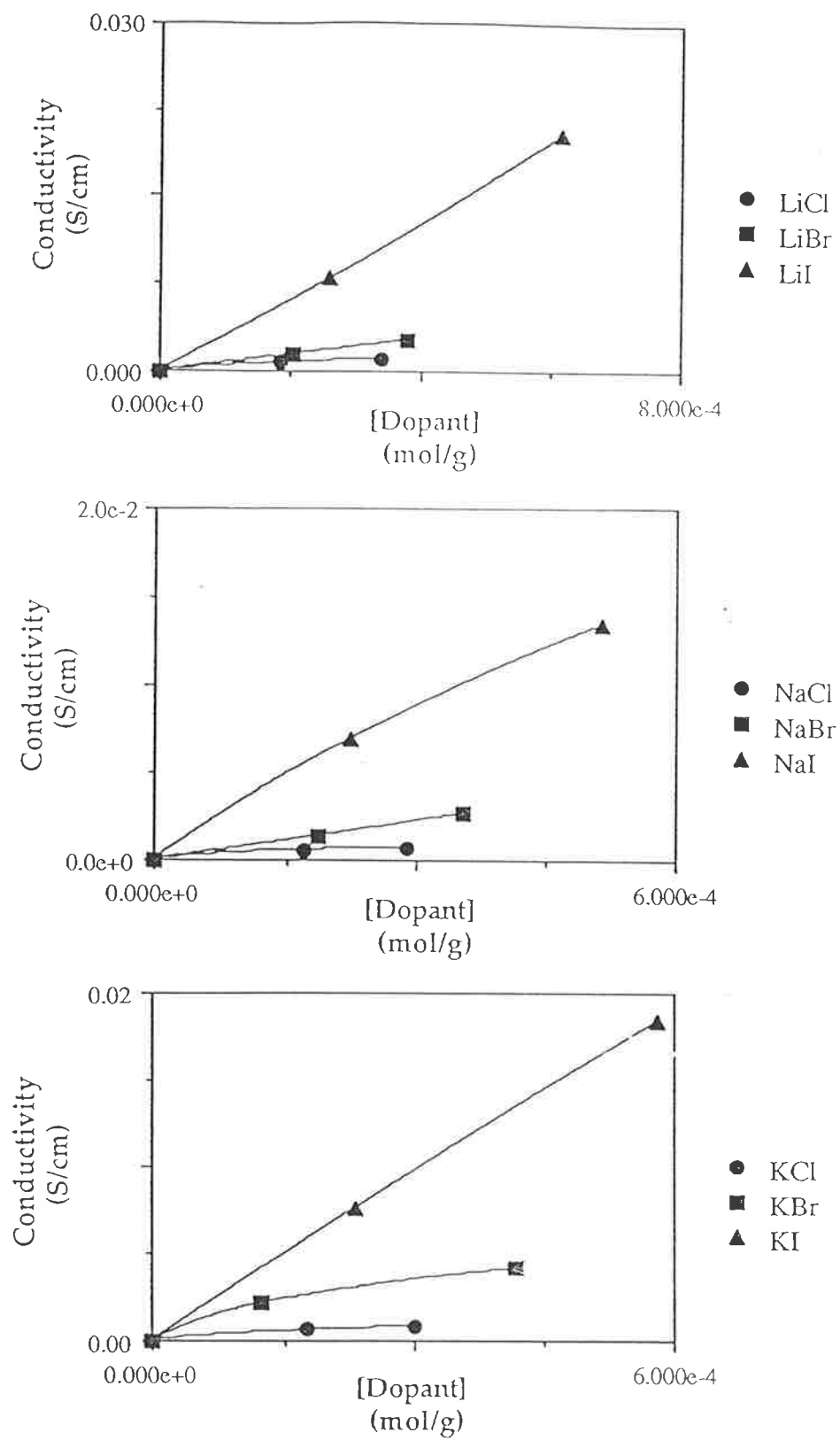


Figure 4.17b

The variation of conductivity with dopant concentration for pHEMA samples hydrated in alkali halide solutions; the effect of varying the anion.

by a combination of both anion and cation related effects.

It should be noted that all samples hydrated in electrolyte solutions exhibited significant increases in conductivity despite a reduction in EWC for some samples. This suggests that the number of charge carriers available has the greatest effect on the conductivity of the gel electrolytes studied. The variation of conductivity with dopant concentration for a range of alkali halide doped samples is presented in Figures 4.17a and 4.17b.

For each cation,  $\text{Li}^+$ ,  $\text{Na}^+$  and  $\text{K}^+$ , it was found that samples hydrated in iodide solutions exhibited much higher conductivity when compared to samples hydrated in bromide solutions which in turn were more conductive than samples hydrated in chloride solutions. Conductivity is not only dependent on the number of available charge carriers but also on their mobility. The mobility of iodide ions must thus be greater than that of bromide ions which is greater than the mobility of chloride ions. Diffusion measurements by Tighe et al.<sup>(12,13)</sup> have shown this to be true for the transport of ions across undoped pHEMA gel samples. They found the order of permeability of salts to be consistent with the changing influence of ionic structure on behaviour found in the lyotropic series and regarded both size and water structuring effects as important in determining the transport properties of an ion in a hydrated polymer matrix. However, it must be noted that the measurements of Tighe et al. were obtained by monitoring the flow of electrolytes through fully hydrated undoped pHEMA gels.

As a consequence of the sample preparation method in this work, it is suggested that the differences in conductivity result primarily from the effect of electrolytes on the EWC of the samples. The hydration of pHEMA in iodide electrolytes leads to a drastic increase in the EWC. Given that for undoped pHEMA it is believed that up to 20wt% water is tightly bound to the polymer, and water sorbed at >35wt% is believed to be free water<sup>(16)</sup>, it is suggested that increasing the EWC from that of undoped pHEMA will only

result in greater amounts of free mobile water. Conversely, the decrease in EWC caused by the sorption of bromide and chloride electrolytes will decrease the amount of free water present. These changes in the water phase not only alter the mobility of the water phase but also decrease the amount water in the gel structure limiting ion motion. These alterations of the water phase will have a significant effect on the conductivity.

The conductivity of samples hydrated in solutions of polyatomic anions is shown below (Figure 4.18). The conductivity is dependent on the effect of the electrolyte on hydration. pHEMA samples sorbed in  $\text{LiClO}_4$  had much greater conductivities than those hydrated in  $\text{K}_2\text{CO}_3$ . This can be ascribed, primarily, to charge density and geometric factors.

It should be noted that for samples hydrated in solutions of the same anion the conductivity did not vary significantly with the nature of the cation.

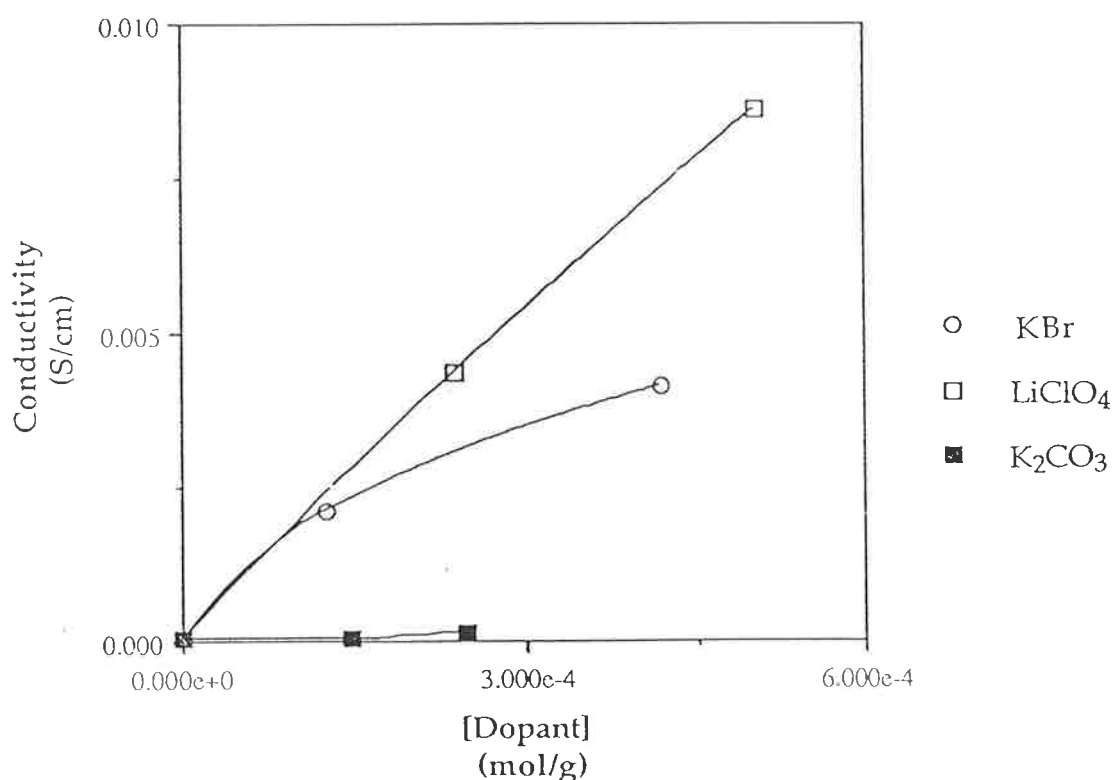


Figure 4.18

The variation in conductivity with dopant concentration for pHEMA samples hydrated in polyatomic anion solutions. Electrolytes as listed above. KBr data is included for comparison.

#### 4.9 Summary.

Hydrogels hydrated in electrolyte solutions yield a range of water contents dependent on the nature of the electrolyte employed. When compared to undoped samples significant increases in conductivity resulted from hydration in electrolyte solutions even for samples that caused a decrease in EWC. At low water contents in dehydration experiments, the doped gels also exhibited higher conductivities than for undoped samples of like water content. This would suggest that for a given hydrogel the determining factor in its conductivity is the dopant concentration.

However when comparing different doped samples it is necessary to not only consider the dopant concentration but also the nature of the dopant employed. Large variations in conductivity were achieved for pHEMA gels when they were hydrated in alkali halide solutions by altering the halide anion used. Primarily this variation resulted from the ability of the anion to enhance or interfere with the hydrophobic bonding of the gel network thus altering the water sorbing capabilities of the hydrogel. This in turn leads to variations in the availability and mobility of the conductive phase, the occluded water, which must in turn limit the mobility of the charge carriers, the dopant ions. Tighe et al. (12,13) measured the ion transport properties of pHEMA based on diffusion measurements and concluded that size and charge considerations result in variable permeability, yielding an order of ions similar to the lyotropic series. This would also be a factor in determining the conductivity of the samples studied here, however given the nature of sample preparation and experimentation in this work, this effect is thought to be secondary to the water ordering effect of the dopant.

More subtle variation in conductivity was achieved through the addition of crosslinkers to the pHEMA gels. Again, as for the undoped samples, increasing the crosslinker concentration was found to decrease the conductivity. More flexible crosslinkers, i.e. as  $n$  increased for 3mol%

OED/HEMA samples, yielded increases in conductivity. The variation in conductivity is due to the water structuring effect of the addition of the crosslinker. It is noteworthy that salting-out effects were larger for KBr doped samples at higher crosslinker concentrations.

The addition of KBr to all copolymers altered their AC impedance. At full hydration and 25°C all samples exhibited higher touch down frequencies than for undoped samples. Freezing point depressions were experienced for all samples whose conductivities were measured when cooled. The magnitude of the depression was greater than anticipated from the concentration of the dopant solution used for hydration and can be ascribed to water ordering effects of the polymer network. The magnitude of the depression increased with dopant concentration and crosslinker (EGDMA) concentration. In dehydration experiments the transition from single semi-circle AC impedance behaviour to the superposition of two semi-circles tended to occur at lower water contents for doped samples in comparison to similar undoped samples. This would suggest that the dopant could reorder water in such a way as to provide enhanced continuity of the conducting phase at low water contents.

## CHAPTER FIVE

### *Characterization*

#### 5.1 Introduction

It has been noted by Gray<sup>(1)</sup> that the conductive phase within gel electrolytes is the solvent phase that is supported by the polymer. It follows that the structure of the solvent phase is the major factor in determining the conductive properties of gel electrolytes. However ion-doped hydrogels systems are complex and numerous interactions can take place between polymer, water and electrolyte. Such interactions have been summarised by Zaikov et al.<sup>(2)</sup> (Table 4.1). The conductivity of pHEMA has been shown in this work to be sensitive to a number of environmental parameters: water content, crosslink density, crosslink nature, temperature, dopant concentration and dopant nature. To understand more fully the relative importance of the various interactions it is necessary to characterize the interactions of polymer, water and electrolyte.

Differential Scanning Calorimetry has been used to investigate the ratio of freezing to nonfreezing water in a number of HEMA based hydrogels in both the doped and undoped forms<sup>(3-9)</sup>. Nonfreezing water has been ascribed to the water which is bound tightly to the polymer network<sup>(6)</sup>. The mobility of charge carriers, and hence the conductivity, will be dependent on the ratio of freezing to nonfreezing water which in turn will be dependent on the structure of the polymer network and the concentration and nature of the electrolytic dopant employed. Comparison of the conductivity for 3mol% OED/HEMA copolymers with the DSC data of Allen et al.<sup>(7)</sup> have shown the ratio of freezing to nonfreezing water varies in a similar manner to the conductivity for such gels.

The specific volume of a polymer is only partly occupied by molecules. The random array of macromolecules leads to imperfections in the packing order and this unoccupied free volume is presumed to consist of holes of molecular sizes. Flory and Fox<sup>(10,11)</sup> argued that free volume was essential for molecular motion by rotation or translation. Hydrogels have been described<sup>(12)</sup> as being composed of statistically distributed microchannels or fluctuating pores created by the mobility of segments within an interpenetrating network in the presence of a solvent where these pores are formed and removed as a result of the thermal motion of the polymer chains. Given that motion of charge carriers is believed to take place through these pores, and their formation is related to the free volume of the system, the monitoring of free volume will assist in understanding the conductivity behaviour.

Thermal Mechanical Analysis has been used to measure the dimensional changes of the polymers studied in both the dry and hydrated state. TMA has been shown by Allen et al.<sup>(13)</sup> to be a most convenient technique for studying dimensional changes provided sufficient care is taken with the selection and preparation of samples. The relatively short duration of TMA experiments (hours) and the requirement of small samples make TMA a preferable option to more conventional dilatometric techniques. TMA enables the calculation of linear expansion coefficients which in turn can be used to give a measure of the free volume of the system.

Positron Annihilation Lifetime Spectroscopy is another non destructive technique used to measure free volume. The parameters  $\tau_3$  and  $I_3$ , the mean lifetime and relative number of annihilations resulting from the orthopositronium (oPs) pickoff mechanism, yield a measure of the average size and distribution of free volume sites within polymers. In this work the PALS technique has been applied to fully hydrated hydrogels, both doped and undoped, with varying crosslink density and nature.



## 5.2 Differential Scanning Calorimetry

### 5.2.1 Introduction

DSC enables the calculation of the relative amounts of freezing and non-freezing water within hydrogel samples. The ratio of these two types of water present in the samples studied provides a qualitative indication of the microscopic viscosity; non-freezable water tends to be tightly bound to the polymer and is less mobile than freezable water. It has already been established that the variation in the ratio of freezing water to non freezing water is similar to the variation in conductivity for 3mol% OED/HEMA copolymers (Fig 3.6).

In this study it has been assumed that the enthalpy of melting of frozen water in the hydrogel samples has not been altered by its the presence of the polymer network. Some doubt has been raised over the validity of this assumption<sup>(4,14)</sup> but it has been shown that the heat of fusion of water absorbed in polymers is nearly identical to the heat of fusion of pure water<sup>(15,16)</sup>. The method employed here to determine the amount of freezing water is consistent with that used by others<sup>(17-20)</sup> and thus enables comparison to be made between samples with different crosslinking density, nature of crosslinker and dopant.

Allen et al.<sup>(7)</sup> showed that cooling and heating procedures need to be clearly defined as slight variation of these experimental parameters can lead lead to both variation in the form of the melting endotherm recorded but also the amount of freezing water recorded. All samples in this work were cooled from 298K to 190K and held at this temperature for 15 minutes before warming to 290K at 10K.min<sup>-1</sup>.

### 5.2.2 Variation of Freezing Water with Copolymer Composition

Percentages of freezing water present are shown in Table 5.1 for

pHEMA and copolymers with EGDMA and in Table 5.2 for several 3mol% OED/HEMA copolymers.

**Table 5.1**

Freezing water determination for EGDMA/HEMA copolymers. The results are given both as a percentage of the total hydrogel weight (A) and as a percentage of the weight of water in the hydrogel (B).

	EWC(%)	A(%)	B(%)
pHEMA	40.4	12.9	31.8
0.6mol% EGDMA/HEMA	36.3	7.1	19.5
1.5mol% EGDMA/HEMA	32.9	2.7	8.3
3.0mol% EGDMA/HEMA	27.7	1.7	6.2

It is clear that the introduction of EGDMA reduces not only the EWC but also decreases the amount of the available water that is able to freeze. EGDMA is less hydrophilic than HEMA and its introduction will thus decrease the water sorbing capabilities of the network. The addition of EGDMA to the network will result in a tighter less mobile network with decreased ability to swell in water.

**Table 5.2**

Freezing water determination for 3mol%OED/HEMA copolymers. The results are given both as a percentage of the total hydrogel weight (A) and as a percentage of the weight of water in the hydrogel (B).

	EWC(%)	A(%)	B(%)
pHEMA	40.4	12.9	31.8
3.0mol% EGDMA/HEMA	27.7	1.7	6.2
3.0mol% DiEGDMA/HEMA	33.3	2.2	6.6
3.0mol% TEGDMA/HEMA	33.8	3.3	9.8
3.0mol% P400/HEMA	34.7	6.6	18.9

All samples crosslinked with OEDs exhibited a decrease in the amount of freezing water compared to pHEMA however, the magnitude of the decrease is dependent on the nature of crosslinker employed. The results gained for the variation in freezing water with  $n$ , the number of ethylene glycol units in the crosslinker, for 3mol% OED/HEMA were in agreement with those found by Allen et al.<sup>(7)</sup> for like samples. The amount of freezing water present was found to increase as  $n$  increased.

### 5.2.3 Variation of Freezing Water with KBr Concentration

The EWC and percentages of freezing water present in pHEMA samples hydrated in KBr solutions are shown in Table 5.3. The introduction of KBr resulted in a decrease in the EWC which was greater for samples hydrated in more concentrated KBr solutions.

Previous sorption measurements by Refojo<sup>(21)</sup> have attributed such decreases resulting from electrolyte presence to an enhancement of hydrophobic bonding within the polymer network. The presence of KBr also alters the structure of the occluded water as is reflected in the decrease in the amount of freezing water as the KBr concentration increased.

**Table 5.3**

Freezing water determination for pHEMA samples hydrated in KBr solutions of varying concentration. The results are given both as a percentage of the total hydrogel weight (A) and as a percentage of the weight of water in the hydrogel (B).

KBr(M)	EWC(%)	A(%)	B(%)
1.0	39.6	11.6	29.3
0.75	39.7	11.6	28.9
0.5	40.0	11.4	28.6
0.25	40.2	12.4	31.3
0	40.4	12.9	31.8

Similar DSC measurements were carried out on a range of 3mol% OED/HEMA copolymers and the percentages of freezing water determined are presented in Table 5.4. Decreases in both the EWC and the amount of freezing water were experienced for all crosslinked samples that were hydrated in KBr solutions. It should be noted that the decrease in freezing water was greater for samples where  $n$ , the number of ethylene glycol units in the crosslinker, was smaller. This could suggest that the decrease in freezing water could be due to a polymer/electrolyte/water interaction that could inhibit the formation of clusters of water that are able to form ice on cooling

**Table 5.4**

Freezing water determination for 3mol%OED/HEMA copolymers hydrated in 1M KBr solutions. The results are given both as a percentage of the total hydrogel weight (A) and as a percentage of the weight of water in the hydrogel (B).

	EWC(%)	A(%)	B(%)
pHEMA	39.6	11.6	29.3
3.0mol% EGDMA/HEMA	27.0	0.6	2.3
3.0mol% DiEGDMA/HEMA	32.5	0.3	2.5
3.0mol% TEGDMA/HEMA	32.8	1.7	5.3
3.0mol% P400/HEMA	34.0	3.2	9.4

#### 5.2.4 Variation of Freezing Water with Nature of Dopant

The hydration of pHEMA samples in a range of electrolytes yielded samples of varying EWC in accordance with previous sorption work<sup>(21)</sup>. The EWC and the amount of freezing water, measured by DSC, present in pHEMA samples hydrated in a range of electrolyte solutions are presented in Table 5.5.

It is clear from the data recorded for the samples hydrated in alkali halide solutions that the nature of the anion has a significant role in determining the EWC and the amount of freezing water of the resulting gels. Samples hydrated in iodide solutions experienced increases in both the EWC

and the freezing water whereas samples hydrated in bromide and chloride solutions experienced decreases in both EWC and freezing water, the decrease being greater for samples hydrated in chloride solutions. The larger softer iodide ion has been suggested<sup>(21)</sup> to form a liaison with the network resulting in a polyelectrolyte effect which results in an increase in both EWC and freezing water. Samples hydrated in polyatomic anion solutions, that is carbonate and perchlorate solutions, had markedly different EWC and water structuring. The sample hydrated in  $\text{LiClO}_4$  resulted in a gel of increased EWC and freezing water content whereas the sample hydrated in  $\text{K}_2\text{CO}_3$  had reduced EWC and freezing water content compared to pHEMA hydrated in deionised water.

**Table 5.5**

Freezing water determination for pHEMA samples hydrated in several 1M electrolyte solutions. The results are given both as a percentage of the total hydrogel weight (A) and as a percentage of the weight of water in the hydrogel (B). The ratio of freezing water to non-freezing water,  $m_f/m_{nf}$ , is also given.

Electrolyte	EWC(%)	A(%)	B(%)	$m_f/m_{nf}$
-	40.4	12.9	31.8	0.469
LiCl	33.3	3.1	9.1	0.103
NaCl	28.2	2.7	9.5	0.106
KCl	29.7	2.8	9.5	0.104
LiBr	38.3	10.0	25.9	0.353
NaBr	35.6	9.3	26.1	0.354
KBr	39.6	11.6	29.3	0.414
LiI	53.7	23.8	44.3	0.796
NaI	51.5	24.2	47.1	0.886
KI	50.5	22.7	44.9	0.817
$\text{K}_2\text{CO}_3$	21.4	2.7	12.7	0.144
$\text{LiClO}_4$	50.9	21.6	42.5	0.737

The variation of freezing water for samples hydrated solutions of different cations but same anion revealed no general trends. However, the nature of the cation will still contribute to the determination of the water structuring in the gel through interaction with the polar moieties of the repeat unit.

The variation in both the conductivity and the ratio of freezing water to non-freezing water is presented in Figure 5.1. With the exception of the sample hydrated in NaI, similar trends are shown for the samples hydrated in alkali halide solutions suggesting that the structure of the water within the gel is a determining factor in the conductivity. It should be noted that the nature of the electrolyte dopant used varied the EWC and thus must contribute to the determination of the water structure in doped gels.

### 5.2.5 Summary

The nature of water sorbed by doped pHEMA based gel electrolytes is dependent on both the polymer network and the nature of the electrolytic dopant employed. Increases in crosslinking reduce the relative proportion of freezing water present in the gels with this decrease being less for samples crosslinked with OEDs of greater values of  $n$ . Variation in the nature of the anion was found to have a greater effect on the ratio of freezing water to non-freezing water.

Previous data collected by Allen et al.<sup>(7)</sup> and the results of this work show that there is a positive correlation between the change in conductivity and the variation in the ratio of freezing water to non freezing water suggesting that the structure of the occluded water is a determining factor in the conductivity of pHEMA gel electrolytes. As a consequence of this relationship, it would be of interest in the future to measure the ratio of freezing water to non-freezing water for progressively dehydrated samples to investigate whether this correlation holds for samples of variable hydration.

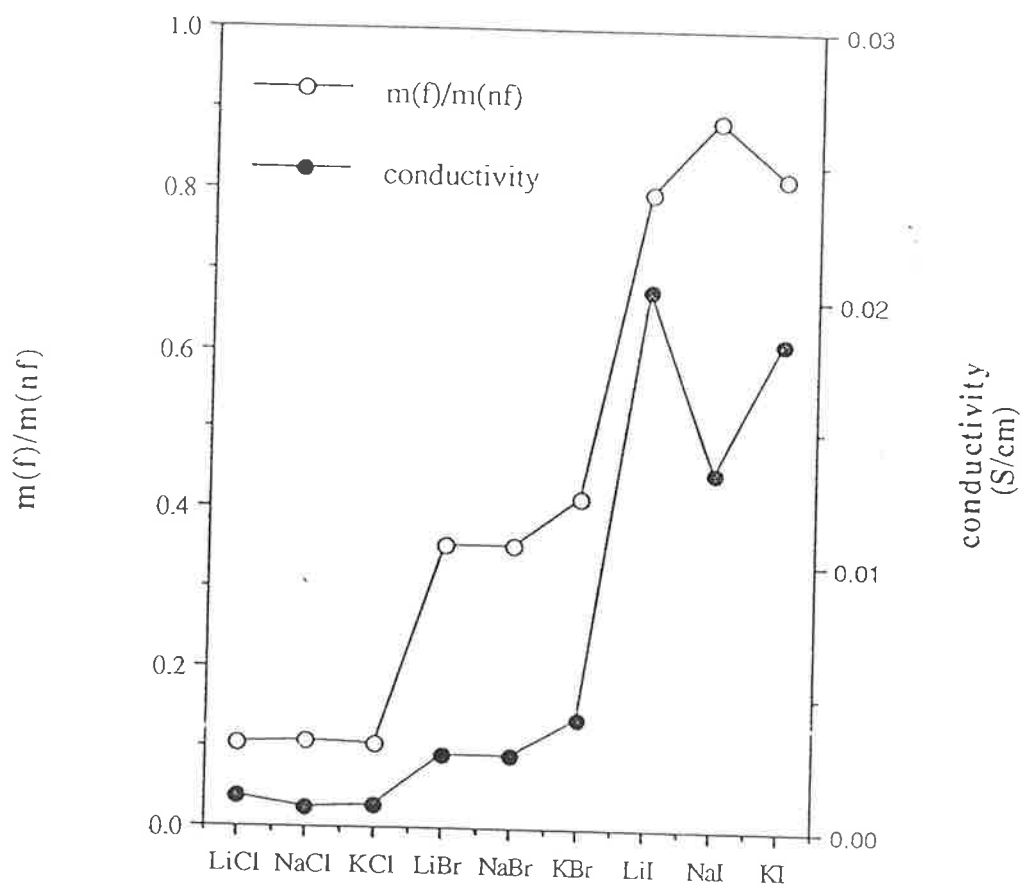


Figure 5.1

The variation in conductivity and the ratio of freezing water to non freezing water ( $m(f)/m(nf)$ ) for pHEMA samples hydrated in several 1.0M electrolyte solutions.

## 5.3 Thermal Mechanical Analysis

### 5.3.1 Introduction

The thermal expansion of polymers on heating is dependent on internal molecular interactions and is the result of both inter and intrachain vibrational modes. Intrachain vibration is governed by the nature of the covalent bonds in the polymer whereas interchain vibration is controlled by secondary interactions such as hydrogen bonding and van der Waal's forces. Interchain vibration has been shown to make a greater contribution to the thermal expansion of polymer crystals by Swan<sup>(22)</sup>: the thermal expansivities were shown to be greater along the chain axis than perpendicular to it when measured for polymer crystals.

The TMA enables the collection of length-temperature ( $\Delta L$  v T) curves from which the linear expansion coefficients can be determined. Linear glass and liquid expansion coefficients,  $\alpha_g'$  and  $\alpha_l'$  respectively, are taken as the slope of the  $\Delta L$  v T curve in glass and liquid regions. The expansion coefficients of a polymer are not independent of temperature but generally show an increase with temperature, however there is a large change in the expansion coefficient on passing through the glass transition, hence it is conventional to ignore the gradual increase in  $\alpha_g'$  with temperature<sup>(23)</sup>. The linear expansion coefficients are expressed as:

$$\alpha' = l_0^{-1} \cdot \frac{dl}{dT} = l_0^{-1} \cdot \frac{dl}{dt} \cdot \frac{dt}{dT} \quad \text{Eqn 5.1}$$

where  $l_0$  and  $l$  are the initial and instantaneous lengths of the sample,  $dT/dt$  is the heating rate and  $dl/dt$  and  $dl/dT$  are the change in length of the sample with respect to time and temperature respectively. The linear thermal expansion coefficient of an unoriented amorphous polymer is normally assumed to isotropic, thus the cubic thermal expansion coefficient,  $\alpha$ , can be



approximated as  $\alpha = 3\alpha'$ <sup>(23,24)</sup>.

Free volume is the subject of several models including that presented by Simha and Boyer<sup>(25)</sup>. According to this model, free volume is frozen in to the polymer structure remaining constant in the glassy state and as such the hole size and distribution of free volume is believed to remain fixed below T<sub>g</sub>. However, the glass will continue to expand or contract with changes in temperature due to the normal expansion process of all molecules by thermal agitation. It should be noted that above T<sub>g</sub>, the free volume increases resulting from the larger expansion of the liquid state compared to the glassy state<sup>(26)</sup>.

Simha and Boyer<sup>(25)</sup> proposed that the difference between the glass and the liquid expansion coefficients reflect the expansivity of the free volume fraction,  $f$ , where:

$$f = \frac{V_f}{V} = \Delta\alpha T_g \quad \text{Eqn 5.2}$$

$V$  is the specific volume,  $V_f$  is the free volume and  $\Delta\alpha$  is the free volume expansivity. A range of values for  $f$  have been evaluated for several polymer systems and are summarised by Lai<sup>(27)</sup>. Lai and others have discussed the limitations of this relationship, especially the assumption that the linear expansion coefficient remains invariant with temperature, however, the overall trends relating to the changes in free volume will remain valid. The change in free volume resulting from changes in several environmental parameters such as crosslink density and nature and dopant has been investigated. An attempt has also been made to understand the dimensional changes of copolymers at several hydration levels.

### 5.3.2 Dimensional Changes in pHEMA

#### 5.3.2.a *The Effect of the nature and concentration of Crosslinking.*

Glass and liquid expansion coefficients and the free volume fractions for pHEMA and several OED/HEMA copolymers are presented in Table 5.6. The glass expansion coefficient was found to be  $46.4 \times 10^{-6}\text{K}^{-1}$  for dry pHEMA. This value compares favourably with the results of Lai<sup>(27)</sup> in length contraction experiments ( $\alpha_g' = 42.1 \times 10^{-6}\text{K}^{-1}$ ). Lai also measured the expansivities of several other acrylate polymers, such as poly(methyl methacrylate), poly(ethyl methacrylate) and poly(methyl acrylate), and found  $\alpha_g'$  to be comparatively low for pHEMA; this was attributed to hydrogen bonding.. A liquid expansion coefficient of  $\alpha_l' = 170.2 \times 10^{-6}\text{K}^{-1}$  was recorded for dry pHEMA.

Table 5.6

Thermal expansion coefficients and free volume fractions for pHEMA and its copolymers with several OEDs. Glass transition temperatures as calculated by Allen et al.<sup>(30)</sup> by torsion pendulum. All samples were dry.

Polymer	T <sub>g</sub> (°C)	$\alpha_g'$ ( $10^{-6}\text{K}^{-1}$ )	$\alpha_l'$ ( $10^{-6}\text{K}^{-1}$ )	$3(\alpha_l' - \alpha_g')$ ( $10^{-6}\text{K}^{-1}$ )	f
pHEMA	125	46.4	170.2	371.4	0.148
0.3mol% EGDMA/HEMA	-	29.2	149.8	361.8	-
0.6mol% EGDMA/HEMA	-	38.1	140.6	307.5	-
1.5mol% EGDMA/HEMA	-	30.2	203.0	518.4	-
3.0mol% EGDMA/HEMA	136.7	44.0	126.2	246.0	0.100
3.0mol% DiEGDMA/HEMA	-	30.6	107.0	229.2	-
3.0mol% TEGDMA/HEMA	127	33.0	118.5	256.5	0.103
3,0mol% P400/HEMA	111	33.0	112.3	237.9	0.105

It is evident from the data presented that, in general, the addition of any crosslinker resulted in decreases in both  $\alpha_g'$  and  $\alpha_l'$ . The variations in  $\alpha_g'$  and  $\alpha_l'$  are clearly shown for 3.0mol%OED/HEMA copolymers in Figure

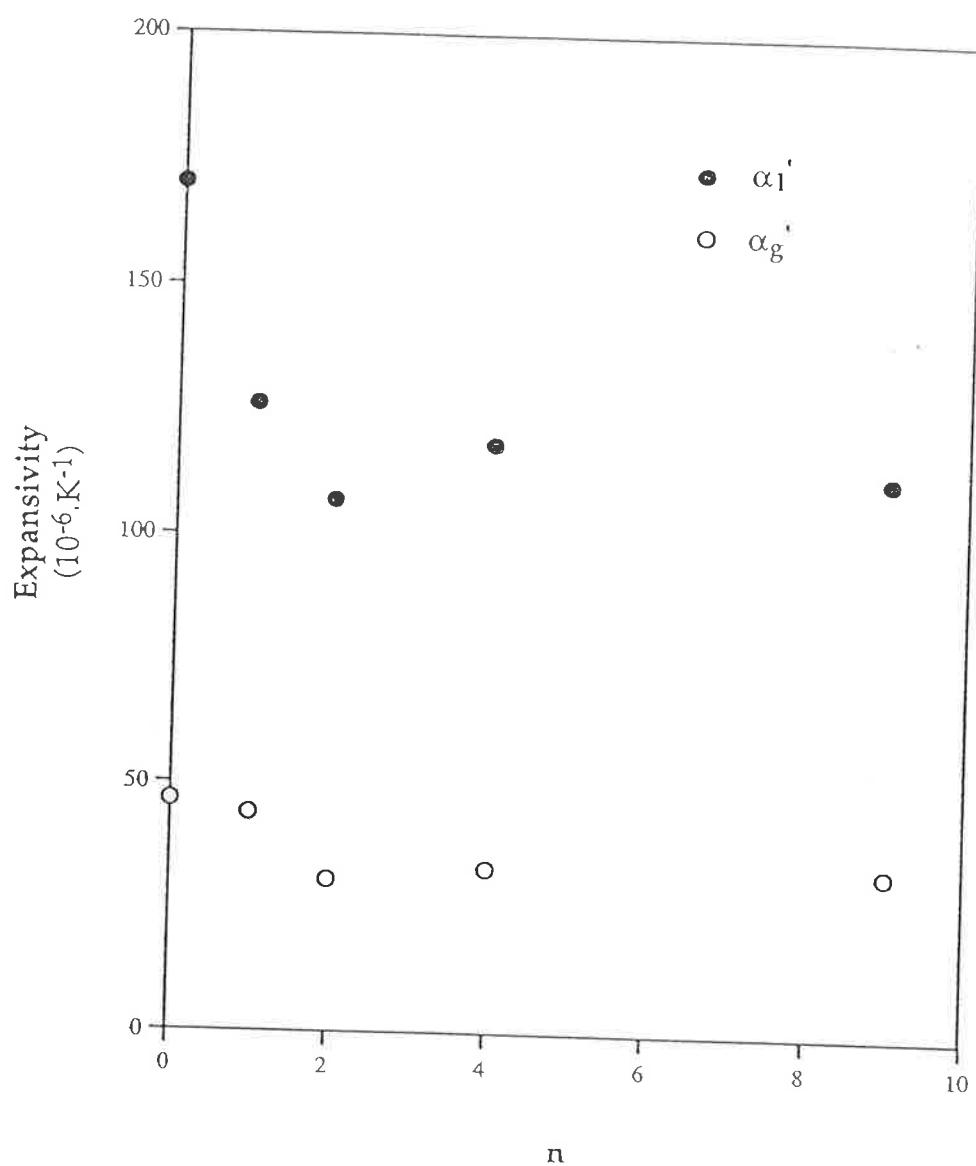


Figure 5.2

The variation in the liquid and glass expansion coefficients,  $\alpha_g'$  and  $\alpha_l'$ , for dry 3mol% OED/HEMA copolymers. (n is the number of ethylene glycol units in the OED.)

5.2. It should be noted that the free volume fraction,  $f$ , was found to decrease on the introduction of 3mol% EGDMA yet as  $n$  was increased from 1 to 9  $f$  increased minimally. The introduction of a crosslinker results in tighter networks with greater secondary bonding interaction between polymer chains and thus less free volume. As  $n$ , the number of ethylene glycol units in the crosslinker, is increased it would be anticipated that the increased length of the crosslink would result in greater free volume. However the lack in variation of the free volume fraction suggests that the copolymers investigated are insufficiently crosslinked for the nature of the crosslink to become a significant factor in the determination of the free volume fraction of the dry samples.

### 5.3.2.b *The Effect of Dopant.*

Length contraction experiments by Lai<sup>(27)</sup> on dry KBr doped pHEMA samples revealed that increasing KBr concentration led to a decrease in length contraction and an increase in the temperature at which contraction of aged samples began and finished. This was attributed to ion/polymer interactions that reduced segmental mobility of the polymer. These observations were consistent with the hypothesis<sup>(29)</sup> that adsorption of the polymer onto filler molecules leads to an increase in  $T_g$ . Glass and liquid expansion coefficients and the free volume fractions for pHEMA and several OED/HEMA copolymers are presented in Table 5.7.

It was found that, in general,  $\alpha_g'$  and  $\alpha_l'$  were lower for doped pHEMA copolymers than undoped samples suggesting that the introduction of KBr impedes molecular motion of the polymer network. The variation in  $\alpha_g'$  and  $\alpha_l'$  for a range of 3mol%OED polymers doped in 1M KBr solutions before drying is presented in Figure 5.3. Similar trends as for the undoped samples (Figure 5.2) were exhibited as  $n$  increased. Free volume fractions have not been calculated due to the lack of quantitative on the effect of KBr on the  $T_g$  of

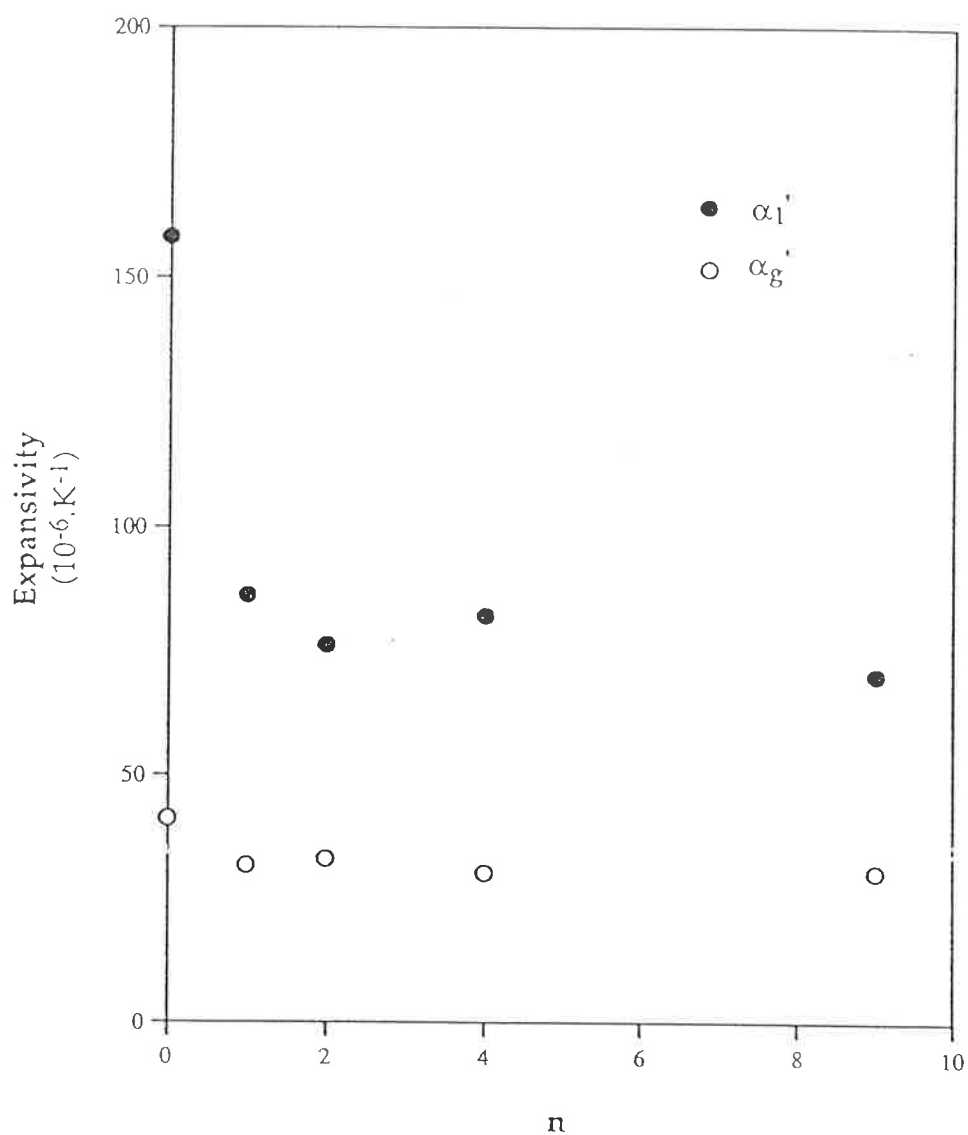


Figure 5.3

The variation in the liquid and glass expansion coefficients,  $\alpha_g'$  and  $\alpha_l'$ , for dry KBr doped 3mol% OED/HEMA copolymers. Samples were hydrated in 1M KBr prior to drying. (n is the number of ethylene glycol units in the OED.)

copolymers investigated here. Length contraction experiments by Allen et al.<sup>(13)</sup> suggest an increase in T<sub>g</sub>, and thus a decrease in free volume.

Table 5.7

Thermal expansion coefficients for doped pHEMA and its copolymers with several OEDs. All samples were dry.

Polymer	[KBr] <sub>ss</sub> (M)	[KBr] <sub>p</sub> (mol/g)	$\alpha_g'$ (10 <sup>-6</sup> K <sup>-1</sup> )	$\alpha_l'$ (10 <sup>-6</sup> K <sup>-1</sup> )	3( $\alpha_l'$ - $\alpha_g'$ ) (10 <sup>-6</sup> K <sup>-1</sup> )
pHEMA	0.5	1.25×10 <sup>-4</sup>	38.6	153.2	343.8
	1.0	4.17×10 <sup>-4</sup>	41.2	158.1	350.7
0.3mol%	0.5	1.26×10 <sup>-4</sup>	33.9	140.5	319.8
EGDMA/HEMA	1.0	3.33×10 <sup>-4</sup>	41.0	141.0	300.0
0.6mol%	0.5	1.39×10 <sup>-4</sup>	35.9	135.8	299.7
EGDMA/HEMA	1.0	3.43×10 <sup>-4</sup>	30.1	123.9	281.4
1.5mol%	0.5	1.65×10 <sup>-4</sup>	35.6	140.5	314.7
EGDMA/HEMA	1.0	3.43×10 <sup>-4</sup>	35.2	111.1	227.7
3.0mol%	0.5	1.09×10 <sup>-4</sup>	35.3	98.0	188.1
EGDMA/HEMA	1.0	1.39×10 <sup>-4</sup>	31.7	86.2	163.5
3.0mol%	0.5	1.64×10 <sup>-4</sup>	32.8	95.8	189.0
DiEGDMA/HEMA	1.0	3.46×10 <sup>-4</sup>	33.0	76.3	129.9
3.0mol%	0.5	1.91×10 <sup>-4</sup>	32.3	114.7	247.2
TEGDMA/HEMA	1.0	3.82×10 <sup>-4</sup>	30.2	82.1	155.7
3.0mol%	0.5	1.93×10 <sup>-4</sup>	31.6	96.0	193.2
P400/HEMA	1.0	3.74×10 <sup>-4</sup>	30.5	70.3	119.4

### 5.3.2.c The Effect of Hydration.

A series of pHEMA samples at varying levels of hydration were cooled slowly (2K/min) from room temperature to -60°C. The length-temperature plots ( $\Delta L$  v T) of these samples on warming from -60°C to 25°C are presented

in Figure 5.4. Note that fully hydrated pHEMA (EWC=40.4wt%) has a  $T_g$  of  $0^\circ\text{C}$ <sup>(30)</sup> indicating that the plots shown cover mostly the glassy region.

It is evident that as the water content increases the glass expansion coefficient,  $\alpha_g'$ , also increases as revealed by the increasing slope of the  $\Delta L$  v  $T$  plots. An interesting phenomenon took place in samples of greater than 34wt% water content; a sharp increase and corresponding decrease in the  $\Delta L$  v  $T$  plot is observed in the vicinity of  $0^\circ\text{C}$ . As this behaviour is only apparent in samples of high hydration levels, and the abrupt expansion of these samples is accompanied by a contraction at temperatures around  $0^\circ\text{C}$ , it would appear that a phase transition experienced by the absorbed aqueous phase may play some role in this phenomenon.

This behaviour was also observed for a range of 3mol% OED/HEMA polymers at full hydration (Figure 5.5). Again, in the vicinity of  $0^\circ\text{C}$  all samples exhibited an abrupt expansion and an accompanying contraction, with the size of this expansion and contraction greatest for samples with longer crosslinks and thus higher water contents. Such behaviour also suggests that a phase transition experienced by the absorbed water phase may play some role in this phenomenon. It is interesting to note that the contraction occurs in stages for some of the samples, especially the 3mol% TEGDMA/HEMA, as revealed by the shoulders in the trace where the contraction takes place. It is suggested that this phenomenon is of an heterogeneous nature. It should also be noted that the initial slope of these  $\Delta L$  v  $T$  plots increases as  $n$ , the number of ethylene glycol units in the crosslinks, increases and thus the water content at full hydration.

Despite the trends that suggest a phase transition in the water phase of the hydrogels contributes to this expansion behaviour, the phenomenon is not fully understood. The magnitude of the expansion at temperatures just below  $0^\circ\text{C}$  of the samples is much greater than the literature glass expansion coefficient for ice ( $\alpha_{g(ice)} = 51 \times 10^{-6} \text{ K}^{-1}$ <sup>(52)</sup>) suggests that it is unlikely to be due

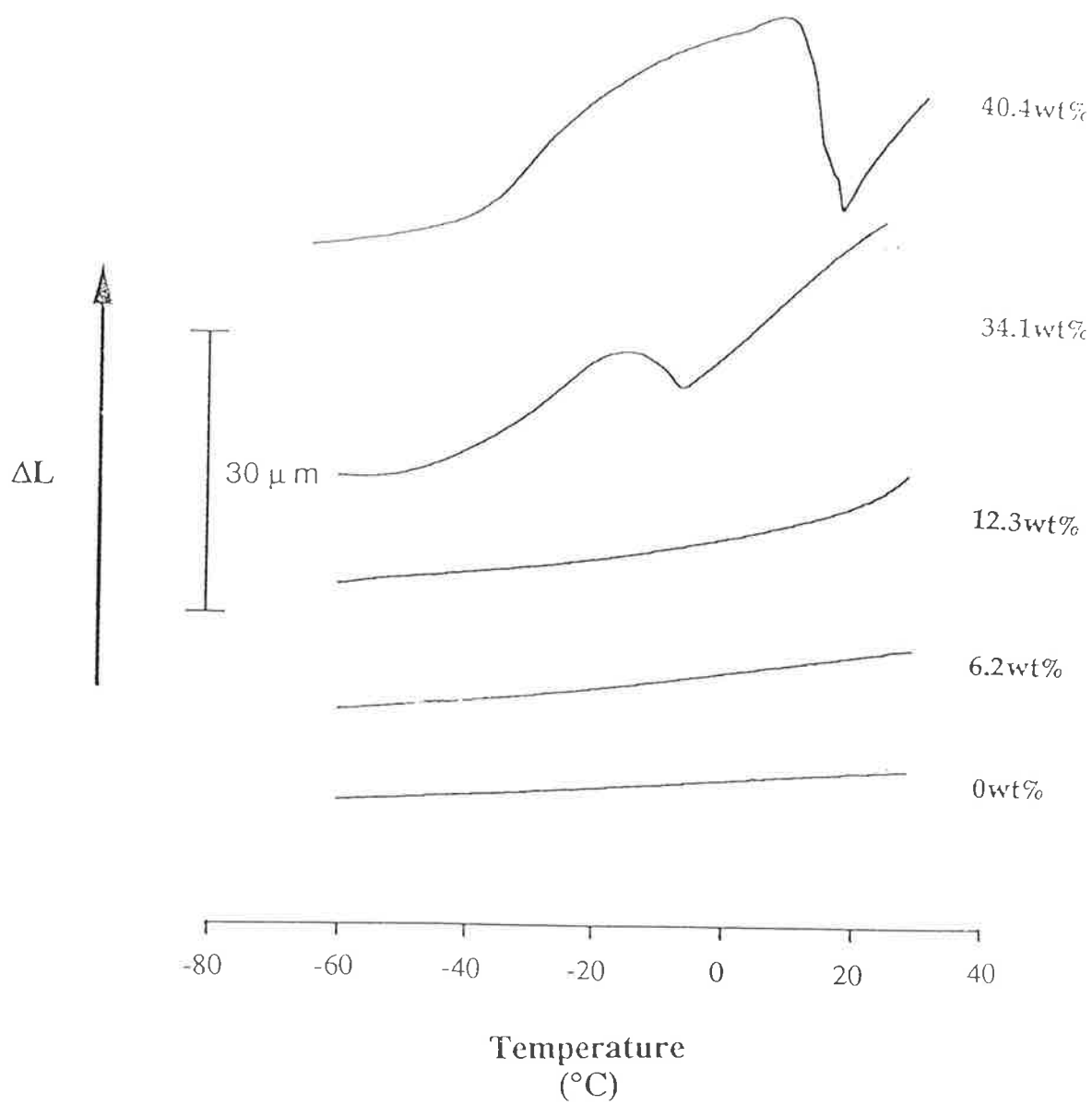


**Figure 5.4**  
 $\Delta L$ -T plots for pHEMA at several water contents.(Water contents as specified above.)



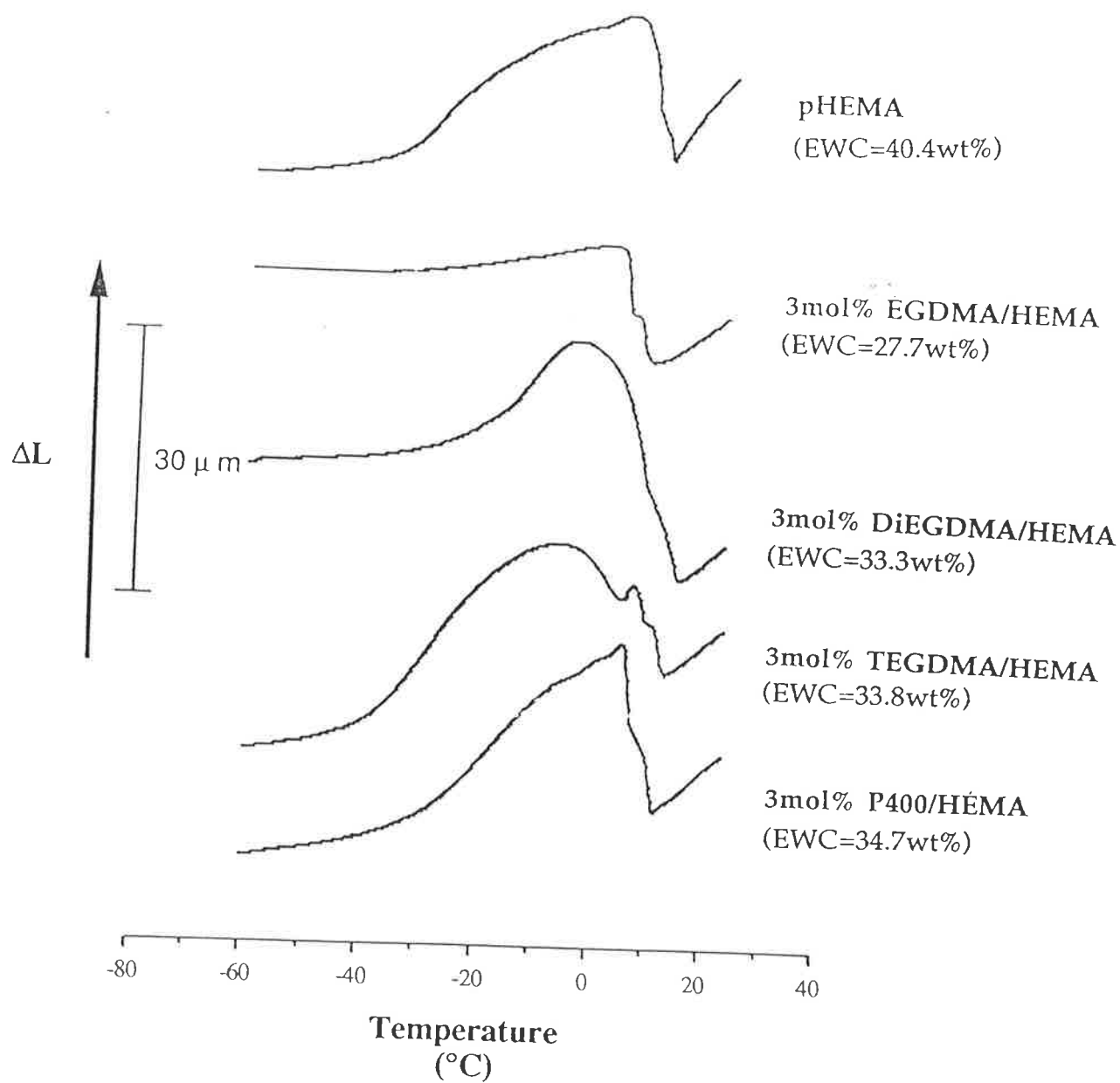


**Figure 5.5**  
 $\Delta L$ -T plots for 3mol% OED/HEMA copolymers at full hydration.

solely to such a transition yet more complex water/polymer behaviour is suspected. However, these results are interesting and suggest the need for more extensive experimentation and analysis. It would be of interest to examine the expansion of a pHEMA gel with some solvent other than water used to see whether a phase transition of the occluded phase is a crucial factor in such behaviour.

Despite the need for further work to understand the interesting behaviour exhibited by samples of high water content, it is apparent from all the data collected that increasing the water content, by increasing the hydration or altering the crosslinking agent, increases the glass expansion coefficient. If the hypothesis of Haldon and Simha<sup>(28)</sup> is considered, whereby the magnitude of the glass expansion coefficient is believed to reflect the free volume fraction of a given sample, then increasing the water content of the polymers studied increases their free volume fraction. This is consistent with the plasticising action of water on pHEMA which has been shown by the dynamic mechanical analysis of Allen et al.<sup>(30)</sup> to result in a reduction in T<sub>g</sub>.

### 5.3.3 Summary

Glass and liquid expansion coefficients,  $\alpha_g'$  and  $\alpha_l'$ , were found to decrease with increases in crosslinking and dopant concentration in the dry state. The variation in the free volume fraction of undoped 3mol% OED/HEMA copolymers followed the same trend as for the variation in EWC at full hydration. The introduction of water into pHEMA copolymers increases the glass expansion coefficient and at high water contents leads to an interesting expansion/contraction phenomenon that appears to be related in some way to the partial freezing of the occluded phase.

## 5.4 Positron Annihilation Lifetime Spectroscopy

### 5.4.1 Introduction

Positron annihilation lifetime spectroscopy (PALS) is a very sensitive non destructive technique for the measurement of free volume that relies upon the sensitivity of orthopositronium (oPs) to localised electron density in condensed matter. PALS has been used to investigate free volume in a number of polymeric systems and such studies have shown orthopositronium (oPs) sensitivity to structural changes resulting from fatigue<sup>(31)</sup>, degree of cure<sup>(32)</sup>, thermoset crosslink density<sup>(33)</sup>, weathering and corrosion resistance of coatings<sup>(34)</sup>, miscibility of copolymer blends<sup>(35,36)</sup> and physical aging in glassy polymers<sup>(37)</sup>. Extensive reviews of the scope of PALS as a free volume probe for polymeric systems have been written by Jean<sup>(38)</sup> and Zipper and Hill<sup>(39)</sup>.

PALS has also been used to study the influence of absorbed water on the free volume characteristics of several polymers. Studies on the interaction of water with nylon<sup>(40,41)</sup>, protective epoxy coatings<sup>(42,43)</sup>, various polyamides<sup>(44)</sup>, DNA<sup>(45)</sup>, protein<sup>(46)</sup>, and poly (vinyl alcohol)<sup>(47)</sup> are available in the literature; in each of these studies, nonlinear relationships between  $\tau_3$ , the mean oPs annihilation lifetime and  $I_3$ , the relative oPs annihilation intensity, have been reported with increasing water content. Many systems exhibit a decrease in  $\tau_3$  with water content for low water contents. This has been ascribed to the absorption of water molecules into free volume cavities effectively reducing their size and decreasing the mean oPs lifetime. At low hydration there is insufficient water to provide the structural order required for either swelling of the polymer or annihilations of oPs to take place in the water phase and thus the water acts as a filler.

After the initial decrease in  $\tau_3$ , a steady increase with increasing water content is observed in all systems. This has been ascribed to the aggregation of

water causing the swelling of the polymer and an enlargement of the free volume cavities resulting in an increase in  $\tau_3$ . It should be noted that the occluded water phase may also contribute to the annihilation spectra as annihilations take place in bulk water ( $\tau_3 = 1.80\text{ns}$ ,  $I_3 = 28 \pm 2\%$ )<sup>(48,49)</sup>. Such annihilations are best described by the bubble model of oPs lifetimes in liquids in which the oPs essentially creates free volume, or blows a bubble, around itself. The size of this bubble determines the oPs lifetime in the same manner that free volume size determines oPs lifetime in solid polymers. The size of this bubble is determined by the relative magnitudes of the liquid surface tension and the repulsive forces between the oPs and the surrounding liquid<sup>(50)</sup>, in this case the occluded aqueous phase.

All studies have revealed a decrease in the oPs intensities,  $I_3$ , with the addition of water. Heater<sup>(41)</sup> attributed this behaviour to the possible reaction of oPs with other species in the water leading to the formation of unstable complexes. These complexes annihilate with shorter lifetimes by other mechanisms and thus do not contribute to  $I_3$  data. Singh et al.<sup>(40)</sup> have proposed that the decrease may be due to the absorbed water molecules changing the free volume cell geometry. Studies of DNA with water uptake by Walrum and Eldrup<sup>(45)</sup> show a similar decrease in  $I_3$  over the first 25% of absorbed water. However, on the addition of water above 25% uptake there was a gradual increase in  $I_3$  as it approached the value reported for pure water<sup>(48,49)</sup>. This increase was postulated to be due to the increasing number of annihilations occurring with bulk water as more water is added.

The introduction of dopant ions into hydrogels results in a number of interactions (Table 4.1) which have already been shown to alter the EWC and the conductivity and suggest that the addition of dopant will change the free volume characteristics of the hydrogels. It was expected that the PALS experiments with ion doped hydrogels may yield data that would be difficult to interpret as a number of interactions must be considered. There exists

evidence<sup>(51)</sup> that paramagnetic ions and chloride ions can lead to oPs quenching and shorter  $\tau_3$  values. The introduction of a competing mechanism to Ps formation, oPs inhibition, results from the addition of salts that cause an increase in the dipole character of polymer molecules and an increasing localization of negative charge and will yield lower  $I_3$  values. It is believed that the formation of oPs is chemically inhibited in favour of positron capture caused by the presence of anions<sup>(51)</sup>. The introduction of ions to the occluded water will alter its surface tension and density thus affecting the oPs lifetime contribution of the water within the gel.

PALS has been shown to be a method of investigating free volume that is sensitive to the effect of occluded water on the free volume characteristics of polymeric systems. PALS has been used to investigate the effect of crosslinking and dopant nature on the free volume characteristics, reflected by  $I_3$  and  $\tau_3$ , of a series of fully hydrated gels.

#### 5.4.2 Free volume characteristics of undoped pHEMA based gel electrolytes.

PALS experiments revealed that for pHEMA at full hydration (EWC=40.4wt%) the oPs pickoff lifetime ( $\tau_3$ ) was  $2.326 \pm 0.032$  ns and the oPs pickoff intensity ( $I_3$ ) was  $22.508 \pm 0.370$  %; errors that are quoted refer to the population standard deviations of these results.

Hodge<sup>(47)</sup> in an investigation of poly(vinyl alcohol) found that as the water content was increased, the values of  $\tau_3$  and  $I_3$  approached the values recorded for water and thus assumed that the observed values of  $\tau_3$  and  $I_3$  could be taken as the sum of the weighted contributions from the polymer and the water, that is

$$\tau_{3(net)} = A\tau_{3(water)} + (1-A)\tau_{3(polymer)} \quad \text{Eqn 5.3}$$

$$I_{3(net)} = AI_{3(water)} + (1-A)I_{3(polymer)} \quad \text{Eqn 5.4}$$

where  $\tau_{3(net)}$ ,  $\tau_{3(polymer)}$  and  $\tau_{3(water)}$  are the oPs lifetimes for the system, as measured, water and polymer respectively and  $I_{3(net)}$ ,  $I_{3(polymer)}$  and  $I_{3(water)}$  are the oPs pickoff intensities for the system, polymer and water respectively; A is the amount of water in which oPs can annihilate via the bubble mechanism. Annihilation of oPs can only take place in clusters of water molecules where there is sufficient water for a bubble to form, that is when the oPs can be completely surrounded. It is assumed that these clusters of water molecules are also able to sufficiently order themselves on cooling for crystallisation to take place. Consequently, to evaluate  $\tau_3$  and  $I_3$  of the pHEMA gels studied, A is the amount of freezing water within the gel which has been measured in this work by DSC (Section 5.2). To calculate  $\tau_{3(polymer)}$  and  $I_{3(polymer)}$  the experimentally obtained values for the hydration water,  $\tau_3=1.897\text{ns}$  and  $I_3=17.795\%$ , were used. The corrected values for pHEMA are  $\tau_{3(polymer)}= 2.389 \text{ ns}$  and  $I_{3(polymer)}= 22.201\%$ . It should also be noted that this model also implies that regions of nonfreezing water have insufficient size to

Table 5.8

The variation in EWC, conductivity,  $\tau_{3(net)}$ ,  $I_{3(net)}$ ,  $\tau_{3(polymer)}$  and  $I_{3(polymer)}$  for 3mol% OED/HEMA copolymers at full hydration and 22°C.

Sample	EWC (%)	$\sigma$ (S/cm)	$\tau_{3(net)}$ (ns)	$I_{3(net)}$ (%)	$\tau_{3(p)}^*$ (ns)	$I_{3(p)}^\ddagger$ (%)
pHEMA	40.4	$2.86 \times 10^{-5}$	2.328	22.508	2.392	23.206
1.5mol% EGDMA/HEMA	32.9	$2.06 \times 10^{-6}$	2.299	21.959	2.310	24.660
3.0mol% EGDMA/HEMA	27.7	$1.08 \times 10^{-6}$	2.203	19.872	2.208	19.908
3.0mol% DiEGDMA/HEMA	33.3	$1.55 \times 10^{-6}$	2.179	20.294	2.185	20.350
3.0mol% TEGDMA/HEMA	33.8	$2.47 \times 10^{-6}$	2.283	21.079	2.296	21.191
3.0mol% P400/HEMA	34.7	$5.47 \times 10^{-6}$	2.175	21.022	2.195	21.250

\*  $\tau_{3(p)} = \tau_{3(polymer)}$

‡  $I_{3(p)} = I_{3(polymer)}$

directly influence the oPs annihilation rate and they therefore act as a filler decreasing the amount of free volume - a mechanism postulated in nylon<sup>(41)</sup> and other poly(amide) systems<sup>(44)</sup>. Hodge<sup>(47)</sup> found that all nonfreezing water in poly(vinyl alcohol) could be attributed to hydrogen bound water. Despite DSC measurements (Section 5.2.2) revealing this not to be the case for pHEMA (i.e. non freezing water > 20wt%), it is believed that the corrections applied are still valid.

The oPs pickoff lifetimes and relative intensities for pHEMA and several OED/HEMA copolymers are given in Table 5.8. Similar trends were exhibited by  $\tau_3$  and  $I_3$  in both corrected and uncorrected forms as would be expected given the nature of the corrections employed (Eqn. 5.3, 5.4). As  $n$ , the number of ethylene glycol units in the crosslink, was increased for 3mol% OED/HEMA copolymers at full hydration,  $\tau_{3(\text{polymer})}$  was found to decrease. All samples recorded lower values of  $\tau_{3(\text{polymer})}$  than pHEMA (Figure 5.6.a) and, in general, the rate of decrease in  $\tau_{3(\text{polymer})}$  also decreased as  $n$  increased. If experimental error is considered only a slight decrease in the average size of the free volume sites was experienced as  $n$  increased from 1 to 9. This appears to suggest that although the length of the crosslink increases as  $n$  increases, the flexibility of the crosslink enables more efficient packing of the polymer network thus slightly decreasing the size of the free volume sites. Repeated measurements of the 3mol% TEGDMA/HEMA sample failed to explain the unexpectedly high value of  $\tau_{3(\text{polymer})}$  obtained.

$I_{3(\text{polymer})}$  was lower for all 3mol% crosslinked samples than for pHEMA. However, an interesting trend in  $I_{3(\text{polymer})}$  was exhibited as  $n$  was increased from 1 to 9 (Figure 5.6.b); as  $n$  was increased from 1 to 4 there was a relatively large increase in the frequency of the free volume sites when compared with the apparent invariance of the frequency of free volume sites as  $n$  was increased from 4 to 9. The ability of the crosslink to be involved in secondary bonding, such as intra chain hydrogen bonding, will increase as  $n$ ,

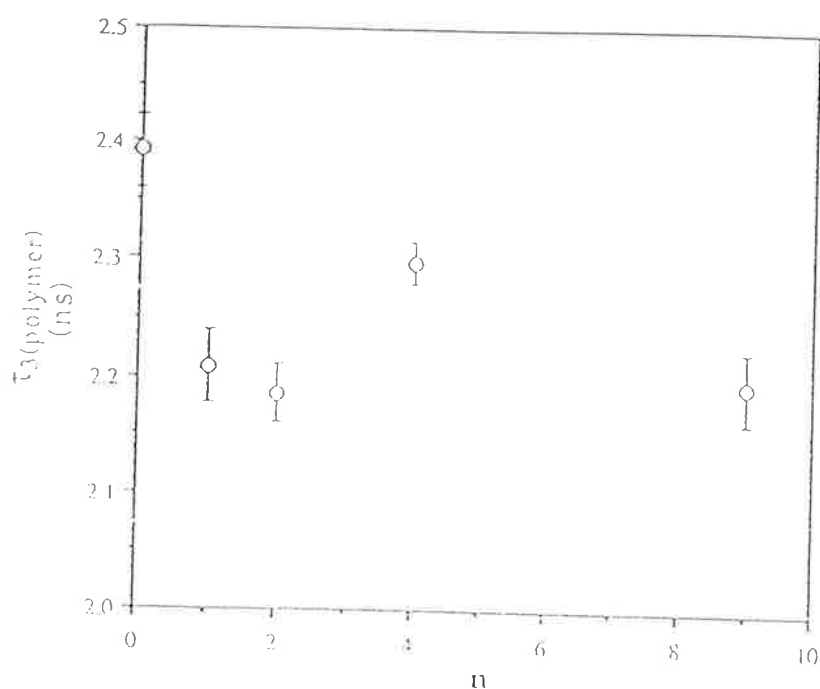


Figure 5.6.a

The variation in  $\tau_3(\text{polymer})$  for several 3mol% OED/HEMA copolymers at full hydration. (Error bars represent population standard deviations of the recorded data.)

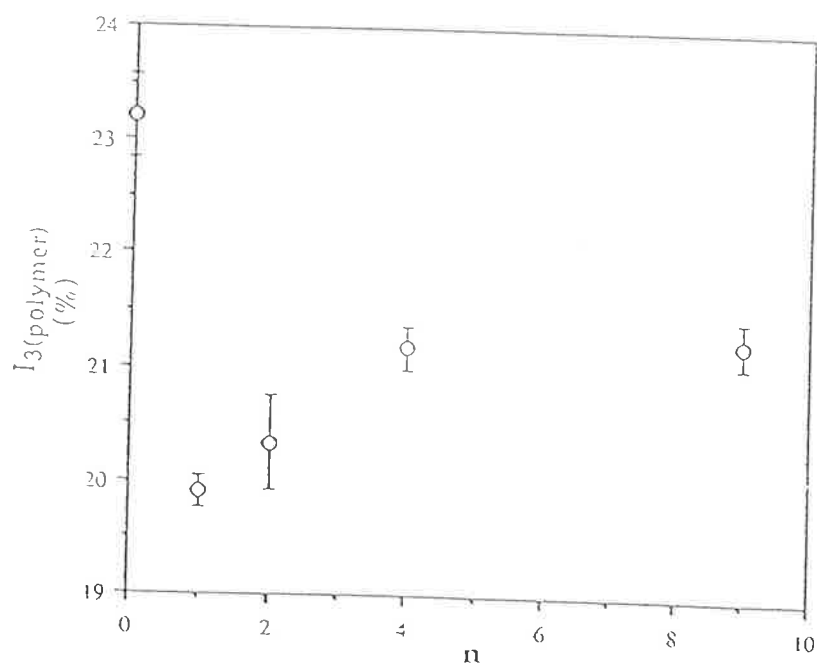


Figure 5.6.b

The variation in  $I_3(\text{polymer})$  for several 3mol% OED/HEMA copolymers at full hydration. (Error bars represent population standard deviations of the recorded data.)



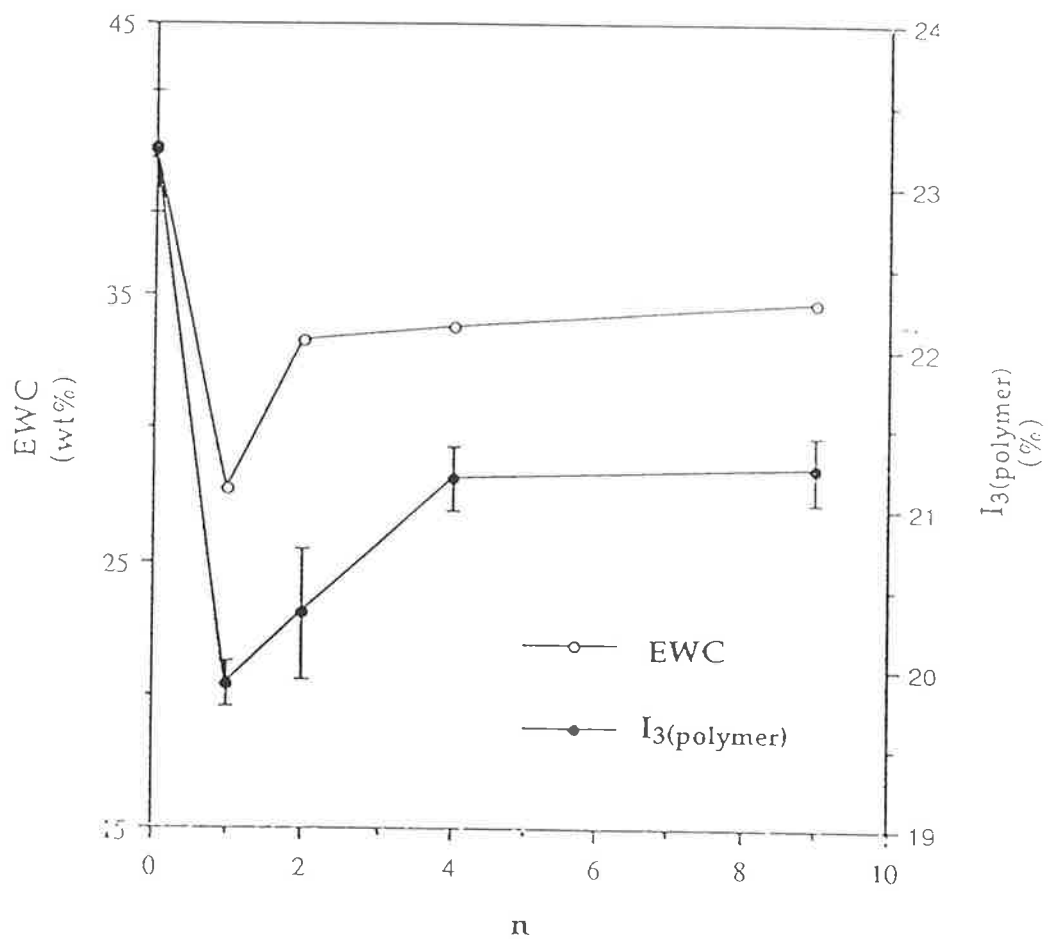


Figure 5.7

The variation in  $I_3(\text{polymer})$  and EWC for several 3mol% OED/HEMA copolymers at full hydration. (Error bars represent population standard deviations of the recorded data.)

and the flexibility of the crosslink, increases and could lead to a limitation in the frequency of free volume sites as a result of steric hindrance. The variation in  $I_{3(\text{polymer})}$  with increasing  $n$  is compared to the change in EWC for 3mol% OED/HEMA copolymer in Figures 5.7. It appears that the frequency of the free volume sites attributable to the polymer network follows a similar trend as the variation in the EWC for 3mol% OED/HEMA copolymers at full hydration. This would suggest that the number of free volume sites resulting from the polymer network is a significant factor in the determination of the EWC of a hydrogel.

### 5.4.3 Free volume characteristics of doped pHEMA based gel electrolytes.

#### 5.4.3a KBr doped gel electrolytes

PALS experiments were undertaken on a range of OED/HEMA hydrogels that had been hydrated in 1M KBr. The oPs pickoff lifetimes and relative intensities are presented in Table 5.9. The experimental data were corrected for contributions to both  $\tau_{3(\text{net})}$  and  $I_{3(\text{net})}$  arising from the presence of KBr solution within the network utilising values of  $\tau_3$  and  $I_3$  recorded for a 1M KBr solution ( $\tau_3 = 1.824$  ns,  $I_3 = 16.498\%$ ). It should be noted that  $\tau_3$  and  $I_3$  were less for the 1M KBr solution than for the deionised water suggesting that there may be oPs quenching and oPs inhibition taking place.

The introduction of KBr to the hydration solution results in a decrease in both the EWC and the amount of freezing water in pHEMA samples and its copolymers (Section 5.2.3). In comparison to the undoped sample, the doped pHEMA sample exhibited a decrease in  $I_{3(\text{polymer})}$  ( $I_{3(\text{polymer})} = 19.042\%$ ) and an increase in  $\tau_{3(\text{polymer})}$  ( $\tau_{3(\text{polymer})} = 2.438$  ns). The decrease in  $I_{3(\text{polymer})}$  may in part be attributed to oPs inhibition. The doped OED/HEMA samples have similar KBr concentration (Table 5.7) and so it is believed that comparison of  $\tau_{3(\text{polymer})}$  and  $I_{3(\text{polymer})}$  is valid as all samples will have experienced similar oPs quenching and inhibition.

Table 5.9

The variation in EWC, conductivity,  $\tau_{3(net)}$ ,  $I_{3(net)}$ ,  $\tau_{3(polymer)}$  and  $I_{3(polymer)}$  for several 3mol% OED/HEMA copolymers hydrated in 1M KBr and at full hydration.

Sample	EWC (%)	$\sigma$ (S/cm)	$\tau_{3(net)}$ (ns)	$I_{3(net)}$ (%)	$\tau_{3(p)}^*$ (ns)	$I_{3(p)}^\ddagger$ (%)
pHEMA	39.6	$4.13 \times 10^{-3}$	2.367	18.747	2.913	17.53
1.5mol% EGDMA/HEMA	32.3	$6.61 \times 10^{-4}$	2.313	19.623	2.322	19.47
3.0mol% EGDMA/HEMA	27.0	$1.70 \times 10^{-4}$	2.258	17.967	2.261	17.9
3.0mol% DiEGDMA/HEMA	32.5	$7.73 \times 10^{-4}$	2.256	17.694	2.259	17.61
3.0mol% TEGDMA/HEMA	32.8	$8.57 \times 10^{-4}$	2.171	18.478	2.177	18.31
3.0mol% P400/HEMA	34.0	$8.70 \times 10^{-4}$	2.142	18.774	2.153	18.47

\*  $\tau_{3(p)} = \tau_{3(polymer)}$

‡  $I_{3(p)} = I_{3(polymer)}$

The variation in both  $\tau_{3(polymer)}$  and  $I_{3(polymer)}$  with  $n$ , the number of ethylene glycol units, in 3mol% OED/HEMA copolymers is shown in Figures 5.8a and 5.8b. Similar trends are revealed as for undoped samples. All crosslinked samples yielded lower  $\tau_{3(polymer)}$  than pHEMA. As  $n$  was increased from 1 to 9,  $\tau_{3(polymer)}$  decreased slightly again suggesting that longer more flexible crosslinks are able to pack in such a way so as to limit the size of free volume sites. The number of free volume sites, reflected in  $I_{3(polymer)}$ , was lower for all doped crosslinked samples than for doped pHEMA at full hydration. A similar trend was revealed for crosslinked doped samples as was shown by undoped samples. If experimental error is taken into account,  $I_{3(polymer)}$  increased as  $n$  was increased from 1 to 4 but did not vary significantly as  $n$  was increased from 4 to 9. This is also similar to the variation in EWC shown by 3mol% OED/HEMA copolymers hydrated in

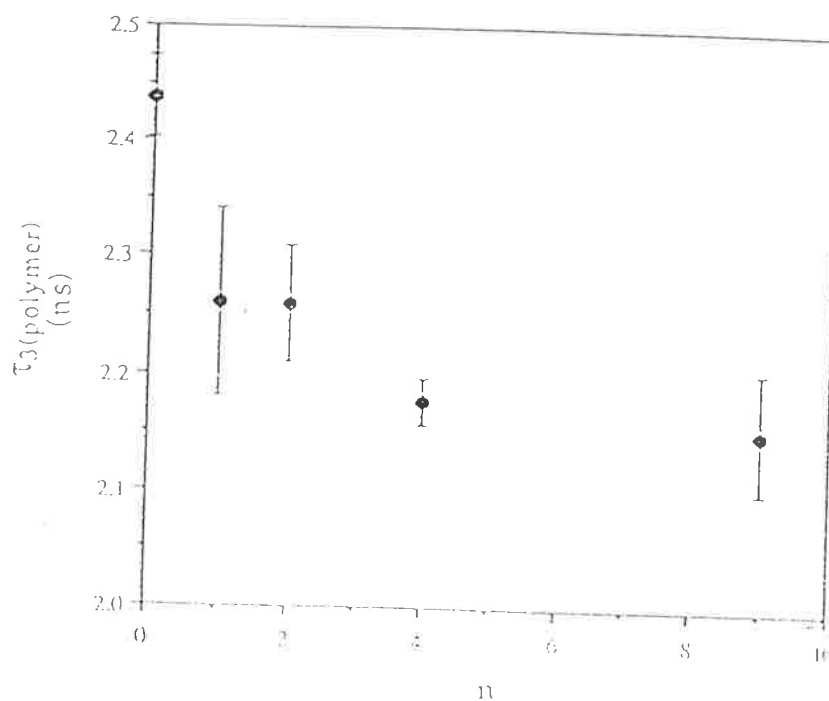


Figure 5.8.a

The variation in  $\tau_3(\text{polymer})$  for several 3mol% OED/HEMA copolymers hydrated in 1M KBr solutions. (Error bars represent population standard deviations of the recorded data.)

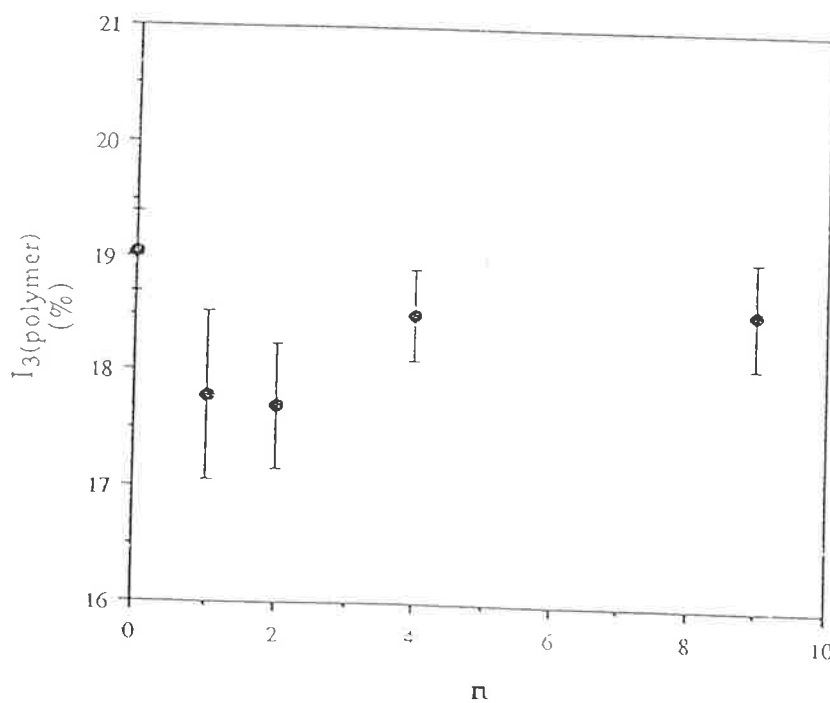
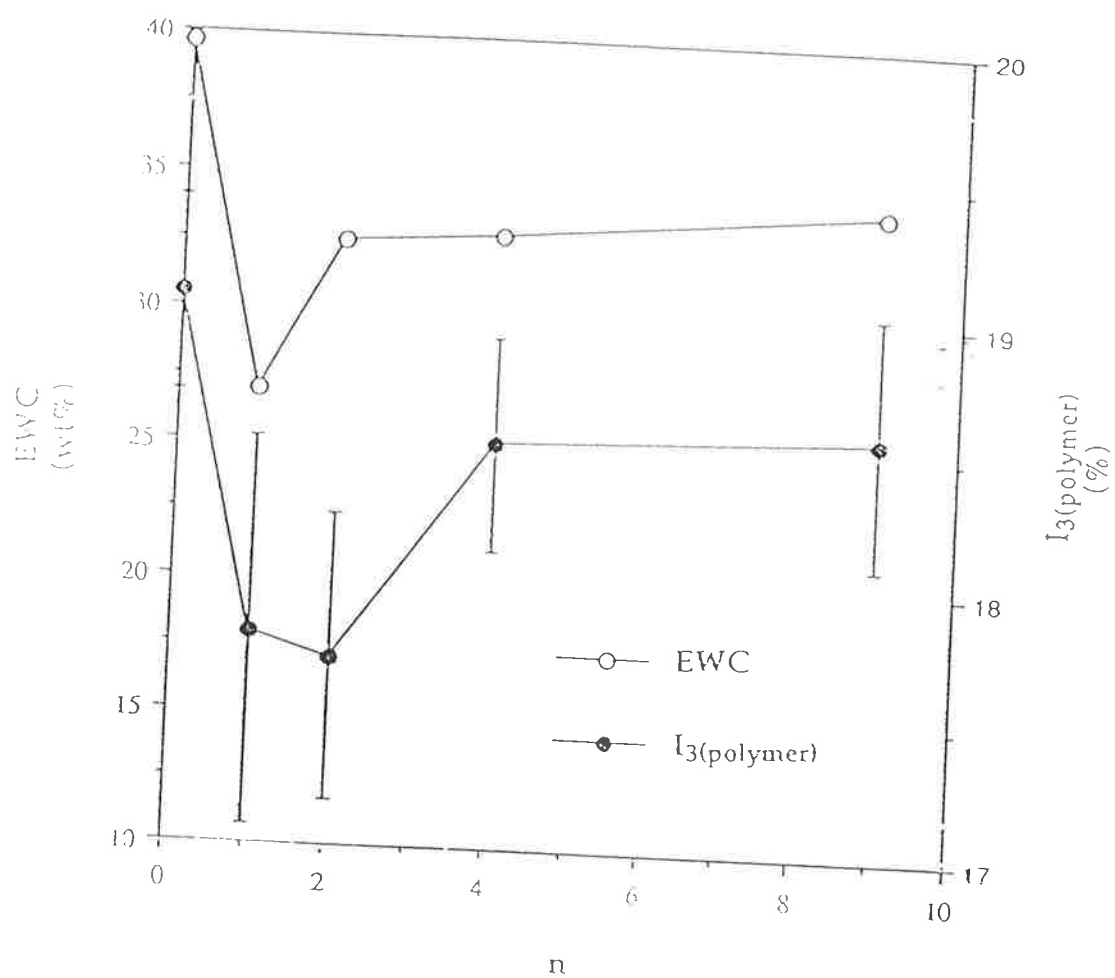


Figure 5.8.b

The variation in  $I_3(\text{polymer})$  for several 3mol% OED/HEMA copolymers hydrated in 1M KBr solutions. (Error bars represent population standard deviations of the recorded data.)



**Figure 5.9**  
The variation in  $I_3(\text{polymer})$  and EWC for several 3mol% OED/HEMA copolymers hydrated in 1M KBr solutions. (Error bars represent population standard deviations of the recorded data.)

1MKBr (Figure 5.9).

#### 5.4.3b The variation of dopant in pHEMA gel electrolytes

As a preliminary investigation, PALS experiments were conducted on pHEMA samples that had been hydrated in a range of 1M electrolyte solutions. The experimentally obtained data,  $\tau_{3(net)}$  and  $I_{3(net)}$ , are presented in Table 5.10. No corrections have been applied to the raw data to date because there exists insufficient experimental data on the free volume characteristics of the electrolyte solutions involved.

It is interesting to note, however, that for samples hydrated in potassium halide solutions that  $I_{3(net)}$  follows the same order as the EWC of these samples, that is  $I_{3(net)KI} > I_{3(net)KBr} > I_{3(net)KCl}$ . This result is by no means conclusive given the lack of data necessary to perform the appropriate corrections but, given the parallel trends exhibited for  $I_{3(polymer)}$  and EWC by fully hydrated undoped 3mol% OED/HEMA copolymers, it is sufficient to suggest that further work is warranted.

Table 5.10

The variation in EWC, conductivity,  $\tau_{3(net)}$  and  $I_{3(net)}$  for pHEMA gels, hydrated in 1M solutions of several electrolytes, at full hydration.

Electrolyte	EWC (%)	$\sigma$ (S/cm)	$\tau_{3(net)}$ (ns)	$I_{3(net)}$ (%)
-	40.4	$2.86 \times 10^{-5}$	2.328	22.508
KBr	39.6	$4.13 \times 10^{-3}$	2.367	18.747
KI	50.5	$1.84 \times 10^{-2}$	2.094	19.324
KCl	29.7	$8.05 \times 10^{-4}$	2.307	18.465
LiBr	38.3	$2.66 \times 10^{-3}$	2.156	18.110
NaBr	35.6	$2.71 \times 10^{-3}$	2.233	18.966

#### 5.4.4 Summary

The introduction of crosslinkers into the pHEMA hydrogels investigated has been shown to reduce both the number and the size of free volume cavities present for the complete range of crosslinkers investigated. For 3mol% OED/HEMA copolymers, whether hydrated in either deionised water or 1M KBr solution, the mean oPs lifetime,  $\tau_3$ , was shown to decrease slightly as  $n$  was increased from 1 to 9. This decrease in the free volume cavity size is believed to be due to the increased flexibility of the crosslink enabling more efficient packing of the network. The variation in  $I_3$ , the relative oPs annihilation intensity, was found to be similar to the variation in EWC as  $n$  increased, in both the doped and undoped 3mol% OED/HEMA samples investigated. It is suggested that the number of free volume cavities is significant in determining the EWC of a crosslinked gel.

No direct comparison has been made between the data of the undoped samples and the doped samples as the complexity of such polymer/water/electrolyte systems leads to numerous interactions that can result in oPs inhibition and oPs quenching. Data was collected for pHEMA samples hydrated in several electrolyte solutions but further work is required before any conclusions can be made.

#### 5.5 Summary

The free volume characteristics of pHEMA hydrogels have been investigated by TMA and PALS. In the dry state, TMA results revealed that both the introduction of crosslinkers and KBr decreased the free volume, however the decrease in free volume arising from the introduction of a crosslinking agent was dependent on the nature of the crosslinker employed; the calculated free volume fractions of dry 3mol% OED/HEMA copolymers followed the same general trend as their EWC at full hydration.

PALS measurements on fully hydrated doped and undoped samples

revealed a decrease in the size of the free volume sites arising from crosslinking. A slight decrease in  $\tau_3$  was experienced by 3mol% OED/HEMA copolymers as  $n$  increased and this was ascribed to more efficient packing of the larger more flexible crosslinks. The variation in  $I_3$  for 3mol% OED/HEMA copolymers was similar to the variation in EWC for these samples in both the doped and undoped forms suggesting the number of free volume cavities is a determining factor in the EWC of these polymers. No comparisons were made between the data gained for the doped and undoped hydrogels because of the uncertainty associated with the validity of the corrections employed for the doped samples. Raw data was obtained for samples hydrated in a range of electrolyte solutions but the study remains incomplete.

DSC measurements revealed that the ratio of freezing to non-freezing water was dependent on the amount and nature of both the crosslinker and the dopant employed in the gels studied. Increased crosslinking reduced the relative amount of freezing water present with this decrease being less for samples crosslinked with OEDs with greater values of  $n$ . The nature of the dopant anion employed was found to have a significant effect on the ratio of freezing water to non-freezing water. Variations in the freezing/non-freezing water ratio were found to correlate well with conductivity data.

These results confirm the classification of the pHEMA/water/electrolyte systems as gel electrolytes. Although the nature of the polymer network and its associated free volume characteristics appears to control the EWC of the gel, it is the nature of the occluded water phase, reflected in the freezing/non-freezing water ratio, that appears to determine the conductivity, i.e. the polymer acts as a support to the conducting phase.



## CHAPTER SIX

### *Conclusions*

At the commencement of this project, it was clear that most research groups involved in hydrogels were divided into two groups; one group was endeavouring to achieve high ionic conductivities through the variation of gel and dopant and the other was concerned with the nature of polyelectrolytes to bring about dimensional changes on the application of an external electrical stimulus or a pH change. Both groups relied upon the absorbed water to provide a conductive medium. In the author's opinion, and from the evidence obtained in the local research group<sup>(1-4)</sup>, it was evident that there was much that was not known about the state of water absorbed in even the simplest of gels. It was for this reason that pHEMA gel electrolytes, and some simple derivatives, were made the focus of this study. The aim of this study was to investigate the conductivity of pHEMA gel electrolytes and improve the understanding of the nature of the absorbed water in such hydrogels.

Gray<sup>(5)</sup> defines a gel electrolyte as a polymer/solvent/salt system in which the polymer is secondary in the conducting matrix and acts merely as a support for the low molecular weight high dielectric solvent which solvates the ions and acts as the conducting medium. The conductivity behaviour exhibited by the pHEMA/water/dopant system studied in this work is indicative of its classification as a gel electrolyte.

Initially, the conductivity of fully hydrated pHEMA (EWC=40.4wt%) was found to be  $2.86 \times 10^{-6} \text{ S.cm}^{-1}$  which was noticeably less than that of the hydration water ( $\sigma = 6.6 \times 10^{-5} \text{ S.cm}^{-1}$ ), a fact that can be explained in terms of the water ordering effects of the polymer network. Water/polymer

interactions lead to less mobile water, which in turn decreases the microscopic viscosity of the conducting phase. The viscosity of the conducting phase is inversely proportional to the mobility of the charge carriers within the conducting phase (Walden's rule, Eqn. 3.7) and thus increases in the viscosity result in decreased conductivity (Eqn. 1.2).

The effect of the variation of the water content on conductivity was investigated in two ways; the introduction of OED crosslinkers yielded hydrogels of reduced EWC through alteration of the nature of the polymer network and progressive dehydration enabled a study of the conductivity with decreasing water content for individual copolymers. In general, a decrease in water content resulted in a a reduction in conductivity.

Introducing EGDMA in increasing amounts to pHEMA networks led to decreased EWC; EGDMA is more hydrophobic than HEMA and its incorporation into the polymer matrix yields tighter less mobile polymer networks with decreased swelling ability. The conductivity and EWC of EGDMA/HEMA copolymers decreased as EGDMA concentration was increased. However, the decrease in conductivity was markedly different than the decrease in EWC. Even small amounts of EGDMA caused significant decreases in conductivity (Figure 3.3) yet studies<sup>(6,7)</sup> have shown that the water uptake of pHEMA to be relatively insensitive to degrees of crosslinking. This lack of variation in EWC at low levels of crosslinking has been attributed to the existence of a secondary non-covalent network. This network, for which there exists several possible explanations, would appear to have a minimal effect on the conductivity of EGDMA/HEMA copolymers. The different trends in EWC and conductivity (Figure 3.3) are ascribed to the alteration of the structure of the occluded water phase resulting from the change in the nature of the polymer network. DSC measurements (Section 5.2.2) revealed a decrease in the ratio of freezing water to non-freezing water as EGDMA concentration was increased in EGDMA/HEMA copolymers.

The AC impedance plots yielded supplementary information on the conductivity behaviour. The ideality of the semi-circular portion of the locus,  $\phi$ , decreased as EGDMA increased suggesting a decrease in the continuity of the conducting phase, that is the occluded water. Increased EGDMA concentration decreases the mobility of the polymer network and leads to an increase in capacitance.

The nature of the crosslinking agent employed was also found to have a significant effect on the conductivity. Both EWC and conductivity were lower for all 3mol% OED/HEMA copolymers than for pHEMA (Table 3.4) but as  $n$ , the number of ethylene glycol units, was increased from 1 to 9 the conductivity increased almost linearly but EWC increased in a limited manner (Figure 3.5). The increase in EWC has been shown to be controlled by two factors; not only does the hydrophilicity of the crosslinker increase with  $n$ , but the increased flexibility of the crosslink enables more efficient packing of the polymer network limiting polymer/water interaction through steric hindrance and thus limiting water uptake. These competing factors limit the increase in EWC as  $n$  is increased. Free volume investigations by PALS yielded a similar trend for  $I_3$ , an indication of the number of free volume sites, in hydrated 3mol% OED/HEMA copolymers (Figure 5.7). It would appear that the hydration level of a polymer and its free volume characteristics are closely related. Furthermore, DSC measurements (Section 5.2.2) revealed a similar trend for both the conductivity and the ratio of freezing to non-freezing water as  $n$  was increased for 3mol% OED/HEMA copolymers. The structure of the water phase, and thus its microscopic viscosity, is a determining factor in the conductivity of such copolymers.

Progressive dehydration of pHEMA resulted in a continuous decrease in conductivity. However, trends were revealed that correlate positively with the description of water in pHEMA offered by McBrierty<sup>(8)</sup>. The absorbed water not only provides the conducting medium, but it also plasticises the

polymer network, liberating segmental motion of the network, which in turn increases the continuity of the conducting phase and also swells the polymer which leads to enhanced mobility of the conducting phase.

The largest increase in conductivity resulted from the first 20wt% water; initially the absorbed water provides the conducting phase and liberates polymer network segmental motion through plasticisation. Water absorbed between 20wt% and 35wt% has a less significant plasticisation ability which further decreases for water absorbed at hydration levels >35wt%. The amount of the conducting phase increases as water content increases as does the microscopic viscosity of the water phase. The cessation of large scale segmental motion ( $T_g=25^\circ\text{C}$  at ca. 20wt% water<sup>(9)</sup>) is believed to contribute to the change in conductivity behaviour at 20wt% water content.

Similar conductivity behaviour during dehydration was observed for several OED/HEMA copolymers, with both variation in the concentration and nature of the crosslinker investigated. It should be noted that, in general, these copolymers exhibited a two stage decrease on the removal of the absorbed water as their EWC tended to be less than 35wt% as a result of crosslinking. Copolymers of greater crosslinker concentration were found to have a lower conductivity over the entire hydration range studied. The changes in conductivity behaviour for several of the OED/HEMA samples investigated agreed with the hypothesis that the glass transition contributes to changes in conductivity behaviour however, insufficient  $T_g$  data on some of the OED/HEMA copolymers exists to fully substantiate this claim.

It should be noted that the dehydration experiments reflect the negligible contribution of the polymer network to the conductivity of the gel electrolytes investigated in this work;  $\log(\text{conductivity})$  was found to be of the order of -12 at very low hydration levels suggesting pHEMA and its copolymers are insulators in the dry state. It is noted that the water in pHEMA has  $\text{pH}=6$ <sup>(10)</sup> resulting from a lack of ionising functionalities of the

polymer network; this is indicative of the negligible contribution that makes to the conductivity of the gel electrolytes studied.

The AC impedance spectra of all hydrogels exhibited a transformation from a single semi-circular locus to the superposition of two semi-circles at some water content during the dehydration. This change in behaviour has been ascribed to morphological change, with respect to the conductivity, in the hydrogels. It is suggested that this change is due to the presence of portions of the polymer/water structure that are unable to support conductivity. As the water content was further decreased, the AC impedance plots reverted to single semi-circular behaviour suggesting an increase in the discontinuous nature of the conducting phase. Similar behaviour, indicative of the heterodispersion of the water in pHEMA hydrogels at low water contents has been reported for the variation in the nature of the  $\alpha$ -transition of the dynamic mechanical analysis of Allen et al.<sup>(2)</sup>.

The change in the locus of the AC impedance plot occurred at 12.1wt% hydration level for pHEMA. Interestingly, as EGDMA concentration was increased, the water content at which this change in the AC impedance behaviour eventuated also increased suggesting that less mobile polymer networks limit the continuity of the conducting phase. However, this transition took place at ca. 10.4wt% for 3mol% DiEGDMA, TEGDMA and P400 copolymers suggesting that sufficiently flexible crosslinks may promote the continuity of the conducting phase.

Conductivity was found to exhibit an Arrhenian dependence on temperature (Section 3.7). In general,  $\log(\text{conductivity})$  v  $1/T$  plots revealed two regions of linear behaviour with differing activation energy. A sharp decrease in  $\log(\text{conductivity})$  and an increase in activation energy occurred at sub-zero temperatures on cooling. The conductivity reverted to the original style of behaviour at ca. 0°C on warming. The transition was reflected in a change in the AC impedance locus; the original semi-circular locus

transformed to the superposition of two semi-circles suggesting a decrease in the continuity of the conducting phase. The original activation energy on cooling,  $E_{a1}$ , was greater for ore crosslinked samples yet the activation energy after the change in the conductivity behaviour,  $E_{a2}$ , was greater for less crosslinked samples. The temperature at which the change in conductivity behaviour took place decreased with an increase in EGDMA concentration. All this evidence suggests that the transition is due to the partial freezing of the water phase; a reversible morphological change, the freezing point depression and the trends in  $E_{a1}$  and  $E_{a2}$  correlate with the different freezing capabilities of the gels revealed by DSC (Section 5.2.2). For pHEMA  $E_{a1}=15.0\text{kJ/mol}$  which is comparable to the activation energy calculated for water ( $15.5\text{kJ/mol}^{(11)}$ ) supporting Gray's definition in which the polymer behaves as a support for the conducting medium.

It was noted that the conductivity above  $0^\circ\text{C}$  on warming was slightly higher than at similar temperatures during the initial cooling of the sample. TMA experiments (Section 5.3.2.c) revealed an interesting expansion/contraction phenomenon in this temperature range on warming samples that had been cooled to  $-60^\circ\text{C}$ . This behaviour warrants further investigation with a view to understanding any possible link between the expansion/contraction phenomenon and the recorded conductivity trends over that temperature range.

In summary, all the changes in the conductivity behaviour of undoped pHEMA samples investigated in this work arise from changes to the structure and the amount of the occluded water phase. However Gray's definition<sup>(5)</sup> of a gel electrolyte underplays the significance of the polymer network in the pHEMA gel electrolytes investigated; the nature of the polymer network controls the EWC and the structure of the absorbed water through polymer/water interactions and thus effects the conductivity albeit in a passive manner.

The introduction of an electrolytic dopant, such as KBr, resulted in large increases in conductivity, compared to undoped samples, of the hydrogels studied for the whole range of dopants employed. The nature of the dopant led to anion dependent variation in the EWC; samples hydrated in iodide solutions had increased EWC, whereas those hydrated in bromide and chloride solutions had reduced EWC with decreases exhibited by samples hydrated in chloride solutions. The change in conductivity for samples hydrated in different dopants followed the same order as EWC. The variation in conductivity was mirrored by a similar trend in the ratio of freezing water to non-freezing water as evaluated by DSC (Figure 5.1).

The majority of experiments were carried out on KBr doped samples as KBr had the least effect on the EWC of the dopants investigated. As KBr concentration was increased, EWC decreased and conductivity increased for all the copolymers investigated. The number of charge carriers,  $n$  (Eqn 1.2) is the determining factor in the conductivity of KBr doped samples. The decrease in EWC was found to be relatively greater for more crosslinked samples.

It should be noted that the conductivities of pHEMA samples hydrated in KBr solutions were of the order of 2.5% to 3.0% of the conductivities of the hydration solutions. The large decrease is ascribed to the presence of the polymer network as an impediment to ion motion and also the increased microscopic viscosity of the water phase resulting from polymer/water and polymer/water/ion interactions. Plots of the conductivity against KBr concentration (Figures 4.4, 4.6) revealed, in general, a negative deviation from a linear increase in conductivity due to ion/ion interaction and also the electrophoretic and relaxation effects.

Dehydration experiments exhibited similar trends as for undoped samples. However, in general, doped samples revealed two regions of conductivity behaviour as a result of their reduced EWC arising from the

presence of KBr. The change in conductivity behaviour attributed to appearance of interfacial water, at 20wt% water content for undoped pHEMA, occurred at lower water contents for samples of higher KBr concentration. Given the antiplasticising effect of KBr on dry pHEMA<sup>(12)</sup>, this trend casts doubt over the suggestion that the glass transition contributes to the change in conductivity behaviour. The change in the nature of the AC impedance plots occurred at lower water contents for samples of higher KBr concentration; it is suggested that the KBr ions may be able to order the water phase in a manner conducive to a more continuous conductive phase at low water contents.

Doped copolymer samples subjected to temperature cycling exhibited similar conductivity trends as undoped samples. The freezing transition temperature decreased with increased KBr concentration; this decrease was greater than that calculated for KBr solutions of similar concentration and is attributed to water/polymer and water/polymer/ion interactions.  $E_{a1}$  was generally found to decrease as KBr concentration increased but was greater than that calculated for similar electrolyte solutions suggesting that the polymer network, and its interactions with water and ions, impedes conductivity.  $E_{a2}$  was greater for doped samples reflecting the importance of freezable water to the motion of ions and their associated hydration spheres.

An attempt has been made to delineate between the relative importance of the several parameters varied in the study of the conductivity of the pHEMA gel electrolytes but this has been difficult to achieve due to the complexity of the numerous interactions in polymer/water/electrolyte systems (Table 4.1). The AC impedance analysis techniques proved to be valuable, providing information on morphological changes, with respect to conductivity, occurring within the gels as they were subjected to various environmental and structural changes. It should be noted that significant variation in conductivity of the pHEMA gel electrolytes studied was achieved



through relatively minor variation of the variables investigated which would appear to suggest that these materials have the potential to be used in sensory applications given the correct conditions under which to perform.

# *References*

## Chapter 1

1. J. Burt, *J. Chem. Soc.*, 1171(1910).
2. M. Goehring and D. Voight, *Naturwissenschaften*, **18**, 482 (1953).
3. F.M. Gray, *Solid Polymer Electrolytes: Fundamentals and Technological Applications*, VCH Publishers Ltd., Cambridge, 1991, Chapter 1, pp 1.
4. J.S. Miller, *Adv. Mater.*, **5**(7/8), 587 (1993).
5. B. Scrosati, *Mater. Sci. Forum*, **42**, 207 (1989).
6. M. Gauthier, M. Armand and D. Muller in *Electroresponsive Molecular and Polymeric Systems: 1*, Ed. T.A. Skotheim, Marcel Dekker Inc., New York, 1988, pp41.
7. A.G. MacDiarmid and M. Maxfield in *Electrochemical science and technology of polymers*, Ed. R.G. Linford, Elsevier Applied Science, New York, 1987, pp67.
8. B.C. Tofield, R.M. Dell and J. Jensen, *AERE Harewell Report 11261* (1984).
9. H. Shirakawa, E.J. Louis, A.G. MacDiarmid, C.K. Chiang and A.J. Heeger, *J. Chem. Soc. Chem. Comm.*, 578 (1977).
10. L.W. Shacklette, R.L. Elsenbaumer, R.R. Chance, J.M. Sowa, D.M. Ivory, G.G. Miller and R.H. Baughman, *J. Chem. Soc., Chem. Commun.*, 361 (1982).
11. A.F. Diaz, K.K. Kanazawa and G.P. Gardini, *J. Chem. Soc., Chem. Commun.*, 635 (1979).
12. C.K. Chiang, M.A. Druy, S.C. Gau, A.J. Heeger, E.J. Louis, A.G. MacDiarmid, Y.W. Park and H. Shirakawa, *J. Am. Chem. Soc.*, **100**, 1013 (1978).
13. C.K. Chiang, C.R. Fincher Jr., Y.W. Park, A.J. Heeger, H. Shirakawa, E.J. Louis, S.C. Gau and A.G. Macdiarmid, *Phys. Rev. Lett.*, **39**, 1098 (1977).
14. S. Roth, *Mater. Sci. Forum*, **42**, 1(1989).
15. B.E. Fenton, J.M. Parker and P.V. Wright, *Polymer*, **14**, 589 (1973).
16. M.B. Armand in *Fast Ion Transport in Solids*, Eds. P. Vashishta, J.N. Mundy, and G.D. Shenoy, Elsevier North-Holland, Amsterdam 1979.

17. F.M. Gray in *Polymer Electrolyte Reviews-1*, Eds. J.R. MacCallum, C.A. Vincent, Elsevier, London, 1987, pp 139.
18. G.T. Davis, C.K. Chiang and C.A. Harding, *Solid State Ionics*, **18/19**, 321 (1986).
19. R. Dupon, B.L. Papke, M.A. Ratner and D.F. Shriver, *J. Electrochem. Soc.*, **131**, 586 (1984).
20. R.D. Armstrong and M.D. Clarke, *Electrochimica Acta*, **29**, 1443 (1984).
21. M. Watanabe, M. Togo, N. Ogata, T. Kobayashi and T. Ohtaki, *Macromolecules*, **17**, 2908 (1984).
22. D.F. Shriver, B.L. Papke, M.A. Ratner, R. Dupon, T. Wong and M. Brodwin, *Solid State Ionics*, **5**, 83 (1981).
23. P.M. Blonsky and D.F. Shriver, *J. Am. Chem. Soc.*, **106**, 6854 (1984).
24. D. A. Seanor in, *Electrical Properties of Polymers*, Ed. D.A. Seanor, Academic Press, New York, 1982, Chapter 1.
25. M. Mandel in *Encyclopaedia of Polymer Science and Engineering*, Second Edition, Eds. H.F. Mark, N.M. Bikales, C.G. Overberger, G. Menges and J.I. Kroschwitz, Wiley Interscience, New York, 1988, Vol.11, pp 739.
26. A.M. Voice, J.P. Southall, V. Rogers, K.H. Matthews, G.R. Davies, J.E. McIntyre and I.M. Ward, *Polymer*, **35**(16), 3363 (1994).
27. E. Zygadlo-Monikowska, Z. Florjanczyk and W. Wieczorek, *J.M.S. - Pure Appl. Chem.*, **A31**(9), 1121 (1994).
28. E. Tsuchida, H. Ohno and K. Tsunemi, *Electrochimica Acta*, **28**(5), 591 (1983).
29. K. Tsunemi, H. Ohno and E. Tsuchida, *Electrochimica Acta*, **28**(6), 833 (1983).
30. H. Matsuda, O. Hiroyuki, K. Mizoguchi and E. Tsuchida, *Polym. Bull.*, **7**, 271 (1981).
31. M. Watanabe, M. Kanba, H. Matsuda, K. Tsunemi, K. Mizoguchi, E. Tsuchida and I. Shinohara, *Makromol. Chem., Rapid Commun.*, **2**, 741 (1981).

32. T. Kabata, T. Fujii, O. Kimura, T. Ohsawa, Y. Matsuda and M. Watanabe, *Polym. Adv. Tech.*, **4**, 205 (1993).
33. S. Reich and I. Michaeli, *J. Polym. Sci., Polym. Phys. Ed.*, **13**, 9 (1975).
34. F. Croce, S.D. Brown, S.G. Greenbaum, S.M. Slane and M. Salomon, *Chem. Mater.*, **5**, 1268 (1993).
35. M.B. Armand, *Solid State Batteries*, Eds. C.A.C. Sequeira, A. Hooper, NATO ASI Series, Martinus Nijhoff, Dodrecht, 1985.
36. S.M Aharoni and S.F. Edwards, *Macromolecules*, **22**, 3361 (1989).
37. Y. Sakai, Y. Sadaoka, M. Matugushi, I. Hiramatsu and K. Hirayama, in *Proceedings of the 3rd International Meeting on Chemical Sensors*, Cleveland, OH, p273 (1990).
38. E. I. du Pont de Nemours Co., *U.S. Pat.* 2,028,012 (1936).
39. E. I. du Pont de Nemours Co., *Ind. Chem. Eng.*, **28**, 1160 (1936).
40. O. Wichterle and D. Lim, *Nature*, **165**, 117 (1960).
41. O. Wichterle and D. Lim, *U.S. Pat.* 2,976,576, March 28 (1961).
42. D.J. Bennett, *PhD Thesis*, University of Adelaide (1991).
43. M. Refojo, 'Contact Lenses', in *Encyclopaedia of Polymer Science and Technology*, Wiley, New York, 1976; Supplement Vol. 1, pp195-219.
44. T. A. Jadwin, A.S. Hoffmann and W.R. Vieth, *J. Appl. Polym. Sci.*, **14**, 1339 (1970).
45. J. Kopecek and J. Vacik, *Coll. Czech. Chem. Commun.*, **38**, 854 (1973).
46. B.D. Ratner and I.F. Miller, *J. Biomed. Mater. Res.*, **7**, 353 (1973).
47. J. Vacik, M. Czakova, J. Exner, J. Kalal and J. Kopecek, *Coll. Czech. Chem. Commun.*, **42**, 2786 (1977).
48. M. Tollar, M. Stol and K. Kliment, *J. Biomed. Mater. Res.*, **3**, 305 (1969).
49. S. M. Lazarus, J.N. LaGuerre, H. Kay, S.R. Weinberg and B.S. Levowitz, *J. Biomed. Mater. Res.*, **5**, 129 (1971).
50. G.M. Zetner, J.R. Cardinal and S.W. Kim, *J. Pharm. Sci.*, **67**, 1352 (1978).

51. M.L. Davies and B.J. Tighe, *Selective Electrode Rev.*, **13**, 159 (1991).
52. S. Sevcik, J. Stamberg and P. Schmidt, *J. Polym. Sci.*, **C16**, 821 (1967).
53. J. Stamberg and S. Sevcik, *Coll. Czech. Chem. Commun.*, **31**, 1009 (1966).
54. P.E.M. Allen, D.J. Bennett, A.M. Hounslow and D.R.G. Williams, *Eur. Polym. J.*, **28**(10), 1179 (1992).
55. H.B. Lee, J.D. Andrade and M.S. Jhon, *Polym. Prepr.*, **15**, 706 (1974).
56. A. Yamada-Nosaka, K. Ishikiriyama, M. Todoka and H. Tanzawa, *J. Appl. Polym. Sci.*, **39**, 2443 (1990).
57. P.E.M. Allen, D.J. Bennett and D.R.G. Williams, *Eur. Polym. J.*, **29**(2/3), 231 (1993).
58. G. Smyth, F.X. Quinn and V.J. McBrierty, *Macromolecules*, **21**, 3198 (1988).
59. Y.K. Sung, D.E. Gregonis, M.S. Jhon and J.D. Andrade, *J. Appl. Polym. Sci.*, **26**, 3179 (1981).
60. M. Van Bos, E. Schacht, W.E. Roorda and H.E. Junginger, *Polym. Comm.*, **32**(1), 20 (1991).
61. P.H. Corkhill, A.M. Jolly, C.O. Ng and B.J. Tighe, *Polymer*, **28**, 1758 (1987).
62. D.G. Pedley and B.J. Tighe, *Br. Polym. J.*, **11**, 130 (1979).
63. J.A. Bouwstra, J.C. van Miltenburg, W.E. Roorda and H.E. Junginger, *Polym. Bull.*, **18**, 337 (1987).
64. H.B. Lee, M.S. Jhon and J.S. Andrade, *J. Colloid Interface Sci.*, **51**(2), 225 (1975).
65. P.G. Bruce in *Polymer Electrolyte Reviews-1*, Eds. J.R. MacCallum, C.A. Vincent, Elsevier, London, 1987, pp 237.
66. M. Watanabe, S. Oohashi, K. Sanui, N. Ogata, T. Kobayashi and Z. Ohataki, *Macromolecules*, **18**, 1945 (1985).
67. G.P. Simon, *Ph.D. Thesis*, University of Adelaide (1986).
68. M. Refojo and H. Yasuda, *J. Appl. Polym. Sci.*, **9**, 2425 (1965).
69. J. Janacek and J. Hasa, *Coll. Czech. Chem. Commun.*, **31**, 2186 (1966).

- 70 M. Refojo, *J. Polym. Sci. , Polym. Chem. Ed.*, **5**, 3103 (1967).
71. B.D. Ratner and I.F. Miller, *J. Polym. Sci., Polym. Chem. Ed.*, **10**, 2425 (1972).
72. J.H. Collett, D.E.M. Spillane and E.J. Pywell, *Polym. Prep.*, **28**, 141 (1987).
73. J.R. MacCallum and C.A. Vincent in *Polymer Electrolyte Reviews-1*, Eds.J.R. MacCallum and C.A. Vincent, Elsevier, London, 1987, pp 23.
74. K. Dusek, M. Bohadanecky and J. Vosicky, *Coll. Czechoslov. Chem. Comm.*, **42**, 1599 (1977).
75. M.F. Refojo, *J. Polym. Sci., A-1*, **5**, 3103 (1967).
76. K. Nakamura, *Polymer J.*, **8**(3), 267 (1976).
77. P.E.M. Allen, C.-H. Lai and D.R.G. Williams, *Eur. Polym. J.*, **29**(10), 1293 (1993).
78. S.M. Murphy, C.J. Hamilton and B.J. Tighe, *Polymer*, **29**, 1887 (1988).
- 79.F.X. Quinn, V.J. McBrierty, A.C. Wilson and G.D. Friends, *Macromolecules*, **23**, 4576 (1990).
80. S.H. Oh, R. Ryoo and M.S. Jhon, *Macromolecules*, **23**, 1671 (1990).
81. C.J. Hamilton, S.M. Murphy, N.D. Atherton and B.J. Tighe, *Polymer*, **29**, 1879 (1988).

## Chapter 2

1. S. Hagias, Private Communication.
2. G.F. Cowperthwaite, J.J. Foy and M.A. Malloy, in *Biomedical and Dental Applications*, C.G. Geblen and F.F. Koblitz, Eds., Plenum Press, New York, 1981, pp.397.
3. J.E.Moore in *Chemistry and Properties of Crosslinked Polymers*, S.S.Labena, Ed., Academic Press, New York, 1977, pp. 535.
- 4 M.Atсутa and D.T.Turner, *J.Polym.Sci.,Polym. Phys.Ed.*, **20**, 1609 (1982).
5. D.J. Bennett, *Honours Thesis*, University of Adelaide, (1985).
6. P.E.M.Allen, G.P.Simon, D.R.G.Williams and E.H.Williams, *Eur. Polym. J.*, **22**, 549 (1986).
7. P.E.M.Allen, G.P.Simon, D.R.G.Williams and E.H.Williams, *Macromolecules*, **22**, 809 (1989).
8. P.H. Corkhill, A.M. Jolly, C.O. Ng and B.J. Tighe, *Polymer*, **28**, 1758 (1987).
9. J. Perry (Ed.), *Chemical Engineers Handbook*, McGraw-Hill Book Company, New York (1934).
10. J.R. MacDonald, *J.Chem.Phys.*, **61**, 3977, (1974).
11. W.I. Archer and R.D. Armstrong in *Electrochemistry*, Vol.7, The Royal Society of Chemistry, London, 1980, pp157.
12. P.G. Bruce in *Polymer Electrolyte Reviews-1*, Eds. J.R. MacCallum, C.A. Vincent (Elsevier, London 1987) pp237.
13. W. Brandt, S. Berko and W.W. Walker, *Physical Rev.*, **120**(4), 1289 (1960).
14. M. Eldrup, *Positron Annihilation*, North Holland Publishing Company (1982).
15. Y.C. Jean, *Microchem. J.*, **42**, 72 (1990).
16. A.J. Hill, *PhD Dissertation*, Duke University, Durham, NC. USA. (1990).



17. M.D. Zipper and A.J. Hill, *Mater. Forum.*, (Materials Characterization Review, Ed G. Schaeffer), **18**, 215 (1994).

18. W. Puff, *Comput. Phys. Commun.*, **30**, 359 (1983).



### Chapter 3

1. J. Vacik and J. Kopecek, *J. Appl. Polym. Sci.*, **19**, 3029 (1975).
2. H. Xu, J.K. Vij and V.J. McBrierty, *Polymer*, **35**(2), 227 (1994).
3. K. Pathmanathan and G.P. Johari, *J. Polym. Sci.: Part B: Polymer Physics Edition*, **28**, 675 (1990).
4. H.B. Lee, M.S. Jhon and J.S. Andrade, *J. Colloid Interface Sci.*, **51**(2), 225 (1975).
5. P.G. Bruce in *Polymer Electrolyte Reviews-1*, Eds. J.R. MacCallum, C.A. Vincent (Elsevier, London 1987) pp237.
6. J.R. Owen in *Comprehensive Polymer Science: the synthesis, characterization, reactions and applications of polymers*, Eds. C. Booth, C. Price, Pergamon Press, London, 1989, vol. 2, pp 669.
7. M.E. Orazem, P. Argawal and L. H. Garcia-Rubio, *J. Electroanal. Chem.*, **378**, 51 (1994).
8. I.C. Hardy and D.F. Shriver, *J. Am. Chem. Soc.*, **107**, 3823 (1985).
9. C.J. Hamilton, S.M. Murphy, N.D. Atherton and B.J. Tighe, *Polymer*, **29**, 1879 (1988).
10. P.H. Corkhill, A.M. Jolly, C.O. Ng and B.J. Tighe, *Polymer*, **28**, 1758 (1987).
11. P.E.M. Allen, D.J. Bennett and D.R.G. Williams, *Eur. Polym. J.*, **29**(2/3), 231 (1993).
12. F. Kohlrausch and A. Heydweiller, *Z. phys. Chem.*, **14**, 317 (1894).
13. R.A. Robinson and R.H. Stokes, *Electrolyte Solutions*, 2nd Edn., Butterworths, Sydney (1970).
14. G. Smyth, F.X. Quinn and V.J. McBrierty, *Macromolecules*, **21**, 3198 (1988).
15. M. Watanabe, M. Kanba, K. Nagaoka and I. Shinohara, *J. Polym. Sci., Polym. Phys.*, **21**, 939 (1983).
16. E.D. Becker, *High resolution NMR: theory and chemical applications*, 2nd edn., Academic Press, New York (1980).

17. S.Hagias, *unpublished data*.
18. P.E.M. Allen, D.J. Bennett, A.M. Hounslow and D.R.G. Williams, *Eur. Polym. J.*, **28**(10), 1179 (1992).
19. P.E.M. Allen, D.J. Bennett and D.R.G. Williams, *Eur. Polym. J.*, **28**(10), 1173 (1992).
20. P.E.M. Allen, D.J. Bennett and D.R.G. Williams, *Eur. Polym. J.*, **28**(4), 347 (1992).
21. M.F. Refojo and H Yasuda, *J. Appl. Polym. Sci.*, **9**, 2425 (1965).
22. J. Janacek and J. Hasa, *Coll. Czech. Chem. Commun.*, **31**, 2186 (1966).
23. M. F. Refojo, *J. Polym. Sci., Polym. Chem. Ed.*, **5**, 3103 (1967).
24. B.D. Ratner and I.F. Miller, *J. Polym. Sci., Polym. Chem. Ed.*, **10**, 2425 (1972).
25. D.J. Bennett, *Ph.D. Thesis*, University of Adelaide (1991).
26. G.P. Simon, *Ph.D. Thesis*, University of Adelaide (1986).
27. M.L. Davies and B.J. Tighe, *Selective Electrode Rev.*, **13**, 159 (1991).
28. M.S. Jhon and J.D. Andrade, *J. Biomed. Mater. Res.*, **7**, 509 (1973).
29. C.A.J. Hoeve in *Water in Polymers*, ACS Symposium Series, Ed. S.P. Rowland, **127**, 347 (1980).
30. A. Barnes, P.H. Corkhill and B.J. Tighe, *Polymer*, **29**, 2191 (1988).
31. W.E. Roorda, J.A. Bouwstra, M.A. de Vries, C. Kosho and H.E. Junginger, *Therm. Chim. Acta*, **112**, 111 (1987).
32. A. Yamada-Nosaka, K. Ishikiriyama, M. Todoki and H. Tanzawa, *J. Appl. Polym. Sci.*, **39**, 2443 (1990).
33. Y.K. Sung, D.E. Gregonis, M.S. Jhon and J.D. Andrade, *J. Appl. Polym. Sci.*, **26**, 3719 (1981).
34. H.B. Lee, J.D. Andrade and M.S. Jhon, *Polym. Prepr.*, **15**, 706 (1974).
35. M. Watanabe, S. Oosashi, K. Sanui, N. Ogata, T. Kobayashi and Z. Ohtaki, *Macromolecules*, **18**, 1945 (1985).

36. S. Reich and I. Michaeli, *J. Polym. Sci., Polym. Phys. Ed.*, **13**, 9 (1975).
37. D. Dobos, *Electrochemical Data*, Elsevier, Budapest (1975).
38. A.J. Kovacs, *Adv. Polym. Sci.*, **3**, 396 (1963).
39. T. G. Fox, *Bull. Am. Phys. Soc.*, **1**, 123 (1953).
40. M. Gordon and J.S. Taylor, *J. Appl. Chem.*, **2**, 493 (1952).
41. F.N. Kelly, *J. Polym. Sci.*, L549 (1961).
42. E.A. DiMarzio and J.H. Gibbs, *J. Polym. Sci.*, **A-1**, 1417 (1963).
43. E.A. DiMarzio and J.H. Gibbs, *J. Polym. Sci.*, **XL**, 121 (1959).

## Chapter 4

1. G.E. Zaikov, A.P. Iordanskii and V.S. Markin in *Diffusion of Electrolytes in Polymers*, New Concepts in Polymer Science Series, Ed. C.R.H.I. de Jonge, VSP, Utrecht, (1988), pp73.
2. "Water, A Comprehensive Treatise: The Physics and Physical Chemistry of Water", Ed. F. Franks, Plenum Press, New York(1972), Vol. 1.
3. H.S. Frank and M.W. Evans, *J. Phys. Chem.*, **13**, 507 (1945).
4. H.S. Frank and W.Y. Wen, *Disc. Faraday Soc.*, **24**, 133 (1957).
5. E.D. Becker, *High resolution NMR: theory and chemical applications*, 2nd edn., Academic Press, New York (1980).
6. P.E.M. Allen, D.J. Bennett and D.R.G. Williams, *Eur. Polym. J.*, **29**(2/3), 231 (1993).
7. M.F. Refojo, *J. Polym. Sci.: Part A-1*, **5**, 3103 (1967).
8. K. Dusek, M. Bohdanecky and V. Vosicky, *Coll. Czech. Chem. Commun.*, **42**, 1599 (1977).
9. S.K. Kang and M.S. Jhon, *J. Polym. Sci.:Part A: Polymer Chemistry*, **31**, 1243 (1993).
10. S.H. Oh, R. Ryoo and M.S. Jhon, *Macromolecules*, **23**, 1671 (1990).
11. F.X. Quinn, V.J. McBrierty, A.C. Wilson and G.D. Friends, *Macromolecules*, **23**, 4576 (1990).
12. C.J. Hamilton, S.M. Murphy, N.D. Atherton and B.J.Tighe, *Polymer*, **29**, 1879 (1988).
13. S.M. Murphy, C.J. Hamilton and B.J. Tighe, *Polymer*, **29**, 1887 (1988).
14. R.A. Robinson and R.H. Stokes, *Electrolyte Solutions*, 2nd Edn., Butterworths, Sydney (1970).
15. K. Pathmanathan and G.P. Johari, *J. Polym. Sci., Polym. Phys. Ed.*, **28**, 675 (1990).

16. G. Smyth, F.X. Quinn and V.J. McBrierty, *Macromolecules*, **21**, 3198 (1988).
17. P.E.M. Allen, D.J. Bennett and D.R.G. Williams, *Eur. Polym. J.*, **28**(10), 1173 (1992).
18. P.E.M. Allen, C.-H. Lai and D.R.G. Williams, *Eur. Polym. J.*, **29**(10), 1293 (1993).
19. P.G. Bruce in *Polymer Electrolyte Reviews-1*, Eds. J.R. MacCallum, C.A. Vincent, Elsevier, London (1987) pp237.
20. M. Watanabe, S. Oosashi, K. Sanui, N. Ogata, T. Kobayashi and Z. Ohtaki, *Macromolecules*, **18**, 1945 (1985).
21. D. Dobos, *Electrochemical Data*, Elsevier, Budapest (1975).

## Chapter 5

1. F.M. Gray in *Polymer Electrolyte Reviews-1*, Eds.J.R. MacCallum, C.A. Vincent, Elsevier, London, 1987.
2. G.E. Zaikov, A.P. Iordanskii and V.S. Markin in *Diffusion of Electrolytes in Polymers*, New Concepts in Polymer Science Series, Ed. C.R.H.I. de Jonge ,VSP, Utrecht, (1988).
3. H.B. Lee, M.S. Jhon and J.S. Andrade, *J. Colloid Interface Sci.*, **51**(2), 225 (1975).
4. J.A. Bouwstra, J.C. van Miltenburg, W.E. Roorda and H.E. Junginger, *Polym. Bull.*, **18**, 337 (1987).
5. P.H. Corkhill, A.M. Jolly, C.O. Ng and B.J. Tighe, *Polymer*, **28**, 1758 (1987).
6. G. Smyth, F.X. Quinn and V.J. McBrierty, *Macromolecules*, **21**, 3198 (1988).
7. P.E.M. Allen, D.J. Bennett and D.R.G. Williams, *Eur. Polym. J.*, **29**(2/3), 231 (1993).
8. C.J. Hamilton, S.M. Murphy, N.D. Atherton and B.J. Tighe, *Polymer*, **29**, 1879 (1988).
9. S.M. Murphy, C.J. Hamilton and B.J. Tighe, *Polymer*, **29**, 1887 (1988).
10. T.G. Fox and P.J. Flory, *J. Am. Chem. Soc.*, **70**, 2384 (1948).
11. T.G. Fox and P.J. Flory, *J. Appl. Phys.*, **21**, 581 (1950).
12. K. Pathmanathan and G.P. Johari, *J. Polym. Sci.:Part B: Polym. Phys. Ed.*, **28**, 675 (1990).
13. P.E.M. Allen, C.-H. Lai and D.R.G. Williams, *Eur. Polym. J.*, **29**(10), 1293 (1993).
14. L.D. Kuntz and W. Kauzman, *Adv. Protein Chem.*, **28**, 239 (1974).
15. H. Yasuda, H.G. Olf, B. Crist, C.E. Lamaze and A. Peterlin in *Water Structure at the Water-Polymer Interface*, H.H.G. Jellinek Ed., Plenum Press, New York (1975).
16. R.A. Nelson, *J.Appl. Polym. Sci.*, **21**, 645 (1977).
17. P.H. Corkhill and B.J. Tighe, *Polymer*, **33**, 1526 (1990).

18. D.G. Pedley and B.J. Tighe, *Br. Polym J.*, **11**, 130 (1979).
19. N. Murase, K. Gonda and T. Watanabe, *J. Phys. Chem.*, **90**, 5421 (1986).
20. D.J. Bennett, *Ph.D. Thesis*, University of Adelaide, 1991.
21. M. Refojo, *J. Polym. Sci. Pt. A-1*, **5**, 3103 (1967).
22. P.R. Swan, *J. Polym. Sci.*, **56**, 403 (1962).
23. D. W. van Krevelen, *Properties of Polymers: Their Estimation and Correlation with Chemical Structure*, 2nd Ed., Elsevier (1976).
24. L.C.E. Struik, *Internal Stresses, Dimensional Instabilities and Molecular Orientations in Plastics*, Interscience (1962).
25. R. Simha and R.F. Boyer, *J. Chem. Phys.*, **37**(5), 1003 (1962).
26. G.E. Roberts and E.F.T. White in *The Physics of Polymer Glasses*, R.N. Haward (Ed.), Applied Science Publishers, Chpt3. (1973).
27. C-H. Lai, *Ph.D. thesis*, University of Adelaide (1992).
28. R.A. Haldon and R. Simha, *J. Appl. Phys.*, **39**(3), 1890 (1968).
29. G.J. Howard and R.A. Shanks, *J. Appl. Polym. Sci.*, **26**, 3099 (1981).
30. P.E.M. Allen, D.J. Bennett and D.R.G. Williams, *Eur. Polym. J.*, **28**(10), 1173 (1992).
31. L.B. Liu, A.F. Lewis, J.C. Lewis, X. Li and D.W. Gidley, *Proc. MRS Symp. R2 Boston MA.*, Nov26-Dec1 (1990).
32. D.H.D. West, K.J. McBrierty and C.F.G. Delaney, *Appl. Phys.*, **18**, 85 (1979).
33. K. Jeffrey and R.A. Pethick, *Eur. Polym. J.*, **30**(2), 153 (1994).
34. C. Szeles, A. Vertes, M.L. White and H. Leidheiser, *Nucl. Meth. Phys. Res. A*, **A271**, 688 (1990).
35. M.D. Zipper, G.P. Simon, P. Cherry and A.J. Hill, *J. Polym. Sci.: Part B Polym. Phys.*, **32**, 1237 (1994).
36. G.P. Simon, M.D. Zipper and A.J. Hill, *J. Appl. Polym Sci.*, **52**, 1191 (1994).
37. A.J. Hill, *Ph.D. Dissertation*, Duke University, Durham, NC. USA (1990).



38. Y.C. Jean, *Microchem. J.*, **42**, 72 (1990).
39. M.D. Zipper and A.J. Hill, *Mater. Forum*, **18** (Materials Characterization Review, G. Schaeffer Ed.), 215 (1994).
40. J.J. Singh, T.L. Clair, H.H. Holt and W. Mock Jr., *Nucl Instrum. Meth. Phys. Res.*, **221**, 427 (1984).
41. K.J. Heater *unpublished data* (1991).
42. R.C. MacQueen and R.D. Granata, *J. Appl. Polym. Sci. B: Polym. Phys.*, **31**, 971 (1993).
43. R.C. MacQueen and R.D. Granata, *Mater. Sci. Forum*, **105-110**, 1649 (1992).
44. M. Welander and F.H.J. Maurer, *Mater. Sci. Forum*, **105-110**, 1815 (1992).
45. J.M. Warman and M. Eldrup, *Biopolymers*, **25**, 1865 (1986).
46. R.B. Gregory, K.J. Chai and W. Su, *Mater. Sci. Forum*, **105-110**, 1577 (1992).
47. R.M. Hodge, *Ph.D. Thesis*, Monash University, Vic. Australia (1994).
48. R.E. Green and R.E. Bell, *Canad. J. Phys.*, **36**, 1684 (1958).
49. G. Fabri, E. Gemagnoli, I.F. Querica and E. Turrisi, *Nuovo Cimento*, **30**, 21 (1962).
50. Yu V. Zelenev and A.I. Filip'ev, *Sov. Phys.: Solid State*, **18**(5), 787 (1976).
51. V.I. Goldanskii, *At. Energy Rev.*, **6**, 3 (1968).
52. R. Resnick and D. Halliday, *Physics*, pp537, Wiley, Tokyo (1967).

## Chapter 6

1. P.E.M. Allen, D.J. Bennett and D.R.G. Williams, *Eur. Polym. J.*, **28**(4), 347 (1992).
2. P.E.M. Allen, D.J. Bennett and D.R.G. Williams, *Eur. Polym. J.*, **28**(10), 1173 (1992).
3. P.E.M. Allen, D.J. Bennett, A.M. Hounslow and D.R.G. Williams, *Eur. Polym. J.*, **28**(10), 1179 (1992).
4. P.E.M. Allen, D.J. Bennett and D.R.G. Williams, *Eur. Polym. J.*, **29**(2/3), 231 (1993).
5. F.M. Gray in *Polymer Electrolyte Reviews-1*, Eds. J.R. MacCallum and C.A. Vincent, Elsevier, London, pp187 (1987).
6. M. Refojo and H. Yasuda, *J. Appl. Polym. Sci.*, **9**, 2425 (1965).
7. J. Janacek and J. Hasa, *Coll. Czech. Chem. Commun.*, **31**, 2186 (1966).
8. G. Smyth, F.X. Quinn and V.J. McBrierty, *Macromolecules*, **21**, 3198 (1988).
9. D.J. Bennett, *Ph.D Thesis*, University of Adelaide (1991).
10. C.J. Hamilton, S.M. Murphy, N.D. Atherton and B.J. Tighe, *Polymer*, **29**, 1879 (1988).
11. *calculated from data in*: D.Dobos, *Electrochemical Data*, Elsevier, Budapest (1975).
12. P.E.M. Allen, C.-H. Lai and D.R.G. Williams, *Eur. Polym. J.*, **29**(10), 1293 (1993).